Characterization of the gut peptidome and the function of brain-gut peptides with regard to food intake and metabolism in *Drosophila melanogaster* and the agricultural pest *Delia radicum*

(Aufklärung des Darmpeptidoms und der Funktion von „brain-gut“-Peptiden in Bezug zu Nahrungsaufnahme und Stoffwechsel bei *Drosophila melanogaster* und dem landwirtschaftlichen Schädling *Delia radicum*)

Philipps Universität Marburg

Dissertation

zur Erlangung des Doktorgrades
der Naturwissenschaften (Dr. rer. nat.)

dem Fachbereich Biologie
der Philipps-Universität Marburg
vorgelegt von:

Dipl.-Biol. Wencke Reiher
aus Chemnitz

Marburg, 2013

Vom Fachbereich Biologie der Philipps-Universität Marburg (Hochschulkennziffer: 1180)
als Dissertation angenommen am:

Erstgutachter: Prof. Dr. Christian Wegener
Zweitgutachter: Prof. Dr. Uwe Homberg

Tag der mündlichen Prüfung:

Contents

1 Erklärung des Eigenanteils an den Publikationen/Manuskripten

Gemäß § 9, Absatz 1 der „Promotionsordnung der Mathematisch-Naturwissenschaftlichen Fachbereiche und des Medizinischen Fachbereichs für seine mathematisch-naturwissenschaftlichen Fächer der Philipps-Universität Marburg“ (Fassung vom 15.07.2009) können „Publikationen, die aus der Promotionsarbeit hervorgegangen sind und in angesehenen Zeitschriften […] veröffentlicht oder eingereicht wurden, [...] als Dissertationsleistung anerkannt werden (kumulative Dissertation). In diesen Fällen ist [...] in einer gesonderten Erklärung darzulegen, welchen Anteil die Doktorandin oder der Doktorand an den Publikationen hatte. Diese Erklärung ist von der Betreuerin oder dem Betreuer sowie von den Promovierenden zu unterschreiben [...].“

Der Anteil der Doktorandin an den Publikationen/Manuskripten wird im Folgenden dargestellt:

Kapitel 5.1: Peptidomics and peptide hormone processing in the *Drosophila* midgut.
W. Reiher, C. Shirras, J. Kahnt, S. Baumeister, R. E. Isaac and C. Wegener

Experimente:
- Probenvorbereitung für LC/MS: Kreuzung, Hitzeschocken und Präparation der Versuchsfliegen sowie Peptidextraktion, z.T. mit Unterstützung von C. Wegener
- Kapillar-HPLC: Durchführung aller Peptidauftrennungen
- Massenspektrometrie: Durchführung aller Messungen, z.T. mit Unterstützung von J. Kahnt, und Auswertung der Daten
- Immunfärbungen: Durchführung sämtlicher Schritte einschließlich Auswertung am konfokalen Laser-Scanning-Mikroskop
- Fluoreszenzmikroskopie: Durchführung sämtlicher Schritte

Manuskript:
- Text: Verfassen der Kapitel „Abstract“, „Materials and Methods“ (außer Abschnitt „*In situ* Hybridization in the Larval Midgut“), „Results“ und „Discussion“ in Zusammenarbeit mit C. Wegener
- Tabellen: Erstellung aller Tabellen
- Abbildungen: Anfertigung aller Bildtafeln und Abbildungen außer Abb. 1

Kapitel 5.2: Peptidomics of the agriculturally damaging larval stage of the cabbage root fly *Delia radicum* (Diptera: Anthomyiidae).
J. Zoephel, W. Reiher, K.-H. Rexer, J. Kahnt and C. Wegener

- Betreuung der Studentin J. Zöphel, deren Masterarbeit Grundlage für die Publikation war, in Zusammenarbeit mit C. Wegener

Experimente:
- Kapillar-HPLC: Durchführung aller Peptidauftrennungen, z. T. in Zusammenarbeit mit J. Zöphel, die ich in die Benutzung des Gerätes eingewiesen habe
- Massenspektrometrie: Durchführung aller Messungen von Peptidextrakten (d.h. ohne direktes Profiling), z. T. in Zusammenarbeit mit J. Zöphel, die ich in die Benutzung des Gerätes eingewiesen habe
- Datenbankeinträge: Eingabe der Peptidsequenzen und weiterer erforderlicher Daten für die UniProt-Datenbank

• Immunfärbungen: Unterstützung von J. Zöphel bei der Benutzung des konfokalen Laser-Scanning-Mikroskops und bei der Anfertigung der Bildtafeln

Manuskript:

• Text: Korrekturen und Ergänzungen zum Text für das Manuskript (und zum ursprünglichen Text der Masterarbeit von J. Zöphel)
• Tabellen: Korrekturen
• Abbildungen: Korrekturen und Überarbeitung an mehreren Abbildungen; insbesondere Überprüfung und einige Korrekturen der abgebildeten MS/MS-Spektren und zugeordneten Peptidsequenzen

Kapitel 5.3: Dissecting the pleiotropic function of allatostatin A cells in *Drosophila*—which subset regulates feeding, activity or gut motility?

W. Reiher, J. Chen, P. Cognigni, C. P. Christov, I. Miguel-Aliaga, J. A. Veenstra and C. Wegener

Experimente:

• Kreuzungen zur Herstellung der Ausgangsfliegenlinien
• Immunfärbungen: Durchführung sämtlicher Schritte einschließlich Auswertung am konfokalen Laser-Scanning-Mikroskop, mit Unterstützung von S. Klühspies
• Capillary Feeder-Assay und Defäkations-Assay: Durchführung sämtlicher Schritte einschließlich Auswertung, mit Unterstützung von C. P. Christov, P. Cognigni und I. Miguel-Aliaga
• Aktivitätsmessungen: Durchführung sämtlicher Schritte des Experiments zu Abb. S1; statistische Auswertung der Daten zu Abb. 6 und S2
• Messung der Mitteldarmbewegungen: Durchführung sämtlicher Schritte einschließlich Auswertung

Manuskript:

• Text: Verfassen des gesamten Manuskripts, mit Überarbeitungen und Ergänzungen durch C. Wegener, Kapitel „Materials and methods“ in Zusammenarbeit mit C. Wegener, J. Chen und J. A. Veenstra
• Tabellen: Erstellung aller Tabellen, Korrekturen durch C. Wegener
• Abbildungen: Anfertigung aller Bildtafeln und Abbildungen, Korrekturen durch C. Wegener

....

Doktorandin Betreuer

2 Zusammenfassung

Regulatorische Peptide, zu denen Neuropeptide und Peptidhormone zählen, sind Signalmoleküle, die der Zell-Zell-Kommunikation dienen und an der Kontrolle vielfältiger biologischer Prozesse in Insekten und anderen vielzelligen Tieren beteiligt sind. Durch Forschung an Säugetieren konnte die Bedeutung von Peptiden aus dem Nervensystem, dem Verdauungstrakt sowie anderen Geweben für die Regulation von Energiebalance, Metabolismus und Nahrungsaufnahme demonstriert werden. Auch etliche Insekten-Neuropeptide sind als effektive metabolische Regulatoren bekannt. Zudem enthält der Mitteldarm der Insekten – wie der Verdauungstrakt bei Säugetieren – zahlreiche endokrine Zellen, wobei die Diversität der enteroendokrinen Insekten-Peptide deren Bedeutung für den Metabolismus und die Nahrungsaufnahme erahnen lässt.

In der ersten Studie meines Projekts haben wir das Mitteldarm-Peptidom von adulten und larvalen *Drosophila melanogaster* charakterisiert. Dafür wurden die Peptide aus dem Mitteldarmgewebe extrahiert und anschließend ihre Strukturen mittels LC-MS/MS (Reversed-phase-HPLC, offline gekoppelt mit MALDI-TOF/TOF-Massenspektrometrie) analysiert. Auf diese Weise konnten wir 24 Peptide identifizieren, die von 9 verschiedenen Peptid-Vorläufermolekülen abstammen: AstA, MIP, AstC, CCHamid1, CCHamid2, sNPF, DTK, DH_{31} und PDF. In einer vorangegangenen Studie konnte mit Immunfärbungen weder PDF noch sNPF in enteroendokrinen Zellen von Adulten gefunden werden. Da jedoch Fortsätze von PDF- bzw. sNPF-produzierenden Neuronen an bestimmten Bereichen des adulten Mitteldarms entdeckt wurden, gehen wir davon aus, dass die Detektion dieser Peptide in den Mitteldarmextrakten adulter Fliegen auf diese Innervationen zurückzuführen war. Die Strukturen von CCHamid1, CCHamid2 und DH_{31} waren vor unserer Untersuchung zwar vorhergesagt, jedoch noch nicht biochemisch charakterisiert worden. Alle 24 Peptide konnten in identischer Form im Nervensystem nachgewiesen werden und stellen somit „brain-gut“-Peptide dar.
Peptide werden generell als Teile größerer Vorläufermoleküle hergestellt, die mehrere Prozessierungsschritte durchlaufen, bis schließlich die bioaktiven Peptide entstehen. Die Spaltung der Propeptide wird durch Subtilisin-ähnliche Prohormon-/Proprotein-Konvertasen (PC) katalysiert. In *Drosophila* wurden drei Gene identifiziert, die für Subtilisin-ähnliche Enzyme codieren. Außerdem konnte gezeigt werden, dass für die Prozessierung von Neuropeptidhormonen dPC2 (=AMON) erforderlich ist. Um mehr über die Prozessierungsschritte bei Mitteldarmpeptiden zu erfahren, haben wir die Verteilung von *amon-Gal4*-getriebenem GFP untersucht und festgestellt, dass es auch in enteroendokrinen Zellen auffindbar war. Außerdem zeigte eine LC-MS/MS-Analyse, dass die Detektierbarkeit der meisten (in Adulten) bzw. aller (in Larven) Darmpeptide nach einer temporären AMON-Defizienz stark herabgesetzt war, was darauf hinweist, dass die Peptidmengen insgesamt reduziert waren und AMON generell für die Bildung von Darmpeptiden benötigt wird. Die umfassende Kenntnis der Strukturen von *Drosophila*-Darmpeptiden bietet fortan eine Grundlage für eine detaillierte Untersuchung ihrer Funktionen.

Mit der zweiten Studie meines Projektes konnten wir die Kenntnis von Peptidstrukturen in wichtigen Insekten weiter ausbauen, und wechselten dabei vom Modellorganismus (*Drosophila*) zum Schadinsekt (der Kleinen Kohlfliege/Kohlmade *Delia radicum*). Wir haben das Peptidom der Kohlmade – d.h. jenes Stadiums, das durch Wurzelfraß wirtschaftlichen Schaden verursacht – mittels LC-MS/MS-Analyse von Peptidextrakten bzw. direktem Profiling von Neurohämalorganen untersucht. Da Genomsequenz- oder EST-Informationen zu dieser Spezies fehlen, haben wir die Peptide anhand unserer Tandem-MS-Daten manuell *de novo*-sequenziert und dabei die Sequenzen von bekannten Insektenpeptiden sowie einigen zuvor in adulten Kohlfliegen identifizierten Neuropeptiden zu Vergleichszwecken herangezogen. Die Sequenzierung der extrahierten Peptide konnte durch

vorheriges Labeln mit SPITC (4-Sulfophenyl-Isothiocyanat) vereinfacht werden. SPITC beeinflusst bekanntermaßen die Ladung der Peptidfragmente, die während der Tandem-MS entstehen, und reduziert dadurch die Komplexität von MS/MS-Spektren, wodurch deren Interpretation erleichtert wird. Durch die Analyse von ZNS, Neurohämalorganen und Därmen konnten wir 38 Peptide aus diversen Peptidfamilien charakterisieren: AstA, AstC, FMRFamid-artige Peptide, Kinine, CAPA-Peptide, Pyrokinine, sNPF, Myosuppressin, Corazonin, SIFamid, Sulfakinine, Tachykinine, NPLP1-Peptide, AKH and CCHamid1. Zudem konnten wir ein neues Peptid („Yamid“) identifizieren, das Sequenzähnlichkeit zum Eclosionshormon-Vorläufermolekül bei einigen *Drosophila*-Arten aufweist.
Zusätzlich zur Peptidomik-Analyse haben wir per Immunfärbung auch die Verteilung bestimmter Typen von peptidbildenden Neuronen und enteroendokrinen Zellen untersucht. Dabei zeigte sich, dass die Verteilungsmuster der angefärbten Zellen weitgehend mit denen in *Drosophila* übereinstimmten, und dass einige Peptidfamilien der LC-MS/MS-Identifikation entgangen sind. In Zukunft könnten unsere Ergebnisse für die Entwicklung einer peptidbasierten Strategie zum zielgerichteten Management der Kohlfliege genutzt werden. Zudem sprechen die gefundenen Übereinstimmungen der peptidergen Systeme von *Delia* und *Drosophila* dafür, dass *Drosophila* im Hinblick auf die peptiderge Regulation der Nahrungsaufnahme und des Stoffwechsels als genetisch zugängliches Modell für Schadinsekten dienen kann.

In der abschließenden Studie zu meinem Projekt haben wir die Rolle von Allatostatin A (AstA) untersucht – einer Peptidfamilie, die typischerweise in Insekten (und anderen Arthropoden) vorkommt und bei Vertretern verschiedenster Insektenordnungen mehrere mit dem Stoffwechsel in Verbindung stehende Prozesse beeinflusst. Daher werden AstA-Peptide als mögliche Kandidaten für eine peptidbasierte Kontrolle von Schadinsekten angesehen. Da AstA in den ersten beiden Studien sowohl im ZNS als auch in enteroendokrinen Zellen bei *Delia* und *Drosophila* nachgewiesen werden konnte, haben wir *Drosophila* gewählt, um mit den verfügbaren genetischen und molekularen Werkzeugen die Wirkung von AstA zu untersuchen. In vorangegangenen Studien konnte bereits demonstriert werden, dass AstA eine Rolle für die Regulation des Stoffwechsels und der Nährstoffhomöostase in *Drosophila* spielt. Um ein umfassenderes Bild der AstA-Wirkungsweise zu erhalten, haben wir uns der Frage gewidmet, ob sich spezifische Effekte auf die Aktivität bestimmter Subsets der zahlreichen bei adulten Taufliegen vorkommenden AstA-produzierenden Zellen (=AstA-Zellen) zurückführen lassen. AstA-Neurone finden sich in verschiedenen Regionen des Nervensystems, wie dem Zentralgehirn, dem Unterschlundganglion, den Medullae und dem Thorakoabdominalganglion. Der Thorax enthält außerdem einige periphere AstA-Neurone. Der Enddarm wird von mehreren zentralen AstA-Neuronen innerviert, wobei einzelne Fortsätze bis auf den angrenzenden Abschnitt des hinteren Mitteldarms reichen. Zusätzlich existieren zahlreiche AstA-produzierende enteroendokrine Zellen, die im Epithel des posterioren Mitteldarms verstreut liegen.
Durch Anwendung des Gal4/UAS-Systems haben wir den hitzesensitiven TrpA1-Kanal in verschiedenen AstA-Zellsubsets exprimiert und die Effekte der temperaturinduzierten Zellaktivierung auf die Nahrungsaufnahme, die lokomotorische Aktivität und die Defäkation untersucht. Durch die thermogenetische Aktivierung der AstA-Zellen wurde die Nahrungsaufnahme der Fliegen signifikant reduziert und die lokomotorische Aktivität beträchtlich vermindert. Aus unseren Ergebnissen konnten wir schließen, dass die Aktivierung von zwei Paar AstA-bildenden Neuronen des posterioren lateralen Protocerebrums (=PLP-Neurone) und/oder der enteroendokrinen AstA-Zellen ausreichen würde, um die festgestellten Effekte hervorzurufen. Die Kombination unserer Daten mit den Ergebnissen einer vorangegangenen Studie legte zudem nahe, dass die PLP-Neurone das Sättigungsgefühl stimulieren, wohingegen die enteroendokrinen AstA-Zellen die Lokomotion regulieren.

Aufgrund der engen Verbindung von AstA und dem hinteren Abschnitt des Darmes haben wir einen möglichen Effekt der Aktivierung der AstA-Zellen auf die Exkretion sowie die Defäkation untersucht. Bei dem dafür angewendeten Assay wurde das Fliegenfutter mit einem pH-Indikatorfarbstoff versetzt, um anschließend die Ausscheidungen der Fliegen automatisiert (bezüglich Anzahl, Größe, Farbe, Farbstoffdichte etc.) analysieren zu können. Obwohl die thermogenetische Aktivierung der AstA-Zellen keinen signifikanten Effekt erkennen ließ, deuteten unsere Ergebnisse darauf hin, dass AstA die Defäkation direkt und indirekt zu beeinflussen scheint, wohingegen kein Effekt auf Wasser- und Ionenhomöostase festgestellt werden konnte.

Da von verschiedenen anderen Insektenarten bereits bekannt war, dass AstA die Darmmotilität beeinflussen kann, wollten wir überprüfen, ob dies auch für *Drosophila* zutrifft. Mittels *in vitro*-Versuch testeten wir die Wirkung von synthetischen AstA-Peptiden auf isolierte Mitteldärme und konnten eine dosisabhängige Inhibition der Mitteldarmmotilität feststellen. Die Reduktion der Mitteldarmbewegungen war bei einer AstA-4-Konzentration von 10^{-7} M oder höher signifikant. Um herauszufinden, über welchen der beiden AstA-Rezeptoren (DAR-1 oder DAR-2) diese Reaktion hervorgerufen wurde, haben wir beide Rezeptortranskripte separat per RNAi in der Mitteldarmmuskulatur herunterreguliert. Während die *DAR-1*-RNAi keine Beeinträchtigung des myoinhibitorischen Effekts von AstA-4 nach sich zog, erwies sich AstA-4 (auch bei einer Konzentration von 10^{-6} M) als wirkungslos, wenn die *DAR-2*-Expression herunterreguliert wurde.

Alles in allem scheint AstA, indem es das Sättigungsempfinden, die Lokomotion, die Darmperistaltik und möglicherweise auch die Defäkation steuert, verschiedene Ebenen des Stoffwechsels und unterschiedliche Gewebe zu beeinflussen, und dabei mehrere mit der Nahrungsaufnahme sowie auch untereinander in Verbindung stehende Prozesse zu fördern. Wir beabsichtigen, in zukünftigen Experimenten die Art und Weise der AstA-Wirkung näher zu beleuchten und die vielfältigen Effekte dieser Peptide weiter aufzuklären.

3 Summary

Regulatory peptides, which comprise neuropeptides and peptide hormones, are cell-cell signaling molecules that control a variety of biological processes in insects and other metazoans. Research on mammals demonstrated the importance of peptides generated in the nervous system, the intestine and other tissues for the regulation of energy balance, metabolism and food intake. Similarly, several insect neuropeptides are known to be effective metabolic regulators. Furthermore, the insect midgut—like the mammalian digestive system—contains numerous endocrine cells, and the diversity of insect enteroendocrine peptides gives a hint at their relevance for metabolism and feeding behavior.

In the first study of my project, we characterized the midgut peptidome of adult and larval *Drosophila melanogaster* by extraction of peptides from midgut tissue and subsequent LC-MS/MS (Reversed-phase HPLC, offline coupled with MALDI-TOF/TOF mass spectrometry) analysis of peptide structures. By this means we identified 24 peptides originating from 9 different peptide precursors: AstA, MIP, AstC, CCHamide1, CCHamide2, sNPF, DTK, DH_{31} and PDF. Since, in a previous study, neither PDF nor sNPF could be discovered in enteroendocrine cells of adults by immunostaining, but processes of PDF- and sNPF-producing neurons were found to innervate parts of the adult midgut, we concluded that the detection of these peptides in midgut extracts of adult flies resulted from innervations. The structures of CCHamide1, CCHamide2 and DH_{31} had been predicted prior to our study, but not yet characterized biochemically. All 24 peptides were found in identical form within the CNS and thus represent brain-gut peptides.
Peptides are generally produced as parts of larger precursor molecules that undergo several steps of processing to achieve the final, bioactive peptide structure. The cleavage of the propeptide is known to be catalyzed by subtilisin-like prohormone/proprotein convertases (PC). Three *Drosophila* genes coding for subtilisin-like enzymes have been identified, and processing of *Drosophila* neuropeptide hormones was previously shown to require dPC2 (=AMON). In investigation of the processing pathway of midgut peptides, we found *amon-Gal4*-driven GFP localized within enteroendocrine cells. Moreover, the detectability of most (in adults) or all (in larvae) gut peptides by LC-MS/MS was strongly reduced by a temporary AMON deficiency, suggesting a general decrease of peptide levels and thus a general need of AMON for gut peptide production. The comprehensive information on the structures of *Drosophila* gut peptides now provides a background for a detailed investigation of their functions.

In the second study of my project, we could expand the knowledge on peptide structures of relevant insects, changing from a model (*Drosophila*) to a pest species (the cabbage root fly/cabbage maggot *Delia radicum*). We investigated the peptidome of the cabbage maggot—i.e. the stage which causes economic damage by feeding on plant roots—by LC-MS/MS analysis of peptide extracts and direct profiling of tissue from neurohemal organs. Due to the lack of genomic or EST data for this species, we employed manual *de novo* sequencing, supported by comparison of the sequence information that we obtained by tandem MS with the structures of peptides already known from other insects, as well as neuropeptides previously found in adult cabbage root flies. Labeling of extracted peptides with SPITC (4-sulfophenyl isothiocyanate) prior to analysis assisted in peptide sequencing. SPITC is known to influence the charge of the peptide fragments created during tandem MS, thus reducing complexity and facilitating interpretation of MS/MS spectra. By analysis of CNS, neurohemal organ and gut tissue, we could characterize 38 peptides belonging to diverse peptide families: AstA, AstC, FMRFamide-like peptides, kinins, CAPA peptides, pyrokinins, sNPF, myosuppressin, corazonin, SIFamide, sulfakinins, tachykinins, NPLP1-peptides, AKH and CCHamide1. Moreover, we identified a

new peptide ("Yamide") with sequence similarity to the eclosion hormone precursor of several *Drosophila* species.
In addition to the peptidomic analysis, we investigated the distribution of several types of peptide-producing neurons and enteroendocrine cells by immunostaining and found that, in most cases, staining patterns were largely similar to *Drosophila*, and that several peptide families have been missed in our LC-MS/MS analysis. In the future, our results could be of use for the development of a targeted, peptide-based management of cabbage root flies. The observed similarities in the peptidergic systems also suggest that *Drosophila* can serve as a genetically accessible pest species model in terms of peptidergic regulation of feeding and metabolism.

In the final study of my project, we analyzed the role of allatostatin A (AstA), a peptide family commonly occurring in insects (and other arthropods) and shown to pleiotropically influence metabolism-related processes across insect orders. Therefore, AstA peptides are regarded as possible candidates for a peptide-based control of insect pests. Since AstA was found to be present in the CNS and enteroendocrine cells in *Drosophila* and *Delia* in the first studies, we chose *Drosophila* due to the genetic and molecular tools available to investigate AstA signaling. Previous studies had already demonstrated a role for AstA in metabolic regulation and nutritional homeostasis of *Drosophila*. We were interested in a wider picture of AstA action and addressed the question whether specific effects were connected to the activity of certain subsets of the numerous AstA-producing cells (=AstA cells) found in adult fruit flies. AstA neurons are located in different regions of the nervous system, including the central brain, the subesophageal ganglion, the medullae and the thoracico-abdominal ganglion. The thorax also contains a few peripheral AstA neurons. Some of the thoracico-abdominal ganglion neurons innervate the hindgut and also send projections to the posteriormost portion of the midgut. In addition, a large number of enteroendocrine AstA cells are scattered across the epithelium of the posterior midgut.
Using the Gal4/UAS system we expressed the heat-sensitive TrpA1 channel in different subsets of AstA cells and investigated the effects of temperature-induced cell activation on feeding, locomotor activity and defecation behavior. Thermogenetic activation of AstA cells significantly reduced food intake of flies, and also considerably diminished their locomotor activity. Our experimental data led us to conclude that the activation of two pairs of AstA-producing posterior lateral protocerebrum (PLP) neurons and/or the AstA enteroendocrine cells would be sufficient to evoke the observed effects. The combination of these results with findings of a previous study suggested that the PLP neurons function to promote satiety, while AstA from gut endocrine cells regulates locomotor activity.
Due to the close relation of AstA with the posterior gut portion, we investigated a possible influence of AstA cell activation on excretion and defecation. For this, we applied an assay which included supplementation of fly food with a pH indicator dye and subsequent automated analysis of deposits (number, size, color, dye density etc.). Although no significant effect was visible upon thermogenetic activation of AstA cells, our findings indicated that AstA might directly and indirectly influence defecation behavior, while no effect on water and ion homeostasis could be observed.
Because AstA has previously been shown to influence gut motility in several other insect species, we aimed at finding out if this would also apply to *Drosophila*. We tested the effect of synthetic AstA peptides on isolated midguts *in vitro* and observed a dose-dependent inhibition of midgut motility. The reduction of midgut movement was significant at an AstA-4 concentration of 10^{-7} M or higher. To find out which of the two AstA receptors (DAR-1 or DAR-2) mediated this effect, we separately downregulated both receptor transcripts in the gut musculature via RNAi. AstA-4 was ineffective at inhibiting midgut motility if *DAR-2* expression was downregulated—even if the peptide dose was

increased to 10^{-6} M. Downregulation of *DAR-1* expression did not diminish the myoinhibitory effect of AstA-4.

Altogether, by influencing satiety, locomotion, gut peristalsis and possibly also defecation, AstA appears to affect different levels of metabolism and different tissues, seemingly promoting several interrelated processes connected to food intake. In future experiments, we plan to shed light on the mode of AstA action and to further unravel the diverse effects of these peptides.

4 Introduction and outline

4.1 General background: Peptide signals in insects

Neuropeptides and peptide hormones—also referred to as "regulatory peptides"—are the largest group of cell-cell signaling molecules. They originate from the nervous system or endocrine cells and control cell or tissue function. A part of the neuropeptides is used both within the nervous system and also as peptide hormones that are produced by neurosecretory cells and released into the hemolymph at neurohemal regions to reach other organs [1, 2]. Diverse biological processes in metazoans are regulated by regulatory peptides and their receptors, which appeared early in evolution—several neuropeptides could be identified in cnidarians [3]—and diversified along with the phylogeny of both protostomes and deuterostomes [1, 4].

Most knowledge on insect peptide signaling stems from studies on neuropeptides, which primarily function by activation of G protein-coupled receptors [1, 4, 5]. As neuropeptides are more or less involved in all physiological processes during an insect's life cycle (including developmental processes, behavior, metabolic events and reproduction) [5], the importance of studying insect peptide signaling is evident—not only in view of a better physiological understanding of the most species-rich animal class and the role of insect model organisms for research, but also with regard to the potential it holds for a targeted control of those insect representatives that have a direct negative impact on human life, e.g. as disease vectors or agricultural pests.

4.2 Aims of this thesis

The superordinate topic of this thesis is the role of regulatory peptides for the regulation of insect metabolism, including feeding behavior. Our first study (5.1) was a peptidomic approach to take an inventory of gut peptides in *Drosophila*. Furthermore, we were interested in the biosynthetic pathway for peptide production, more precisely whether AMON, a proprotein convertase previously shown to be necessary for the production of neuropeptide hormones, also participates in gut peptide processing. Enteroendocrine peptides in insects likely are important regulators of metabolism, but have still not been receiving adequate attention. Knowledge on the structures of the bioactive peptides in this model species will provide a basis for future research and possible understanding of the relevance of enteroendocrine signaling.

The second study (5.2) addressed the cabbage root fly *Delia radicum*. By feeding on the roots, the larvae of this species can cause severe damage to crops cultivated in the northern temperate region. To provide a first basis for the understanding (and potential future manipulation) of peptide signaling in cabbage maggots, we set about identifying peptides from the gut, CNS and neurohemal organs—this task being a challenge, since no genomic or EST data was available for *Delia*. Besides the peptide structures, we were likewise interested in the distribution of peptidergic cells, also in comparison with *Drosophila*, which might provide a very useful and specific model for *Delia* research.

The intention of the final study (5.3) was to analyze the functions of allatostatin A (AstA) peptides, which—like in several representatives of other insect orders—have been implicated in the control of metabolism-related processes in *Drosophila*, and thus deserved further attention and investigation. AstA is produced by cells in diverse regions of the nervous system as well as endocrine cells of the midgut, and we wondered whether different effects could be assigned to different subsets of AstA-producing cells.

4.3 Recent advances in insect peptide research

The complete genome sequence of *Drosophila melanogaster* was published in 2000 [6] and since then was accessible to scientists worldwide via the GenBank [7] and other sequence databases. Therefore, *Drosophila melanogaster* was the second metazoan organism with a fully sequenced genome, following soon after the publication of the *Caenorhabditis elegans* genome sequence [8]. The genome data accelerated genetic research and the understanding of genome assembly as well as gene function, structure and regulation [9]. Subsequently, information for many more insect genomes has become available [10], and the international "i5k Insect and other Arthropod Genome Sequencing Initiative", launched in 2011, is attempting to sequence the genomes of 5000 insect and other arthropod species within the next years, encouraging the community to suggest species for sequencing [11, 12]. The growth of information found in genome and also EST databases simultaneously promoted research on insect regulatory peptides as their sequences could now be predicted and identified—the same holding true for the peptide receptors that could be deorphanized [5, 10].

Although peptides can be predicted from the genome sequence by BLAST screens and bioinformatics methods, these tools are unable to reveal the final products of peptide precursor genes with certainty. The structure of the bioactive peptides is the result of several steps of precursor processing and potential post-translational modifications, which can differ between developmental stages or tissues [5, 13]. Therefore, biochemical analysis of peptides via peptidomics—i.e. a combination of mass spectrometry and other methods such as liquid chromatography—is needed for structural characterization. Soon after the completion of the *Drosophila* genome project, the fruit fly emerged as one of the few insect species for which a substantial part of the peptidome was characterized. In 2002, 28 neuropeptides—including peptides that had been unknown or predicted incorrectly—were identified from the larval CNS [14], a number that increased through later studies [e.g. 15]. The adult CNS peptidome was analyzed in 2009 [16]. In addition to those studies, which employed sophisticated methods for sample preparation prior to mass spectrometry (mostly liquid chromatography), direct peptide profiling—a method that comprises direct MALDI-TOF mass spectrometric analysis of defined tissue—was applied to analyze peptides stored in neurohemal regions and other peptide hormone release sites [17, 18]. Currently, more than 70 neuropeptides and peptide hormones are known from *Drosophila*, some of them still awaiting biochemical proof [1]. Moreover and astonishingly, new, unpredicted *Drosophila* peptide precursor genes are still being identified—most recently *natalisin* (*NTL*), which was likewise found in other insect and also crustacean genomes [19].

By now, not just *Drosophila* but several more insects have been the object of peptidomic analyses, e.g. *Aedes aegypti* [20], *Apis mellifera* [21–24] and *Tribolium castaneum* [25, 26]. Study of insect peptide signaling has potential to benefit research beyond the field of insect physiology or phylogenetic research, as several mammalian neuropeptides and/or their receptors have orthologs in insects [see 5 and references therein].

4.4 Allatostatin A (AstA)

4.4.1 Occurrence of AstA in insects and other invertebrates

The first allatostatins were discovered by their ability to *in vitro* inhibit the production and release of juvenile hormone by the corpora allata (CA) of the cockroach *Diploptera punctata* [27–30]. Since then, these AstA peptides (also called A-type, *D. punctata*-type or FGL-amide allatostatins) could be identified from a range of insects—more precisely from every investigated insect species with the

exception of *Tribolium castaneum* [5, 25, 26]—as well as other invertebrates. AstA peptides share a common C-terminal sequence motif (Y/F)XFG(L/I)-amide [31, 32], which constitutes or rather contains the active core region of the peptides [33, 34]. Functional analyses showed that AstA peptides are multifunctional peptides (see below), their allatostatic property being limited to cockroaches, crickets and termites [35]. In the locust *L. migratoria* a CA-modulating role was shown for Dippu-AstA peptides, which was either stimulatory or inhibitory depending on the peptide concentration and basal JH release rate of the CA [36]. In general, the allatostatic activity of AstA in an insect species correlates with an intense innervation of the CA by AstA neurons of the pars lateralis [37]. However, the relevance of AstA-positive innervations that were found within the CA of different lepidopterans is still unknown [38, 39].

In representatives of other insect orders, allatostatic activity has been demonstrated for the likewise pleiotropic B-type or C-type allatostatins [35, 40]. The designation of these three peptide groups as "allatostatins" appears unfortunate, since they are structurally and genetically unrelated and allatostatic properties are absent in most insect species. A more general role and probably a prior function of allatostatins A, B and C is the inhibition of muscle contractions [35, 40].

AstA peptides were also found to be widespread within the nervous system (including the stomatogastric nervous system and neurohemal sites) of crustaceans, in which they function as inhibitory neuromodulators or myomodulators to regulate motor activity of the foregut and heart [see 41 and references therein] as well as the hindgut [42]. Moreover, application of Dippu-allatostatins onto skeletal muscles of *Idotea* and *Eriphia* resulted in inhibitory modulation of muscle fiber activation [43]. Kwok et al. [44] found that Dippu-allatostatins can stimulate the production and release of methyl farnesoate from mandibular organs (the crustacean homolog of the insect CA) of a crayfish *in vitro*. Methyl farnesoate is a hormone that is structurally very similar to the insect juvenile hormones (especially JH III) and is thought to be involved in the regulation of molting, reproduction, development and other processes in crustaceans [45]. Evidence for the expression of *AstA* not only in the nervous system but also in the gut of crustaceans was found in the prawn [46].

The occurrence of allatostatin A-like molecules in invertebrate species outside of insects or crustaceans was also demonstrated, mostly as immunoreactivity in neurons using antisera raised against insect AstA peptides [e.g. 47–53]. Additionally, gene sequences encoding putative AstA-like peptides were found in tardigrades [31], chelicerates [54], as well as *C. elegans* and other nematodes [55].

4.4.2 Corpora allata-unrelated functions of AstA in insects

AstA peptides have been found in central interneurons of a variety of insects, but also in processes of central or stomatogastric neurons that run to peripheral targets ([40], see examples below). Gut innervations are common, but extend over the gut to varying degrees in different insect orders. AstA was also detected in enteroendocrine cells (EECs) of many insect species [40], suggesting important and general functions for the peptides regarding metabolism.

In a range of insects, AstA peptides were shown to act myoinhibitory, e.g. in cockroaches, where they modulate gut peristalsis. In studies on *D. punctata*, AstA inhibited spontaneous or proctolin-induced contractions of the hindgut [56, 57] and midgut [58]. In *L. maderae* reduction of foregut but not hindgut contractions was observed [59], while AstA peptides inhibited hindgut but not foregut motility in *B. germanica* [60].

In the hemipteran *R. prolixus* AstA reduced contractions of the anterior midgut and hindgut [61, 62]. Moreover, AstA diminished proctolin-induced contractions of the fore- and hindgut, as well as

spontaneous contractions and the basal tension of the midgut in the locust *L. migratoria* [63]. In addition to a direct effect on muscles, AstA inhibited *L. migratoria* foregut motility via a second pathway involving the ventricular ganglion, which apparently contains a central pattern generator for the regulation of foregut contractions. AstA was able to modulate the activity pattern of nerves emanating from the ventral ganglion and to reduce the frequency and amplitude of the neurogenic foregut contractions [63].

Experiments on guts of moth larvae showed that AstA peptides dose-dependently reduce peristalsis of the foregut, which is innervated by AstA-immunoreactive axons leaving the frontal ganglion through the recurrent nerve [64–67]. Interestingly, AstC (which like AstA acts as foregut myoinhibitor) and/or allatotropin (which, on the contrary, stimulates foregut peristalsis) have been found in the larval frontal ganglion as well [65, 66, 68, 69]. The co-localization of these antagonistically acting peptides within the same axons suggests the existence of unknown, complex regulatory mechanisms for the control of foregut muscle activity ([67, 68], [for a review see 39]).

Gut innervation by AstA neurons in the blowfly *C. vomitoria* is restricted to the hindgut [70]. In this species, AstA peptides reduce spontaneous contractions of the ileum (the anterior portion of the hindgut) in a manner dependent on peptide dose and identity, and also on the vitellogenic state of female blowflies. Peristalsis of other gut regions of this species was not affected by the application of AstA peptides [70].

The myoinhibitory effect of AstA in insects is not restricted to the gut, but has also been demonstrated for other organs associated with musculature, e.g. the *S. gregaria* oviduct [71], as well as the dorsal vessel in *B. germanica* [72] and *R. prolixus* [61, 62].

Several studies have linked AstA function to metabolism and feeding. Matsui et al. [73] found that pars intercerebralis-ablated *P. americana* kept in constant darkness showed a strong increase in food intake and body size. Under these conditions the animals were also arrhythmic, though overall locomotor activity was unaltered [73], and the number of AstA-producing EECs in the midgut was increased [74]. Moreover, AstA peptides stimulated the secretion of carbohydrate- and protein-metabolizing enzymes in the midgut of several cockroach species *in vitro* [58, 60, 75] and, if injected into *B. germanica*, reduced food intake [60]. In *G. bimaculatus* systemic downregulation of the *AstA* mRNA level via injection of dsRNA influenced food intake and transit through the gut, as well as the activity of digestive enzymes in midgut tissue [76]. Furthermore, AstA inhibited vitellogenin production and release from the fat body in *B. germanica* [77, 78].

A role of AstA in the regulation of energy homeostasis was established for *L. migratoria*, in which it increased the cAMP content and the secretory activity of the glandular part of the corpora cardiaca, which produces AHK [36]. Recently, also for *Drosophila* evidence has been found that AstA is involved in the control of AKH, insulin and other important regulators of energy metabolism (e.g. [79], see below).

4.4.3 AstA in *Drosophila melanogaster*

The genes for two G protein-coupled receptors for AstA peptides (DAR-1/AlstR and DAR-2) were cloned from *Drosophila* and their ligands identified by heterologous expression [80–84]. DAR-1 and DAR-2 show 47% overall amino acid sequence identity [82] and are structurally related to the mammalian somatostatin/galanin/opioid receptor family, with highest amino acid sequence identity to the galanin receptor [80–82]. DAR-1 couples mainly to $G_{i/o}$-type G proteins, whereas DAR-2 was shown to interact with $G_{i/o}$ and other types of G proteins [80, 84].

DAR-1 expression was detected by RT-PCR in larvae, pupae, and adult heads as well as adult bodies (i.e. thorax and abdomen), but seemed to be absent in embryos [80]. Northern blot studies showed that *DAR-2* mRNA is detectable from the embryo up to the adult stage [83]. *DAR-2* expression in the body region of adult flies is much stronger than in the head, and in 3rd instar larvae strong expression was detected in the gut, but only weak expression in the brain.

Four *Drosophila* AstA peptides have been identified [85] and their structures were verified by mass spectrometry [14–16, 80, 86]:

AstA-1: VERYAFGL-amide

AstA-2 (=AstA-2$^{14-21}$): LPVYNFGL-amide

AstA-3: SRPYSFGL-amide

AstA-4: TTRPQPFNFGL-amide

Another peptide (AYMYTNGGPGM) encoded by the *AstA* gene, designated as AstA-2$^{1-11}$, has also been detected [14, 86], but probably represents a non-bioactive side product of precursor processing since it lacks the (Y/F)XFGL-amide motif.

4.4.4 Distribution of AstA peptides in *Drosophila*

AstA-immunoreactive neurons have been found in the brain and ventral/thoracico-abdominal ganglion of larval [87, 88] and adult *Drosophila*, although the number of immunopositive cells is higher in adults ([87, 89], Fig. 4.1). The projections of three pairs of DLAa (dorsolateral abdominal a) neurons leave the CNS through the last abdominal nerves in larvae or the median abdominal nerve in adults. The processes of the DLAa cells innervate the larval hindgut or, in adults, the hindgut and posterior midgut. In addition to the central neurons, two pairs of peripheral AstA-producing cells associated with thoracic neuromeres exist in both stages [87]. Further details are given in section 5.3.

Aside from cells of the nervous system, EECs in the posterior part of the larval and adult posterior midgut are a further source of AstA peptides in *Drosophila* [87, 90, 91].

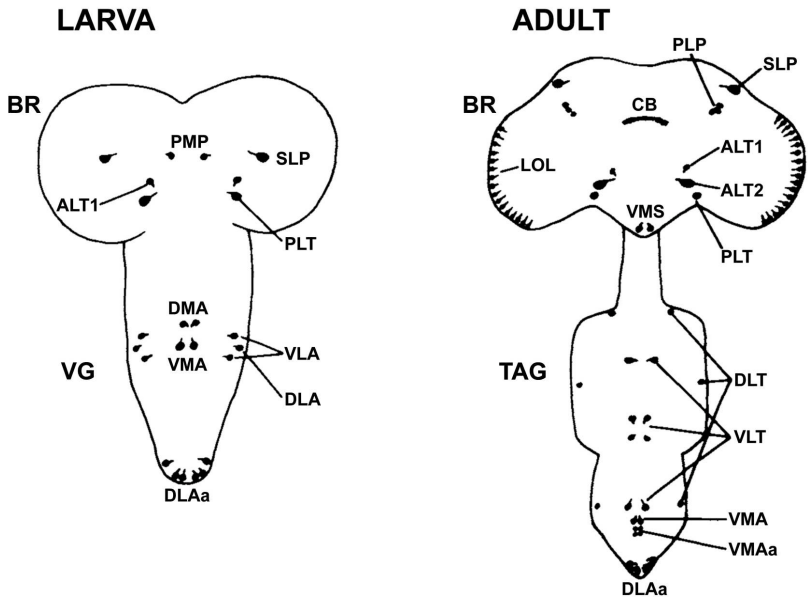

Figure 4.1: Schematic representation of cell bodies showing *Diploptera* allatostatin-like (AstA) immunoreactivity in the *Drosophila* CNS (adopted from [87]). Cells and cell groups are designated according to the location of their somata within the CNS (first letter: A=anterior, D=dorsal, L=lateral, P=posterior, S=superior, V=ventral; second letter: L=lateral, M=medial, O=optic; third letter: A=abdominal, L=lobe, P=protocerebrum, S=subesophageal, T=tritocerebrum (for PLT and ALT) or thoracic (for DLT and VLT), [87]). The fan-shaped part of the central body (CB), which is densely innervated by AstA-immunoreactive projections, is also shown. BR brain, VG ventral ganglion, TAG thoracico-abdominal ganglion.

4.4.5 Function of AstA in *Drosophila*

In *Drosophila* larvae, ubiquitous RNAi to inhibit *DAR-1* or *AstA* expression caused shortened foraging path lengths in the presence, but not in the absence of food, as well as a reduction of *foraging* mRNA levels, characteristics known from the "sitter" phenotype [92]. Two different alleles naturally exist for the *foraging* (= *dg2*) gene, which codes for a cGMP-dependent protein kinase (PKG). The for^{S} allele, which is connected to a lower *foraging* mRNA level and thus lower PKG activity, causes a "sitter" food-search phenotype, whereas the for^{R} allele leads to a higher level of *foraging* mRNA, higher PKG activity and a "rover" foraging behavior [93]. In the presence of food, rover larvae show longer path lengths and consume less than sitter larvae, while, under conditions of food shortage, path length and food consumption are similar for rovers and sitters [94, 95]. Independent of food abundance, rover larvae absorb glucose more efficiently [95].

In a study on adults, Hergarden et al. found that activation of AstA cells via *AstA-Gal4*-driven NaChBac significantly reduced feeding in starved and unstarved flies [96]. The effect was more distinct following food deprivation and under conditions of low food accessibility. AstA cell activation also inhibited the increase of responsiveness to glucose that is seen in controls upon starvation, although the ability of the flies to perceive glucose seemed unaffected. The manipulation also did not alter locomotor activity, energy reserves, starvation resistance or food transit through the gut. Injection of AstA peptides into living flies had no impact on feeding-related phenotypes [96], suggesting that AstA peptides do not function in a hormonal fashion to regulate feeding behavior.

Further functional and anatomical studies reinforced a role for AstA in the regulation of nutritional homeostasis. The DAR-2 receptor is expressed in the AKH cells of the corpora cardiaca, the IPCs

("insulin-producing cells", which produce DILP2, 3 and 5) and in corazonin-producing neurons [79, 97, 98]. AKH and DILPs are important regulators of energy metabolism, energy storage and starvation resistance [1], and also corazonin has been implicated in stress response and energy metabolism [97, 99, 100]. AstA seems to be a positive regulator of IPC, AKH and corazonin cell signaling, since knockdown of *DAR-2* transcript levels in these cells can mimic effects associated with reduced DILP, AKH or corazonin signaling, respectively [79, 98]. AstA signaling itself responds to the uptake of food in a nutrient type-depending manner. Whole-fly *AstA* and *DAR-2* mRNA levels were found to decrease as a consequence of dietary restriction and re-increase following intake of nutritious food [79]. After refeeding with protein-rich food, *AstA* and *DAR-2* mRNA levels were similar to those of control flies that had been fed with carbohydrate-rich food continuously, whereas refeeding with carbohydrate-rich food resulted in a much stronger increase of the two transcripts [79].

4.5 References

1. Nässel DR, Winther ÅME (2010) Drosophila neuropeptides in regulation of physiology and behavior. Prog Neurobiol 92:42–104. doi: 10.1016/j.pneurobio.2010.04.010

2. Fricker LD (2012) Neuropeptides and Other Bioactive Peptides: From Discovery to Function. 1:1–122. doi: 10.4199/C00058ED1V01Y201205NPE003

3. Watanabe H, Fujisawa T, Holstein TW (2009) Cnidarians and the evolutionary origin of the nervous system. Dev Growth Differ 51:167–183. doi: 10.1111/j.1440-169X.2009.01103.x

4. Grimmelikhuijzen CJP, Hauser F (2012) Mini-review: The evolution of neuropeptide signaling. Regul Pept 177, Supplement:S6–S9. doi: 10.1016/j.regpep.2012.05.001

5. Caers J, Verlinden H, Zels S, et al. (2012) More than two decades of research on insect neuropeptide GPCRs: an overview. Front Endocrinol 3:151. doi: 10.3389/fendo.2012.00151

6. Adams MD, Celniker SE, Holt RA, et al. (2000) The genome sequence of Drosophila melanogaster. Science 287:2185–2195.

7. http://www.ncbi.nlm.nih.gov/genbank/

8. C. elegans Sequencing Consortium (1998) Genome sequence of the nematode C. elegans: a platform for investigating biology. Science 282:2012–2018.

9. Ashburner M, Bergman CM (2005) Drosophila melanogaster: A case study of a model genomic sequence and its consequences. Genome Res 15:1661–1667. doi: 10.1101/gr.3726705

10. Boerjan B, Cardoen D, Verdonck R, et al. (2012) Insect omics research coming of age. Can J Zool 90:440–455. doi: 10.1139/z2012-010

11. http://arthropodgenomes.org/wiki/i5K

12. Robinson GE, Hackett KJ, Purcell-Miramontes M, et al. (2011) Creating a Buzz About Insect Genomes. Science 331:1386–1386. doi: 10.1126/science.331.6023.1386

13. Schoofs L, Baggerman G (2003) Peptidomics in Drosophila melanogaster. Brief Funct Genomic Proteomic 2:114–120.

14. Baggerman G, Cerstiaens A, De Loof A, Schoofs L (2002) Peptidomics of the larval Drosophila melanogaster central nervous system. J Biol Chem 277:40368–40374. doi: 10.1074/jbc.M206257200

15. Baggerman G, Boonen K, Verleyen P, et al. (2005) Peptidomic analysis of the larval Drosophila melanogaster central nervous system by two-dimensional capillary liquid chromatography quadrupole time-of-flight mass spectrometry. J Mass Spectrom JMS 40:250–260. doi: 10.1002/jms.744

16. Yew JY, Wang Y, Barteneva N, et al. (2009) Analysis of neuropeptide expression and localization in adult drosophila melanogaster central nervous system by affinity cell-capture mass spectrometry. J Proteome Res 8:1271–1284. doi: 10.1021/pr800601x

17. Predel R, Wegener C, Russell WK, et al. (2004) Peptidomics of CNS-associated neurohemal systems of adult Drosophila melanogaster: a mass spectrometric survey of peptides from individual flies. J Comp Neurol 474:379–392. doi: 10.1002/cne.20145

18. Wegener C, Reinl T, Jänsch L, Predel R (2006) Direct mass spectrometric peptide profiling and fragmentation of larval peptide hormone release sites in Drosophila melanogaster reveals tagma-specific peptide expression and differential processing. J Neurochem 96:1362–1374. doi: 10.1111/j.1471-4159.2005.03634.x

19. Jiang H, Lkhagva A, Daubnerová I, et al. (2013) Natalisin, a tachykinin-like signaling system, regulates sexual activity and fecundity in insects. Proc Natl Acad Sci U S A 110:E3526–3534. doi: 10.1073/pnas.1310676110

20. Predel R, Neupert S, Garczynski SF, et al. (2010) Neuropeptidomics of the mosquito Aedes aegypti. J Proteome Res 9:2006–2015. doi: 10.1021/pr901187p

21. Hummon AB, Richmond TA, Verleyen P, et al. (2006) From the genome to the proteome: uncovering peptides in the Apis brain. Science 314:647–649. doi: 10.1126/science.1124128

22. Audsley N, Weaver RJ (2006) Analysis of peptides in the brain and corpora cardiaca-corpora allata of the honey bee, Apis mellifera using MALDI-TOF mass spectrometry. Peptides 27:512–520. doi: 10.1016/j.peptides.2005.08.022

23. Brockmann A, Annangudi SP, Richmond TA, et al. (2009) Quantitative peptidomics reveal brain peptide signatures of behavior. Proc Natl Acad Sci U S A 106:2383–2388. doi: 10.1073/pnas.0813021106

24. Boerjan B, Cardoen D, Bogaerts A, et al. (2010) Mass spectrometric profiling of (neuro)-peptides in the worker honeybee, Apis mellifera. Neuropharmacology 58:248–258. doi: 10.1016/j.neuropharm.2009.06.026

25. Li B, Predel R, Neupert S, et al. (2008) Genomics, transcriptomics, and peptidomics of neuropeptides and protein hormones in the red flour beetle Tribolium castaneum. Genome Res 18:113–122. doi: 10.1101/gr.6714008

26. Binzer M, Heuer CM, Kollmann M, et al. (2013) The neuropeptidome of Tribolium castaneum antennal lobes and mushroom bodies. J Comp Neurol [Accepted Article]. doi: 10.1002/cne.23399

27. Pratt GE, Farnsworth DE, Siegel NR, et al. (1989) Identification of an allatostatin from adult Diploptera punctata. Biochem Biophys Res Commun 163:1243–1247. doi: 10.1016/0006-291X(89)91111-X

28. Woodhead AP, Stay B, Seidel SL, et al. (1989) Primary structure of four allatostatins: neuropeptide inhibitors of juvenile hormone synthesis. Proc Natl Acad Sci U S A 86:5997–6001.

29. Pratt GE, Farnsworth DE, Fok KF, et al. (1991) Identity of a second type of allatostatin from cockroach brains: an octadecapeptide amide with a tyrosine-rich address sequence. Proc Natl Acad Sci U S A 88:2412–2416.

30. Woodhead AP, Khan MA, Stay B, Tobe SS (1994) Two new allatostatins from the brains of Diploptera punctata. Insect Biochem Mol Biol 24:257–263. doi: 10.1016/0965-1748(94)90005-1

31. Bendena WG, Donly BC, Tobe SS (1999) Allatostatins: A Growing Family of Neuropeptides with Structural and Functional Diversity. Ann N Y Acad Sci 897:311–329. doi: 10.1111/j.1749-6632.1999.tb07902.x

32. Hult EF, Weadick CJ, Chang BSW, Tobe SS (2008) Reconstruction of ancestral FGLamide-type insect allatostatins: A novel approach to the study of allatostatin function and evolution. J Insect Physiol 54:959–968. doi: 10.1016/j.jinsphys.2008.04.007

33. Nachman RJ, Garside CS, Tobe SS (1999) Hemolymph and tissue-bound peptidase-resistant analogs of the insect allatostatins. Peptides 20:23–29. doi: 10.1016/S0196-9781(98)00149-1

34. Kai Z, Xie Y, Huang J, et al. (2011) Peptidomimetics in the Discovery of New Insect Growth Regulators: Studies on the Structure−Activity Relationships of the Core Pentapeptide Region of Allatostatins. J Agric Food Chem 59:2478–2485. doi: 10.1021/jf200085d

35. Stay B, Tobe SS (2007) The Role of Allatostatins in Juvenile Hormone Synthesis in Insects and Crustaceans. Annu Rev Entomol 52:277–299. doi: 10.1146/annurev.ento.51.110104.151050

36. Clark L, Lange AB, Zhang JR, Tobe SS (2008) The roles of Dippu-allatostatin in the modulation of hormone release in Locusta migratoria. J Insect Physiol 54:949–958. doi: 10.1016/j.jinsphys.2008.03.007

37. Weaver RJ, Audsley N (2009) Neuropeptide regulators of juvenile hormone synthesis: structures, functions, distribution, and unanswered questions. Ann N Y Acad Sci 1163:316–329. doi: 10.1111/j.1749-6632.2009.04459.x

38. Audsley N, Duve H, Thorpe A, Weaver RJ (2000) Morphological and physiological comparisons of two types of allatostatin in the brain and retrocerebral complex of the tomato moth, Lacanobia oleracea (Lepidoptera: Noctuidae). J Comp Neurol 424:37–46. doi: 10.1002/1096-9861(20000814)424:1<37::AID-CNE3>3.0.CO;2-9

39. Audsley N, Matthews HJ, Price NR, Weaver RJ (2008) Allatoregulatory peptides in Lepidoptera, structures, distribution and functions. J Insect Physiol 54:969–980. doi: 10.1016/j.jinsphys.2008.01.012

40. Tobe SS, Bendena WG (2006) Chapter 31 - Allatostatins in the Insects. In: Kastin AJ (ed) Handb. Biol. Act. Pept., 1st ed. Academic Press, Burlington, pp 201–206

41. Christie AE, Stemmler EA, Dickinson PS (2010) Crustacean neuropeptides. Cell Mol Life Sci CMLS 67:4135–4169. doi: 10.1007/s00018-010-0482-8

42. Dircksen H, Skiebe P, Abel B, et al. (1999) Structure, distribution, and biological activity of novel members of the allatostatin family in the crayfish Orconectes limosus. Peptides 20:695–712. doi: 10.1016/S0196-9781(99)00052-2

43. Kreissl S, Weiss T, Djokaj S, et al. (1999) Allatostatin modulates skeletal muscle performance in crustaceans through pre- and postsynaptic effects. Eur J Neurosci 11:2519–2530.

44. Kwok R, Rui Zhang J, Tobe SS (2005) Regulation of methyl farnesoate production by mandibular organs in the crayfish, Procambarus clarkii: a possible role for allatostatins. J Insect Physiol 51:367–378. doi: 10.3201/eid1105.040755

45. Nagaraju GPC (2007) Is methyl farnesoate a crustacean hormone? Aquaculture 272:39–54. doi: 10.1016/j.aquaculture.2007.05.014

46. Yin G-L, Yang J-S, Cao J-X, Yang W-J (2006) Molecular cloning and characterization of FGLamide allatostatin gene from the prawn, Macrobrachium rosenbergii. Peptides 27:1241–1250. doi: 10.1016/j.peptides.2005.11.015

47. Rudolph PH, Stay B (1997) Cockroach allatostatin-like immunoreactivity in the central nervous system of the freshwater snails Bulinus globosus (Planorbidae) and Stagnicola elodes (Lymnaeidae). Gen Comp Endocrinol 106:241–250. doi: 10.1006/gcen.1996.6871

48. Smart D, Johnston CF, Curry WJ, et al. (1994) Peptides related to the Diploptera punctata allatostatins in nonarthropod invertebrates: an immunocytochemical survey. J Comp Neurol 347:426–432. doi: 10.1002/cne.903470308

49. Smart D, Johnston CF, Maule AG, et al. (1995) Localization of Diploptera punctata allatostatin-like immunoreactivity in helminths: an immunocytochemical study. Parasitology 110:87–96.

50. Zhu XX, Oliver JH Jr (2001) Cockroach allatostatin-like immunoreactivity in the synganglion of the American dog tick Dermacentor variabilis (Acari: Ixodidae). Exp Appl Acarol 25:1005–1013.

51. Mousley A, Moffett CL, Duve H, et al. (2005) Expression and bioactivity of allatostatin-like neuropeptides in helminths. Int J Parasitol 35:1557–1567. doi: 10.1016/j.ijpara.2005.08.002

52. Simo L, Slovak M, Park Y, Zitnan D (2009) Identification of a complex peptidergic neuroendocrine network in the hard tick, Rhipicephalus appendiculatus. Cell Tissue Res 335:639–655. doi: 10.1007/s00441-008-0731-4

53. Loesel R, Seyfarth E-A, Bräunig P, Agricola H-J (2011) Neuroarchitecture of the arcuate body in the brain of the spider Cupiennius salei (Araneae, Chelicerata) revealed by allatostatin-, proctolin-, and CCAP-immunocytochemistry and its evolutionary implications. Arthropod Struct Dev 40:210–220. doi: 10.1016/j.asd.2011.01.002

54. Donohue KV, Khalil SMS, Ross E, et al. (2010) Neuropeptide signaling sequences identified by pyrosequencing of the American dog tick synganglion transcriptome during blood feeding and reproduction. Insect Biochem Mol Biol 40:79–90. doi: 10.1016/j.ibmb.2009.12.014

55. Nathoo AN, Moeller RA, Westlund BA, Hart AC (2001) Identification of neuropeptide-like protein gene families in Caenorhabditis elegans and other species. Proc Natl Acad Sci 98:14000–14005. doi: 10.1073/pnas.241231298

56. Lange AB, Chan KK, Stay B (1993) Effect of allatostatin and proctolin on antennal pulsatile organ and hindgut muscle in the cockroach, Diploptera punctata. Arch Insect Biochem Physiol 24:79–92. doi: 10.1002/arch.940240203

57. Lange AB, Bendena WG, Tobe SS (1995) The effect of the thirteen Dip-allatostatins on myogenic and induced contractions of the cockroach (Diploptera punctata) hindgut. J Insect Physiol 41:581–588. doi: 10.1016/0022-1910(95)00008-I

58. Fusé M, Zhang JR, Partridge E, et al. (1999) Effects of an allatostatin and a myosuppressin on midgut carbohydrate enzyme activity in the cockroach Diploptera punctata. Peptides 20:1285–1293.

59. Duve H, Wren P, Thorpe A (1995) Innervation of the foregut of the cockroach Leucophaea maderae and inhibition of spontaneous contractile activity by callatostatin neuropeptides. Physiol Entomol 20:33–44. doi: 10.1111/j.1365-3032.1995.tb00798.x

60. Aguilar R, Maestro JL, Vilaplana L, et al. (2003) Allatostatin gene expression in brain and midgut, and activity of synthetic allatostatins on feeding-related processes in the cockroach Blattella germanica. Regul Pept 115:171–177. doi: 10.1016/S0167-0115(03)00165-4

61. Sarkar NR., Tobe SS, Orchard I (2003) The distribution and effects of Dippu-allatostatin-like peptides in the blood-feeding bug, Rhodnius prolixus. Peptides 24:1553–1562. doi: 10.1016/j.peptides.2003.07.015

62. Zandawala M, Lytvyn Y, Taiakina D, Orchard I (2012) Cloning of the cDNA, localization, and physiological effects of FGLamide-related allatostatins in the blood-gorging bug, Rhodnius prolixus. Insect Biochem Mol Biol 42:10–21. doi: 10.1016/j.ibmb.2011.10.002

63. Robertson L, Rodriguez EP, Lange AB (2012) The neural and peptidergic control of gut contraction in Locusta migratoria: the effect of an FGLa/AST. J Exp Biol 215:3394–3402. doi: 10.1242/jeb.073189

64. Duve H, Johnsen AH, Maestro JL, et al. (1997) Identification, tissue localisation and physiological effect in vitro of a neuroendocrine peptide identical to a dipteran Leu-callatostatin in the codling moth Cydia pomonella (Tortricidae: Lepidoptera). Cell Tissue Res 289:73–83.

65. Duve H, East PD, Thorpe A (1999) Regulation of lepidopteran foregut movement by allatostatins and allatotropin from the frontal ganglion. J Comp Neurol 413:405–416.

66. Duve H, Audsley N, Weaver RJ, Thorpe A (2000) Triple co-localisation of two types of allatostatin and an allatotropin in the frontal ganglion of the lepidopteran Lacanobia oleracea (Noctuidae): innervation and action on the foregut. Cell Tissue Res 300:153–163.

67. Matthews HJ, Audsley N, Weaver RJ (2007) Interactions between allatostatins and allatotropin on spontaneous contractions of the foregut of larval Lacanobia oleracea. J Insect Physiol 53:75–83. doi: 10.1016/j.jinsphys.2006.10.007

68. Duve H, Thorpe A (2003) Neuropeptide co-localisation in the lepidopteran frontal ganglion studied by confocal laser scanning microscopy. Cell Tissue Res 311:79–89. doi: 10.1007/s00441-002-0648-2

69. Audsley N, Matthews J, Weaver RJ (2005) Neuropeptides associated with the frontal ganglion of larval Lepidoptera. Peptides 26:11–21. doi: 10.1016/j.peptides.2004.10.011

70. Duve H, Thorpe A (1994) Distribution and functional significance of Leu-callatostatins in the blowfly Calliphora vomitoria. Cell Tissue Res 276:367–379. doi: 10.1007/BF00306122

71. Veelaert D, Devreese B, Schoofs L, et al. (1996) Isolation and characterization of eight myoinhibiting peptides from the desert locust, Schistocerca gregaria: new members of the cockroach allatostatin family. Mol Cell Endocrinol 122:183–190.

72. Vilaplana L, Maestro JL, Piulachs M-D, Bellés X (1999) Modulation of cardiac rhythm by allatostatins in the cockroach Blattella germanica (L.) (Dictyoptera, Blattellidae). J Insect Physiol 45:1057–1064.

73. Matsui T, Matsumoto T, Ichihara N, et al. (2009) The pars intercerebralis as a modulator of locomotor rhythms and feeding in the American cockroach, Periplaneta americana. Physiol Behav 96:548–556. doi: 10.1016/j.physbeh.2008.12.009

74. Matsui T, Sakai T, Satake H, Takeda M (2013) The pars intercerebralis affects digestive activities of the American cockroach, Periplaneta Americana, via crustacean cardioactive peptide and allatostatin-A. J Insect Physiol 59:33–37. doi: 10.1016/j.jinsphys.2012.06.010

75. Sakai T, Satake H, Takeda M (2006) Nutrient-induced alpha-amylase and protease activity is regulated by crustacean cardioactive peptide (CCAP) in the cockroach midgut. Peptides 27:2157–2164. doi: 10.1016/j.peptides.2006.04.009

76. Meyering-Vos M, Woodring J (2008) A-type allatostatins and sulfakinins as satiety effectors in the Mediterranean field cricket Gryllus bimaculatus. Mitteilungen Dtsch Ges Für Allg Angew Entomol 16:409–412.

77. Martín D, Piulachs MD, Bellés X (1996) Inhibition of vitellogenin production by allatostatin in the German cockroach. Mol Cell Endocrinol 121:191–196.

78. Martín D, Piulachs M-D, Bellés X (1998) Allatostatin Inhibits Vitellogenin Release in a Cockroach. Ann N Y Acad Sci 839:341–342. doi: 10.1111/j.1749-6632.1998.tb10788.x

79. Hentze JL, Carlsson MA, Andersen O, et al. (SUBMITTED) The neuropeptide allatostatin A coordinates feeding decisions and metabolism in Drosophila.

80. Birgül N, Weise C, Kreienkamp HJ, Richter D (1999) Reverse physiology in Drosophila: identification of a novel allatostatin-like neuropeptide and its cognate receptor structurally related to the mammalian somatostatin/galanin/opioid receptor family. EMBO J 18:5892–5900. doi: 10.1093/emboj/18.21.5892

81. Lenz C, Søndergaard L, Grimmelikhuijzen CJ (2000) Molecular cloning and genomic organization of a novel receptor from Drosophila melanogaster structurally related to mammalian galanin receptors. Biochem Biophys Res Commun 269:91–96. doi: 10.1006/bbrc.2000.2251

82. Lenz C, Williamson M, Grimmelikhuijzen CJ (2000) Molecular cloning and genomic organization of a second probable allatostatin receptor from Drosophila melanogaster. Biochem Biophys Res Commun 273:571–577. doi: 10.1006/bbrc.2000.2964

83. Lenz C, Williamson M, Hansen GN, Grimmelikhuijzen CJ (2001) Identification of four Drosophila allatostatins as the cognate ligands for the Drosophila orphan receptor DAR-2. Biochem Biophys Res Commun 286:1117–1122. doi: 10.1006/bbrc.2001.5475

84. Larsen MJ, Burton KJ, Zantello MR, et al. (2001) Type A allatostatins from Drosophila melanogaster and Diplotera puncata activate two Drosophila allatostatin receptors, DAR-1 and DAR-2, expressed in CHO cells. Biochem Biophys Res Commun 286:895–901. doi: 10.1006/bbrc.2001.5476

85. Lenz C, Williamson M, Grimmelikhuijzen CJ (2000) Molecular cloning and genomic organization of an allatostatin preprohormone from Drosophila melanogaster. Biochem Biophys Res Commun 273:1126–1131. doi: 10.1006/bbrc.2000.3062

86. Reiher W, Shirras C, Kahnt J, et al. (2011) Peptidomics and peptide hormone processing in the Drosophila midgut. J Proteome Res 10:1881–1892. doi: 10.1021/pr101116g

87. Yoon JG, Stay B (1995) Immunocytochemical localization of Diploptera punctata allatostatin-like peptide in Drosophila melanogaster. J Comp Neurol 363:475–488. doi: 10.1002/cne.903630310

88. Santos JG, Vömel M, Struck R, et al. (2007) Neuroarchitecture of Peptidergic Systems in the Larval Ventral Ganglion of Drosophila melanogaster. PLoS ONE 2:e695. doi: 10.1371/journal.pone.0000695

89. Carlsson MA, Diesner M, Schachtner J, Nässel DR (2010) Multiple neuropeptides in the Drosophila antennal lobe suggest complex modulatory circuits. J Comp Neurol 518:3359–3380. doi: 10.1002/cne.22405

90. Veenstra JA, Agricola H-J, Sellami A (2008) Regulatory peptides in fruit fly midgut. Cell Tissue Res 334:499–516. doi: 10.1007/s00441-008-0708-3

91. Veenstra JA (2009) Peptidergic paracrine and endocrine cells in the midgut of the fruit fly maggot. Cell Tissue Res 336:309–323. doi: 10.1007/s00441-009-0769-y

92. Wang C, Chin-Sang I, Bendena WG (2012) The FGLamide-allatostatins influence foraging behavior in Drosophila melanogaster. PloS One 7:e36059. doi: 10.1371/journal.pone.0036059

93. Osborne KA, Robichon A, Burgess E, et al. (1997) Natural Behavior Polymorphism Due to a cGMP-Dependent Protein Kinase of Drosophila. Science 277:834–836. doi: 10.1126/science.277.5327.834

94. Pereira HS, Sokolowski MB (1993) Mutations in the larval foraging gene affect adult locomotory behavior after feeding in Drosophila melanogaster. Proc Natl Acad Sci U S A 90:5044–5046.

95. Kaun KR, Riedl CAL, Chakaborty-Chatterjee M, et al. (2007) Natural variation in food acquisition mediated via a Drosophila cGMP-dependent protein kinase. J Exp Biol 210:3547–3558. doi: 10.1242/jeb.006924

96. Hergarden AC, Tayler TD, Anderson DJ (2012) Allatostatin-A neurons inhibit feeding behavior in adult Drosophila. Proc Natl Acad Sci U S A 109:3967–3972. doi: 10.1073/pnas.1200778109

97. Veenstra JA (2009) Does corazonin signal nutritional stress in insects? Insect Biochem Mol Biol 39:755–762. doi: 10.1016/j.ibmb.2009.09.008

98. Hentze JL (2013) Regulation of Metabolism and Steroid Production in Insects - A study of Allatostatin A and ecdysone. Dissertation (Ph.D.), Roskilde University

99. Zhao Y, Bretz CA, Hawksworth SA, et al. (2010) Corazonin Neurons Function in Sexually Dimorphic Circuitry That Shape Behavioral Responses to Stress in Drosophila. PLoS ONE 5:e9141. doi: 10.1371/journal.pone.0009141

100. Kapan N, Lushchak OV, Luo J, Nässel DR (2012) Identified peptidergic neurons in the Drosophila brain regulate insulin-producing cells, stress responses and metabolism by coexpressed short neuropeptide F and corazonin. Cell Mol Life Sci 69:4051–4066. doi: 10.1007/s00018-012-1097-z

5 Publications / Manuscripts

5.1 Peptidomics and peptide hormone processing in the *Drosophila* midgut.

W. Reiher, C. Shirras, J. Kahnt, S. Baumeister, R. E. Isaac and C. Wegener

Journal of Proteome Research 10: 1881–1892.

DOI: 10.1021/pr101116g

Published: January 10, 2011

Journal of proteome research

ARTICLE

pubs.acs.org/jpr

Peptidomics and Peptide Hormone Processing in the *Drosophila* Midgut

Wencke Reiher,[†] Christine Shirras,[‡] Jörg Kahnt,[§] Stefan Baumeister,[∥] R. Elwyn Isaac,[⊥] and Christian Wegener*[,†]

[†]Department of Biology, Animal Physiology, Philipps-University Marburg, Marburg, Germany

[‡]School of Health and Medicine, Division of Biomedical and Life Sciences, University of Lancaster, Lancaster, U.K.

[§]Max-Planck Institute of Terrestrial Microbiology, Marburg, Germany

[∥]Department of Biology, Proteomic Facility, Philipps-University Marburg, Marburg, Germany

[⊥]Institute of Integrative and Comparative Biology, University of Leeds, Leeds, U.K.

ABSTRACT: Peptide hormones are key messengers in the signaling network between the nervous system, endocrine glands, energy stores and the gastrointestinal tract that regulates feeding and metabolism. Studies on the *Drosophila* nervous system have uncovered parallels and homologies in homeostatic peptidergic signaling between fruit flies and vertebrates. Yet, the role of enteroendocrine peptides in the regulation of feeding and metabolism has not been explored, with research hampered by the unknown identity of peptides produced by the fly's intestinal tract. We performed a peptidomic LC/MS analysis of the fruit fly midgut containing the enteroendocrine cells. By MS/MS fragmentation, we found 24 peptides from 9 different preprohormones in midgut extracts, including MIP-4 and 2 forms of AST-C. DH_{31}, CCHamide1 and CCHamide2 are biochemically characterized for the first time. All enteroendocrine peptides represent brain−gut peptides, and apparently are processed by *Drosophila* prohormone convertase 2 (AMON) as suggested by impaired peptide detectability in *amon* mutants and localization of *amon*-driven GFP to enteroendocrine cells. Because of its genetic amenability and peptide diversity, *Drosophila* provides a good model system to study peptide signaling. The identification of enteroendocrine peptides in the fruit fly provides a platform to address functions of gut peptide hormones in the regulation of feeding and metabolism.

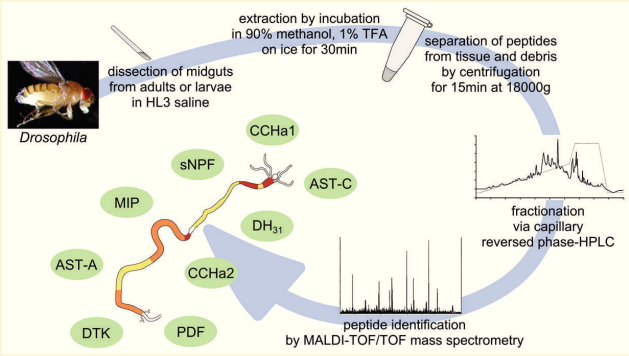

KEYWORDS: MALDI-TOF mass spectrometry, prohormone convertase, peptide hormone, insect, peptide processing, metabolic signaling, feeding, gastrointestinal system

INTRODUCTION

Mammals possess a complex signaling network between the brain, endocrine glands, gut and adipocytes that regulates metabolism and feeding. Because of its implication in obesity-related diseases, this signaling network is receiving increased attention. Peptide hormones play a key role within this network.[1−3] While leptin from adipocytes, insulin from pancreas, and neuropeptide Y (NPY)/Agouti-related peptide (AgRP) as well as αMSH/CART from the hypothalamus are major signals, there are many more peptides from various sources involved in the regulation of metabolism and feeding.[4] Among them, the gastrointestinal peptides form a group that is particularly important for appetite and satiety signaling as well as energy balance.[5−7] These peptide hormones originate from enteroendocrine cells and do not only regulate the secretion of digestive enzymes but also modulate the motility of the gastrointestinal tract. In addition, enteroendocrine cells send information about the nutritive state to appetite control centers in the brain such as the hypothalamus or brain stem.[6,7] For example, the anorexic gut peptide hormones cholecystokinin and PYY act on NPY/AgRP neurons of the hypothalamus.[2,7] Ghrelin acts as orexigenic hormone, with central action on NPY/AgRP neurons of the arcuate nucleus of the hypothalamus.[2,7]

For invertebrates, most knowledge on the peptidergic regulation of metabolism and feeding comes from insects, particularly from lepidopterans and the fruitfly *Drosophila melanogaster*.[8−10] In functional terms, however, fruit fly research has so far only focused on neuropeptides from neurons,[11] as well as (neuro) peptide hormones released from the corpora cardiaca, the main neurohemal organ of the brain/subesophageal ganglion. The results show that, similar to the situation in mammals, several

Received: November 5, 2010
Published: January 10, 2011

Table 1. Peptides Detected in the Midgut[a]

encoding gene[b]	peptide	sequence	$[M + H]^+$
Ast (CG13633)	AST-A1	VERYAFGLamide	953.52
	AST-A2$^{1-11}$	AYMYTNGGPGM	1161.47
	AST-A2$^{14-21}$	LPVYNFGLamide	921.52
	AST-A3	SRPYSFGLamide	925.49
	AST-A4	TTRPQPFNFGLamide	1276.68
Mip (CG6456)	MIP-2	AWKSMNVAWamide	1091.55
	MIP-3	RQAQGWNKFRGAWamide	1603.84
	MIP-4[c]	EPTWNNLKGMWamide	1374.66
	MIP-5	DQWQKLHGGWamide	1253.62
Ast-C (CG14919)	AST-C[c]	QVRYRQCYFNPISCF	1921.88
	AST-C[c]	pQVRYRQCYFNPISCF	1904.86
(CG14358)	CCHa1[c]	SCLEYGHSCWGAHamide	1446.57
(CG14375)	CCHa2[c]	GCQAYGHVCYGGHamide	1348.53
sNPF (CG13968)	sNPF-1$^{4-11}$/ sNPF-2$^{12-19}$	SPSLRLRFamide	974.59
	sNPF-2$^{1-10}$	WFGDVNQKPI	1203.62
	sNPF-3	KPQRLRWamide	982.61
	sNPF-4	KPMRLRWamide	985.59
Tk (CG14734)	DTK-1	APTSSFIGMRamide	1065.55
	DTK-2	APLAFVGLRamide	942.59
	DTK-3	APTGFTGMRamide	936.47
	DTK-4	APVNSFVGMRamide	1076.57
	DTK-5	APNGFLGMRamide	961.50
Dh31 (CG13094)	DH_{31}[c]	TVDFGLARGYSGTQEAKHRMGLAAANFAGGPamide	3149.57
Pdf (CG6496)	PDF[d]	NSELINSLLSLPKNMNDAamide	1972.02

[a] All peptide sequences were verified by MS/MS analysis. Cysteines forming intramolecular disulfide bonds are underlined. [b] Gene designations adopted from FlyBase. [c] Sequence biochemically identified for the first time. [d] From neuron fibres innervating the hindgut and (in adults) posterior midgut, not in enteroendocrine cells.[37,38]

neuropeptides are involved in the control of fly feeding and metabolism, some of which even show sequence and functional homology to their vertebrate counterparts: *Drosophila* insulin-like peptides (DILPs[11−13]), the NPY homologue neuropeptide F (NPF[14−16]), the neuromedin U homologue hugin-Pyrokinin,[17,18] short NPF (sNPF[19,20]), leucokinin[11,21] and adipokinetic hormone (AKH, a glucagon analogue).[22−24] Sulfakinins, homologues of vertebrate cholecystokinin, inhibit feeding in various insect species.[25] In *Drosophila*, sulfakinins decrease the contraction frequency of adult foregut and larval midgut.[26]

In strong contrast to these neuropeptides from the central nervous system, our knowledge on the chemical identity and function of insect peptides from enteroendocrines is poor and mostly stems from larger insects outside the genome-sequenced species. For example, CCAP, allatotropin and RFamides from the gut of cockroaches and lepidopterans regulate the activity and secretion of α-amylase and other digestive enzymes.[27−31] Allatostatin A expressed by endocrine cells in the lepidopteran gut[32,33] reduces feeding and growth rate[34] and regulates the release of digestive enzymes.[31,35] Many gut peptides, like for example, the *Drosophila* tachykinins,[36] either stimulate or inhibit gut motility. However, systemic functional studies do not exist for insect gut peptides even though the insect digestive system contains peptidergic enteroendocrine cells and likely plays an important role both as sender and receiver of metabolic peptide signals. In *Drosophila*, endocrine cells are scattered throughout the midgut, but are absent in the fore- and hindgut.[37,38]. In adult fruit flies, both foregut and hindgut are innervated by the central and peripheral (mainly stomatogastric) nervous system, while only the most anterior and posterior portions of the midgut receive neurite endings.[11] In third instar larvae, neurons of the stomatogastric nervous system are found to innervate the foregut and the most anterior midgut.[39] Additionally, the larval hindgut is innervated,[10] but these neurites do not reach the posterior midgut.

In the past decade, following the publication of the *Drosophila* genome,[40] fruit fly genetics has boosted our knowledge of neuropeptide function in insects (reviewed by Nässel and Winther[10]). It is therefore timely to employ molecular tools available for *Drosophila* to also shed light on the function of insect gut peptides. This will not only be important to understand the evolution of endocrine systems and identify new targets for pest control,[41] but may also provide a genetically accessible model system to study the general role of gut peptides in paracrine signaling within the digestive tract as well as brain−gut signaling in the control of food intake. It is evident that any functional study requires solid knowledge on the chemical identity of the peptides expressed in the fruit fly midgut. Veenstra and colleagues have used an array of peptide antisera to systematically characterize the distribution of peptidergic cells in the fruit fly midgut, the only part of the intestinal tract that contains enteroendocrine cells.[37,38] Their data is backed up by mRNA expression data from the FlyAtlas,[42] yet the chemical identity of the gut peptides in *Drosophila* remained unclear, since peptide hormones are post-translationally processed and modified, and the used antisera do mostly not distinguish between sequence-similar peptides of larger peptide families. Further, differential preprohormone processing between the nervous system and gut may occur.

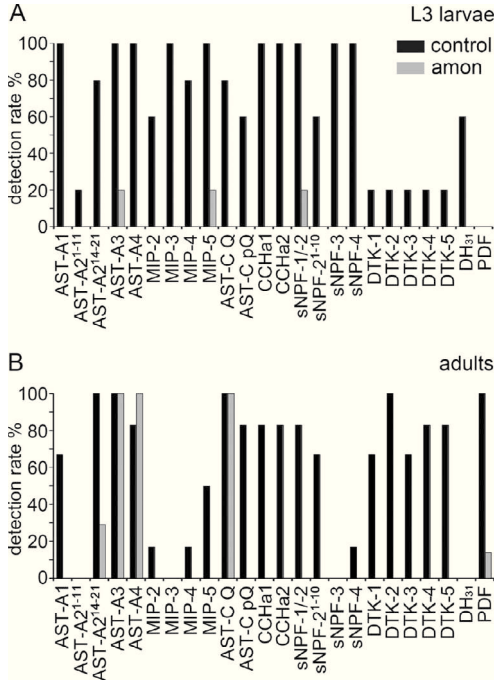

Figure 1. Detection rates of peptides in midgut samples from control and *amon*-deficient flies. (A) Control (black bars, n = 5) and *amon*-deficient (gray bars, n = 5) 3rd instar larvae. Most peptides were undetectable in *amon*-deficient larvae, while AST-A3, MIP-5 and sNPF-1^{4-11}/sNPF-2^{12-19} were detected in one out of 5 trials. (B) Control (black bars, n = 6) and *amon*-deficient (gray bars, n = 7) adults. Again, most peptides were undetectable in *amon*-deficient flies, yet PDF occurred in 1 and AST-$A2^{14-21}$ in 2 out of 7 trials, while AST-A3, AST-A4 and the Gln-form of AST-C were detectable in all samples. Loss of detection indicates that peptide concentrations have fallen below the detection level, while detection indicates that peptide concentrations were above detection level albeit diminished or not.

Therefore, we characterized peptide hormones from the *Drosophila* midgut by capillary RP-HPLC offline coupled with MALDI-TOF MS/MS. Our results show that all of the identified enteroendocrine peptides can be classified as brain−gut peptides that are identically processed in both nervous and gut tissue. As in secretory neurons,[43] *Drosophila* prohormone convertase dPC2 encoded by *amontillado* (*amon*) appears to be a key processing enzyme in the production of peptide hormones in enteroendocrine cells.

MATERIALS AND METHODS

Fly Stocks

The following fly stocks were used: the *amon*-deficient strain *yw*; +/+; $amon^{C241Y}$/*TM3 Sb Ser* y^+ *e*, the heat-shock rescue strain *yw*; *hs-amon*; *Df(3R)Tl-X e*/*TM3 Sb Ser* y^+ *e*,[44] *amon*-$GAL4^{91D}$ (kind gift of Michael Bender and Jeanne Rhea, Athens GA),[44] 386Y-GAL4 (kind gift of Paul Taghert, Saint Louis MO),[45] UAS-GFP.S65T T10 (Bloomington Stock Center) and wildtype Oregon R (OrR). The *amon*-$GAL4^{91D}$ line is a promoter construct containing 464 bp of the 5′ regulatory region (bp −331 to +133), while 386Y-GAL4 carries a P-element insertion within 320 bp of the *amon* 3′ end.[45] Flies were reared at room-temperature or 25 °C on standard cornmeal agar medium and yeast.

In Situ Hybridization in the Larval Midgut

Larvae were dissected in Ringer solution (NaCl 6.5 g/L; KCl 0.14 g/L; $NaHCO_3$ 0.2 g/L; $NaH_2PO_4 \cdot 2H_2O$ 0.01 g/L; $CaCl_2 \cdot 2H_2O$ 0.12 g/L), fixed in 4% paraformaldehyde in phosphate buffered saline (PBS) for 15 min, and rinsed with PBS and 0.1% Tween 20 (PBT), 3 × 5 min.

Samples for hybridization were digested with Proteinase K (50 μg/mL) for 4 min then incubated with glycine in PBT (2 mg/mL) for 5 min. Samples were washed in PBT (2 × 5 min), refixed for 20 min, then washed five times in PBT, each for 5 min. The samples were then washed in equal proportions of hybridization solution (50% formamide, 5× SSC (20× SSC: 3 M NaCl, 0.3 M trisodium citrate), 100 μg/mL salmon sperm DNA, 50 μg/mL heparin, 0.1% Tween 20) and PBT for 10 min, then washed in undiluted hybridization solution for 10 min. Samples were prehybridized in hybridization solution for 1 h at 45 °C. A total of 17 ng of *amontillado* riboprobe was added to the samples in 100 μL of hybridization solution and hybridization occurred overnight at 45 °C. Samples were agitated in fresh hybridization solution for 20 min, then successive washes were performed using decreasing ratios of hybridization solution/PBT (4:1, 3:2, 2:3, 1:4), each for 20 min in 1 mL volume. Samples were washed in PBT for 20 min, then incubated with Anti-DIG (500 μL, diluted 1:2000 with PBT and preabsorbed for 1 h against fresh fixed tissues). Samples were washed with PBT 4 × 20 min, washed in washing buffer (0.1 M NaCl, 5 × 10^{-2} M $MgCl_2$, 0.1 M Tris HCl pH 9.5, 10^{-3} M levamisol, 0.1% Tween 20) for 3 × 5 min, then a solution of SIGMAFAST BCIP/NBT solution (SIGMA) was added according to manufacturer's instructions. After color development, the samples were rinsed with PBT (5 × 5 min). *Amon* digoxigenin-labeled sense and antisense riboprobes were synthesized using the EST cDNA clone GH22014,[46] T7 and SP6 RNA polymerases and digoxigenin-labeled dNTPs according to manufacturer's instructions (Roche Molecular Biochemicals catalogue number 11 175 025 910) as described previously.[36] GH22014 was obtained from the Berkley *Drosophila* Genome Project via Research Genetics (pOT2 vector, Invitrogen Corporation, Carlsbad, CA).

Sample Preparation for LC/MS

Midguts of adults or third instar larvae were dissected in HL3 saline,[47] rinsed for a few seconds in a fresh droplet of HL3, and then directly transferred into 30−40 μL ice-cold 90% methanol/9% water/1% trifluoroacetic acid (TFA) (v/v/v) in a microtube. After 30 min incubation on ice, the sample was centrifuged for 15 min at 18 000*g* to pellet tissue and debris. The supernatant was transferred to a fresh tube, again centrifuged and transferred (larval samples only), and then dried in a Speed-Vac and stored at −20 °C. Batches of about 20 (larval) or 25 (adult) midguts per sample were used for extraction. Low-binding plastics were used throughout. In adults, the corpora cardiaca are situated directly anterior to the midgut. To avoid sample contamination with peptides from the corpora cardiaca, the proventriculus (which is devoid of endocrine cells) as the most anterior part of the midgut was not included in sample preparation for LC/MS. In pilot experiments, we also used homogenization either by sonication in a water bath, or by dispersion (Ultra-Turrax T10, IKA-Werke, Staufen, Germany).

To obtain *amon*-deficient individuals, virgins of *yw*; +/+; $amon^{C241Y}$/*TM3 Sb Ser* y^+ *e* were crossed with *yw*; *hs-amon*; *Df(3R)Tl-X e*/*TM3 Sb Ser* y^+ *e* males. Eggs were collected every morning, and heatshocked for 35 min at 37 °C in a water bath

Table 2. Comparison of Mass Spectrometric Data with Expression Data from *in Situ* Hybridization (ISH)/Immunostaining (IS) for Peptide Precursor Genes and Peptides Listed in Table 1 and *npf* for Different Stages and Organs of *Drosophila*[a]

	adult						L3					
	central nervous system and associated neurohemal structures			midgut			central nervous system and associated neurohemal structures			midgut		
	central nervous system		CC/HCG	endocrine cells	innervation	extracts (this study)	central nervous system		ring gland	endocrine cells	innervation	extracts (this study)
encoding gene	ISH, IS and/or transgenic flies	mass spectrometry	mass spectrometry	ISH, IS and/or transgenic flies	ISH, IS and/or transgenic flies	mass spectrometry	ISH, IS and/or transgenic flies	mass spectrometry	mass spectrometry	ISH, IS and/or transgenic flies	ISH, IS and/or transgenic flies	mass spectrometry
Ast (CG13633)	+[59,79]	+[53,79]		+[37,59]	+[59]	+	+[59,80]	+[51,52]		+[38,56,59]	-[38]	+
Mip (CG6456)	+[79]	+[53,79]		+[37]	-[37]	+	+[57,80]	+[51,52]		+[38,57]	-[38]	+
Ast-C (CG14919)	+[81,82]	+[53]		+[37,82]	-[37]	+	+[58,80−82]			+[38,58]	-[38]	+
(CG14358, CCHa1)						+						+
(CG14375, CCHa2)						+						+
sNPF (CG13968)	+[19,79,83]	+[53,79,83]	+[66]	-[37]	+[37]	+	+[19,80,83]	+[51,52,83]	+[67]	+[38]	+[38]	+
Tk (CG14734)	+[36,63,79]	+[53,63,79]		+[36,37]	-[37]	+	+[36,63,80]	+[52]		+[36,38]	-[38]	+
Dh31 (CG13094)				+[37]	-[37]		+[80]			+[38]	-[38]	+
Pdf (CG6496)	+[84,85]	+[53]		-[37]	+[37]	+	+[80]			-[38]	-[38]	
npf (CG10342)	+[14,86]			+[14,37]	-[37]		+[14,15,80]			+[14,38]	-[38]	

[a] CC/HCG: corpora cardiaca/hypocerebral ganglion. Transgenic flies: UAS/Gal4-mediated reporter gene studies with Gal4 under control of peptide gene promoter.

dx.doi.org/10.1021/pr101116g |*J. Proteome Res.* 2011, 10, 1881–1892

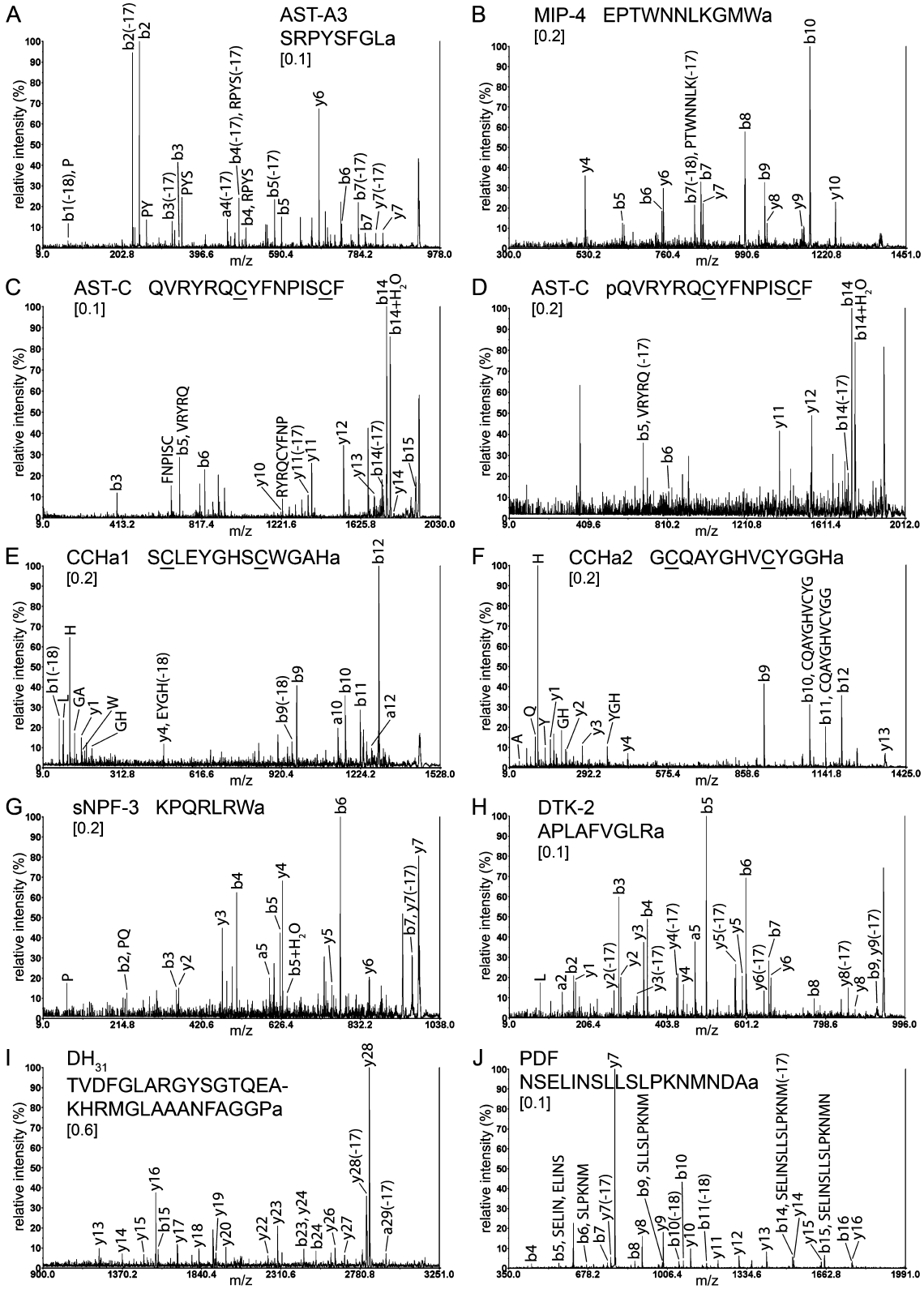

Figure 2. MS/MS spectra of selected peptides from midgut extracts of 3rd instar larvae or adults. (A) PSD-spectrum for AST-A3; (B) PSD-spectrum for MIP-4; (C) PSD-spectrum for AST-C (Q); D) PSD-spectrum for AST-C (pQ); (E) CID-spectrum for CCHa1; (F) CID-spectrum for CCHa2; (G) PSD-spectrum for sNPF-3; (H) PSD-spectrum for DTK-2; (I) PSD-spectrum for DH_{31}; (J) PSD-spectrum for PDF. All other peptides detected in this study could be similarly fragmented and identified. Numbers in squared brackets indicate mass tolerance (m/z) for peak labeling by the Data Explorer Software. a, C-terminal amidation; C...C, cysteines forming intramolecular disulfide bond, which largely persisted during fragmentation, particularly when no collision gas was used.

dx.doi.org/10.1021/pr101116g |*J. Proteome Res.* 2011, 10, 1881–1892

every 24 h for 4 days until the larvae had reached the third instar. Three days later, midguts were dissected. For adult flies, heat-shock was continued until eclosion and then stopped. After 6−10 days without heatshock, midguts of adult flies were dissected. As controls, *yw*; +/*hs-amon*; *amon*^{C241Y}/*TM3 Sb Ser* y^+ *e* and *yw*; +/*hs-amon*; *Df(3R)Tl-X e*/*TM3 Sb Ser* y^+ *e* (resulting from the crossing), as well as Oregon R wildtype flies and larvae were used.

Capillary RP-HPLC

The dried sample was dissolved in 20 μL of water containing 0.1% trifluoroacetic acid (TFA) and sonicated for 15 min in an ultrasonic bath. After centrifugation at 18 000*g* for 15 min, the supernatant was transferred to a fresh tube and manually injected for LC.

Peptides were separated with an UltiMate 3000 Cap system (Dionex, Idstein, Germany) connected to a Proteineer Fraction Collector (Bruker Daltonik GmbH, Bremen, Germany). For cleanup, the sample was loaded onto a reversed phase C18 trap column (Acclaim PepMap100 C18, 5 μm, 100 Å) using eluent A (0.05% TFA in water, v/v) at a flow rate of 20 μL/min. Then the trap column was switched online with the analytical reversed phase column (Acclaim PepMap100 C18, 3 μm, 100 Å). Peptides were eluted by running a linear gradient from 4% to 60% eluent B (80% acetonitrile/0.04% TFA in water, v/v) in 30 min and 60−100% B in 2 min with a flow rate of 2 μL/min. Spotting position on the MALDI target was changed every 30 s. A 1 μL sample fraction and 1 μL of matrix solution (half-saturated α-cyano-4-hydroxycinnamic acid in 60% acetonitrile/40% water/0.1% TFA, v/v/v) were mixed per spot and left to dry. HPLC gradient grade water and acetonitrile were used throughout.

Mass Spectrometry

For offline analysis of the spotted samples, a 4800 *Plus* MALDI TOF/TOF Analyzer (Applied Biosystems/MDS Sciex, Foster City, CA) equipped with a Nd:YAG laser (355 nm wavelength) and the 4800 Series Explorer software version 3.5.1 were used. For external calibration, Applied Biosystems Calibration Mixture 2 was employed. Spectra were acquired in positive ion reflector mode with an acceleration voltage of 20 kV in source 1 and 1 kV in source 2. Laser intensity and the number of laser shots per spectrum were adjusted to sample and instrument condition. Peptides were fragmented by PSD. CID was applied for CCHamide1 and 2, which produce only few fragments in PSD analysis due to an intramolecular disulfide bond that persists during fragmentation. Air was used as collision gas. Samples were measured in batch mode (automatically), except for a few MS/MS spectra which were measured manually.

MS/MS spectra were baseline corrected (advanced baseline correction, correction parameters 32, 0.5, 0.1), noise filtered (correlation factor 0.9) and analyzed using Data Explorer Software 4.10 (Applied Biosystems/MDS Sciex, Foster City, CA).

Immunostaining

Midguts of third instar larvae were dissected in HL3 saline[47] and fixed in 4% paraformaldehyde in 0.01 M PBS for 1.5−2 h at room temperature. Repeated washes with washing buffer (PBT: 0.1 M PBS + 0.3% Triton X) was followed by preincubation with 10% normal goat serum (Dianova, Hamburg, Germany) in PBT for 2 to several hours on a shaker. The following primary antisera were used: mouse anti-GFP (monoclonal; A11120; Invitrogen, Paisley, U.K.), rabbit anti-MIP (polyclonal; kind gift of Manfred Eckert, Jena),[48] rabbit anti-LemTRP (kind gift of Dick Nässel, Stockholm),[49] rabbit anti-AST-A (polyclonal; kind gift of Hans Agricola, Jena).[50] Primary antisera were diluted 1:1000 (anti-GFP) or 1:4000 (others) in PBT containing 5% normal goat serum. Tissues were incubated in the primary antisera solution for 1 day at 4 °C and 0.5−1 day at room temperature on a shaker. After several washing steps, tissues were incubated in secondary antisera (Cy3 or Cy5 conjugated IgG from goat or donkey; Jackson ImmunoResearch, Dianova, Hamburg, Germany) diluted 1:1000 in PBT for 1 day at 4 °C on a shaker. Several washing steps followed. For the final wash, 0.1 M PBS was used, which was then substituted by 80% glycerol in 0.1 M PBS. After gentle mixing with a pipet, the sample was left at 4 °C overnight. The next day, tissues were mounted in 80% glycerol in 0.1 M PBS. Samples were analyzed with a Leica TCS SP5 Confocal Laser Scanning Microscope and Leica LAS software. Images were contrast-enhanced using Photoshop version 10.0 (Adobe Systems, Inc.).

Fluorescence Microscopy

GPF fluorescence of adult and larval midgut tissue from 386Y-Gal4 × UAS-GFP or *amon*-Gal4 × UAS-GFP offspring was analyzed using a SteREO Lumar.V12 fluorescence stereomicroscope (Zeiss, Oberkochen, Germany) equipped with a NeoLumar S 1.5x FWD 30 mm objective (Zeiss, Oberkochen, Germany). Images were acquired with a ProgRes C5 digital microscope camera and ProgRes CapturePro 2.6 software (Jenoptik, Jena, Germany), and contrast-enhanced using Photoshop version 10.0 (Adobe Systems, Inc.). For drawings, the OpenSource software Inkscape 0.48 (www.inkscape.org) was used.

RESULTS

In pilot experiments, we found that peptide extraction with 90% MeOH/1% TFA is more efficient from undisrupted whole midguts than from homogenized samples. This is most likely due to the increased analyte complexity introduced by the gut content and broken cells after homogenization. Intermediate ultrafiltration (Millipore Microcon YM-10) as well as boiling after extraction did also not improve peptide detectability. Therefore, we settled with the fast and easy incubation of midguts in 90% MeOH/1% TFA.

Products of Nine Different Peptide Genes Occur in Midgut Extracts

Twenty-four peptides were detected in midgut samples from OrR wildtype and *amon* control flies, originating from 9 different preproproteins: AST-A, MIP, AST-C, sNPF, DTK, DH_{31}, CHHa1, CHHa2 and PDF (Table 1). Two of the nonamidated peptides, AST-A2$^{1-11}$ and sNPF-2$^{1-10}$ may represent nonbioactive processing products. The peptide detection frequencies for larval and adult midguts are shown in Figure 1 (black bars) and correlate well with the number of peptide immunoreactive cells and mRNA expression levels reported in the literature (see Table 2 and Discussion). The identity of each peptide could be confirmed by MS/MS fragmentation, even though we did not yield complete y or b ion series (Figure 2). Since we dissected complete midguts, the analyzed samples contained peptides from midgut endocrines as well as from innervating neuronal processes. This explains the detection of PDF, which is not produced by gut endocrine cells but by neurons innervating the adult posterior midgut.[37,38] The sequences confirmed by tandem MS fragmentation show that all peptides originating from enteroendocrine cells can be classified as brain-gut peptides.

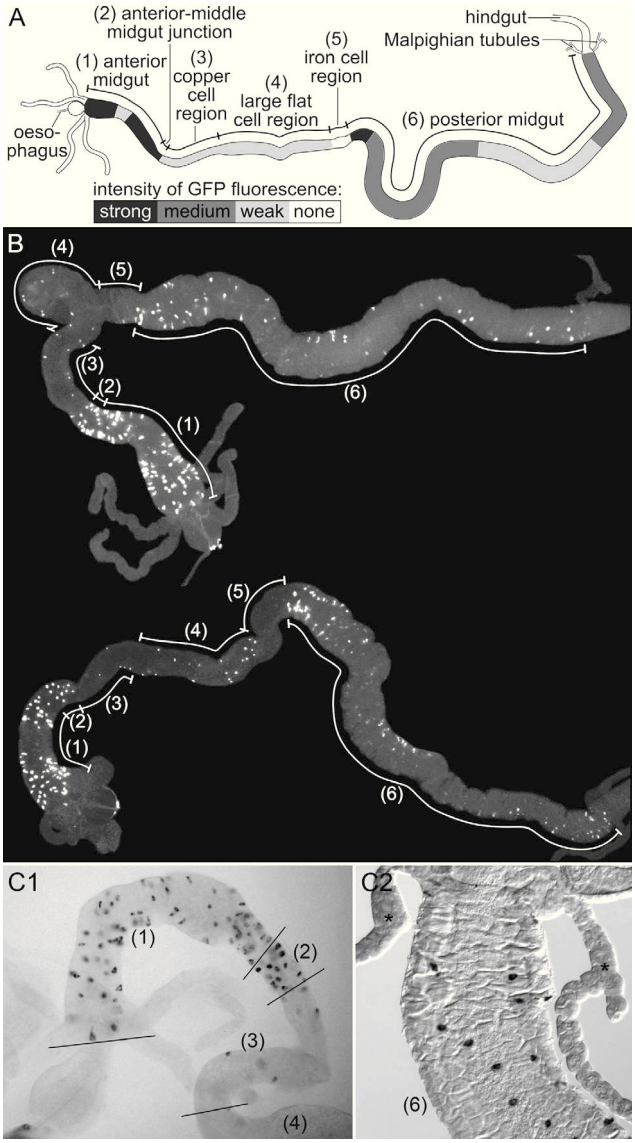

Figure 3. *Amon* expression pattern in the midgut of 3rd instar larvae. (A) Scheme of the distribution of GFP fluorescence intensity in different parts of the midgut of 386Y-Gal4 × UAS-GFP 3rd instar larvae. Designation of midgut sections adopted from Veenstra[38]. The highest number of GFP-expressing cells was found in the anterior midgut and in the anterior-most part of the posterior midgut. The number of GFP-expressing cells was intermediate in the anterior and posterior part of the posterior midgut, and lowest in the rest of the midgut. (B) Pictures of GFP-fluorescent cells in midguts of 386Y-Gal4 × UAS-GFP 3rd instar larvae, numbering as in panel A. PFA-fixated tissue was used to draw the midgut shape in panel A, while the midguts shown in panel B are unfixed and thus contracted. (C) *In situ* hybridization in midguts with an *amon* riboprobe, numbering as in panel A. C1 is a photomontage representing 4 different focal planes. The distribution of labeled cells matches well with the observed pattern in panels A and B. Asterisks mark Malpighian tubules.

Drosophila Prohormone Convertase 2 (AMON) Is Expressed in Enteroendocrine Cells of the Midgut

Our findings above show that brain−gut preproproteins are processed into sequence-identical forms in the brain[51−53] and gut. This suggests that the same processing pathways are active in both tissues. The proprotein convertase AMONTILLADO (AMON) is indispensable for the production of a diversity of bioactive neuropeptides and peptide hormones from neurohemal organs of *Drosophila*.[43,44] Since expression of AMON in cells of the midgut had previously been suggested by immunostaining,[54] we asked whether *amon* is expressed in enteroendocrine cells in the midgut.

In situ hybridization revealed *amon* expression in a characteristic pattern in the larval midgut (Figure 3C) that corresponds well with the distribution of peptide-immunoreactive enteroendocrine cells.[38] We next marked *amon*-expressing cells by expressing GFP under control of *amon* regulatory regions via the GAL4/UAS-system.[55] Both the *amon*-GAL4^{91D} and the 386Y-GAL4 line drove GFP-expression in a characteristic and reproducible pattern in the larval midgut (Figure 3B). Since the different immunoreactive cell types of the midgut epithelium are not as constant in their number and location as, for example, neurons in the nervous system, individual variations occurred. Nevertheless, several regions with characteristic *amon*-driven GFP fluorescence intensities can be differentiated (Figure 3A,B), which match well with the *amon* expression pattern detected by *in situ* hybridization (Figure 3C) and the distribution of peptide-immunoreactive cells.[37,38] In general, GFP expression appeared to be stronger in 386Y-Gal4 × UAS-GFP larvae than in *amon*-Gal4^{91D} × UAS-GFP larvae. Since the expression patterns in the adult midgut showed increased variation and broader expression (data not shown), we used larval midguts to test for localization of AMON in enteroendocrine cells. Immunolabeling of midguts from 386Y-Gal4 × UAS-GFP or *amon*-Gal4^{91D} × UAS-GFP larvae against GFP and AST-A, DTK or MIP revealed that all peptide-immunoreactive cells co-expressed GFP and thus are included in the 386Y-Gal4 and *amon*-Gal4^{91D} expression pattern (Figure 4).

Deficiency of *amon* Results in Impaired Production of Gut Peptide Hormones

The results above indicate that AMON is expressed by enteroendocrine cells, and suggest that AMON is involved in the processing of gut peptide hormones. To test whether AMON is indeed involved in gut peptide processing, we applied the LC/MS analysis workflow in parallel for *amon*-deficient flies and controls. For 3 of the 5 midgut batches from larval and 4 of the 7 midgut batches from adult *amon*-deficient flies (*yw*; +/*hs-amon*; *amon*^{C241Y}/*Df(3R)Tl-X e*), we measured an identical batch of control flies (*yw*; +/*hs-amon*; *amon*^{C241Y}/*TM3 Sb Ser y*$^{+}$ *e* or *yw*; +/*hs-amon*; *Df(3R)Tl-X e*/*TM3 Sb Ser y*$^{+}$ *e*) taken from the same bottles that were of similar age to minimize possible age, food or population density effects on peptide levels. Additionally, we measured 2 batches of OrR wildtype flies each for larvae and adults. Findings for wildtype flies were comparable to *amon* control flies; thus, both groups were combined as "control" in Figure 1.

The results in Figure 1 show that the detection rates of the gut peptides were drastically reduced in midgut extracts of *amon* larvae versus controls (gray bars). Also the detection rate for peptide hormones in the adult midgut dropped drastically with exception of AST-A3, AST-A4 and the Gln-form of AST-C. These three peptides all show a high detection rate (83−100%) in control adults. Taken together, the comparison between control and *amon*-deficient animals shows that a loss of *amon* results in drastically reduced detection rates of gut peptide hormones, suggesting that the level for gut peptides in *amon* flies was strongly reduced and, for most peptides, fell below the detection limit of the mass spectrometer.

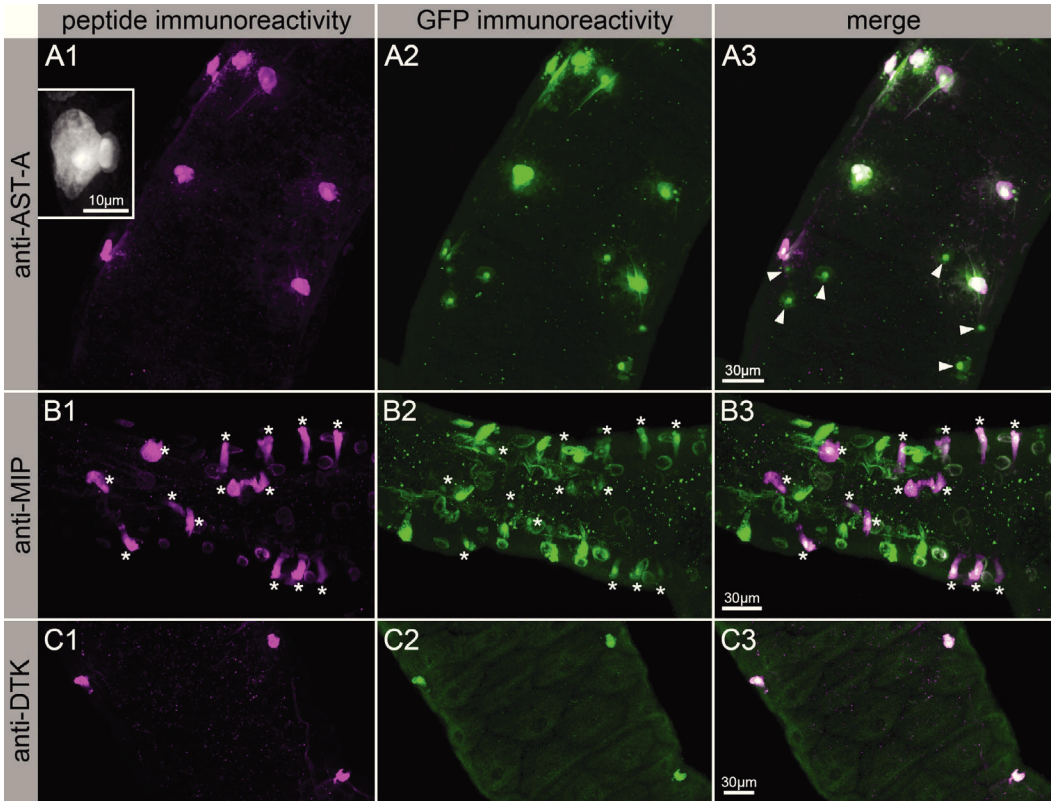

Figure 4. Localization of *amon*-promoter driven GFP in midguts of 3rd instar larvae. (A) AST-A immunoreactive cells colocalize with 386Y-GAL4-driven GFP in the most posterior part of the midgut. Arrowheads mark GFP-expressing cells that are not AST-A immunoreactive. These cells likely produce different peptides. Inset: Detail showing a single AST-A immunoreactive cell. Gut lumen is to the right. (B) MIP-immunoreactive cells colocalize with *amon*-GAL4^{91D}-driven GFP at the anterior-middle midgut junction (cells marked by asterisks). MIP-immunoreactive cells show weaker anti-GFP staining than other endocrines in this region of the midgut. (C) TK-immunoreactive cells colocalize with *amon*-GAL4^{91D}-driven GFP near the posterior boundary of the midgut.

DISCUSSION

Peptidomics Confirm, Refine, and Extend Data from Immunostaining and *in Situ* Hybridization

The presence of AST-A, MIP, AST-C, sNPF, DH_{31} and DTK peptides in the fruit fly midgut had already been suggested by immunostaining and *in situ* hybridization.[36−38,56−59] Our peptidomic analysis now reveals the chemical identity of the bioactive peptide paracopies of these peptide families produced by the midgut. The identification of MIP-4, the full-length pyroGln- and Gln-forms of AST-C and DH_{31} represents the first biochemical characterization of these peptides in *Drosophila*. First evidence for the occurrence of both forms of AST-C had earlier been provided by MS analysis in combination with an acetylation reaction.[53] DH_{31} could also be detected and fragmented in extracts of larval and adult central nervous systems (unpublished). The finding of CCHa1 and CCHa2 is the first proof of expression of these peptides originating from very recently predicted genes first discovered in the silkmoth *Bombyx*.[60] In *Bombyx*, CCHa is expressed in the CNS and in numerous endocrine cells of the midgut.[60] In *Drosophila*, the function and cellular localization of CCHa is still uncharacterized. By LC/MS, we detected mass signals corresponding to both CCHamides in extracts of larval and adult *Drosophila* central nervous systems at retention times similar to the CCHamide transcripts from midgut samples (unpublished). While data from FlyAtlas[42] indicate an upregulation of both CCHamide transcripts in the midgut, we cannot fully exclude that the CCHamides in the midgut extracts originate from innervating neuronal processes and not from enteroendocrine cells.

Though expression in the midgut is suggested by *in situ* hybridization, FlyAtlas data and *npf*-GAL4-driven expression of marker proteins,[14,37,38,42] we did not find NPF. Noteworthy, NPF is also expressed in the CNS,[14] but has so far not been found in any of the peptidomic studies of the CNS.[51−53] If not processed as predicted from the genome, NPF (as well as any other unpredicted peptide) may well have escaped our analysis since we searched for predicted peptide masses and did not perform de novo sequencing of all mass peaks. Also a mass corresponding to TAP-5/DTK-6,[36,61,62] which was not detected in peptidomic studies of CNS tissue,[51−53,63] was absent. This provides further evidence that this peptide is not stored along with the other five DTKs.

Unlike the other peptides, PDF is not expressed in the midgut, and originates from nerves innervating the hindgut and the posteriormost part of the adult midgut.[37,38] The most anterior part of the midgut is innervated by sNPF-immunoreactive neurons with somata in the hypocerebral ganglion.[37,38] Thus, at least part of our sNPF signal may be attributable to neuronal origin in the larva, where also sNPF-immunoreactive enteroendocrine cells have been found.[38] Since sNPF-immunoreactivity is not detectable in cells of the adult midgut,[37] the sNPF signals in adults may entirely be contributable to neuronal origin.

The differences in detection rates for MIPs, AST-C, sNPF, DTKs and DH_{31} between the larval and adult midgut correspond

well with the observed differences in the number of immunoreactive cells[37,38] and expression intensities from the FlyAtlas.[42] Thus, both on the transcript and peptide level, sNPF, DH_{31} and MIPs show a stronger expression in larvae, while DTKs and AST-C are more strongly expressed in the adult midgut.

Comparison of the Midgut Peptidome of the Fruit Fly and Mosquito

Besides our study on *Drosophila*, comprehensive peptidomic data for the insect midgut is only available from a direct mass spectrometric profiling of the rather closely related mosquito *Aedes aegypti*.[64] Midgut endocrines of both Dipteran species process AST-A, MIP, sNPF, and TK. However, DH_{31} and AST-C have only been found in the *Drosophila* midgut. Since it is notoriously difficult to extract larger peptides by direct peptide profiling,[65] DH_{31} may nevertheless still occur in the *Aedes* midgut. In contrast, CAPA-PK was only found in the midgut of *Aedes*, but not in *Drosophila*, where it is an abundant peptide hormone in abdominal neurohemal organs.[66,67] In accordance, SCPb-immunoreactivity (SCPb is a molluscan neuropeptide sequence-related to insect CAPA peptides[68]) was found both in enteroendocrine cells and innervating axons in *Aedes*,[69] while CAPA immunoreactivity is absent from the *Drosophila* gut.[37,38] Since the function of CAPA-PK is still unknown in both species, the functional significance of this difference is unclear.

Endocrine Peptides from the Midgut Can Be Classified as Brain−Gut Peptides

All detected gut peptides occur in identical form in the CNS,[52,53] including the newly confirmed CHHa1 and -2 (Reiher and Wegener, unpublished). The same has been found for *Aedes*,[64] the only other insect species with characterized midgut peptidome so far, and is reminiscent to the situation in mammals and other vertebrates. Earlier reports suggested a differential distribution of tachykinin-related peptides (TRPs) in brain and midgut of cockroaches.[70−72] A more recent mass-spectrometric analysis, however, revealed that all TRPs synthesized by neurons are also produced by gut endocrines.[73] The two previously reported midgut-specific TRPs are N-terminally extended forms of two of the TRPs (LemTRP-2 and -3) occurring in neurons and gut endocrines. These two extended TRPs were only detected in midgut extracts and not in the brain,[70,73] yet extended LemTRP-3 could be immunodetected in neurons.[72] An extended TRP, identified in the midgut of the locust *Schistocerca*,[74] was not detected in a peptidomic study of the nervous system.[75] Thus, while differences in the expression of extended tachykinins exist, a majority of TRPs represent brain−gut peptides also in cockroaches and locusts. In our analysis, we did not detect potential extended forms of DTKs in midgut extracts.

Up to date we can only speculate about the functional consequences of the occurrence of similar peptides in the brain and gut. We note that some of the gut peptides, which all may be released into the circulation and act as hormones, seem to be expressed only in interneurons in the CNS (AST-A, AST-C, DTK), and are not concentrated in neurohemal organs or release sites as shown by direct mass spectrometric peptide profiling.[66,67] These peptides may act within the CNS or in a paracrine fashion (DTK[76]) when released in the CNS, while acting as hormones potentially able to reach peripheral targets or the CNS when released from the gut. Other gut peptides (sNPF, MIP) are also stored in neurohemal release sites or neurohemal areas on peripheral muscles,[66,67,77] suggesting a function both as a gut and neuro-hormone. Whether and how these brain−gut hormones exert differential effects depending on the source of release will be interesting to investigate.

AMON Is a Key Enzyme in the Processing of Peptide Hormones from Gut and CNS

The strongly reduced detectability of gut peptides in *amon* flies suggests that AMON is a key enzyme in the processing of peptide hormones from the gut. This is further supported by the distinct pattern of *amon* expression found by *in situ* hybridization and *amon* promotor-driven GFP. A similar expression pattern has also been found by AMON immunostaining.[54] Furthermore, gut peptide immunoreactivity colocalized with *amon* promotor driven GFP in DTK-, MIP-, and AST-A-producing enteroendocrines.

We have recently found that a mutation in *amon*, the gene coding for *Drosophila* PC2, affects all peptide hormones detectable by mass spectrometric direct profiling of the major neurohemal organs.[43,44] These studies showed a stronger effect on peptide detectability in larvae, suggesting that adult flies possibly have a larger relative pool of neuropeptide hormones than larvae. The same seems to hold also for AST-A and AST-C from the gut. The finding that out of 4 AST-A isoforms detected in control adult guts only AST-A3 and -4 could be detected with a similar rate may suggest that the general level of AST-A peptides, though detectable, is reduced in *amon* mutants. To convincingly show this, however, a proper quantification of peptide levels will be needed.

Taken together, it seems possible that dPC2 AMON is the only PC responsible for the production of the smaller peptide hormones (up to ≈3 kDa) from both gut and the nervous system. Accordingly, peptide preprohormones from both tissues are cleaved into the same bioactive peptides. Thus, *Drosophila* shows a much simpler processing pattern than in mammals, which besides PC2 express further PCs in both nervous system (mainly PC1/3) and gut (PC1/3 and 5/6), and show differences in the peptide patterns between brain and gut due to a differential PC expression.[78]

CONCLUSIONS

The results show that all detected enteroendocrine peptides can be classified as brain−gut peptides which seem to be processed by dPC2 AMON. This now offers the opportunity to use the specific molecular tools available for *Drosophila* to investigate the mechanisms and functional significance of enteroendocrine signaling in the regulation of food intake, energy homeostasis and gut development.

AUTHOR INFORMATION

Corresponding Author

*Philipps-University Marburg, Department of Biology - Animal Physiology, Karl-von-Frisch-Str. 8, D-35032 Marburg, Germany. T: +49-6421-2823411 (office); T: +49-6421-2823405 (lab). Fax: +49-6421-2828941. E-mail: wegener@staff.uni-marburg.de.

The authors declare no conflicts of interest.

ACKNOWLEDGMENT

We are very grateful to Jeanne Rhea and Michael Bender (Athens) and the Bloomington Stock Center for kindly supplying fly lines, to Hans Agricola (Jena), Manfred Eckert (Jena) and

Dick R. Nässel (Stockholm) for the generous gift of antisera, Lotte Søgaard-Andersen (Max-Planck-Institute for Terrestrial Microbiology) for access to the mass spectrometer and Caroline Rylett (deceased, University of Leeds) for preparing riboprobes used in this study. We also thank Martina Kern and Jutta Seyfarth for excellent technical help, Franz Grolig for maintenance of the confocal microscope, Renate Renkawitz-Pohl and Ruth Hyland for fly housing, Dominic Aumann for providing a fly picture, Reinhard Predel for helpful discussions, and Uwe Homberg for general support. Funded by the Deutsche Forschungsgemeinschaft (WE 2652/4-1) and the Biotechnology and Biological Sciences Research Council of the UK (24/S15562).

REFERENCES

(1) Broberger, C. Brain regulation of food intake and appetite: molecules and networks. *J. Intern. Med.* **2005**, *258*, 301–327.

(2) Stanley, S.; Wynne, K.; McGowan, B.; Bloom, S. Hormonal regulation of food intake. *Physiol. Rev.* **2005**, *85*, 1131–1158.

(3) Atkinson, T. J. Central and peripheral neuroendocrine peptides and signalling in appetite regulation: considerations for obesity pharmacotherapy. *Obes. Rev.* **2008**, *9*, 108–120.

(4) Blundell, J. E.; Levin, F.; King, N. A.; Barkeling, B.; Gustafsson, T.; Gustafson, T.; Hellstrom, P. M.; Holst, J. J.; Naslund, E. Overconsumption and obesity: peptides and susceptibility to weight gain. *Regul. Pept.* **2008**, *149*, 32–38.

(5) Murphy, K. G.; Dhillo, W. S.; Bloom, S. R. Gut Peptides in the Regulation of Food Intake and Energy Homeostasis. *Endocr. Rev.* **2006**, *27*, 719–727.

(6) Chaudhri, O. B.; Salem, V.; Murphy, K. G.; Bloom, S. R. Gastrointestinal Satiety Signals. *Annu. Rev. Physiol.* **2008**, *70*, 239–255.

(7) Mendieta-Zerón, H.; López, M.; Diéguez, C. Gastrointestinal peptides controlling body weight homeostasis. *Gen. Comp. Endocrinol.* **2008**, *155*, 481–495.

(8) Bede, J. C.; McNeil, J. N.; Tobe, S. S. The role of neuropeptides in caterpillar nutritional ecology. *Peptides* **2007**, *28*, 185–196.

(9) Audsley, N.; Weaver, R. Neuropeptides associated with the regulation of feeding in insects. *Gen. Comp. Endocrinol.* **2009**, *162*, 93–104.

(10) Nässel, D. R.; Winther, Å. M. Drosophila neuropeptides in regulation of physiology and behavior. *Prog. Neurobiol.* **2010**, *92*, 42–104.

(11) Cognigni, P.; Bailey, A. P.; Miguel-Aliaga, I. Enteric neurons and systemic signals couple nutritional and reproductive status with intestinal homeostasis. *Cell Metab.* **2011**, *13*, 92–104.

(12) Brogiolo, W.; Stocker, H.; Ikeya, T.; Rintelen, F.; Fernandez, R.; Hafen, E. An evolutionarily conserved function of the Drosophila insulin receptor and insulin-like peptides in growth control. *Curr. Biol.* **2001**, *11*, 213–221.

(13) Rulifson, E. J.; Kim, S. K.; Nusse, R. Ablation of insulin-producing neurons in flies: growth and diabetic phenotypes. *Science* **2002**, *296*, 1118–1120.

(14) Brown, M. R.; Crim, J. W.; Arata, R. C.; Cai, H. N.; Chun, C.; Shen, P. Identification of a Drosophila brain-gut peptide related to the neuropeptide Y family. *Peptides* **1999**, *20*, 1035–1042.

(15) Shen, P.; Cai, H. N. Drosophila neuropeptide F mediates integration of chemosensory stimulation and conditioning of the nervous system by food. *J. Neurobiol.* **2001**, *47*, 16–25.

(16) Wu, Q.; Wen, T.; Lee, G.; Park, J. H.; Cai, H. N.; Shen, P. Developmental control of foraging and social behavior by the Drosophila neuropeptide Y-like system. *Neuron* **2003**, *39*, 147–161.

(17) Melcher, C.; Pankratz, M. J. Candidate gustatory interneurons modulating feeding behavior in the Drosophila brain. *PLoS Biol.* **2005**, *3*, e305.

(18) Melcher, C.; Bader, R.; Walther, S.; Simakov, O.; Pankratz, M. J. Neuromedin U and its putative Drosophila homolog hugin. *PLoS Biol* **2006**, *4*, e68.

(19) Lee, K.; You, K.; Choo, J.; Han, Y.; Yu, K. Drosophila short neuropeptide F regulates food intake and body size. *J. Biol. Chem.* **2004**, *279*, 50781–50789.

(20) Lee, K.; Kwon, O.; Lee, J. H.; Kwon, K.; Min, K.; Jung, S.; Kim, A.; You, K.; Tatar, M.; Yu, K. Drosophila short neuropeptide F signalling regulates growth by ERK-mediated insulin signalling. *Nat. Cell Biol.* **2008**, *10*, 468–475.

(21) Al-Anzi, B.; Armand, E.; Nagamei, P.; Olszewski, M.; Sapin, V.; Waters, C.; Zinn, K.; Wyman, R. J.; Benzer, S. The leucokinin pathway and its neurons regulate meal size in Drosophila. *Curr. Biol.* **2010**, *20*, 969–978.

(22) Kim, S. K.; Rulifson, E. J. Conserved mechanisms of glucose sensing and regulation by Drosophila corpora cardiaca cells. *Nature* **2004**, *431*, 316–320.

(23) Lee, G.; Park, J. H. Hemolymph sugar homeostasis and starvation-induced hyperactivity affected by genetic manipulations of the adipokinetic hormone-encoding gene in Drosophila melanogaster. *Genetics* **2004**, *167*, 311–323.

(24) Isabel, G.; Martin, J.; Chidami, S.; Veenstra, J. A.; Rosay, P. AKH-producing neuroendocrine cell ablation decreases trehalose and induces behavioral changes in Drosophila. *Am. J. Physiol.: Regul. Integr. Comp. Physiol.* **2005**, *288*, R531–538.

(25) Downer, K. E.; Haselton, A. T.; Nachman, R. J.; Stoffolano, J. G. Insect satiety: sulfakinin localization and the effect of drosulfakinin on protein and carbohydrate ingestion in the blow fly, Phormia regina (Diptera: Calliphoridae). *J. Insect Physiol.* **2007**, *53*, 106–112.

(26) Nichols, R. The first nonsulfated sulfakinin activity reported suggests nsDSK acts in gut biology. *Peptides* **2007**, *28*, 767–773.

(27) Sakai, T.; Satake, H.; Minakata, H.; Takeda, M. Characterization of crustacean cardioactive peptide as a novel insect midgut factor: isolation, localization, and stimulation of alpha-amylase activity and gut contraction. *Endocrinology* **2004**, *145*, 5671–5678.

(28) Sakai, T.; Satake, H.; Takeda, M. Nutrient-induced alpha-amylase and protease activity is regulated by crustacean cardioactive peptide (CCAP) in the cockroach midgut. *Peptides* **2006**, *27*, 2157–2164.

(29) Harshini, S.; Nachman, R. J.; Sreekumar, S. Inhibition of digestive enzyme release by neuropeptides in larvae of Opisina arenosella (Lepidoptera: Cryptophasidae). *Comp. Biochem. Physiol., Part B: Biochem. Mol. Biol.* **2002**, *132*, 353–358.

(30) Harshini, S.; Nachman, R. J.; Sreekumar, S. In vitro release of digestive enzymes by FMRF amide related neuropeptides and analogues in the lepidopteran insect Opisina arenosella (Walk.). *Peptides* **2002**, *23*, 1759–1763.

(31) Lwalaba, D.; Hoffmann, K. H.; Woodring, J. Control of the release of digestive enzymes in the larvae of the fall armyworm, Spodoptera frugiperda. *Arch. Insect Biochem. Physiol.* **2010**, *73*, 14–29.

(32) Abdel-Latief, M.; Meyering-Vos, M.; Hoffmann, K. H. Type-A allatostatins from the fall armyworm, Spodoptera frugiperda: molecular cloning, expression and tissue-specific localization. *Arch. Insect Biochem. Physiol.* **2004**, *56*, 120–132.

(33) Davey, M.; Duve, H.; Thorpe, A.; East, P. Helicostatins: brain-gut peptides of the moth, Helicoverpa armigera (Lepidoptera: Noctuidae). *Arch. Insect Biochem. Physiol.* **2005**, *58*, 1–16.

(34) Audsley, N.; Weaver, R. J.; Edwards, J. P. In vivo effects of Manduca sexta allatostatin and allatotropin on larvae of the tomato moth, Lacanobia oleracea. *Physiol. Entomol.* **2001**, *26*, 181–188.

(35) Woodring, J.; Diersch, S.; Lwalaba, D.; Hoffmann, K.; Meyering-Vos, M. Control of the release of digestive enzymes in the caeca of the cricket Gryllus bimaculatus. *Physiol. Entomol.* **2009**, *34*, 144–151.

(36) Siviter, R. J.; Coast, G. M.; Winther, A. M.; Nachman, R. J.; Taylor, C. A.; Shirras, A. D.; Coates, D.; Isaac, R. E.; Nässel, D. R. Expression and functional characterization of a Drosophila neuropeptide precursor with homology to mammalian preprotachykinin A. *J. Biol. Chem.* **2000**, *275*, 23273–23280.

(37) Veenstra, J. A.; Agricola, H.; Sellami, A. Regulatory peptides in fruit fly midgut. *Cell Tissue Res.* **2008**, *334*, 499–516.

(38) Veenstra, J. A. Peptidergic paracrine and endocrine cells in the midgut of the fruit fly maggot. *Cell Tissue Res.* **2009**, *336*, 309–323.

(39) Spiess, R.; Schoofs, A.; Heinzel, H. Anatomy of the stomatogastric nervous system associated with the foregut in Drosophila melanogaster and Calliphora vicina third instar larvae. *J. Morphol.* **2008**, *269*, 272–282.

(40) Adams, M. D.; Celniker, S. E.; Holt, R. A.; Evans, C. A.; Gocayne, J. D.; Amanatides, P. G.; Scherer, S. E.; Li, P. W.; Hoskins, R. A.; Galle, R. F.; George, R. A.; Lewis, S. E.; Richards, S.; Ashburner, M.; Henderson, S. N.; Sutton, G. G.; Wortman, J. R.; Yandell, M. D.; Zhang, Q.; Chen, L. X.; Brandon, R. C.; Rogers, Y. H.; Blazej, R. G.; Champe, M.; Pfeiffer, B. D.; Wan, K. H.; Doyle, C.; Baxter, E. G.; Helt, G.; Nelson, C. R.; Gabor, G. L.; Abril, J. F.; Agbayani, A.; An, H. J.; Andrews-Pfannkoch, C.; Baldwin, D.; Ballew, R. M.; Basu, A.; Baxendale, J.; Bayraktaroglu, L.; Beasley, E. M.; Beeson, K. Y.; Benos, P. V.; Berman, B. P.; Bhandari, D.; Bolshakov, S.; Borkova, D.; Botchan, M. R.; Bouck, J.; Brokstein, P.; Brottier, P.; Burtis, K. C.; Busam, D. A.; Butler, H.; Cadieu, E.; Center, A.; Chandra, I.; Cherry, J. M.; Cawley, S.; Dahlke, C.; Davenport, L. B.; Davies, P.; de Pablos, B.; Delcher, A.; Deng, Z.; Mays, A. D.; Dew, I.; Dietz, S. M.; Dodson, K.; Doup, L. E.; Downes, M.; Dugan-Rocha, S.; Dunkov, B. C.; Dunn, P.; Durbin, K. J.; Evangelista, C. C.; Ferraz, C.; Ferriera, S.; Fleischmann, W.; Fosler, C.; Gabrielian, A. E.; Garg, N. S.; Gelbart, W. M.; Glasser, K.; Glodek, A.; Gong, F.; Gorrell, J. H.; Gu, Z.; Guan, P.; Harris, M.; Harris, N. L.; Harvey, D.; Heiman, T. J.; Hernandez, J. R.; Houck, J.; Hostin, D.; Houston, K. A.; Howland, T. J.; Wei, M. H.; Ibegwam, C.; Jalali, M.; Kalush, F.; Karpen, G. H.; Ke, Z.; Kennison, J. A.; Ketchum, K. A.; Kimmel, B. E.; Kodira, C. D.; Kraft, C.; Kravitz, S.; Kulp, D.; Lai, Z.; Lasko, P.; Lei, Y.; Levitsky, A. A.; Li, J.; Li, Z.; Liang, Y.; Lin, X.; Liu, X.; Mattei, B.; McIntosh, T. C.; McLeod, M. P.; McPherson, D.; Merkulov, G.; Milshina, N. V.; Mobarry, C.; Morris, J.; Moshrefi, A.; Mount, S. M.; Moy, M.; Murphy, B.; Murphy, L.; Muzny, D. M.; Nelson, D. L.; Nelson, D. R.; Nelson, K. A.; Nixon, K.; Nusskern, D. R.; Pacleb, J. M.; Palazzolo, M.; Pittman, G. S.; Pan, S.; Pollard, J.; Puri, V.; Reese, M. G.; Reinert, K.; Remington, K.; Saunders, R. D.; Scheeler, F.; Shen, H.; Shue, B. C.; Sidén-Kiamos, I.; Simpson, M.; Skupski, M. P.; Smith, T.; Spier, E.; Spradling, A. C.; Stapleton, M.; Strong, R.; Sun, E.; Svirskas, R.; Tector, C.; Turner, R.; Venter, E.; Wang, A. H.; Wang, X.; Wang, Z. Y.; Wassarman, D. A.; Weinstock, G. M.; Weissenbach, J.; Williams, S. M.; WoodageT; Worley, K. C.; Wu, D.; Yang, S.; Yao, Q. A.; Ye, J.; Yeh, R. F.; Zaveri, J. S.; Zhan, M.; Zhang, G.; Zhao, Q.; Zheng, L.; Zheng, X. H.; Zhong, F. N.; Zhong, W.; Zhou, X.; Zhu, S.; Zhu, X.; Smith, H. O.; Gibbs, R. A.; Myers, E. W.; Rubin, G. M.; Venter, J. C. The genome sequence of Drosophila melanogaster. *Science* **2000**, *287*, 2185–2195.

(41) Fitches, E.; Audsley, N.; Gatehouse, J. A.; Edwards, J. P. Fusion proteins containing neuropeptides as novel insect contol agents: snowdrop lectin delivers fused allatostatin to insect haemolymph following oral ingestion. *Insect Biochem. Mol. Biol.* **2002**, *32*, 1653–1661.

(42) Chintapalli, V. R.; Wang, J.; Dow, J. A. T. Using FlyAtlas to identify better Drosophila melanogaster models of human disease. *Nat. Genet.* **2007**, *39*, 715–720.

(43) Wegener, C.; Herbert, H.; Kahnt, J.; Bender, M.; Rhea, J. M. Deficiency of prohormone convertase dPC2 (AMONTILLADO) results in impaired production of bioactive neuropeptide hormones in Drosophila. *J. Neurochem.*, DOI: 10.1111/j.1471-4159.2010.07130.x, **2011**.

(44) Rhea, J. M.; Wegener, C.; Bender, M. The proprotein convertase encoded by amontillado (amon) is required in Drosophila corpora cardiaca endocrine cells producing the glucose regulatory hormone AKH. *PLoS Genet.* **2010**, *6*, e1000967.

(45) Taghert, P. H.; Hewes, R. S.; Park, J. H.; O'Brien, M. A.; Han, M.; Peck, M. E. Multiple amidated neuropeptides are required for normal circadian locomotor rhythms in Drosophila. *J. Neurosci.* **2001**, *21*, 6673–6686.

(46) Stapleton, M.; Liao, G.; Brokstein, P.; Hong, L.; Carninci, P.; Shiraki, T.; Hayashizaki, Y.; Champe, M.; Pacleb, J.; Wan, K.; Yu, C.; Carlson, J.; George, R.; Celniker, S.; Rubin, G. M. The Drosophila gene collection: identification of putative full-length cDNAs for 70% of D. melanogaster genes. *Genome Res.* **2002**, *12*, 1294–1300.

(47) Stewart, B. A.; Atwood, H. L.; Renger, J. J.; Wang, J.; Wu, C. F. Improved stability of Drosophila larval neuromuscular preparations in haemolymph-like physiological solutions. *J. Comp. Physiol., A* **1994**, *175*, 179–191.

(48) Predel, R.; Rapus, J.; Eckert, M. Myoinhibitory neuropeptides in the American cockroach. *Peptides* **2001**, *22*, 199–208.

(49) Winther, A. M.; Nässel, D. R. Intestinal peptides as circulating hormones: release of tachykinin-related peptide from the locust and cockroach midgut. *J. Exp. Biol.* **2001**, *204*, 1269–1280.

(50) Vitzthum, H.; Homberg, U.; Agricola, H. Distribution of Dip-allatostatin I-like immunoreactivity in the brain of the locust Schistocerca gregaria with detailed analysis of immunostaining in the central complex. *J. Comp. Neurol.* **1996**, *369*, 419–437.

(51) Baggerman, G.; Cerstiaens, A.; De Loof, A.; Schoofs, L. Peptidomics of the larval Drosophila melanogaster central nervous system. *J. Biol. Chem.* **2002**, *277*, 40368–40374.

(52) Baggerman, G.; Boonen, K.; Verleyen, P.; De Loof, A.; Schoofs, L. Peptidomic analysis of the larval Drosophila melanogaster central nervous system by two-dimensional capillary liquid chromatography quadrupole time-of-flight mass spectrometry. *J. Mass Spectrom.* **2005**, *40*, 250–260.

(53) Yew, J. Y.; Wang, Y.; Barteneva, N.; Dikler, S.; Kutz-Naber, K. K.; Li, L.; Kravitz, E. A. Analysis of neuropeptide expression and localization in adult Drosophila melanogaster central nervous system by affinity cell-capture mass spectrometry. *J. Proteome Res.* **2009**, *8*, 1271–1284.

(54) Rayburn, L. Y. M.; Rhea, J.; Jocoy, S. R.; Bender, M. The proprotein convertase amontillado (amon) is required during Drosophila pupal development. *Dev. Biol.* **2009**, *333*, 48–56.

(55) Brand, A. H.; Perrimon, N. Targeted gene expression as a means of altering cell fates and generating dominant phenotypes. *Development* **1993**, *118*, 401–415.

(56) Lenz, C.; Williamson, M.; Hansen, G. N.; Grimmelikhuijzen, C. J. Identification of four Drosophila allatostatins as the cognate ligands for the Drosophila orphan receptor DAR-2. *Biochem. Biophys. Res. Commun.* **2001**, *286*, 1117–1122.

(57) Williamson, M.; Lenz, C.; Winther, A. M.; Nässel, D. R.; Grimmelikhuijzen, C. J.; Winther, M. E. Molecular cloning, genomic organization, and expression of a B-type (cricket-type) allatostatin preprohormone from Drosophila melanogaster. *Biochem. Biophys. Res. Commun.* **2001**, *281*, 544–550.

(58) Williamson, M.; Lenz, C.; Winther, A. M.; Nässel, D. R.; Grimmelikhuijzen, C. J. Molecular cloning, genomic organization, and expression of a C-type (Manduca sexta-type) allatostatin preprohormone from Drosophila melanogaster. *Biochem. Biophys. Res. Commun.* **2001**, *282*, 124–130.

(59) Yoon, J. G.; Stay, B. Immunocytochemical localization of Diploptera punctata allatostatin-like peptide in Drosophila melanogaster. *J. Comp. Neurol.* **1995**, *363*, 475–488.

(60) Roller, L.; Yamanaka, N.; Watanabe, K.; Daubnerová, I.; Zitnan, D.; Kataoka, H.; Tanaka, Y. The unique evolution of neuropeptide genes in the silkworm Bombyx mori. *Insect Biochem. Mol. Biol.* **2008**, *38*, 1147–1157.

(61) Birse, R. T.; Johnson, E. C.; Taghert, P. H.; Nässel, D. R. Widely distributed Drosophila G-protein-coupled receptor (CG7887) is activated by endogenous tachykinin-related peptides. *J. Neurobiol.* **2006**, *66*, 33–46.

(62) Poels, J.; Birse, R. T.; Nachman, R. J.; Fichna, J.; Janecka, A.; Vanden Broeck, J.; Nässel, D. R. Characterization and distribution of NKD, a receptor for Drosophila tachykinin-related peptide 6. *Peptides* **2009**, *30*, 545–556.

(63) Winther, A. M. E.; Siviter, R. J.; Isaac, R. E.; Predel, R.; Nässel, D. R. Neuronal expression of tachykinin-related peptides and gene transcript during postembryonic development of Drosophila. *J. Comp. Neurol.* **2003**, *464*, 180–196.

(64) Predel, R.; Neupert, S.; Garczynski, S. F.; Crim, J. W.; Brown, M. R.; Russell, W. K.; Kahnt, J.; Russell, D. H.; Nachman, R. J. Neuropeptidomics of the mosquito *Aedes aegypti*. *J. Proteome Res.* **2010**, *9*, 2006–2015.

(65) Wegener, C.; Neupert, S.; Predel, R. Direct MALDI-TOF mass spectrometric peptide profiling of neuroendocrine tissue of Drosophila. *Methods Mol. Biol.* **2010**, *615*, 117–127.

(66) Predel, R.; Wegener, C.; Russell, W. K.; Tichy, S. E.; Russell, D. H.; Nachman, R. J. Peptidomics of CNS-associated neurohemal systems of adult Drosophila melanogaster: a mass spectrometric survey of peptides from individual flies. *J. Comp. Neurol.* **2004**, *474*, 379–392.

(67) Wegener, C.; Reinl, T.; Jänsch, L.; Predel, R. Direct mass spectrometric peptide profiling and fragmentation of larval peptide hormone release sites in Drosophila melanogaster reveals tagma-specific peptide expression and differential processing. *J. Neurochem.* **2006**, *96*, 1362–1374.

(68) Predel, R.; Wegener, C. Biology of the CAPA peptides in insects. *Cell. Mol. Life Sci.* **2006**, *63*, 2477–2490.

(69) Moffett, S. B.; Moffett, D. F. Comparison of immunoreactivity to serotonin, FMRFamide and SCPb in the gut and visceral nervous system of larvae, pupae and adults of the yellow fever mosquito Aedes aegypti. *J. Insect Sci.* **2005**, *5*, 20.

(70) Muren, J. E.; Nässel, D. R. Isolation of five tachykinin-related peptides from the midgut of the cockroach Leucophaea maderae: existence of N-terminally extended isoforms. *Regul. Pept.* **1996**, *65*, 185–196.

(71) Muren, J. E.; Nässel, D. R. Seven tachykinin-related peptides isolated from the brain of the Madeira cockroach: evidence for tissue-specific expression of isoforms. *Peptides* **1997**, *18*, 7–15.

(72) Winther, A. M.; Muren, J. E.; Ahlborg, N.; Nässel, D. R. Differential distribution of isoforms of Leucophaea tachykinin-related peptides (LemTRPs) in endocrine cells and neuronal processes of the cockroach midgut. *J. Comp. Neurol.* **1999**, *406*, 15–28.

(73) Predel, R.; Neupert, S.; Roth, S.; Derst, C.; Nässel, D. R. Tachykinin-related peptide precursors in two cockroach species. *FEBS J.* **2005**, *272*, 3365–3375.

(74) Veelaert, D.; Baggerman, G.; Derua, R.; Waelkens, E.; Meeusen, T.; Vande Water, G.; De Loof, A.; Schoofs, L. Identification of a new tachykinin from the midgut of the desert locust, Schistocerca gregaria, by ESI-Qq-oa-TOF mass spectrometry. *Biochem. Biophys. Res. Commun.* **1999**, *266*, 237–242.

(75) Clynen, E.; Schoofs, L. Peptidomic survey of the locust neuroendocrine system. *Insect Biochem. Mol. Biol.* **2009**, *39*, 491–507.

(76) Kahsai, L.; Kapan, N.; Dircksen, H.; Winther, A. M. E.; Nässel, D. R. Metabolic stress responses in Drosophila are modulated by brain neurosecretory cells that produce multiple neuropeptides. *PLoS One* **2010**, *5*, e11480.

(77) Vömel, M.; Wegener, C. Neurotransmitter-induced changes in the intracellular calcium concentration suggest a differential central modulation of CCAP neuron subsets in Drosophila. *Dev. Neurobiol.* **2007**, *67*, 792–808.

(78) Rehfeld, J. F.; Bundgaard, J. R.; Hannibal, J.; Zhu, X.; Norrbom, C.; Steiner, D. F.; Friis-Hansen, L. The cell-specific pattern of cholecystokinin peptides in endocrine cells versus neurons is governed by the expression of prohormone convertases 1/3, 2, and 5/6. *Endocrinology* **2008**, *149*, 1600–1608.

(79) Carlsson, M. A.; Diesner, M.; Schachtner, J.; Nässel, D. R. Multiple neuropeptides in the Drosophila antennal lobe suggest complex modulatory circuits. *J. Comp. Neurol.* **2010**, *518*, 3359–3380.

(80) Park, D.; Veenstra, J. A.; Park, J. H.; Taghert, P. H. Mapping peptidergic cells in Drosophila: where DIMM fits in. *PLoS One* **2008**, *3*, e1896.

(81) Zitnan, D.; Sehnal, F.; Bryant, P. J. Neurons producing specific neuropeptides in the central nervous system of normal and pupariation-delayed Drosophila. *Dev. Biol.* **1993**, *156*, 117–135.

(82) Price, M. D.; Merte, J.; Nichols, R.; Koladich, P. M.; Tobe, S. S.; Bendena, W. G. Drosophila melanogaster flatline encodes a myotropin orthologue to Manduca sexta allatostatin. *Peptides* **2002**, *23*, 787–794.

(83) Nässel, D. R.; Enell, L. E.; Santos, J. G.; Wegener, C.; Johard, H. A. D. A large population of diverse neurons in the Drosophila central nervous system expresses short neuropeptide F, suggesting multiple distributed peptide functions. *BMC Neurosci.* **2008**, *9*, 90.

(84) Helfrich-Förster, C.; Homberg, U. Pigment-dispersing hormone-immunoreactive neurons in the nervous system of wild-type Drosophila melanogaster and of several mutants with altered circadian rhythmicity. *J. Comp. Neurol.* **1993**, *337*, 177–190.

(85) Nässel, D. R.; Shiga, S.; Mohrherr, C. J.; Rao, K. R. Pigment-dispersing hormone-like peptide in the nervous system of the flies Phormia and Drosophila: immunocytochemistry and partial characterization. *J. Comp. Neurol.* **1993**, *331*, 183–198.

(86) Lee, G.; Bahn, J. H.; Park, J. H. Sex- and clock-controlled expression of the neuropeptide F gene in Drosophila. *Proc. Natl. Acad. Sci. U.S.A.* **2006**, *103*, 12580–12585.

5.2 Peptidomics of the agriculturally damaging larval stage of the cabbage root fly *Delia radicum* (Diptera: Anthomyiidae).

J. Zoephel, W. Reiher, K.-H. Rexer, J. Kahnt and C. Wegener

PLoS ONE 7(7): e41543.

DOI: 10.1371/journal.pone.0041543

Published: July 25, 2012

OPEN ACCESS Freely available online

PLoS one

Peptidomics of the Agriculturally Damaging Larval Stage of the Cabbage Root Fly *Delia radicum* (Diptera: Anthomyiidae)

Judith Zoephel[1¤], Wencke Reiher[1,4], Karl-Heinz Rexer[2], Jörg Kahnt[3], Christian Wegener[1,4]*

1 Department of Biology, Animal Physiology, Philipps-University Marburg, Marburg, Germany, **2** Department of Biology, Mycology, Philipps-University Marburg, Marburg, Germany, **3** Max-Planck-Institute of Terrestrial Microbiology, Marburg, Germany, **4** Neurobiology and Genetics, Theodor Boveri Institute, Biocenter, University of Würzburg, Würzburg, Germany

Abstract

The larvae of the cabbage root fly induce serious damage to cultivated crops of the family Brassicaceae. We here report the biochemical characterisation of neuropeptides from the central nervous system and neurohemal organs, as well as regulatory peptides from enteroendocrine midgut cells of the cabbage maggot. By LC-MALDI-TOF/TOF and chemical labelling with 4-sulfophenyl isothiocyanate, 38 peptides could be identified, representing major insect peptide families: allatostatin A, allatostatin C, FMRFamide-like peptides, kinin, CAPA peptides, pyrokinins, sNPF, myosuppressin, corazonin, SIFamide, sulfakinins, tachykinins, NPLP1-peptides, adipokinetic hormone and CCHamide 1. We also report a new peptide (Yamide) which appears to be homolog to an amidated eclosion hormone-associated peptide in several *Drosophila* species. Immunocytochemical characterisation of the distribution of several classes of peptide-immunoreactive neurons and enteroendocrine cells shows a very similar but not identical peptide distribution to *Drosophila*. Since peptides regulate many vital physiological and behavioural processes such as moulting or feeding, our data may initiate the pharmacological testing and development of new specific peptide-based protection methods against the cabbage root fly and its larva.

Citation: Zoephel J, Reiher W, Rexer K-H, Kahnt J, Wegener C (2012) Peptidomics of the Agriculturally Damaging Larval Stage of the Cabbage Root Fly *Delia radicum* (Diptera: Anthomyiidae). PLoS ONE 7(7): e41543. doi:10.1371/journal.pone.0041543

Editor: Subba Reddy Palli, U. Kentucky, United States of America

Received March 16, 2012; **Accepted** June 22, 2012; **Published** July 25, 2012

Funding: This work was funded by the Deutsche Forschungsgemeinschaft (WE 2652/4-1). The funders had no role in study design, data collection and analysis, decision to publish, or preparation of the manuscript.

Competing Interests: The authors have declared that no competing interests exist.

* E-mail: christian.wegener@uni-wuerzburg.de

¤ Current address: Max-Planck-Institute of Terrestrial Microbiology, Marburg, Germany

Introduction

The cabbage root fly *Delia radicum* is a serious pest species on cultivated Brassicaceae (e.g. cabbage, turnip, swede) in the temperate holarctic region. Up to 60–90% of untreated brassica crops can be regionally damaged by a cabbage root fly infestation, while average losses of untreated crop may be somewhat above 20% (see [1], [2] for review). The damaging life stage of *D. radicum* is the larva also known as cabbage maggot. After hatching from eggs deposited at the root base close to the ground, larvae first feed on smaller rootlets. Later on, with growing size, they also attack the main root. This largely subterranean life of the larva and the long emergence period of the adult flies make pesticide control difficult and ineffective [3]. In recent time, *D. radicum* has enlarged its host range and is now attacking rapeseed (*Brassica napus* L.) in several countries, in Germany and Czech Republic since the mid-1990ies [3,4]. Since rapeseed monocultures have increased considerably due to biofuel and oil production, *D. radicum* is causing considerable economic losses additional to the damage to food crops.

Neuropeptides and peptides from endocrine cells (together referred to as regulatory peptides) and especially their synthetic mimetics with improved bioavailability and peptidase-resistance have a high potential for specific and environmentally friendly pest control since they can regulate feeding, development and reproduction (see [5,6]). Though the chemical or biotechnological synthesis of peptides is still comparatively expensive, bioactive peptides can potentially be ectopically expressed in transgenic plants. Also peptide uptake through the insect cuticle or gut can be considerably enhanced by lipophilic and degradation-resistant analogues (e.g. [7]), or by coupling to molecules like lectins which are transported through the gut epithelium [8].

Here we report the mass spectrometric characterisation of 38 peptides (including variants of different size and N-terminal pyroglutamination) from the central nervous system (CNS) and midgut of *D. radicum* larvae. We further describe the cellular distribution of selected sets of peptidergic neurons and enteroendocrine cells, and morphologically characterise the major neurohemal organs of this species. Genomic or EST data are not available for *D. radicum*, and at the onset of our work, no peptide sequence data were available for this species. Recently, however, Audsley and colleagues [9] elucidated the sequence of 20 neuropeptides including variants from the CNS of adult *D. radicum*. Our results confirm the occurrence of all but two of these neuropeptides also in the damaging life stage (i.e. the larva), and reveal further peptides and peptide families that are either absent or have so far not been found in adult flies. The now available peptide data may initiate the development of new specific peptide-

based protection methods against the difficult-to-control cabbage root fly.

Materials and Methods

Insects

Adult *D. radicum* were reared at 20°C and an L:D cycle of 16:8 in a small flight cage [10]. Both dry and wet food was provided. The dry food consisted of dextrose, skim milk powder, soy flour and brewer's yeast in a 10:10:1:1 ratio. The wet food consisted of honey, soy flower and brewer's yeast in a 5:5:1 ratio, if necessary diluted with water. For egg deposition, small pieces of swedes were placed into the fly cage. Swede pieces with deposited eggs were then transferred to breeding boxes (Phytacon vessel, Carl Roth, Karlsruhe, Germany) filled with autoclaved bird sand to prevent mould. After approximately three weeks the first pupae appeared on the sand's surface and were transferred to the fly cage again where adult flies eclosed after about one week.

Drosophila virilis were raised on standard *Drosophila* medium at 18°C or 25°C at L:D 12:12.

Peptide Extraction

Larval ring glands (RGs), central nervous systems (CNS) and midgut tissue were dissected on ice in HL3 saline (80 mM NaCl, 5 mM KCl, 1.5 mM $CaCl_2$, 20 mM $MgCl_2$, 10 mM $NaHCO_3$, 5 mM trehalose, 115 mM sucrose, 5 mM HEPES, adjusted to pH of 7.2 with HCl; [11]) using fine forceps and scissors. The tissues were immediately transferred into 40–60 µl extraction solution (90% methanol, 9% gradient grade water, 1% trifluoroacetic acid (TFA) (v/v)) in an Eppendorf low bind tube and incubated for 30 min on ice. CNS were additionally sonicated in a water bath for 15 min to homogenize tissue before incubating 30 min on ice. Subsequently, the samples were centrifuged at 18,000 g for 15 min and the supernatant (peptides dissolved in extraction solution) was transferred to a fresh Eppendorf low bind tube. 10 µl HPLC grade water was added to the extract and methanol was removed by concentrating the sample to 10 µl in a vacuum centrifuge. The concentrated sample was stored at −20°C until further use.

Peptide Coupling with 4-sulfophenyl Isothiocyanate (SPITC) for LC/MS

Based on the method described by Wang *et al.* [12], the concentrated samples were dissolved in 8 µl solvent (50% acetonitrile, 0.01% TFA, 49.99% HPLC grade water (v/v/v)) and sonicated for 20 min in an ultrasonic water bath. After that, the samples were centrifuged for 15 min at 18,000 g and the supernatant was transferred to a fresh Eppendorf low bind tube. 30 µg/µl SPITC (4-Isothio-cyanatobenzenesulfonic acid, Sigma-Aldrich) was added to yield a 92 mM SPITC solution. Then, 3 µl buffer (136 mM $(NH_4)_2CO_3$) was added and after incubating for 30 min at 55°C, the sample was concentrated to a volume of 10 µl by vacuum centrifugation. Then, 20 µl of 0.5% acetic acid were added and the sample was subjected to HPLC.

Capillary RP-HPLC

The concentrated unlabelled samples were dissolved in 40–60 µl eluent A (98% HPLC grade water, 2% acetonitrile, 0.05% TFA (v/v/v)) for 30 min at room temperature and sonicated for 20 min in a water bath. After centrifugation for 15 min at 18,000 g, the supernatant was transferred to a fresh low bind Eppendorf tube and injected into an UltiMate 3000 capillary HPLC system (Dionex, Idstein, Germany) connected to a Proteineer Fraction Collector (Bruker Daltonik GmbH, Bremen, Germany). SPITC-labelled samples were injected in 0.5% acetic acid. The samples were loaded onto a RP C18 trap column (Acclaim PepMap100 C18, 5 µm, 100 Å) with eluent A at a flow rate of 20 µl/min. Then the flow was switched through the trap column and the analytical RP column (Acclaim PepMap100 C18, 3 µm, 100 Å) with a rate of 2 µl/min. Peptides were eluted with a linear gradient from 4%−60% eluent B (80% acetonitrile, 20% HPLC grade water, 0.04% TFA (v/v/v)) in 30 min. 1 µl sample fraction mixed with 1 µl of matrix solution (half-saturated recrystallised α-cyano-4-hydroxycinnamic acid in 60% acetonitrile, 40% HPLC grade water, 0.1% TFA (v/v/v)) was spotted every 30 s onto a stainless steel MALDI target plate (Applied Biosystems/MDS SCIEX, Foster City, CA, USA).

Sample Preparation for Direct MS Peptide Profiling

Direct peptide profiling was performed on single larval tissues and the dorsal sheath of the adult thoracico-abdominal ganglion (TAG) as described [13]. The tissues were dissected in saline (128 mM NaCl, 2 mM KCl, 1.8 mM $CaCl_2$, 4 mM $MgCl_2$, 36 mM sucrose, 5 mM HEPES, adjusted to pH 7.1 with NaOH; [14]), briefly rinsed in a fresh droplet of Aqua bidest, and then transferred onto a stainless steel MALDI target plate. A small amount of matrix solution (saturated recrystallised α-cyano-4-hydroxycinnamic acid in 30% methanol, 30% ethanol, 0.1% TFA (v/v)) was added with a manual oocyte injector (Drummond Digital, Broomall, PA, USA).

MALDI TOF MS/MS

Masses were analysed with a 4800 *Plus* MALDI TOF/TOF Analyser (Applied Biosystems/MDS SCIEX, Foster City, CA, USA) at a laser wavelength of 355 nm. Settings like laser intensity and the number of sub-spectra per plate spot varied among the samples and were adjusted individually. The device was calibrated with a peptide calibration standard (Applied Biosystems Calibration Mixture 2). Peptides from the LC/MS samples were fragmented by post-source decay (PSD). For direct tissue profiling, both PSD and collision-induced dissociation (CID) were applied depending on sample condition. MS/MS spectra were interpreted using Data Explorer 4.10 software (Applied Biosystems/MDS SCIEX, Foster City, CA, USA).

Data Base Entry

The peptide sequences have been submitted to the Uniprot database (http://www.uniprot.org/); accession numbers are listed in Table 1.

Immunostainings

CNS with and without RG attached were dissected on ice in HL3 saline and immediately fixed in 4% paraformaldehyde in 0.01 M phosphate-buffered saline (PBS), pH 7.1 for 3.5 h at 4°C. Afterwards tissues were washed 5 times for 10 min in PBT (0.1 M PBS with 0.3% TritonX) on a shaker at room temperature (RT). Preincubation with 10% normal goat serum (Dianova, Hamburg, Germany) in PBT for 4 h at RT on a shaker was followed by the incubation with primary antisera diluted in PBT and 10% normal goat serum for 2 days at RT on a shaker. The following polyclonal rabbit primary antibodies were used: anti-Dip-AST-A (kind gift of Hans Agricola, Jena, Germany [15]) diluted 1:5000, anti-RFamide (kind gift of Eve Marder, Brandeis, USA [16]) diluted 1:4000, anti-SIFa (kind gift of Peter Verleyen and Liliane Schoofs, Leuven, Belgium [17]) diluted 1:500, anti-DH31 (kind gift of Jan Veenstra, Bordeaux, France [18]), anti-Lem-Tachykinin-related peptide (kind gift of Dick Nässel, Stockholm, Sweden [19]), anti-MIP and anti-PRXa (kind gift of Manfred Eckert, Jena, Germany

Table 1. Sequences, accession numbers and tissue distribution of the peptides characterised in *D. radicum* larvae.

Peptide	Sequence[a]	Mass $[M+H]^+$	UniProt Accession	CNS	ring gland	tPSOs[b]	aPSOs[b]	midgut	SPITC-labeled[c]	detected in adults [9]
A-type allatostatins										
AST-A_{909}	ARPYSFGLa	909.50	B3EWI2	Y				Y	Y	Y
AST-A_{921}[d]	LPVYNFGLa	921.43	B3EWL8					Y		Y
AST-A_{952}	NRPYSFGLa	952.49	B3EWJ3	Y				Y	Y	Y
AST-A_{953}	VERYAFGLa	953.53	B3EWJ4	Y				Y	Y	Y
C-type allatostatins										
AST-C	pQVRYRQcYFNPIScF	1904.90	B3EWJ5	Y				Y		
AST-C	QVRYRQcYFNPIScF	1921.87	B3EWJ6	Y				Y		
FMRFamide-like peptides										
$FMRFa_{885}$	GDNFMRFa	885.42	B3EWJ7	Y					Y	
$FMRFa_{899}$	GQDFMRFa	899.42	B3EWJ8	Y					Y	
$FMRFa_{925}$	PDNFMRFa	925.44	B3EWJ9	Y		Y			Y	Y
$FMRFa_{942}$	GGNDFMRFa	942.44	B3EWK0	Y		Y			Y	Y
$FMRFa_{971}$[d]	EQDFMRFa	971.50	-			Y				Y
$FMRFa_{996}$	PGQDFMRFa	996.48	B3EWK1	Y		Y				
$FMRFa_{1067}$	APGQDFMRFa	1067.51	B3EWK2	Y		Y				Y
$FMRFa_{1097}$	TPGQDFMRFa	1097.60	B3EWK3	Y		Y			Y	Y
$FMRFa_{1154}$	SAPGQDFMRFa	1154.54	B3EWK4	Y		Y				?[e]
$FMRFa_{1181}$	LPEQDFMRFa	1181.60	B3EWK5	Y		Y			Y	?[e]
$FMRFa_{1185}$	SAQGQDFMRFa	1185.53	B3EWK8	Y		Y			Y	
Yamides										
Ya	LPSIGHYYa	948.50	B3EWK9	Y	Y				Y	
Kinins										
Kinin	NSVVLGKKQRFHSWGa	1741.40	B3EWL0	Y						
putative CAPA-peptides										
CAPA-pyrokinin	AGPSATTGVWFGPRLa	1515.81	B3EWL1	Y	Y		Y		Y	
CAPA-pyrokinin$^{2-15}$	GPSATTGVWFGPRLa	1444.78	B3EWL2	Y	Y				Y	
CAPA-periviscerokinin-1	GGGGTSGLFAFPRVa	1321.72	B3EWL3	Y			Y		Y	
CAPA-periviscerokinin-2	AGLFAQPRLa	971.59	B3EWL4	Y			Y		Y	
putative HUGIN-peptides										
HUG-pyrokinin	SVQFKPRLa	973.59	B3EWL5	Y	Y					Y
short neuropeptide Fs										
sNPF-1$^{4-11}$	SPSLRLRFa	974.61	B3EWL6	Y	Y				Y	Y
sNPF-1	AQRSPSLRLRFa	1329.80	B3EWL7	Y	Y				Y	Y
Myosuppressin										
Myosuppressin	TDVDHVFLRFa	1247.70	B3EWL9	Y	Y				Y	Y
Myosuppressin$^{2-10}$	DVDHVFLRFa	1146.59	B3EWM0	Y						
Corazonin										
Corazonin	pQTFQYSRGWTNa	1369.69	B3EWM1	Y	Y					Y
Corazonin$^{3-11}$	FQYSRGWTNa	1157.56	B3EWM2	Y					Y	
SIFamides										
SIFa	AYRKPPFNGSIFa	1395.74	B3EWH1	Y					Y	
Sulfakinins										
Sulfakinin	GGEEQFDDYGHMRFa	1686.68	B3EWM3	Y					Y	Y
Sulfakinin$^{6-14}$	FDDYGHMRFa	1186.52	B3EWM4	Y					Y	Y
Tachykinin-related peptides										
TK_{1010}	TPTAFYGVRa	1010.55	B3EWM5	Y				Y	Y	

Table 1. Cont.

Peptide	Sequence[a]	Mass $[M+H]^+$	UniProt Accession	CNS	ring gland	tPSOs[b]	aPSOs[b]	midgut	SPITC-labeled[c]	detected in adults [9]
TK_{1116}[f]	GLGNNAFLGVRa	1116.62	B3EWM6	Y				Y	Y	
NPLP1-peptides										
APK[g]	SVAALAAQGLL[YNAPK]	1586.85	B3EWM9	Y					Y	
Adipokinetic hormones										
AKH	pQLTFSPDWa	975.48	B3EWM7		Y					Y
AKHGK	pQLTFSPDWGK	1161.62			Y					Y
AKHGKR	pQLTFSPDWGKR	1317.65			Y					
CCHamide 1 peptides										
CCHa 1	ScLEYGHScWGAHa	1446.56	B3EWM8					Y		

a)Leu and Ile have the same molecular mass. Since we did not obtain distinguishing high-energy collision w-fragments [76], we are unable to distinguish between these two amino acids. Therefore, Leu and Ile in the sequences above have to be considered as predicted only based on the homolog peptides from *Drosophila* or other Dipterans. Small letter c within a sequence indicates cysteines that form an intramolecular disulfide bridge.
b)tPSO = thoracic PSO, aPSO = abdominal PSO, data from direct profiling of the dorsal sheath of the adult thoracico-abdominal ganglion.
c)these peptides could be sequenced in their SPITC-labelled form.
d)Mass peak indicative of this peptide appeared consistently, but could not be fragmented. Sequence adapted from [9].
e)a peptide with similar mass but different sequence (SPKQDFMRFa, 1154.6 Da and KPNQDFMRFa, 1181.6 Da) was reported by Audsley et al. [9].
f)The y9-fragment identifying the sequence order of positions 2–3 could not be found in SPITC-labelled and unlabeled spectra. The sequence LG is assumed since a very similar tachykinin (*Cav*-TKII: GLGNNAFVGVRa) was isolated and Edman-sequenced from the blowfly *Calliphora vomitoria* [73].
g)Only amino acids 1–11 of APK have been fully fragmented and are sequence identical to the N-terminus of APK of *Drosophila melanogaster* [24,28]. The y-fragment representing amino acids 12–16 matches the mass of amino acids 12–15 of *Drosophila* APK plus the mass of tyrosine. Therefore, we assume the listed sequence. The position of the tyrosine and the C-terminal NAPK is not confirmed by fragmentation data.
doi:10.1371/journal.pone.0041543.t001

[20,21] diluted 1:5000. The mouse monoclonal anti-PDF serum (donated by Justin Blau, obtained from the Developmental Studies Hybridoma Bank developed under the auspices of the NICHD and maintained by The University of Iowa, Department of Biology, Iowa City, USA) was diluted 1:100.

After three washing steps with PBT, the samples were incubated with affinity-purified goat-anti rabbit or goat-anti mouse Cy3 or Cy5 IgG (Jackson Immunoresearch, Pa., USA) diluted 1:100 in PBT and 10% normal goat serum for 2 days in constant darkness on a shaker. 3 washing steps of 10 min in PBT followed before a final wash in PBS. Tissues were mounted in 80% glycerol in 0.1 M PBS and analyzed with a confocal laser scanning microscope (TCS SP5, Leica, Wetzlar, Germany).

Scanning Electron Microscopy

Samples were dissected in HL3 saline and fixed in 5% glutaraldehyde in 0.1 M PBS, pH 7.1, for 2 h at 4°C. Then, the samples were briefly dipped into chloroform and fixed further in 5% glutaraldehyde as above overnight. After washing, the samples were postfixed for 2 h in osmiumtetroxide (1% in 0.1 M Sörensen buffer, pH 7.2). Fixed samples were washed in Sörensen buffer and water, dehydrated in ethylene-glycol monoethylether over night followed by three 10 min changes in 100% acetone, and critical-point-dried using a Polaron E3000 (Balzer Union). Afterwards, samples were sputtered with gold particles with a sputter coater (Balzer Union), and then examined on a Hitachi S-530 scanning electron microscope.

Results

LC-MS/MS of Ring Gland Extracts

To characterise the sequence of *D. radicum* neuropeptides, we started with an LC-MS/MS analysis of extracts from 10–40 pooled ring glands (2 runs without, 4 runs with SPITC labelling). Automatic PSD peptide fragmentation was based first on a mass list containing the masses obtained by direct profiling (see below) and masses of biochemically identified *Drosophila* peptides, and subsequently on signal intensity. Some of the extracted peptide samples were coupled with 4-sulfophenyl isothiocyanate (SPITC) to direct fragmentation towards y-fragments [12,22]. The selective enhancement of y-fragments after SPITC labelling strongly decreases the complexity of PSD fragmentation patterns. This facilitates the interpretation of fragment spectra in general [23], and also improved *de novo* sequencing of *D. radicum* peptides considerably.

The LC/MS-analysis revealed the presence of HUG-PK, sNPF-1, sNPF-1^{4-11}, AKH, AKHGK (a processing intermediate of AKH), myosuppressin and corazonin in the ring gland. All peptide sequences were validated by fragmentation (see Table 1). Interestingly, we found and fragmented the $[M+H]^+$ adduct of AKH (975.5 Da, Fig. S1), which in *Drosophila* and other insects is only found as a sodium or potassium adduct (e.g. [24,25,26]). SPITC labelling of an unknown peptide ion with the mass of 948.5 Da yielded a full y-fragment spectrum (Fig. 1). Since leucine and isoleucine are mass-identical and cannot be distinguished based on y-fragments, this fragment spectrum indicates the amino acid sequence (L/I)PS(L/I)GHYYamide. The C-terminal amidation is a unique modification of bioactive neuropeptides [27], hence the sequence and occurrence in the ring gland suggest that this peptide -designated here as Yamide- may be stored and released as a bioactive peptide hormone. Yamide shows no sequence-similarity with any hitherto sequenced insect peptide, suggesting it constitutes a new insect peptide family.

Neuropeptides from the Central Nervous System

For identification and sequence analysis of peptides from the larval CNS, we performed LC-MS/MS of a SPITC-labelled and an unlabeled extract of 40 CNS with attached ring glands. Peptides were then identified by aligning the measured fragmen-

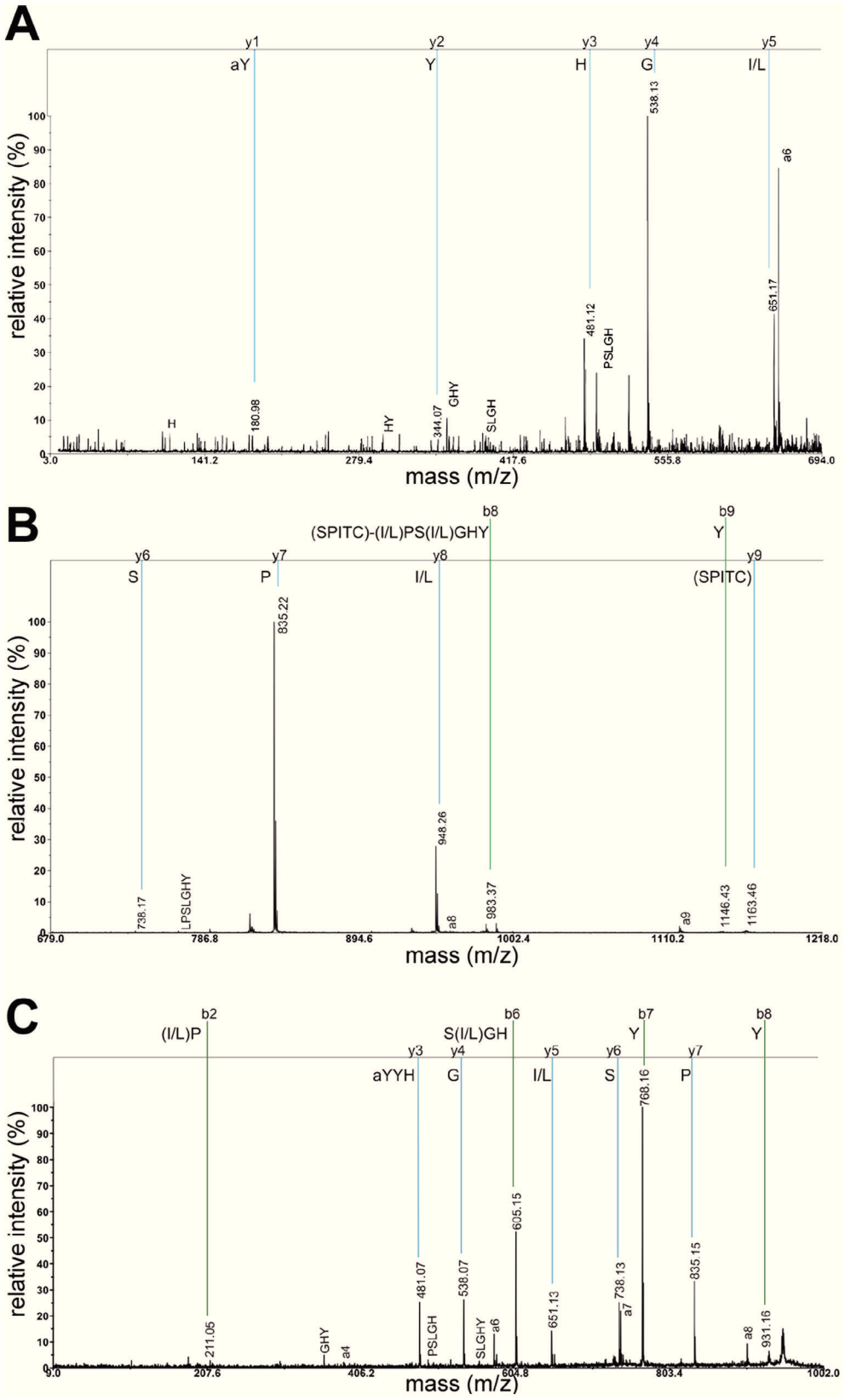

Figure 1. MS/MS spectrum of Yamide. A+B) SPITC-labelled; C) unlabeled. A+B) The fragment spectrum was divided, therefore the relative intensities vary. y-fragments are labelled with blue lines, b-fragments with green lines. Internal and a-fragments are shown as well.
doi:10.1371/journal.pone.0041543.g001

tation patterns with known peptides from *Drosophila* [25,28] and adult *D. radicum* [9] as well as through manual *de novo* fragment annotation. The data revealed the presence of three A-type allatostatins, one C-type allatostatin with and without N-terminal pyroGlu, 10 FMRFa-like peptides, Yamide, CAPA-PK, CAPA-PK[2–15], HUG-PK, CAPA-PVK-1 and -2, sNPF-1 and sNPF-1[4–11], myosuppressin, myosuppressin[2–10], SIFamide, sulfakinin, sulfakinin[6–14], corazonin and corazonin[3–11], two tachykinin-related peptides and a peptide very similar to *Drosophila* APK [28]. The sequences of these peptides are given in Table 1, the fragmentation spectra are shown in Fig. S2, S3, S4, S5, S6, S7, S8, S9, S10, S11, S12, S13, S14, S15, S16, and S17. Since sequences of *D. radicum* prepropeptide genes or ESTs are not available, it is difficult to rationally assign numbers for the different paracopies of the multicopy peptide families AST-A, tachykinin-related peptides and FMRFamides. As a neutral system, we therefore refer to the peptides with their mass as index (e.g. AST-A_{909} instead of AST-A-1). Instead of the typical C-terminal sequence PRVa, CAPA-PVK-2 from *D. radicum* ends on PRLamide, which has hitherto only been observed in the closely related flesh fly *Neobellieria bullata* as well as locusts (see [29]). Additionally, we also yielded the sequence of a kinin from direct peptide profiling and fragmentation of ventral ganglion fragments (Fig. 2). This kinin is sequence-identical to the kinin of *Drosophila* species [30].

Peptides from the Midgut

Two LC-MS/MS runs of peptide extracts from 20 and 25 *D. radicum* larval midguts respectively led to the identification of four A-type allatostatins, one C-type allatostatin occurring with and without N-terminal pyroGlu, two tachykinin-related peptides and CCHamide1 (Table 1). AST-A_{909} and AST-A_{953}, the AST-C and the two tachykinins had also been detected in the CNS by LC-MS/MS. AST-A_{921} has been found in the CNS by Audsley and colleagues [9]. All but one midgut peptide can thus be classified as brain-gut peptides. CCHamide1 was exclusively detectable in the midgut, but represents a brain-gut peptide in *Drosophila melanogaster* [31] and may have escaped detection in the *D. radicum* CNS.

Direct Peptide Profiling and Fragmentation of Peptide Hormones from Neurohemal Organs

To identify potential neuropeptide hormones among the characterised peptides, we performed direct peptide profiling of isolated neurohemal tissues from individual larvae. The neurohemal organs associated with the CNS are the major source of neuropeptide hormones in insects. They consist of the corpora cardiaca (CC, containing terminals of secretory neurons with somata in the pars lateralis and pars intercerebralis), and the thoracic and abdominal perisympathetic organs (PSOs, containing terminals of secretory neurons with somata in the thoracic and abdominal neuromeres respectively). The CC also comprise an endocrine compartment containing the adipokinetic hormone (AKH)-producing cells. Scanning electron microscopy shows that the morphology of these organs in *D. radicum* larvae is typical for a cyclorrhaphan (Fig. 3): the CC are fused with the corpora allata and prothoracic gland and form a ring gland (Fig. 3A). Each thoracic neuromere shows a blind-ending thoracic PSO at its dorsal surface as also shown for *Drosophila* and *Calliphora* [32,33]. Unlike *Drosophila*, however, *D. radicum* appears to have four instead of three abdominal PSOs, visible as swellings of the median/transverse nerves (Fig. 3B).

Earlier studies in *Drosophila* and other flies showed that direct mass spectrometric profiling of neurohemal organs leads to specific extraction and detection of peptides, while non-peptidergic signals are largely absent (e.g. [24,25,30,34,35]). A typical direct profile of a larval ring gland is shown in Figure 4A. The masses of 948.5 Da, 974.5 Da, 997.4/1013.4 Da, 1247.6 Da, 1329.8 Da and 1369.6 Da correspond to Yamide, sNPF-1[4–11], AKH (Na^+ and K^+ adduct), myosuppressin (MS), sNPF-1 and corazonin from the ring gland of various *Drosophila* species [25,30]. *D. radicum* CAPA-PK[2–15] (1444.7 Da) and, with much less intensity, CAPA-PK (1515.2

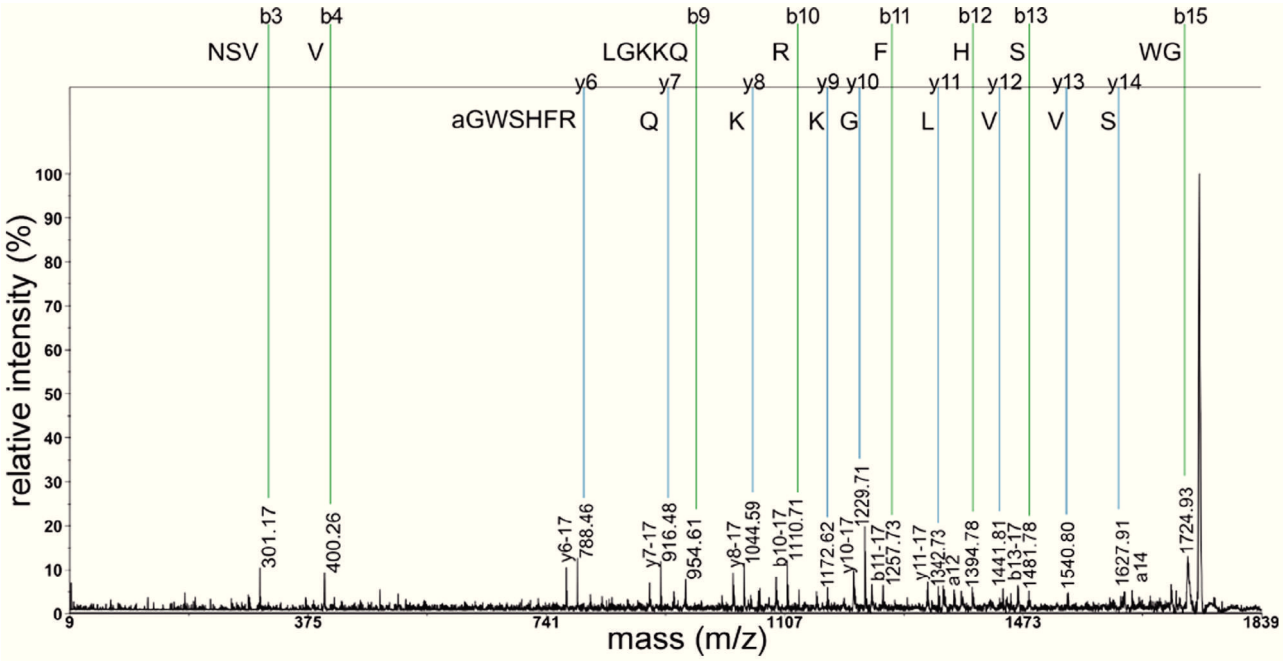

Figure 2. MS/MS PSD spectrum of kinin, obtained by direct profiling of a piece of the ventral ganglion.
doi:10.1371/journal.pone.0041543.g002

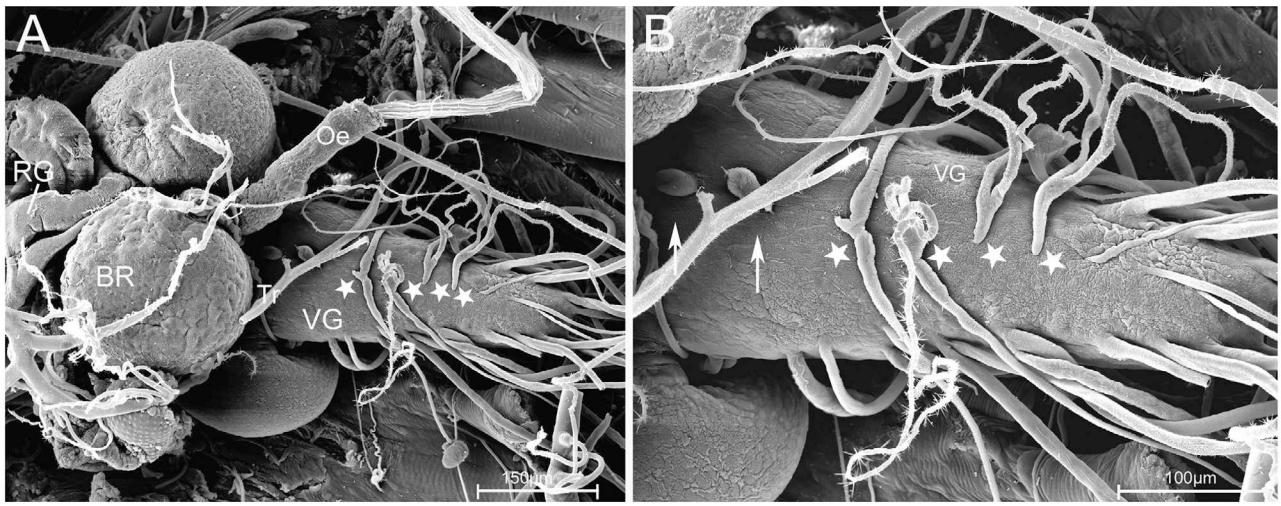

Figure 3. Morphology of the neurohemal organs of a *D. radicum* larva, scanning electron microscopy. A) Dorsal view of the larval nervous system consisting of the two brain hemispheres (BR) and the ventral ganglion (VG, to the right) comprising the suboesophageal, thoracic and abdominal neuromeres. The ring gland (RG) is visible to the left, attached to the brain. The stars mark the abdominal PSOs. B) Enlarged picture of the ventral ganglion. Four abdominal PSOs (stars) are visible as thickenings of the median/transverse nerve. Also two blindly-ending thoracic PSOs (arrows) are visible. Oe = oesophagus, Tr = trachea.
doi:10.1371/journal.pone.0041543.g003

Da) were consistently abundant. Also the AKH processing intermediates AKHGK (1161.6 Da) and AKHGKR (1317.6 Da) could consistently be detected, as well as *D. radicum* HUG-PK (973.6 Da) previously identified by Audsley and colleagues [9] in the adult CC. Subsequent direct PSD/CID fragmentation confirmed the identity of these peptides and the sequence data obtained by LC-MS/MS of CNS extracts (see Table 1). Further consistently detected masses were 939.4 Da, 955.4 Da, 1121.6 Da, 1125.5 Da, 1141.5 Da, 1143.6 Da and 1259.6 Da. None of these masses could be sequenced by direct fragmentation. The monoisotopic peak distribution however suggests that these masses represent peptides which thus remain to be characterised.

The PSOs are very small structures that are very difficult to separate from the larval CNS. Their homolog in adult cyclorrhaphan flies is the dorsal sheath of the adult thoracico-abdominal ganglion (TAG) [32,33,36,37,38,39] which is much easier to dissect. A typical profile of this adult dorsal sheath is shown in Figure 4B (anterior "thoracic" region) and Figure 4C (posterior "abdominal" region).

The profiles of the thoracic region showed many different mass peaks, most of which corresponded to FMRFa-like peptides, while the posterior region is enriched in masses corresponding to CAPA peptides. With the exception of $FMRFa_{899}$, all FMRFamide-like peptides identified by LC-MS/MS in whole CNS extracts could also be detected in the thoracic dorsal sheath preparation. This may suggest that $FMRFa_{899}$ represents a degradation or processing intermediate of $FMRFa_{1185}$. A consistent mass peak of 971.5 Da indicates the presence of $FMRFa_{971}$ (EQDFMRFa) reported from adult *D. radicum* [9]. This peptide had not been found by LC-MS and could not be fragmented. Also APSQDFMRFa with an oxidised mass of 1113.5 Da characterised by Audsley *et al.* [9] from adult cabbage root flies was not found by LC-MS/MS of CNS extracts. However, a matching mass peak consistently occurred in direct profiles of the thoracic preparation but could not be fragmented - it may thus equally well represent the oxidised form of the mass-identical TPGQDFMRFa (= $FMRFa_{1097}$). The peaks corresponding to $FMRFa_{1097}$ and $FMRFa_{1154}$ gave higher signal intensities than other FMRFa-like peptides, suggesting that the peptides are encoded in three and two copies in the *fmrf* prepropeptide gene respectively (e.g. [24,25]). Alternatively, if APSQDFMRFa also occurs in the larva albeit undetected, the peak at 1097.6 Da represents the integrated intensity of both APSQDFMRFa and TPGQDFMRFa.

The profiles of the abdominal dorsal sheath preparation only showed four peaks, corresponding to CAPA-PVK-1 and -2, CAPA-PK and a mass of 2217.2 Da. The same preparation in other fly species show also three CAPA peptides [24,34] plus -at least in *Drosophila* species- a non-amidated cleavage product in the 2200 Da range (CAPA precursor protein B (CPPB)) [25,30]. While a direct fragmentation could not be achieved, it is therefore likely that the peak at 2217.2 Da represents the CPPB of *D. radicum*.

Distribution Pattern of Peptidergic Cells

To compare the general cellular architecture of peptidergic systems in *D. radicum* larvae with that of other flies, we performed immunofluorescent stainings with a host of peptide antisera.

Peptidergic neurons in the CNS and ring gland. *AST-A IR:* Clusters of AST-A IR cell bodies and descending neurites are prominent in the brain and ventral ganglion (Fig. 5A-C), and are highly similar in number and morphology to the bilateral pairs of AST-A PMP, LP and LT neurons in the brain, and the DMA, VMA, LA and LAa neurons in the ventral ganglion of larval *Drosophila* [40,41]. *D. radicum* has, however, further pairs of AST-A IR brain neurons, e.g. in the posterior protocerebrum (Fig. 5B). Like in *Drosophila*, the LAa neurons send neurites to the hindgut through segmental nerve 8/9 and the ring gland is devoid of AST-A IR; neurites projecting towards the ring gland could not be detected (Fig. 5A). Also in adult *Calliphora*, posterior AST-A IR LAa-like neurons innervate the hindgut, and the CC are devoid of AST-A IR [42].

SIFamide IR: Two pairs of strongly SIFamide-immunoreactive somata are located in the pars intercerebralis (Fig. 5D-E). Their axons project to contralateral parts of the protocerebrum and descend through the entire ventral ganglion. Thus, the pattern is identical to that of the larval SIFamide neurons in *Drosophila*

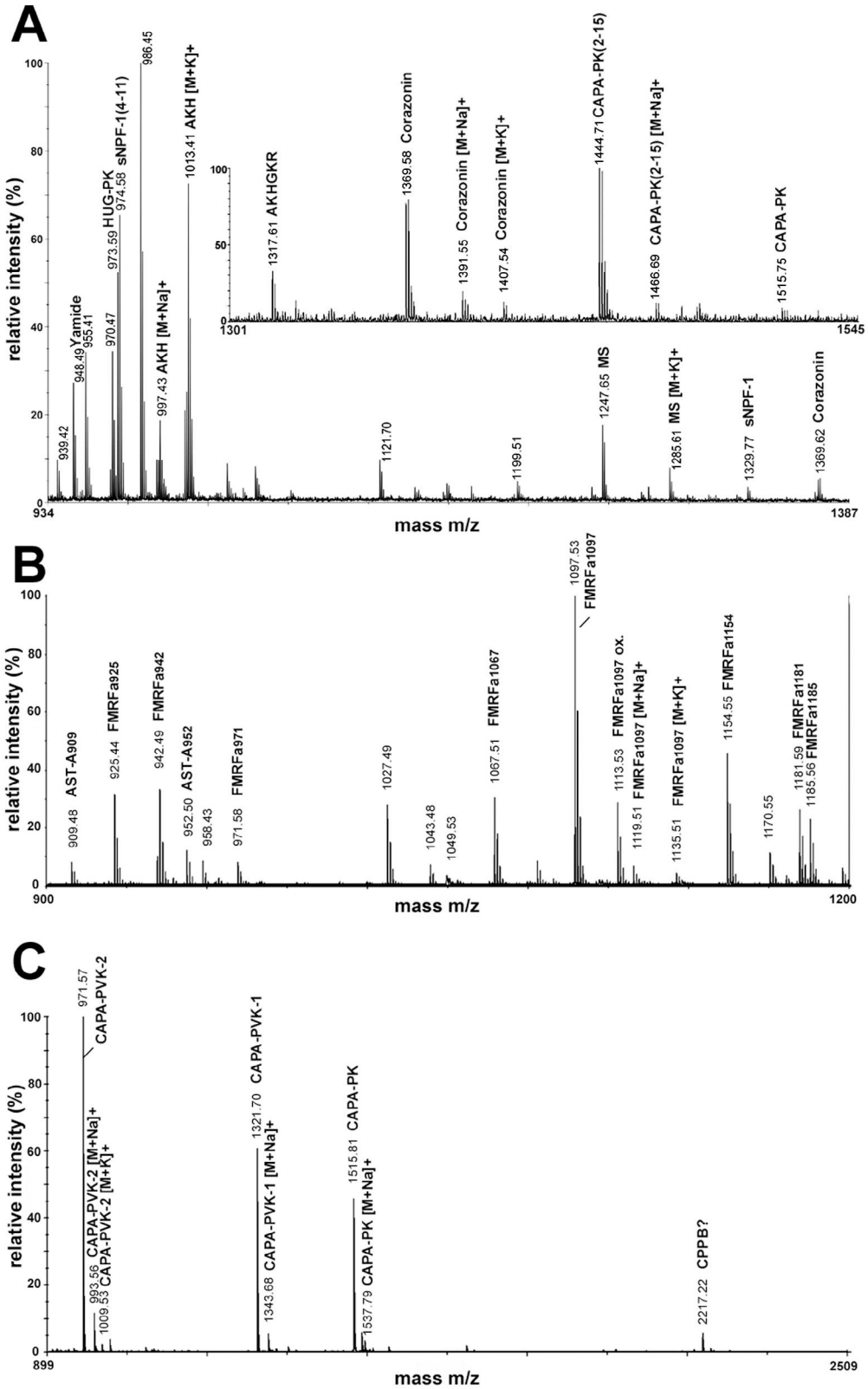

Figure 4. Typical spectra from direct peptide profiling. (A) Profile of the larval ring gland, (B) the anterior (thoracic), and (C) posterior (abdominal) portion of the adult dorsal sheath of the TAG. For some peptides, sodium and potassium adducts are visible besides the typical $[M+H]^+$ adducts.

doi:10.1371/journal.pone.0041543.g004

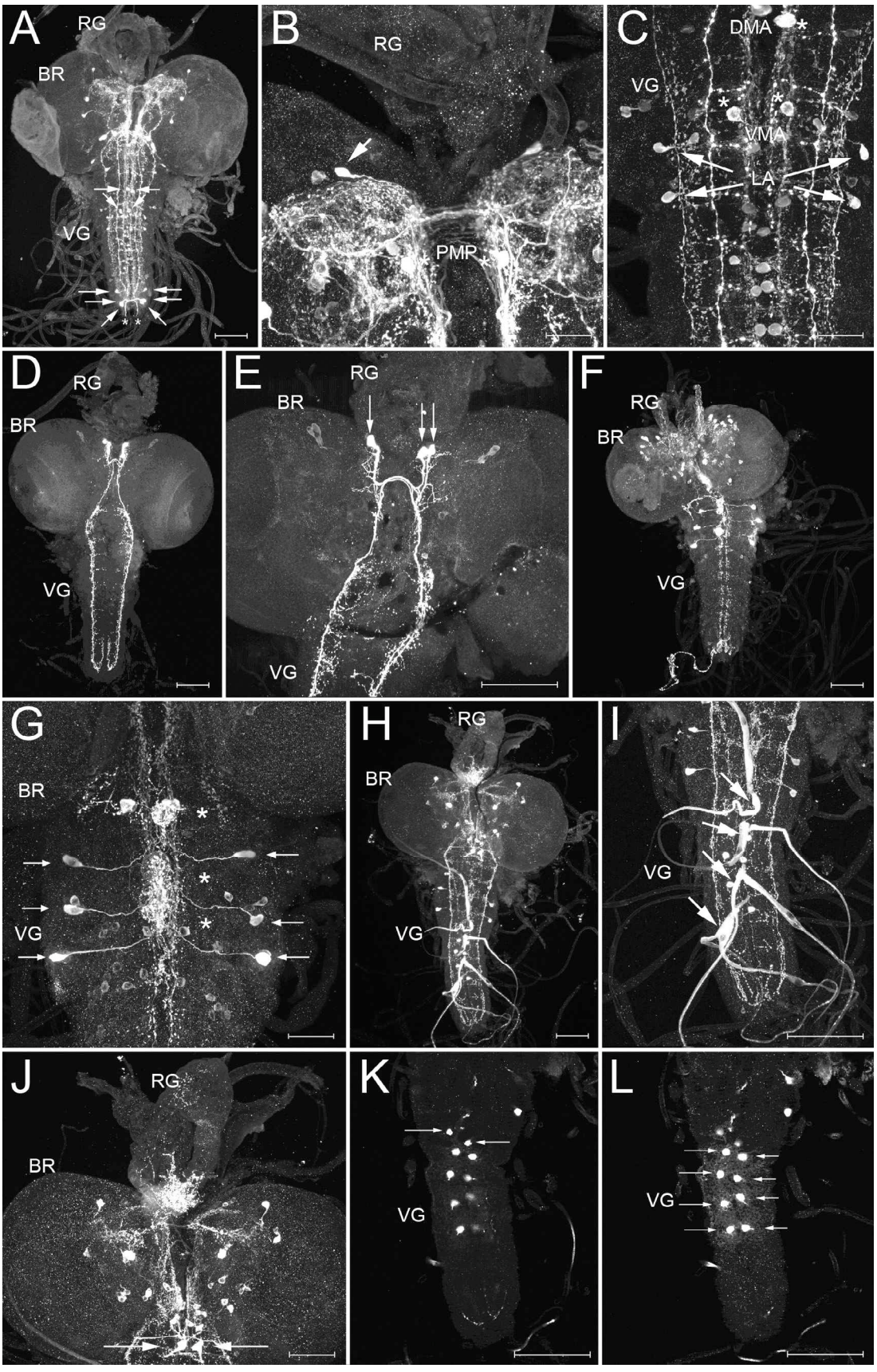
A
RG
BR
VG
B
RG
PMP
C
DMA
VG
VMA
LA
D
RG
BR
VG
E
RG
BR
VG
F
RG
BR
VG
G
BR
VG
H
RG
BR
VG
I
VG
J
RG
BR
K
VG
L
VG

Figure 5. Wholemount immunostainings of the larval CNS. A-C) AST-A immunoreactivity. A) Dorsal overview (maximum projection). Arrows point to prominently stained somata in the ventral ganglion. Exiting neurites innervating the hindgut are marked by an asterisk. B) Detail of the dorsal protocerebrum showing a pair of strongly labelled PMP-like neurons (asterisks) and a strongly labelled neuron not described in *Drosophila* (arrow). C) Detail of the metathoracic and first abdominal neuromeres, showing the strongly labelled MA (asterisks) and LA (arrows) neurons, and further very weakly stained cells at the midline. D-E) SIFa immunoreactivity. D) Dorsal overview (maximum projection) of the two pairs of SIFa neurons in the protocerebrum, that send contralaterally descending fibres through the ventral ganglion. E) Close-up showing the arborisation pattern of the descending fibres. Somata are marked by arrows. F-G) FMRFa-like IR. F) Dorsal overview (maximum projection) of the whole CNS. Immunoreactive somata are most prominent in the dorsal protocerebrum and the thoracic neuromeres. G) Detail of the thoracic neuromeres. The thoracic PSOs are strongly stained in a varicose fashion likely due to stored peptide vesicles (asterisks). A pair of strongly stained Tv neurons is visible in each neuromere (arrows). H-L) PRXa-like IR. H) Dorsal overview (maximum projection) of the whole CNS. Immunoreactive somata are most prominent in the dorsal protocerebrum, suboesophageal ganglion and the anterior abdominal neuromeres. I) Detail showing the ventral ganglion with four pairs of strongly stained median/transverse nerves in the anterior abdominal neuromeres. The swellings along the median and transverse nerves represent the abdominal PSOs (arrows). J) Detail showing the brain, ring gland and suboesophageal ganglion. Somata in the protocerebrum are visible. The strong immunoreactivity in the ring gland is due to innervation by the CC-MS neurons (arrows) in the suboesophageal ganglion. K) Detail showing the ventral ganglion with a pair of strongly stained neurons (arrows) anterior to the Va neurons. This pair seems to be a different cell type than the Va neurons due to differences in shape and the lack of neurohemal projections. L) Detail showing the ventral ganglion with four pairs of strongly stained Va neurons (arrows) in the anterior abdominal neuromeres. BR = brain, RG = ring gland, VG = ventral ganglion. Scale bars = 150 μm, in B, C, G and J = 50 μm.
doi:10.1371/journal.pone.0041543.g005

melanogaster and adult *Neobellieria (Sarcophaga) bullata* [17,41] and other insects [17].

FMRFamide IR: The used antiserum recognises not only FMRFamide-like peptides, but (less strongly) also other peptides with a C-terminal RFamide (sNPF, sulfakinin, myosuppressin, neuropeptide F). Relatively weak FMRFamide IR is visible in the ring gland and in bilaterally symmetric somata in the pars intercerebralis (Fig. 5F-G). Since sNPF-1 and myosuppressin are the only RFamides found via mass spectrometry in the ring gland, at least part of this IR is likely to be attributable to sNPF-containing secretory or myosuppressin neurons. A pair of strongly stained secretory neurons is visible in each of the three thoracic neuromeres (Fig. 5G). These neurons innervate the thoracic PSOs and appear to be homolog to the FMRFamide-like peptide expressing Tv neurons of *Drosophila melanogaster* [41,43]. Similar neurons have also been described in larvae of *Lucilia cuprina* [35], *Sarcophaga bullata* [39] and *Calliphora erythrocephala* [33].

PRXamide IR: PRXamide IR labels pyrokinins and periviscerokinins ending on either PRLamide or PRVamide [21]. Prominent PRXamide IR is visible in the CC part of the ring gland, and the abdominal PSOs/transverse nerves 1–4 (Fig. 5H-L). The MS data and the situation in *Drosophila melanogaster* [25] indicates that the ring gland staining represents HUG-PK and CAPA-PK$^{2-15}$, while the aPSO staining represents both CAPA-PK and CAPA-PVKs. Large neurosecretory cells (Fig. 5J) in the suboesophageal neuromeres -likely homologs of the hugin-expressing CC-MS-1 and capa-expressing CC-MS-2 cells of *Drosophila* [44,45,46]- provide the immunoreactivity of the ring gland. Each of the four abdominal PSOs (see Fig. 3) is innervated by a pair of neurons homolog to the Va neurons of *Drosophila* (Fig. 5K-L, [47]). The number of Va neuron pairs thus matches that of abdominal PSOs like in *Drosophila melanogaster* larvae which, however, only have three PSOs and Va neuron pairs respectively [32].

Diuretic hormone-31 (DH31) IR: The antiserum against DH31 stained a complex pattern of somata with broad arborisations in both the brain and ventral ganglion (Fig. 6A-C). Again the overall pattern was very similar to that described in the *Drosophila melanogaster* maggot [48]. The ring gland is innervated by DH31-positive neurites that most likely originate from somata in the pars intercerebralis. Unlike most peptidergic terminals that end in the CC part, these DH31-immunoreactive neurites end in a neurite meshwork in the region of the corpora allata. This opens the possibility that DH31 may play a role in the regulation of juvenile hormone synthesis or release.

Myoinhibiting peptide (MIP) IR: The pattern of MIP immunoreactivity in the brain and ventral ganglion (Fig. 6D-F) was again strongly reminiscent to the situation in *Drosophila melanogaster* [49]. Strongly stained neurons and descending neurites are prominent in the brain (Fig. 6D). In the protocerebrum, one pair of neurites projects contralaterally dorsal to the foramen (Fig. 6E). One pair of median cells in the suboesophageal neuromeres, and a pair of lateral cells in the thoracic and all but the last abdominal neuromeres are stained (Fig. 6F). In larval *Drosophila melanogaster*, similar cells express also CCAP [50]. MIP immunoreactivity also occurred in intrinsic endocrine cells of the glandular CC part of the ring gland (Fig. 6E). Since MIPs could not be detected in the ring gland by mass spectrometry in *D. radicum* and other fly species [9,25,30,51], and since in all insects the intrinsic endocrine cells produce AKH, it seems unlikely that the MIP IR in the ring gland represents the occurrence of MIPs. The antiserum recognises the C-terminus of Pea-MIP (GGWamide), and we thus rather assume a cross-reaction with AKH (ending Wamide) in the ring gland, while the staining in the CNS is more likely to be MIP-specific.

Tachykinin-related peptide (TK) IR: Bilaterally symmetric TK-immunoreactive cells are situated in both brain and ventral ganglion (Fig. 6G-H). No TK-IR was observed in neurohemal organs. Again, the number, pattern of somata and projections is very similar to the situation in *Drosophila* [19,52] and also the blowfly *Calliphora vomitoria* [53], with prominent descending neurites originating in the brain and running along a lateral tract throughout the ventral ganglion. Unlike in *Drosophila* and *Calliphora*, however, TK-immunoreactive somata were not discernible in the suboesophageal ganglion.

Pigment dispersing factor (PDF) IR: Two different clusters of PDF immunoreactive neurons could be observed (Fig. 6I-K). One cluster of four cells is located in each half of the brain, sending projections to the dorsal protocerebrum and to the putative larval optic neuropile (Fig. 6J). The number, morphology and PDF IR identify these cells as homologs of the lateral neurons (LNs) of larval *Drosophila melanogaster* [54]. The second group of PDF-immunoreactive cells is located in abdominal neuromeres 8 and 9, again identical to the situation in *Drosophila melanogaster* [41,54]. Like in the fruit fly [54], their axons exit the ventral ganglion through segmental nerve a8 and innervate the hindgut (Fig. 6K, Fig. 7A). Both LNs and the abdominal neurons also occur in the housefly, though additional PDF-immunoreactive neurons neither found in *Drosophila melanogaster* nor *D. radicum* have been described for larval *Musca domestica* [55].

Peptidergic enteroendocrine cells. Tachykinin-like-immunoreactive enteroendocrine cells (EECs) occurred in a region possibly presenting the anterior-middle midgut junction, and scattered throughout the posterior midgut (Fig. 7B). In larval

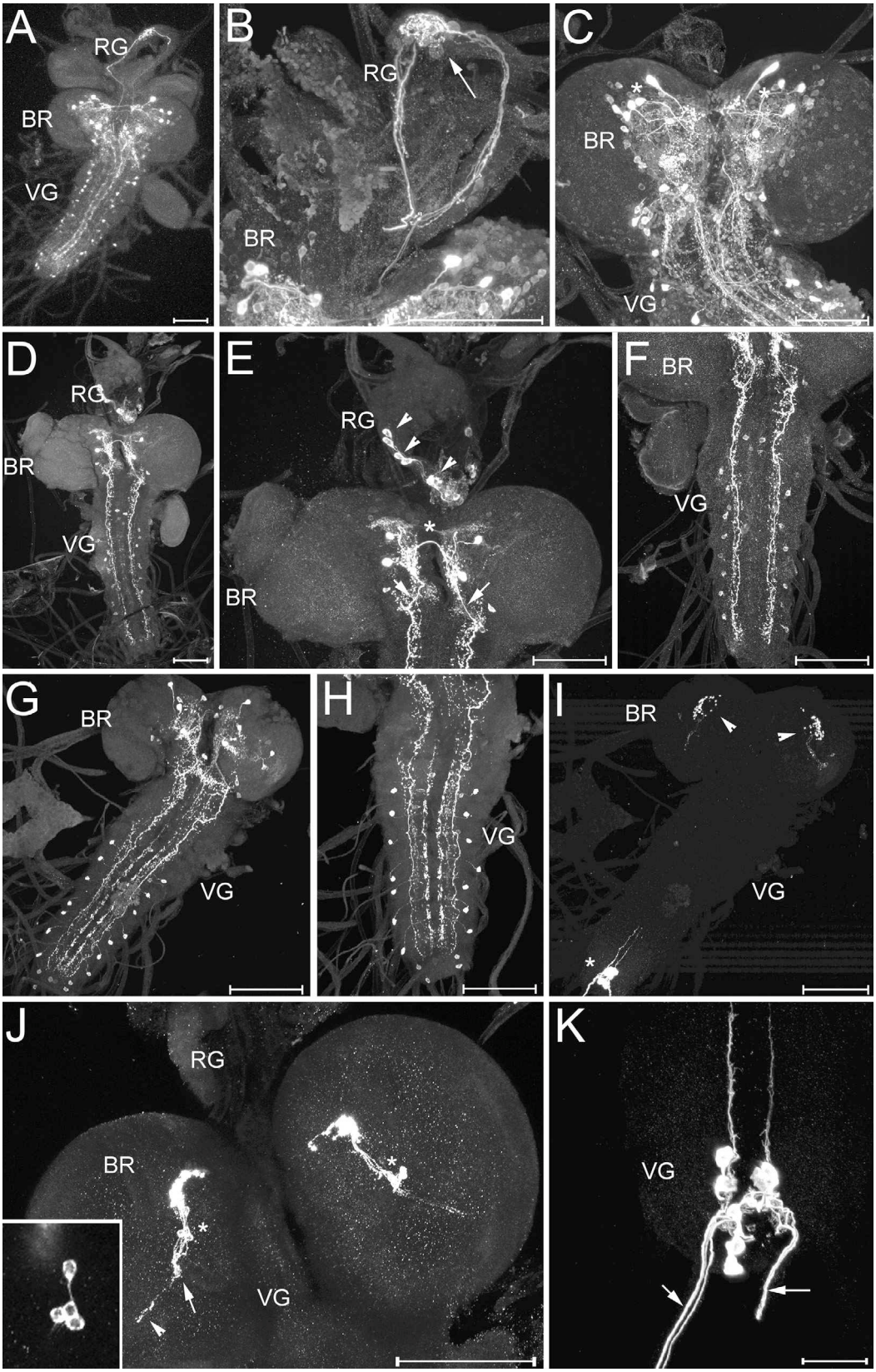

Figure 6. Wholemount immunostainings of the larval CNS. A-C) DH31 immunoreactivity. A) Dorsal overview (maximum projection). Large strongly stained somata in the protocerebrum and further smaller cells are visible, as well as paired lateral neurons in the ventral ganglion. B) Detail of the protocerebrum and ring gland. Several DH31-immunoreactive fibres project over the whole ring gland and branch intensely around the corpora

allata (arrow). C) Close-up of the brain and suboesophageal neuromeres shows that many neurons are DH31-immunoreactive. The most strongly stained neurons in the dorsal protocerebrum (asterisks) may represent the neurosecretory neurons innervating the ring gland, but their exact projection pattern could not be singled out from the dense arborisations. D-F) MIP immunoreactivity. D) Dorsal overview (maximum projection). E) Close-up of the brain and ring gland. Two pairs of large and strongly stained neurons in the brain are visible. While the more dorsal pair appears to send a neurite to the contralateral brain hemisphere (asterisk), the more ventral pair seems to give rise to the descending bilateral fibre (arrows) that projects through the whole ventral nerve cord. Even more ventral in the brain, a pair of smaller neurites is stained. Their processes could not be followed. In the ring gland, intrinsic cells in the corpora cardiaca are labelled (arrow heads). These cells most likely do not produce MIP but are cross-reacting AKH endocrines. F) Close-up of the ventral ganglion. The descending fibres with small branchings and varicosities along their track are visible. One pair of lateral cells in the thoracic and abdominal neuromeres are also stained. G-H) Tachykinin-like peptide immunoreactivity. G) Dorsal overview (maximum projection) and H) magnification of the ventral ganglion. Note the absence of stained somata in the suboesophageal ganglion. I-K) PDF-like immunoreactivity. I) Dorsal overview (maximum projection). The lateral neurons (LNs) in each brain hemisphere with strongly stained arborisations in the dorsal protocerebrum (arrowheads), and the abdominal neurons (asterisk) with neurites projecting to the hindgut are visible. J) Close-up of the two brain hemispheres, each with a group of LNs (asterisks) sending neurites to the dorsal protocerebrum and to the putative larval optic neuropile (arrow). Interestingly, some neurites appear to project beyond the optic neuropile (arrowhead), possibly along the entering optic ("Bolwig") nerve. The inset shows a magnification of the four LNs. K) Close-up of the PDF-neurons in the last abdominal neuromeres which send neurites through the last segmental nerves towards the hindgut (arrows) BR = brain, RG = ring gland, VG = ventral ganglion. Scale bars = 150 μm, in K = 50 μm.

doi:10.1371/journal.pone.0041543.g006

Drosophila melanogaster, tachykinin-like immunoreactive EECs have only been found in the posterior midgut; more anterior parts seem to be devoid of tachykinin-like IR [52,56]. Both in *Drosophila* and *D. radicum* larvae, the highest density of Tk-IR cells in the posterior midgut is seen in the short portion closest to the hindgut.

Like in *Drosophila melanogaster* [40], AST-A-immunoreactive EECs are located in the posterior midgut, and AST-A-IR neurites from the CNS innervate the hindgut (Fig. 8A). The AST-A-IR EECs are apically elongated and teardrop-shaped, thus reminiscent of the typical structure of open type EECs (Fig. 8A).

Strongly stained myoinhibitory peptide (MIP)-IR cells are densely located in a relatively short midgut portion possibly representing the anterior-middle midgut junction (Fig. 8B). Thus, these cells are another common attribute of *D. radicum* and *Drosophila* larvae. Smaller MIP-IR EECs occur in the middle and posterior midgut, whereas in *Drosophila* these portions of the gut show only weak MIP immunoreactivity.

Numerous diuretic hormone 31 (DH31)-IR EECs are located in the posterior portion of the anterior midgut, where they are largest and show open EEC type-like cytoplasmic extensions (Fig. 9). Smaller and more roundish DH31-IR cells are also found in the middle midgut and posterior midgut (Fig. 9).

In general, the pattern of immunoreactivity in the larval midgut is very similar to that described in *Drosophila melanogaster* for AST-A [40,56], while smaller differences occur for TK-, MIP-and DH31-immunoreactive EECs. Like in the fruit fly larva [56], also the larval *D. radicum* hindgut is innervated by PDF-immunoreactive neurites which do not reach the midgut (Fig. 7A).

Yamide is also Present in Drosophila Species and Represents an Eclosion Hormone-related Peptide

C-terminal amidation is a unique modification of regulatory peptides, and is generated from a C-terminal glycine residue by a specific set of enzymes occurring in peptidergic cells [27]. Peptides originating from the break-down of proteins therefore do not carry an amidation signal. The presence of a Yamide signal in direct profilings of the neurohemal ring gland suggests that this peptide is released as a neurohormone, while its amidation may suggest bioactivity. Since peptides are evolutionarily strongly conserved, it would be surprising if Yamide, a peptide without published homologs in other insect species, only occurred in *D. radicum*. An unrestricted blast search based on the sequence LPSIGHYYG identified a highly similar sequence only for *Drosophila* species outside the *melanogaster* group (Fig. 10A). The identified sequence in the non-*melanogaster* fruitflies represents a short peptide stretch of the respective eclosion hormone precursor. This stretch is N-terminally joined to the signal peptide, and C-terminally extended by KR, the processing signal for prohormone convertases. It is also present in the EH prepropeptide of *melanogaster* fruitflies and the relatively closely related mosquitoes and moths, yet with a differing sequence and without an amidation signal (Fig.10A). This predicts that for the *Drosophila* species outside the *melanogaster* group, a Yamide is produced during the normal processing of eclosion hormone. In *Drosophila*, eclosion hormone is stored and released from the ring gland, which predicts that also Yamide should be stored in this neurohemal organ. To test this, we directly profiled the ring gland of wandering L3 larvae of *Drosophila virilis* by MALDI-TOF MS. In all preparations (n = 16), a prominent peak of the predicted mass 785.43 Da was detectable (Fig. 10B). Tandem MS of this peak yielded a complete fragmentation spectrum indicating the sequence LPSIGHYa and thus confirming the presence of Yamide in *Drosophila virilis* (Fig. 10C).

Discussion

We have chemically characterised 38 peptides (including variants of different size and N-terminal pyroglutamination) from the nervous system, neurohemal organs and midgut of larval *D. radicum*. Of these peptides, sNPF [57], HUG-pyrokinin [58], kinins [59,60,61,62], CAPA-PVKs [44,63], AST-A [64] and AKH [65,66,67] have important effects on feeding and diuresis in *Drosophila* and other Dipterans. Since it is likely that the function of these peptides is conserved within the Diptera, their signalling pathways are potential targets for a chemical control of *D. radicum* larvae. The available peptide sequence data for *D. radicum* maggots and adults now allow physiological and pharmacological studies with native peptides in this species, and may possibly provide a platform for the future development of peptide-based protectants against cabbage maggot infestation.

The SPITC Labelling Approach Strongly Improved MALDI-TOF/TOF De Novo Sequencing

Peptide fragmentation by mass spectrometry has largely substituted traditional peptide sequencing methods since it in principle allows *de novo* sequencing of peptides from very little material. A caveat for MALDI-based mass spectrometric peptide fragmentation is that the obtained fragmentation patterns can be very complex due to the many different types of fragments that are generated. These include N- and C-terminal fragments, immonium ions and internal fragments, sometimes accompanied by satellite peaks caused by the loss of water or ammonia. In species with sequenced genome this is rarely a problem, since the whole fragment spectrum can be predicted from the respective candidate gene. Not surprisingly, most insect species with characterised

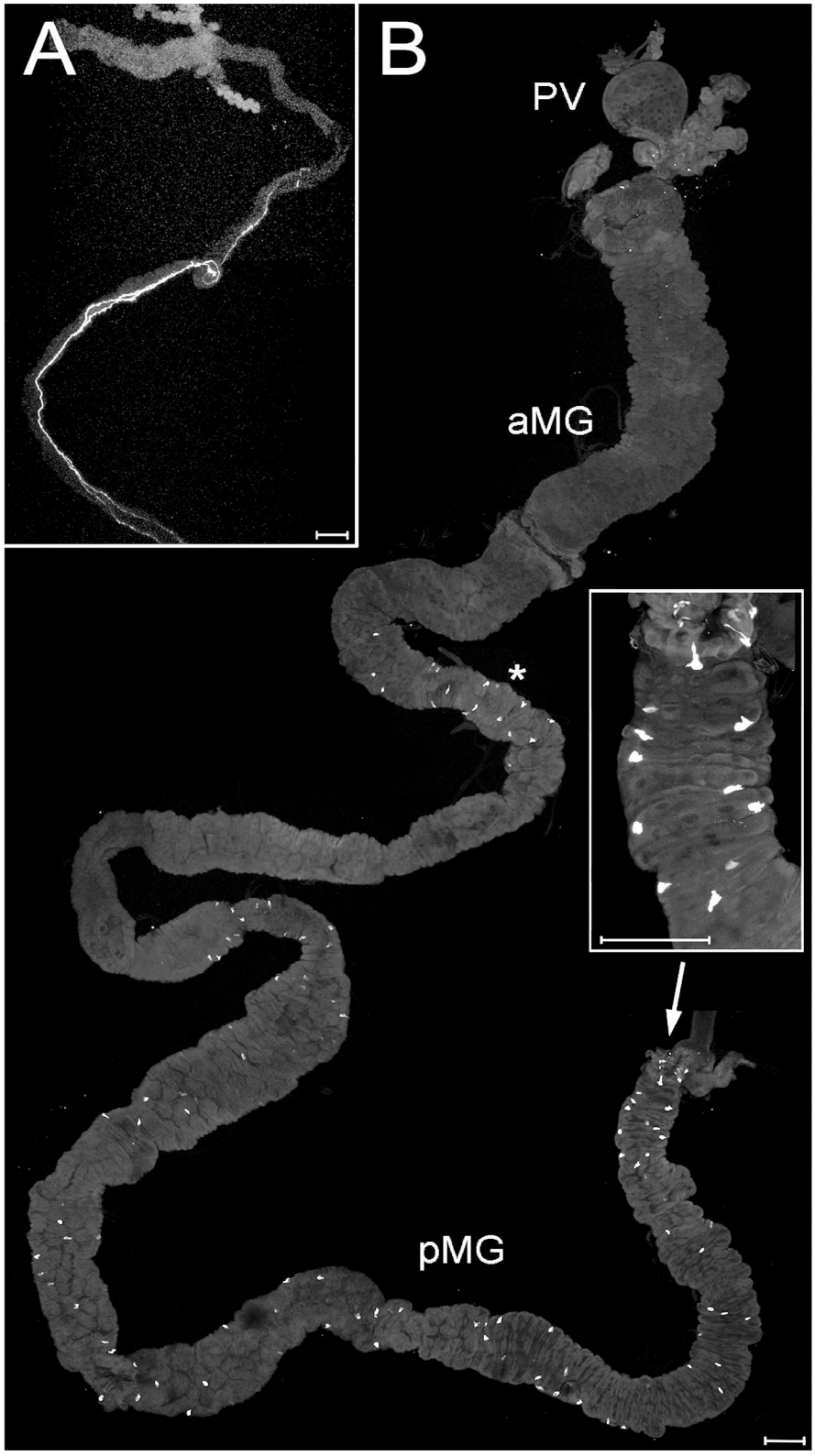

Figure 7. PDF and tachykinin-like immunoreactivity in the larval gut. A) PDF-immunoreactive neurites innervate the hindgut, but do not reach the midgut or Malpighian tubules. B) Tachykinin-like-immunoreactive EECs are visible in a region possibly representing the anterior-middle midgut junction (asterisk). Further immunoreactive cells are scattered throughout the posterior midgut. The most posterior midgut portion is shown enlarged in the inset. PV = proventriculus, aMG = anterior midgut, pMG = posterior midgut. Scale bars = 150 μm.
doi:10.1371/journal.pone.0041543.g007

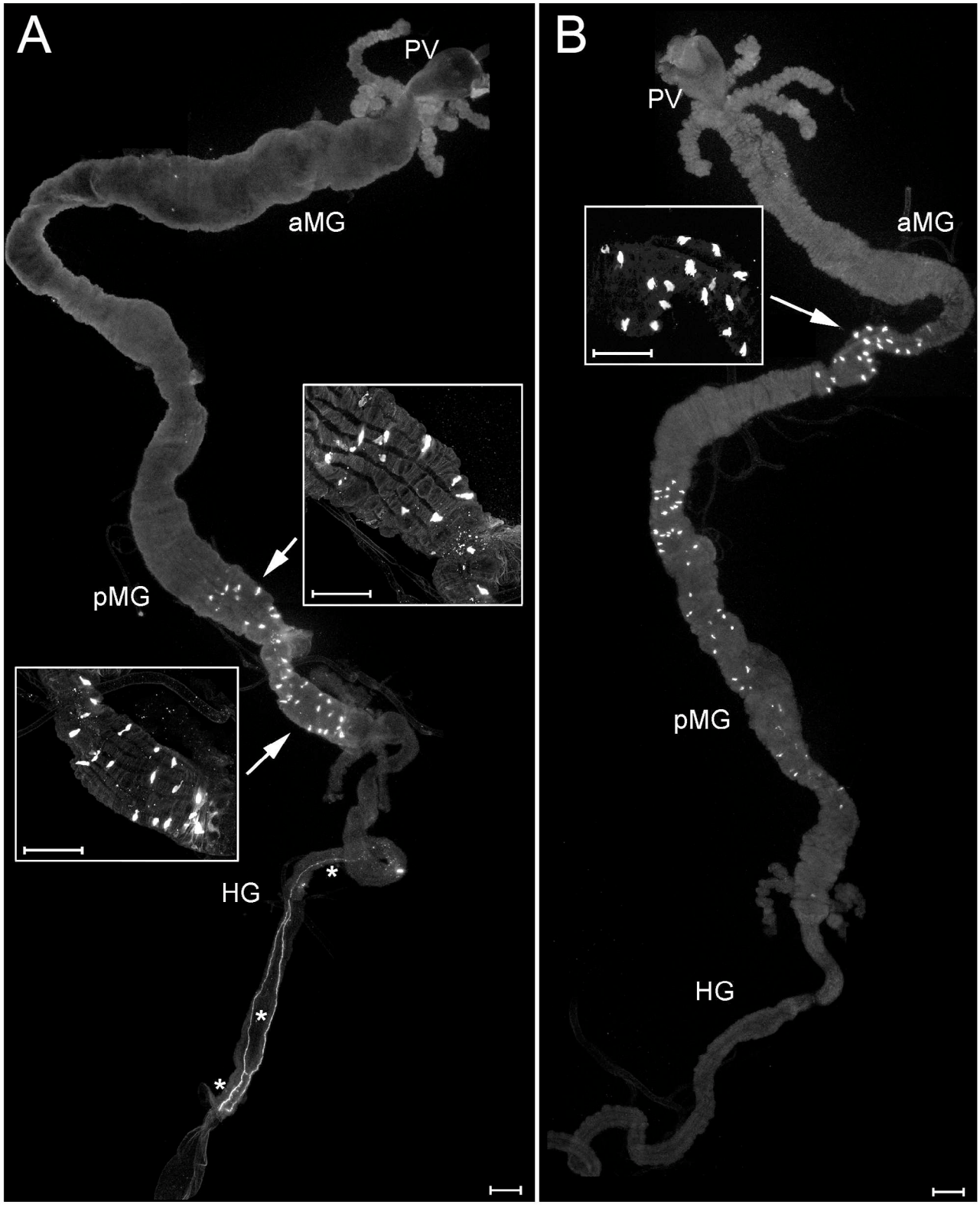

Figure 8. AST-A and MIP (AST-B) immunoreactivity in the larval gut. A) AST-A immunoreactive EECs are located in the posterior midgut, their typical tear-drop like shape is visible in the insets. On the hindgut, AST-A immunoreactive neurites are labelled (asterisks). B) MIP-immunoreactive EECs are densely located in the anterior middle midgut (inset), smaller cells are visible throughout the posterior middle and posterior midgut. PV = proventriculus, aMG = anterior midgut, pMG = posterior midgut, HG = hindgut. Scale bars = 150 μm.
doi:10.1371/journal.pone.0041543.g008

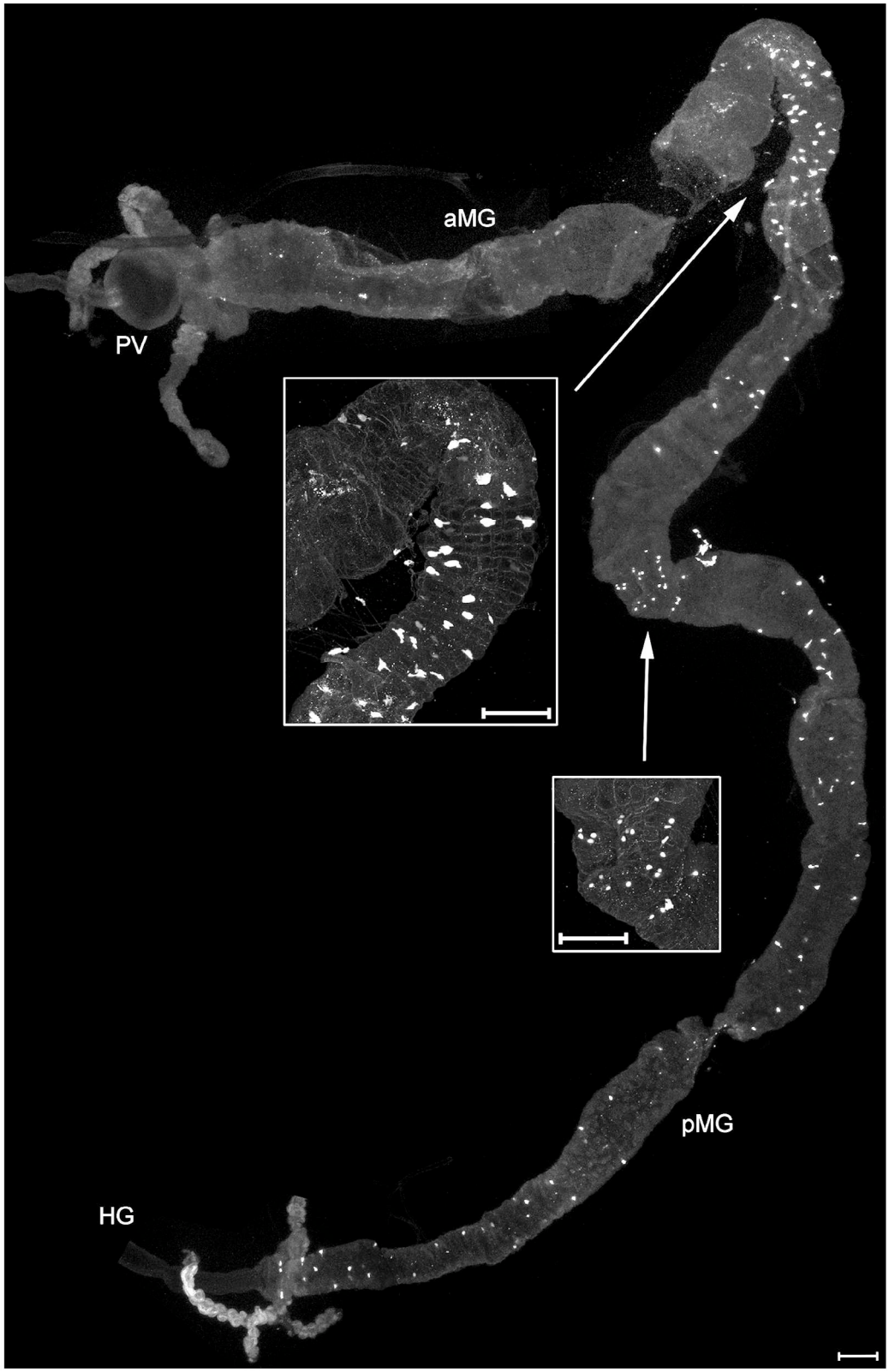

Figure 9. DH31 immunoreactivity in the larval gut. Parts of the midgut containing stained EECs are enlarged in the insets. DH31-immunoreactive EECs are located throughout the middle and posterior midgut, and are also densely distributed around the presumptive anterior-middle midgut junction. PV = proventriculus, aMG = anterior midgut, pMG = posterior midgut, HG = hindgut. Scale bars = 150 μm.
doi:10.1371/journal.pone.0041543.g009

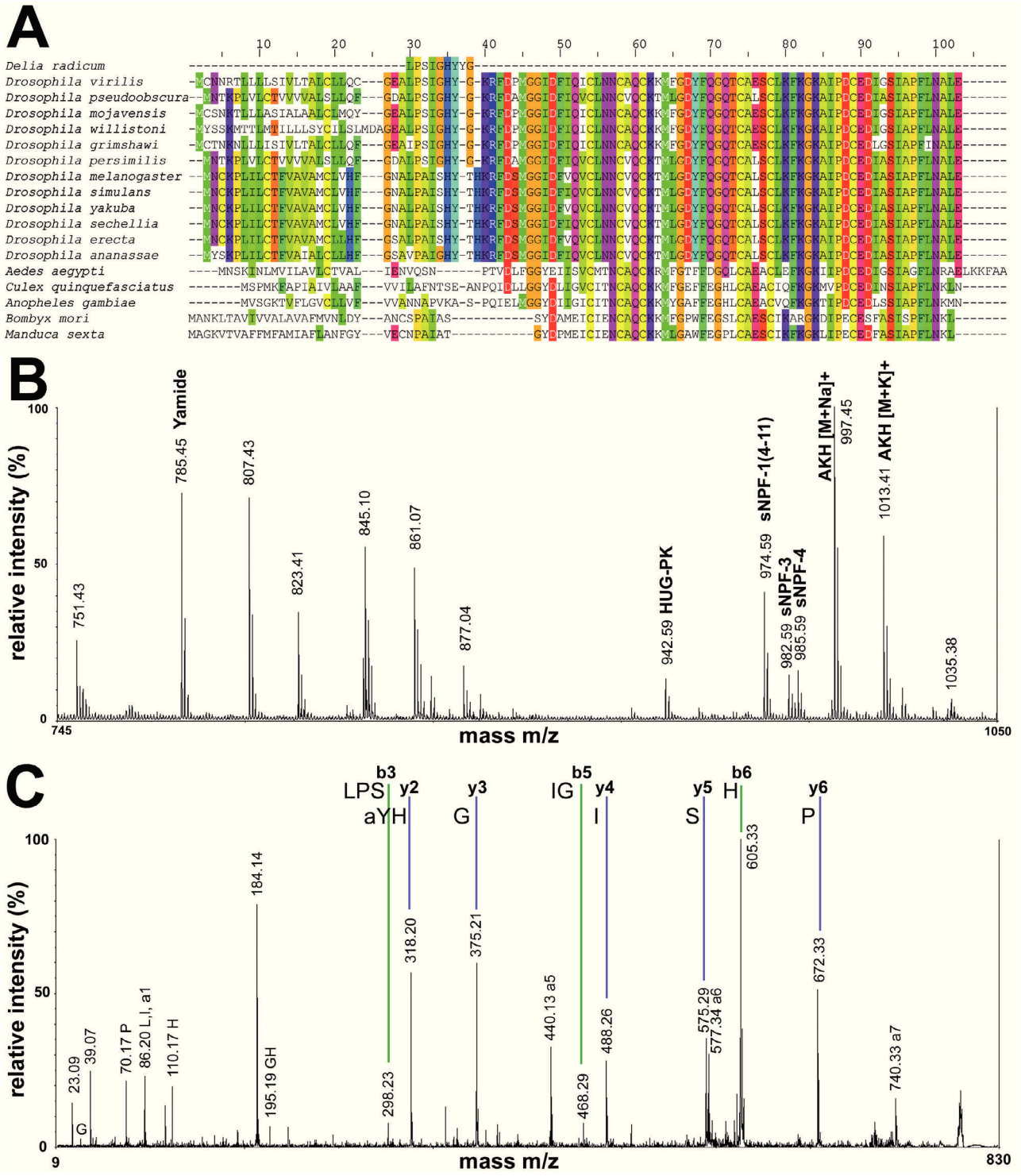

Figure 10. Yamide in Dipterans and moths. A) Alignment of the eclosion hormone prepropeptides of different fly, mosquito and moth species with *D. radicum* Yamide (aligned at position 30), generated with Jalview 2 [77]. The predicted signal peptide cleavage site locates at aligned position 29. In all *Drosophila* species, the Yamide-aligning sequences are followed by a dibasic cleavage site (KR, at aligned position 40), which is absent in mosquitoes and moths. An amidation signal (G) precedes this cleavage sites in fruitflies outside the *melanogaster* group, while the flies of the *melanogaster* group possess the sequence TH instead. B) Direct mass spectrometric profile of the ring gland of a wandering third instar larva of *Drosophila virilis*. Several mass peaks are visible, which above 900 Da represent known neuropeptides. The mass peak at 785.45 corresponding to *Drosophila virilis* Yamide typically showed a high relative intensity comparable with that of the abundant sNPF-1$^{4-11}$ and AKH peptide hormones. C) Combined post-source and collision-induced decay spectrum of the mass peak at 785.45 Da reveals the identity of *Drosophila virilis* Yamide.
doi:10.1371/journal.pone.0041543.g010

peptidomes belong to those (still rather rare) species with a sequenced genome. Considerable peptidomic data for species without sequenced genome or EST data banks exist only for large insects such as cockroaches, locusts and blowflies for which enough peptide could be extracted for traditional Edman sequencing (see [68]) or *de novo* mass spectrometric sequencing [69,70,71]. Since SPITC labelling directs fragmentation towards y-fragments [12,22], it strongly decreased the complexity of the PSD fragmentation pattern in this study. This allowed us to characterise a substantial (so clearly not the full) complement of peptides present in the comparatively small cabbage root fly larvae for which no genomic or suitable EST sequences are available. Our results confirm and extend previous results from adult cabbage root flies [9], suggesting that the neuropeptide complement does not change qualitatively between the maggot and adult fly. Also in *Drosophila*, the peptide complement does not change qualitatively during postembryonic development [24,25,28]. Nevertheless, our sequence data differ from those of Audsley and colleagues for $FMRFa_{1154}$ (SAPGQDFMRFa vs. SPKQDFMRFa) and $FMRFa_{1181}$ (LPEQDFMRFa vs. KPNQDFMRFa), contradictions which will be solved once the *D. radicum fmrf* gene sequence is available. The FMRFamide-like peptides represent the most variable group of insect neuropeptides, and the available fly genes suggest a very high degree of internal variation [30,72]. Moreover, strain-specific FMRFamide-like peptides have been reported for *Lucilia cuprina* [35]. Therefore, it is also possible that the different sequences obtained in this study (based on a laboratory strain originating from Germany) and the study of Audsley *et al.* [9] (based on a UK laboratory strain) are genuine and reflect genetic variation between separated populations.

Immunostainings Confirm the Mass Spectrometric Data and Show that Peptide Families have been Missed by MS

The observed patterns of immunoreactivity for AST-A, SIFa, FMRFamide-like peptides, pyrokinins/periviscerokinins and tachykinin-like peptides confirm the peptide distribution found by direct peptide profiling of neurohemal organs and LC/MS of the CNS and gut. The immunostainings against PDF, MIP and DH31 show, however, that there are further *D. radicum* peptides which we were unable to characterise. Larger peptides such as insulins, eclosion hormone etc. are notoriously difficult for peptidomics and were also not found here. At least, however, PDF, DH31 and MIPs could be detected by LC/MS in *Drosophila melanogaster* [28,31] and may be also detectable in *D. radicum* with improved chromatographic separation reducing ion suppression. Thus, while the available sequence for 38 peptides puts *D. radicum* on the list of the best characterised Dipterans in terms of peptides, there are certainly more peptides to be discovered in this species.

D. radicum Shows Fly-typical Presence and Distribution of Peptide Hormones

In general, the peptide families identified in *D. radicum* are common in cyclorrhaphan fly species (e.g. [24,25,28,30,31,35,51,71]), and the peptide hormone complement in neurohemal organs and enteroendocrine cells is typical for this fly group [24,25,30,56,31,35,34,51]. Moreover, our anatomical results emphasise that the gross distribution and projection patterns of the immunostained peptidergic neurons and enteroendocrine cells in *D. radicum* is largely similar to that in *Drosophila melanogaster* and other less well investigated flies (see section 3.4), even though differences may occur in finer details (e.g. the dendritic projection patterns) which we have not studied here. This chemical and anatomical similarity of peptidergic systems between *D. radicum* and *Drosophila melanogaster* suggests that the fruit fly may well constitute a useful genetically amenable (neuro)endocrine model for cyclorrhaphan pest species besides its importance as a general developmental or neurobiological model organism. This is particularly evidenced by sequence-identical peptides in *Drosophila melanogaster*, *D. radicum* and other flies (e.g. sNPF-1, myosuppressin, SIFamide). Nevertheless, from a peptidomic perspective, *D. radicum* is clearly closer to the blowflies than to *Drosophila melanogaster*. For example, the sulfakinin and tachykinin sequences are much more similar to that of *Calliphora vomitoria* [73,74] than *Drosophila melanogaster* [19,28]. Thus, our sequence data is in support of the phylogenetically grouping of Anthomyiidae, Sarcophagidae and Calliphoridae within the Calyptratae, a sister group of the Ephydroidea (*Drosophila* and allies) [75].

In light of the above, the restricted occurrence of the Yamide in Anthomyiidae and *Drosophila*-species outside the *melanogaster* group is remarkable. Our mass spectrometric data show that Yamide is stored in higher concentrations in the ring gland, but this might simply be a consequence of its C-terminal glycine (absent in e.g. *Drosophila melanogaster*) which is amidated due to co-processing and co-packaging with eclosion hormone. We therefore assume that Yamide represents an evolutionary caprice without biological function, at least until a receptor for this peptide family has been identified.

Supporting Information

Figure S1 MS/MS spectrum of unlabeled AKH.
(TIF)

Figure S2 MS/MS spectrum of AST-A909, SPITC-labelled.
(TIF)

Figure S3 MS/MS spectrum of FMRFa885, SPITC-labelled.
(TIF)

Figure S4 MS/MS spectrum of FMRFa899, SPITC-labelled.
(TIF)

Figure S5 MS/MS spectrum of FMRFa996, unlabeled.
(TIF)

Figure S6 MS/MS spectrum of FMRFa1097 with an oxidised methionine (1113.5 Da), SPITC-labelled.
(TIF)

Figure S7 MS/MS spectrum of FMRFa1154, unlabeled.
(TIF)

Figure S8 MS/MS spectrum of FMRFa1181, SPITC-labelled.
(TIF)

Figure S9 MS/MS spectrum of FMRFa1185, SPITC-labelled.
(TIF)

Figure S10 MS/MS spectrum of CAPA-PK, SPITC-labelled.
(TIF)

Figure S11 MS/MS spectrum of CAPA-PVK-1, SPITC-labelled.
(TIF)

Figure S12 MS/MS spectrum of CAPA-PVK-2, SPITC-labelled.
(TIF)

Figure S13 MS/MS spectrum of SIFa, SPITC-labelled.
(TIF)

Figure S14 MS/MS spectrum of sulfakinin6-14, SPITC-labelled.
(TIF)

Figure S15 MS/MS spectrum of TK1116, SPITC-labelled.
(TIF)

Figure S16 MS/MS spectrum of TK1010, SPITC-labelled.
(TIF)

Figure S17 MS/MS spectrum of APK, SPITC-labelled.
(TIF)

Acknowledgments

We are very grateful to Bernd Ulber (Göttingen) for the kind gift of pupae and valuable advice on *Delia* culturing, to Hans Agricola (Jena), the DSHB (Iowa), Manfred Eckert (Jena), Eve Marder (Brandeis), Dick Nässel (Stockholm), Jan Veenstra (Bordeaux) and Peter Verleyen/Liliane Schoofs (Leuven) for the generous gift of antisera. We also thank Jan Veenstra for the hint regarding Yamide and EH, Lotte Søgaard-Andersen (MPI for Terrestrial Microbiology, Marburg) and Stefan Baumeister (Proteomics Facility, Department of Biology, Philipps-University Marburg) for access to mass spectrometer and fraction collector, Franz Grolig (Philipps-University Marburg) for maintenance of the confocal microscope and Uwe Homberg (Philipps-University Marburg) for general support.

Author Contributions

Conceived and designed the experiments: JZ WR CW. Performed the experiments: JZ WR KHR JK CW. Analyzed the data: JZ WR CW. Contributed reagents/materials/analysis tools: JK KHR. Wrote the paper: JZ WR CW.

References

1. Finch S (1989) Ecological considerations in the management of Delia pest species in vegetable crops. Annu Rev Entomol 34: 117–137.
2. Finch S, Collier R (2000) Integrated pest management in field vegetable crops in northern Europe - with focus on two key pests. Crop Protection 19: 817–824.
3. Erichsen E, Hünmörder S (2005) Kohlfliegenauftreten im Raps. Gesunde Pflanzen 57: 149–157.
4. Muska F, Kazda J, Cerka R (2008) Cabbage maggot (Delia radicum) as a potential rapeseed (Brassica napus L.) pest in the Czech Republic. Can we make use of the German experience? Nachrichtenbl Deut Pflanzenschutzd 60: 252–258.
5. Gäde G, Goldsworthy G (2003) Insect peptide hormones: a selective review of their physiology and potential application for pest control. Pest Manag Sci 59: 1063–1075.
6. Scherkenbeck J, Zdobinsky T (2009) Insect neuropeptides: structures, chemical modifications and potential for insect control. Bioorg Med Chem 17: 4071–4084.
7. Nachman RJ, Mahdian K, Nässel DR, Isaac RE, Pryor N, et al. (2011) Biostable multi-Aib analogs of tachykinin-related peptides demonstrate potent oral aphicidal activity in the pea aphid Acyrthosiphon pisum (Hemiptera: Aphidae). Peptides 32: 587–594.
8. Fitches E, Audsley N, Gatehouse JA, Edwards JP (2002) Fusion proteins containing neuropeptides as novel insect control agents: snowdrop lectin delivers fused allatostatin to insect haemolymph following oral ingestion. Insect Biochem Mol Biol 32: 1653–1661.
9. Audsley N, Matthews HJ, Down RE, Weaver RJ (2011) Neuropeptides associated with the central nervous system of the cabbage root fly, Delia radicum (L). Peptides 32: 434–440.
10. Zohren E (1968) Laboruntersuchungen zu Massenzucht, Lebensweise, Eiablage und Eiablageverhalten der Kohlfliege, Chortophila brassicae Bouché (Diptera, Anthomyiidae). Z Angew Entomol 62: 139–188.
11. Stewart BA, Atwood HL, Renger JJ, Wang J, Wu CF (1994) Improved stability of Drosophila larval neuromuscular preparations in haemolymph-like physiological solutions. J Comp Physiol A 175: 179–191.
12. Wang D, Kalb SR, Cotter RJ (2004) Improved procedures for N-terminal sulfonation of peptides for matrix-assisted laser desorption/ionization post-source decay peptide sequencing. Rapid Commun Mass Spectrom 18: 96–102.
13. Wegener C, Neupert S, Predel R (2010) Direct MALDI-TOF mass spectrometric peptide profiling of neuroendocrine tissue of Drosophila. Methods Mol Biol 615: 117–127.
14. Jan LY, Jan YN (1976) Properties of the larval neuromuscular junction in Drosophila melanogaster. J Physiol (Lond) 262: 189–214.
15. Vitzthum H, Homberg U, Agricola H (1996) Distribution of Dip-allatostatin I-like immunoreactivity in the brain of the locust Schistocerca gregaria with detailed analysis of immunostaining in the central complex. J Comp Neurol 369: 419–437.
16. Marder E, Calabrese RL, Nusbaum MP, Trimmer B (1987) Distribution and partial characterization of FMRFamide-like peptides in the stomatogastric nervous systems of the rock crab, Cancer borealis, and the spiny lobster, Panulirus interruptus. J Comp Neurol 259: 150–163.
17. Verleyen P, Huybrechts J, Baggerman G, Van Lommel A, De Loof A, et al. (2004) SIFamide is a highly conserved neuropeptide: a comparative study in different insect species. Biochem Biophys Res Commun 320: 334–341.
18. Veenstra JA, Agricola H-J, Sellami A (2008) Regulatory peptides in fruit fly midgut. Cell Tissue Res 334: 499–516.
19. Winther AME, Siviter RJ, Isaac RE, Predel R, Nässel DR (2003) Neuronal expression of tachykinin-related peptides and gene transcript during postembryonic development of Drosophila. J Comp Neurol 464: 180–196.
20. Predel R, Rapus J, Eckert M (2001) Myoinhibitory neuropeptides in the American cockroach. Peptides 22: 199–208.
21. Eckert M, Herbert Z, Pollak E, Molnar L, Predel R (2002) Identical cellular distribution of all abundant neuropeptides in the major abdominal neurohemal system of an insect (Periplaneta americana). J Comp Neurol 452: 264–275.
22. Gevaert K, Demol H, Martens L, Hoorelbeke B, Puype M, et al. (2001) Protein identification based on matrix assisted laser desorption/ionization-post source decay-mass spectrometry. Electrophoresis 22: 1645–1651.
23. Leon IR, Neves-Ferreira AGC, Valente RH, Mota EM, Lenzi HL, et al. (2007) Improved protein identification efficiency by mass spectrometry using N-terminal chemical derivatization of peptides from Angiostrongylus costaricensis, a nematode with unknown genome. J Mass Spectrom 42: 1363–1374.
24. Predel R, Wegener C, Russell WK, Tichy SE, Russell DH, et al. (2004) Peptidomics of CNS-associated neurohemal systems of adult Drosophila melanogaster: a mass spectrometric survey of peptides from individual flies. J Comp Neurol 474: 379–392.
25. Wegener C, Reinl T, Jänsch L, Predel R (2006) Direct mass spectrometric peptide profiling and fragmentation of larval peptide hormone release sites in Drosophila melanogaster reveals tagma-specific peptide expression and differential processing. J Neurochem 96: 1362–1374.
26. König S, Albers C, Gäde G (2005) Mass spectral signature for insect adipokinetic hormones. Rapid Commun Mass Spectrom 19: 3021–3024.
27. Prigge ST, Mains RE, Eipper BA, Amzel LM (2000) New insights into copper monooxygenases and peptide amidation: structure, mechanism and function. Cell Mol Life Sci 57: 1236–1259.
28. Baggerman G, Boonen K, Verleyen P, De Loof A, Schoofs L (2005) Peptidomic analysis of the larval Drosophila melanogaster central nervous system by two-dimensional capillary liquid chromatography quadrupole time-of-flight mass spectrometry. J Mass Spectrom 40: 250–260.
29. Predel R, Wegener C (2006) Biology of the CAPA peptides in insects. Cell Mol Life Sci 63: 2477–2490.
30. Wegener C, Gorbashov A (2008) Molecular evolution of neuropeptides in the genus Drosophila. Genome Biol 9: R131.
31. Reiher W, Shirras C, Kahnt J, Baumeister S, Isaac RE, et al. (2011) Peptidomics and Peptide hormone processing in the Drosophila midgut. J Proteome Res 10: 1881–1892.
32. Santos JG, Pollák E, Rexer KH, Molnár L, Wegener C (2006) Morphology and metamorphosis of the peptidergic Va neurons and the median nerve system of the fruit fly, Drosophila melanogaster. Cell Tissue Res 326: 187–199.
33. Nässel DR, Ohlsson LG, Cantera R (1988) Metamorphosis of identified neurons innervating thoracic neurohemal organs in the blowfly: Transformation of cholecystokininlike immunoreactive neurons. J Comp Neurol 267: 343–356.
34. Predel R, Russell WK, Tichy SE, Russell DH, Nachman RJ (2003) Mass spectrometric analysis of putative capa-gene products in Musca domestica and Neobellieria bullata. Peptides 24: 1487–1491.
35. Rahman MM, Fromm B, Neupert S, Kreusch S, Predel R (2009) Extended FMRFamides in dipteran insects: conservative expression in the neuroendocrine system is accompanied by rapid sequence evolution. Gen Comp Endocrinol 162: 52–58.
36. Duve H, Thorpe A, Nässel DR (1988) Light- and electron-microscopic immunocytochemistry of peptidergic neurons innervating thoracico-abdominal neurohaemal areas in the blowfly. Cell Tissue Res 253: 583–595.
37. Truman JW (1990) Metamorphosis of the central nervous system of Drosophila. J Neurobiol 21: 1072–1084.
38. Schubiger M, Wade AA, Carney GE, Truman JW, Bender M (1998) Drosophila EcR-B ecdysone receptor isoforms are required for larval molting and for neuron remodeling during metamorphosis. Development 125: 2053–2062.

39. Sivasubramanian P (1991) FMRFamide-like immunoreactivity in the ventral ganglion of the fly Sarcophaga bullata: metamorphic changes. Comp Biochem Physiol C 99: 507–512.
40. Yoon JG, Stay B (1995) Immunocytochemical localization of Diploptera punctata allatostatin-like peptide in Drosophila melanogaster. J Comp Neurol 363: 475–488.
41. Santos JG, Vömel M, Struck R, Homberg U, Nässel DR, et al. (2007) Neuroarchitecture of peptidergic systems in the larval ventral ganglion of Drosophila melanogaster. PLoS One 2: e695.
42. Duve H, Thorpe A (1994) Distribution and functional significance of Leucallatostatins in the blowfly Calliphora vomitoria. Cell Tissue Res 276: 367–379.
43. Schneider LE, Sun ET, Garland DJ, Taghert PH (1993) An immunocytochemical study of the FMRFamide neuropeptide gene products in Drosophila. J Comp Neurol 337: 446–460.
44. Kean L, Cazenave W, Costes L, Broderick KE, Graham S, et al. (2002) Two nitridergic peptides are encoded by the gene capability in Drosophila melanogaster. Am J Physiol 282: R1297–1307.
45. Bader R, Colomb J, Pankratz B, Schröck A, Stocker RF, et al. (2007) Genetic dissection of neural circuit anatomy underlying feeding behavior in Drosophila: distinct classes of hugin-expressing neurons. J Comp Neurol 502: 848–856.
46. Siegmund T, Korge G (2001) Innervation of the ring gland of Drosophila melanogaster. J Comp Neurol 431: 481–491.
47. O'Brien MA, Taghert PH (1998) A peritracheal neuropeptide system in insects: release of myomodulin-like peptides at ecdysis. J Exp Biol 201: 193–209.
48. Park D, Veenstra JA, Park JH, Taghert PH (2008) Mapping peptidergic cells in Drosophila: where DIMM fits in. PLoS One 3: e1896.
49. Williamson M, Lenz C, Winther AM, Nässel DR, Grimmelikhuijzen CJ, et al. (2001) Molecular cloning, genomic organization, and expression of a B-type (cricket-type) allatostatin preprohormone from Drosophila melanogaster. Biochem Biophys Res Commun 281: 544–550.
50. Vömel M, Wegener C (2007) Neurotransmitter-induced changes in the intracellular calcium concentration suggest a differential central modulation of CCAP neuron subsets in Drosophila. Dev Neurobiol 67: 792–808.
51. Inosaki A, Yasuda A, Shinada T, Ohfune Y, Numata H, et al. (2010) Mass spectrometric analysis of peptides in brain neurosecretory cells and neurohemal organs in the adult blowfly, Protophormia terraenovae. Comp Biochem Physiol A 155: 190–199.
52. Siviter RJ, Coast GM, Winther AM, Nachman RJ, Taylor CA, et al. (2000) Expression and functional characterization of a Drosophila neuropeptide precursor with homology to mammalian preprotachykinin A. J Biol Chem 275: 23273–23280.
53. Lundquist CT, Clottens FL, Holman GM, Riehm JP, Bonkale W, et al. (1994) Locustatachykinin immunoreactivity in the blowfly central nervous system and intestine. J Comp Neurol 341: 225–240.
54. Helfrich-Förster C (1997) Development of Pigment-dispersing hormone-immunoreactive neurons in the nervous system of Drosophila melanogaster. J Comp Neurol 380: 335–354.
55. Pyza E, Siuta T, Tanimura T (2003) Development of PDF-immunoreactive cells, possible clock neurons, in the housefly Musca domestica. Microsc Res Tech 62: 103–113.
56. Veenstra JA (2009) Peptidergic paracrine and endocrine cells in the midgut of the fruit fly maggot. Cell Tissue Res 336: 309–323.
57. Lee K-S, You K-H, Choo J-K, Han Y-M, Yu K (2004) Drosophila short neuropeptide F regulates food intake and body size. J Biol Chem 279: 50781–50789.
58. Melcher C, Pankratz MJ (2005) Candidate gustatory interneurons modulating feeding behavior in the Drosophila brain. PLoS Biol 3: e305.
59. Cognigni P, Bailey AP, Miguel-Aliaga I (2011) Enteric neurons and systemic signals couple nutritional and reproductive status with intestinal homeostasis. Cell Metab 13: 92–104.
60. Al-Anzi B, Armand E, Nagamei P, Olszewski M, Sapin V, et al. (2010) The leucokinin pathway and its neurons regulate meal size in Drosophila. Curr Biol 20: 969–978.
61. Veenstra JA, Pattillo JM, Petzel DH (1997) A single cDNA encodes all three Aedes leucokinins, which stimulate both fluid secretion by the malpighian tubules and hindgut contractions. J Biol Chem 272: 10402–10407.
62. Radford JC, Terhzaz S, Cabrero P, Davies S-A, Dow JAT (2004) Functional characterisation of the Anopheles leucokinins and their cognate G-protein coupled receptor. J Exp Biol 207: 4573–4586.
63. Pollock VP, McGettigan J, Cabrero P, Maudlin IM, Dow JAT, et al. (2004) Conservation of capa peptide-induced nitric oxide signalling in Diptera. J Exp Biol 207: 4135–4145.
64. Hergarden AC, Tayler TD, Anderson DJ (2012) Allatostatin-A neurons inhibit feeding behavior in adult Drosophila. Proc Natl Acad Sci USA 109: 3967–3972.
65. Kim SK, Rulifson EJ (2004) Conserved mechanisms of glucose sensing and regulation by Drosophila corpora cardiaca cells. Nature 431: 316–320.
66. Lee G, Park JH (2004) Hemolymph sugar homeostasis and starvation-induced hyperactivity affected by genetic manipulations of the adipokinetic-hormone-encoding gene in Drosophila melanogaster. Genetics 167: 311–323.
67. Isabel G, Martin JR, Chidami S, Veenstra JA, Rosay P (2005) AKH-producing neuroendocrine cell ablation decreases trehalose and induces behavioral changes in Drosophila. Am J Physiol - Reg Integr Comp Physiol 288: R531–538.
68. Gäde G (1997) The explosion of structural information on insect neuropeptides. Progr Chem Organic Natural Products 71: 1–127.
69. Clynen E, Schoofs L (2009) Peptidomic survey of the locust neuroendocrine system. Insect Biochem Mol Biol 39: 491–507.
70. Predel R (2006) Cockroach neuropeptides: sequences, localization, and physiological actions. In: H S, editor. Invertebrate neuropeptides and hormones. Trivandrum, Kerala: Transworld Research Network. 127–155.
71. Verleyen P, Huybrechts J, Sas F, Clynen E, Baggerman G, et al. (2004) Neuropeptidomics of the grey flesh fly, Neobellieria bullata. Biochem Biophys Res Commun 316: 763–770.
72. Taghert PH, Schneider LE (1990) Interspecific comparison of a Drosophila gene encoding FMRFamide-related neuropeptides. J Neurosci 10: 1929–1942.
73. Lundquist CT, Clottens FL, Holman GM, Nichols R, Nachman RJ, et al. (1994) Callitachykinin I and II, two novel myotropic peptides isolated from the blowfly, Calliphora vomitoria, that have resemblances to tachykinins. Peptides 15: 761–768.
74. Duve H, Thorpe A, Scott AG, Johnsen AH, Rehfeld JF, et al. (1995) The sulfakinins of the blowfly Calliphora vomitoria. Peptide isolation, gene cloning and expression studies. Eur J Biochem 232: 633–640.
75. Wiegmann BM, Trautwein MD, Winkler IS, Barr NB, Kim J-W, et al. (2011) Episodic radiations in the fly tree of life. Proc Natl Acad Sci 108: 5690–5695.
76. Nachman RJ, Russell WK, Coast GM, Russell DH, Predel R (2005) Mass spectrometric assignment of Leu/Ile in neuropeptides from single neurohemal organ preparations of insects. Peptides 26: 2151–2156.
77. Waterhouse AM, Procter JB, Martin DMA, Clamp M, Barton GJ (2009) Jalview Version 2–a multiple sequence alignment editor and analysis workbench. Bioinformatics 25: 1189–1191.

Supporting Information

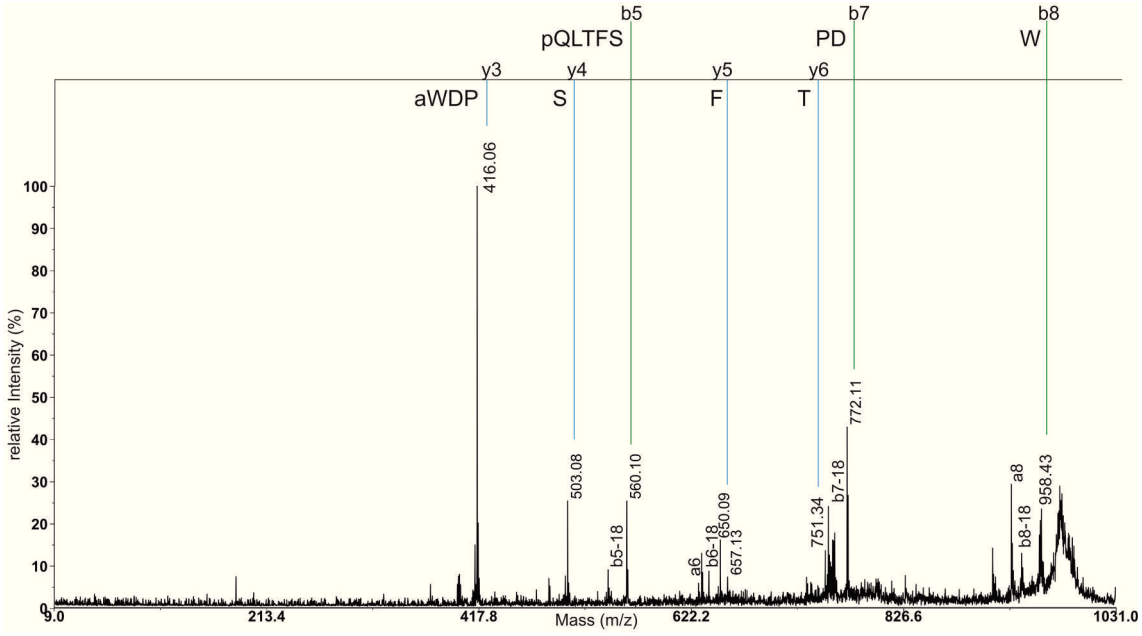

Supplemental Figure S1:

MS/MS spectrum of unlabelled AKH.

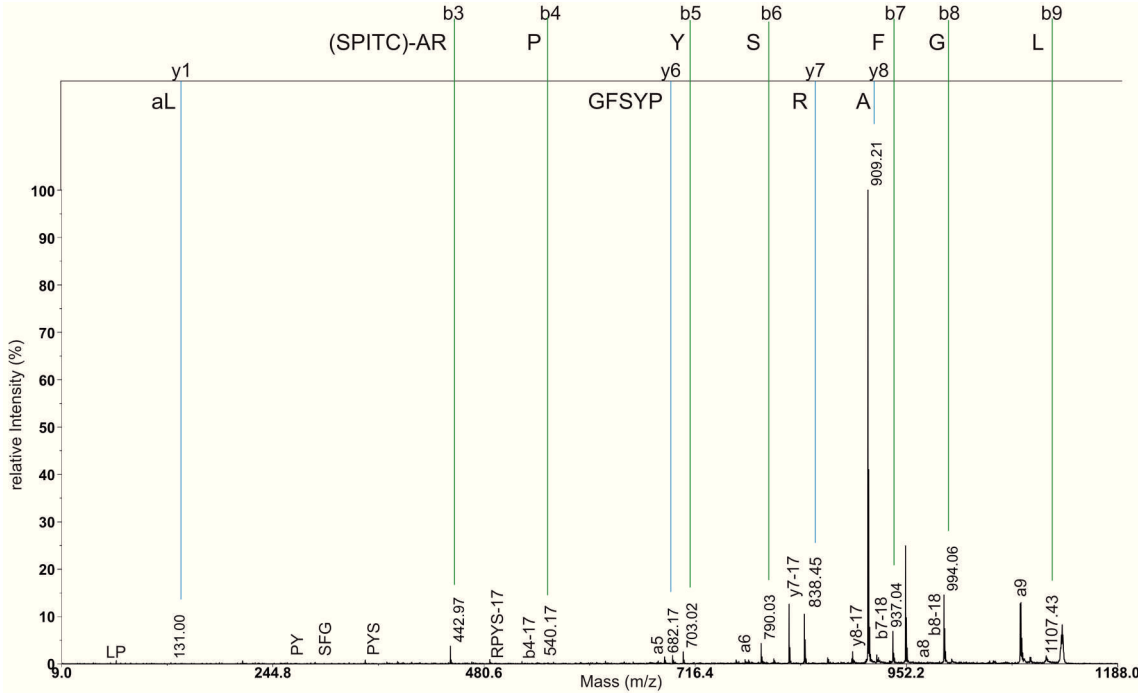

Supplemental Figure S2:

MS/MS spectrum of AST-A_{909}, SPITC-labelled.

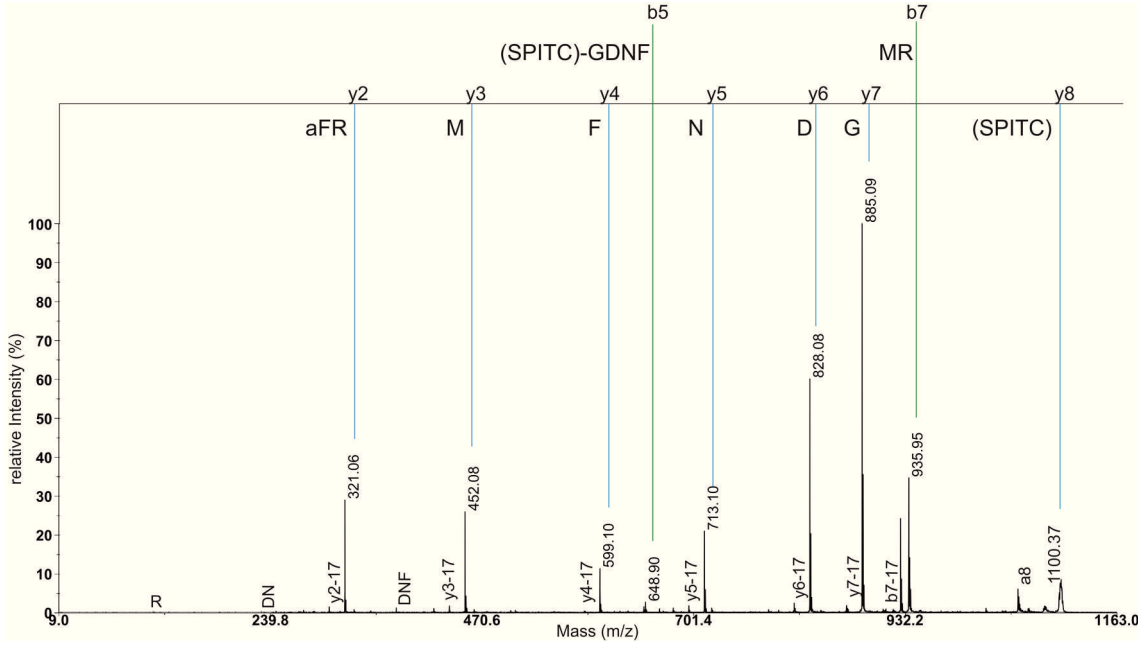

Supplemental Figure S3:

MS/MS spectrum of $FMRFa_{885}$, SPITC-labelled.

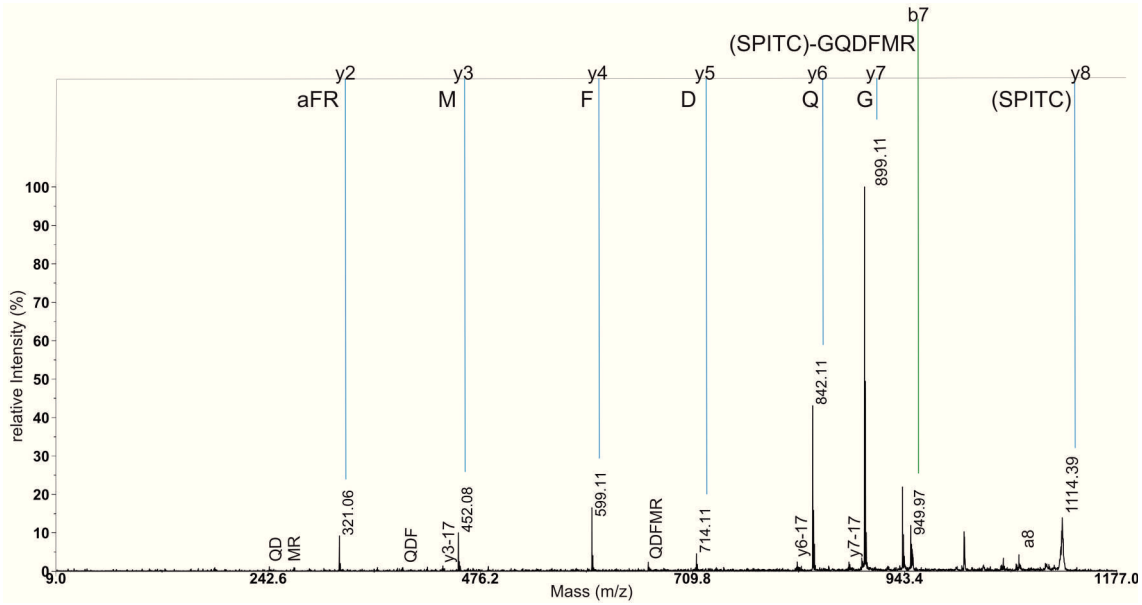

Supplemental Figure S4:

MS/MS spectrum of $FMRFa_{899}$, SPITC-labelled.

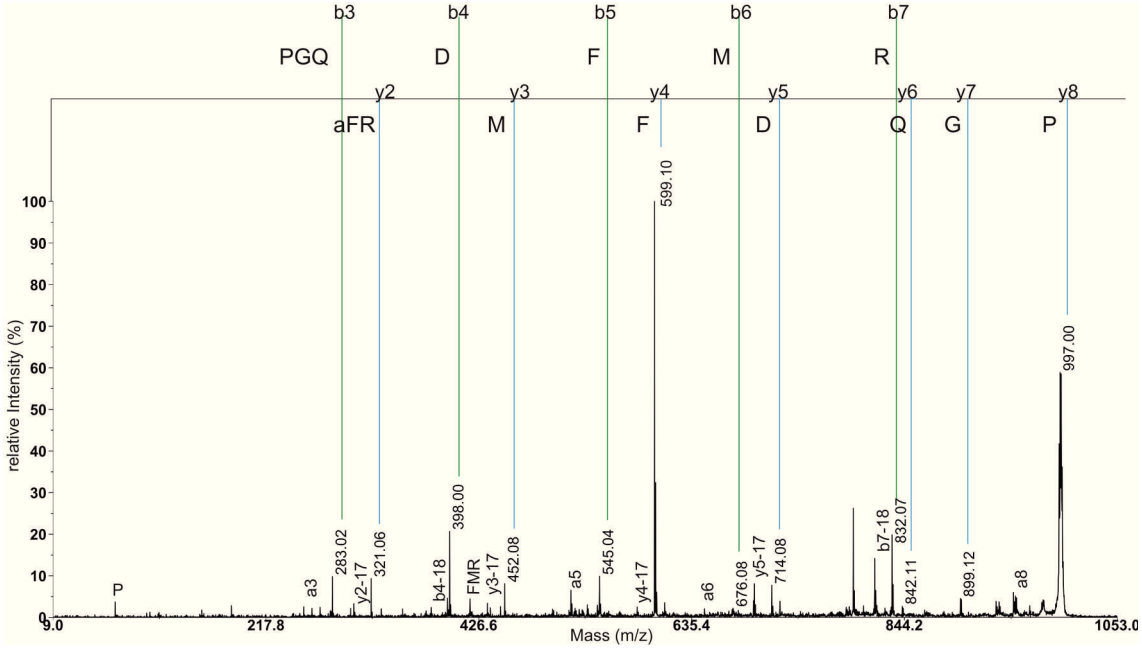

Supplemental Figure S5:

MS/MS spectrum of $FMRFa_{996}$, unlabelled.

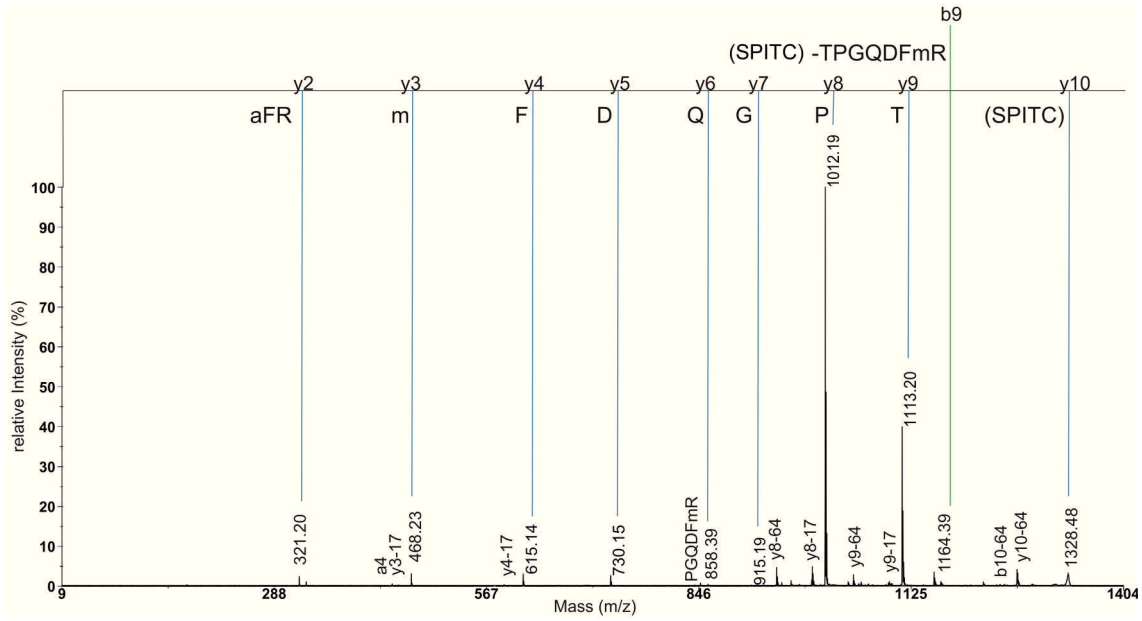

Supplemental Figure S6:

MS/MS spectrum of $FMRFa_{1097}$ with an oxidized methionine (1113.5 Da), SPITC-labelled.

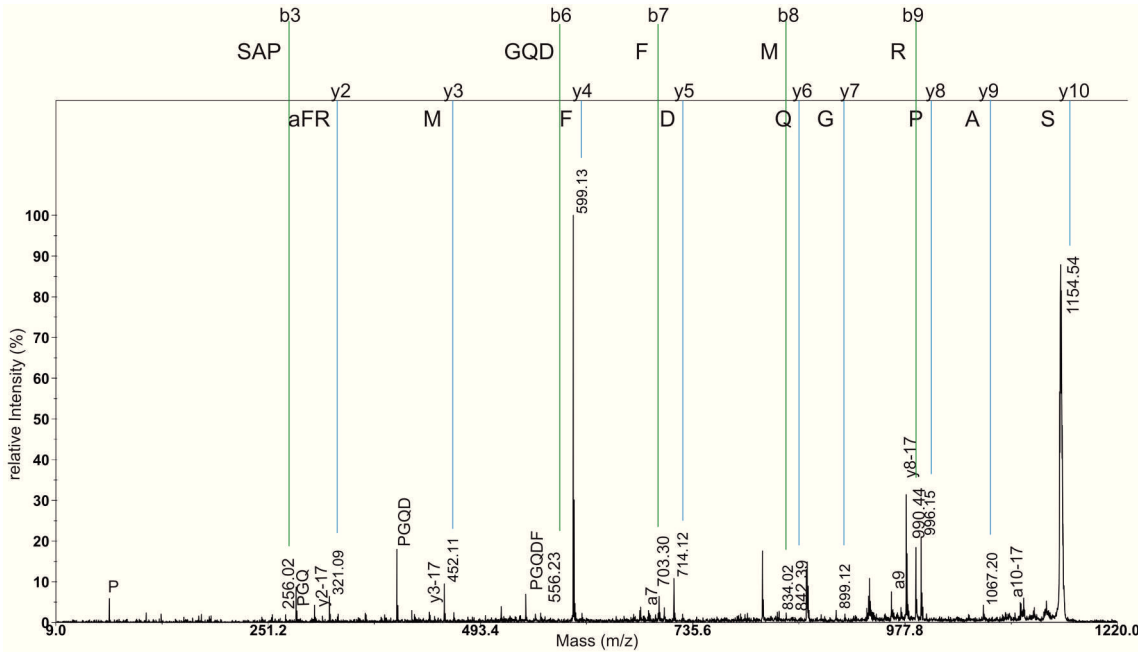

Supplemental Figure S7:

MS/MS spectrum of $FMRFa_{1154}$, unlabelled.

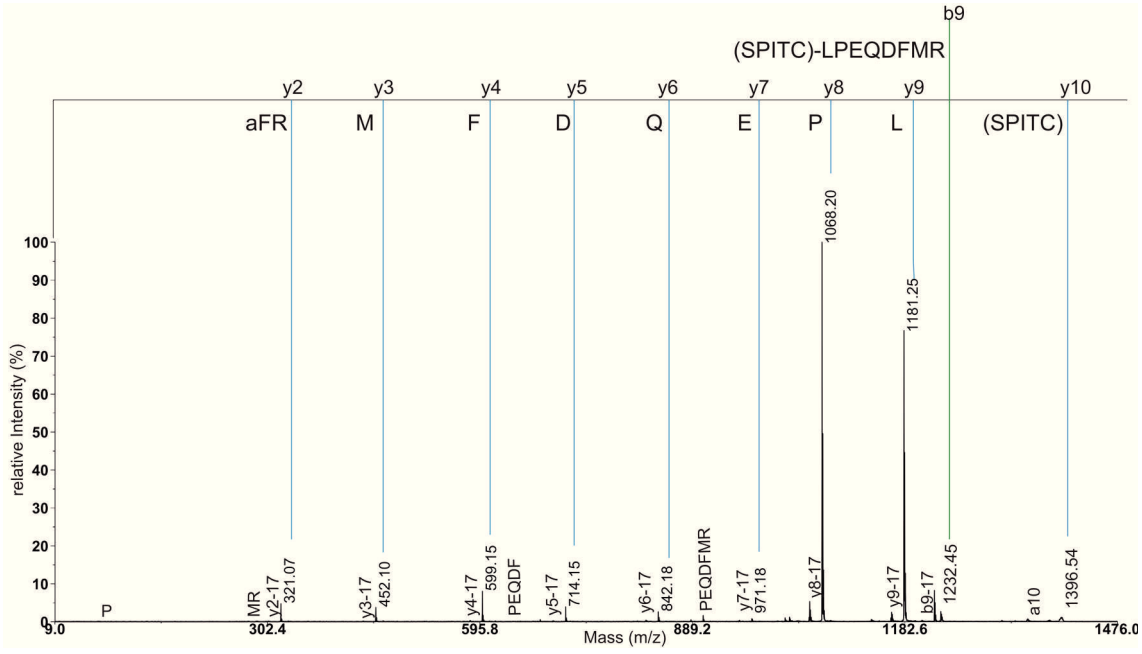

Supplemental Figure S8:

MS/MS spectrum of $FMRFa_{1181}$, SPITC-labelled.

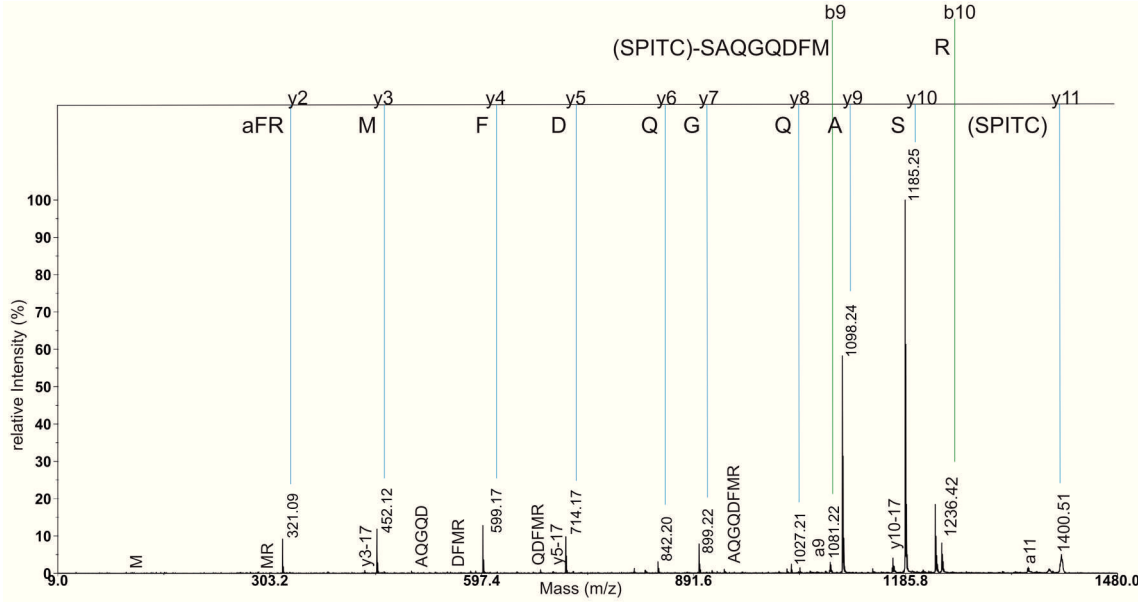

Supplemental Figure S9:

MS/MS spectrum of $FMRFa_{1185}$, SPITC-labelled.

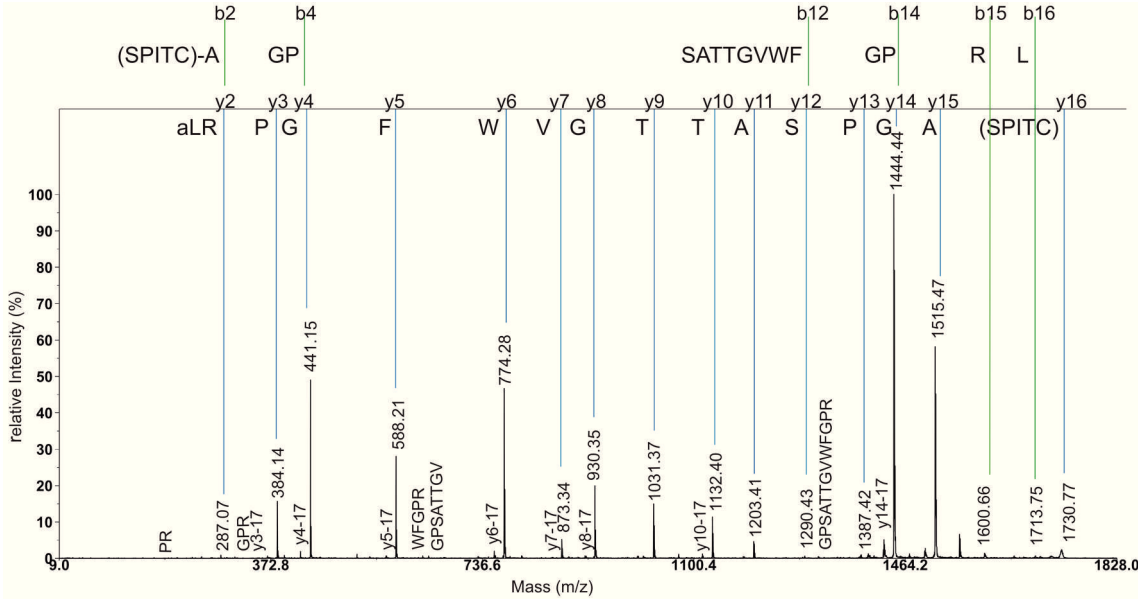

Supplemental Figure S10:

MS/MS spectrum of CAPA-PK, SPITC-labelled.

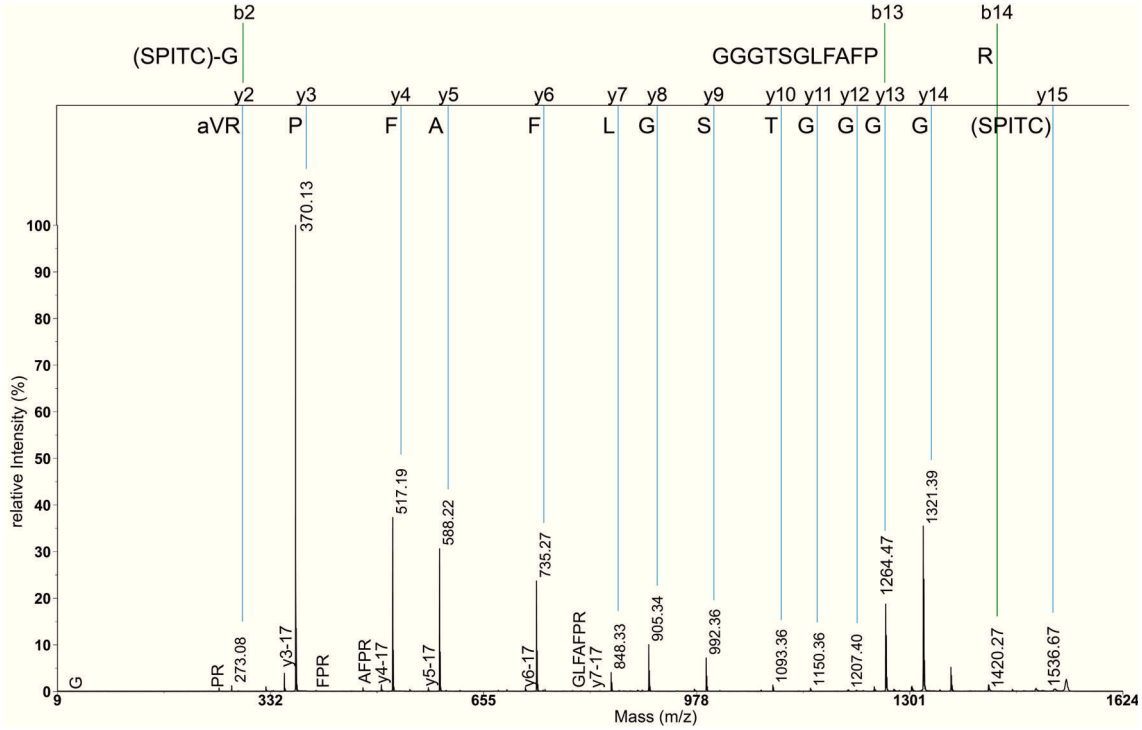

Supplemental Figure S11:

MS/MS spectrum of CAPA-PVK-1, SPITC-labelled.

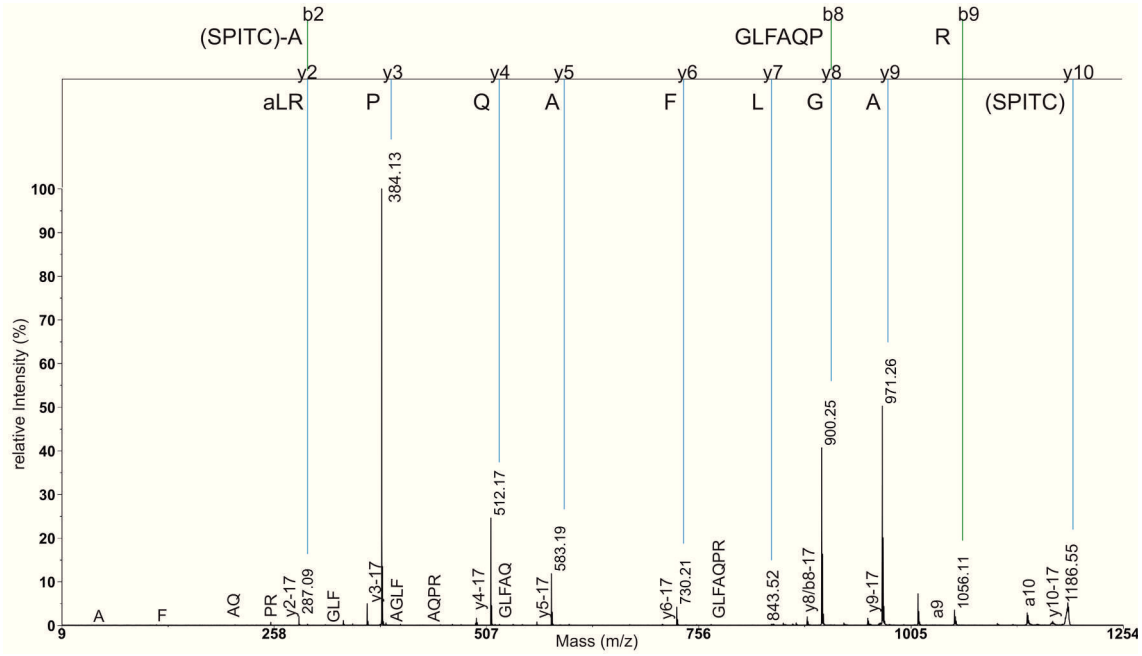

Supplemental Figure S12:

MS/MS spectrum of CAPA-PVK-2, SPITC-labelled.

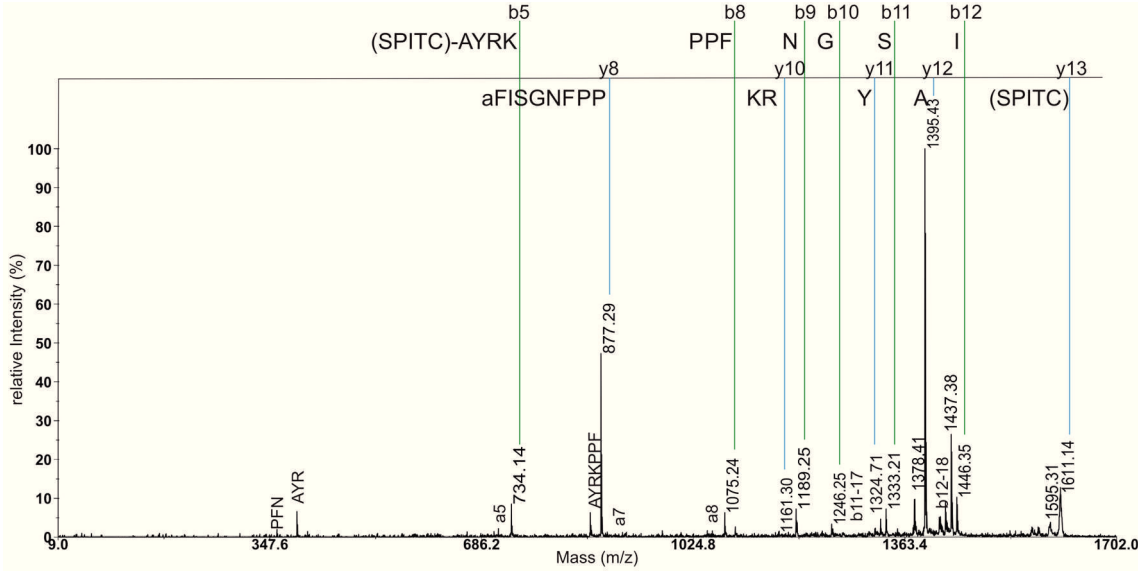

Supplemental Figure S13:

MS/MS spectrum of SIFa, SPITC-labelled.

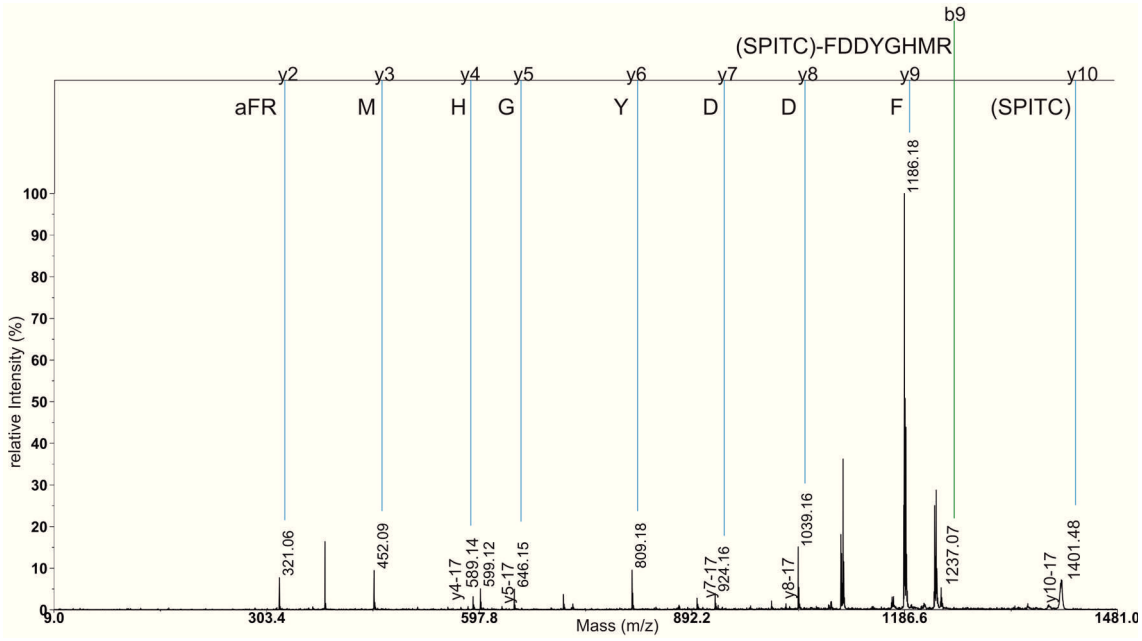

Supplemental Figure S14:

MS/MS spectrum of sulfakinin$^{6-14}$, SPITC-labelled.

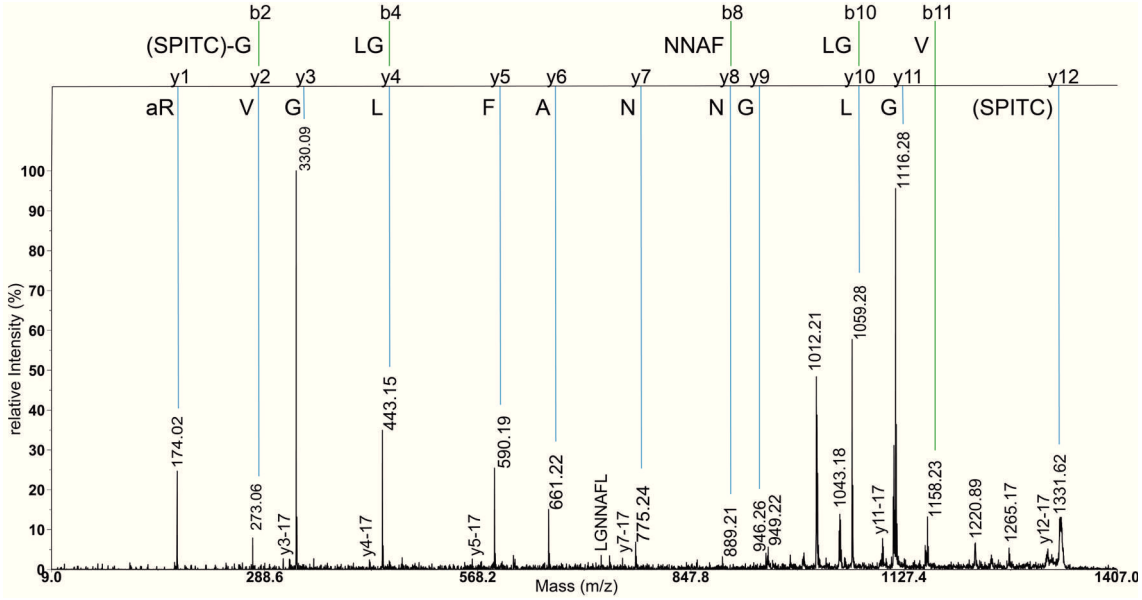

Supplemental Figure S15:

MS/MS spectrum of TK_{1116}, SPITC-labelled.

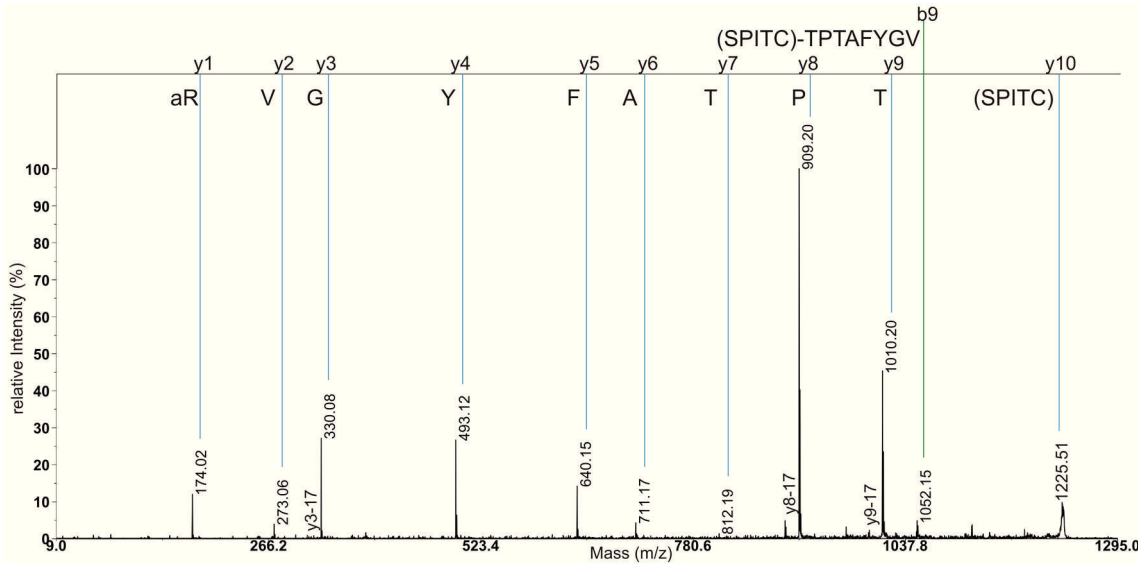

Supplemental Figure S16:

MS/MS spectrum of TK_{1010}, SPITC-labelled.

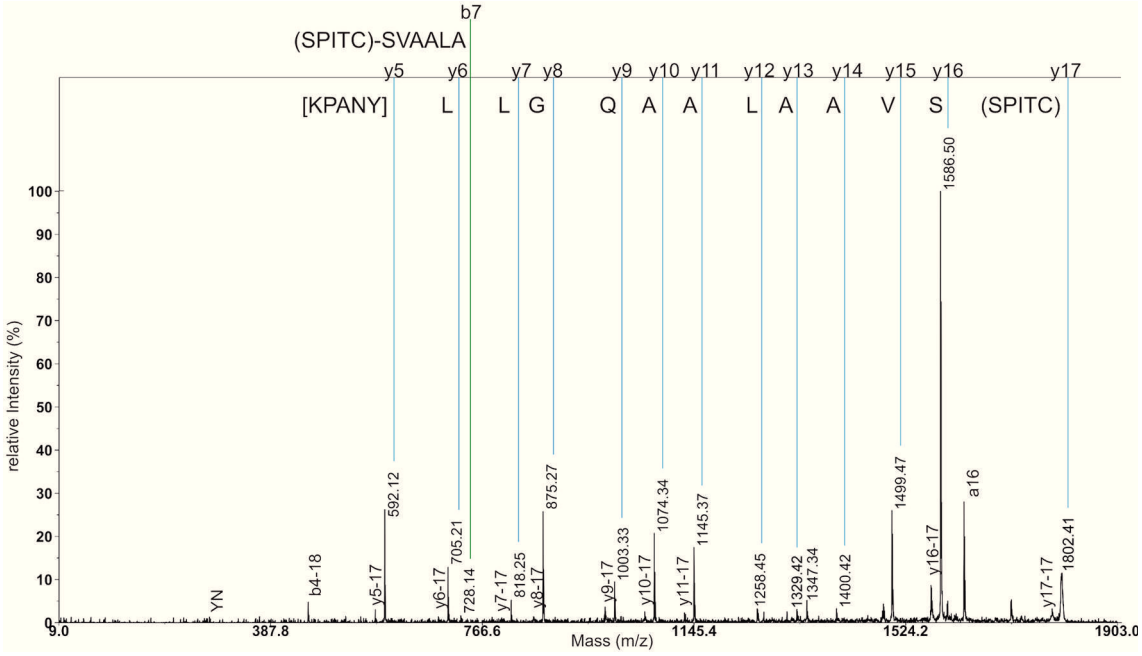

Supplemental Figure S17:

MS/MS spectrum of APK, SPITC-labelled.

5.3 Dissecting the pleiotropic function of allatostatin A cells in *Drosophila*—which subset regulates feeding, activity or gut motility?

W. Reiher, J. Chen, P. Cognigni, C. P. Christov, I. Miguel-Aliaga, J. A. Veenstra and C. Wegener

Manuscript

Dissecting the pleiotropic function of allatostatin A cells in *Drosophila*—which subset regulates feeding, activity or gut motility?

Wencke Reiher[1], Jiangtian Chen[1], Paola Cognigni[2], Christo P. Christov[3], Irene Miguel-Aliaga[2], Jan A. Veenstra[4], Christian Wegener[1]

[1] Neurobiology and Genetics, Theodor-Boveri Institute, Biocenter, University of Würzburg, Würzburg, Germany

[2] Genes and Metabolism, MRC Clinical Sciences Centre, Faculty of Medicine, Imperial College London, London, UK

[3] Cell Biology, Department of Zoology, University of Cambridge, Cambridge, UK

[4] Neurogenetics of Cognitive Abilities, Aquitaine Institute for Cognitive and Integrative Neuroscience, University of Bordeaux 1, Talence, France

Corresponding author:

Prof. Dr. Christian Wegener
Lehrstuhl für Neurobiologie und Genetik
Theodor-Boveri Institut
Biozentrum
Universität Würzburg
Am Hubland
97074 Würzburg
Germany

christian.wegener@uni-wuerzburg.de

Abstract

In animals, regulation of metabolism-related processes and behaviors, e.g. food consumption, is important to replenish energy stores after times of food shortage and to prevent obesity. The brain-gut peptide allatostatin A (AstA) has been implicated in the control of *Drosophila* metabolism. Here, we shed light on the complexity of AstA action by dissecting functional subgroups of AstA cells. We show that activation of a subset of AstA brain neurons, i.e. the PLP neurons, and AstA-producing gut endocrine cells significantly reduces feeding, but also strikingly inhibits fly locomotor activity. Integrating findings of a previous study, we conclude that AstA from the PLP neurons functions as satiety factor, while AstA secreted by enteroendocrine cells regulates locomotion in a hormonal manner. We also demonstrate that different subsets of AstA cells influence defecation behavior. But although processes of AstA neurons with somata in the thoracico-abdominal ganglion seem to contact the rectal epithelium, activation of these neurons did not result in detectable changes of acid-base ratio or water content of excreta. Furthermore, we show that the AstA receptor DAR-2 is expressed in the midgut-associated musculature and mediates a dose-dependent inhibition of midgut motility caused by AstA. Our results reveal subset-dependent functions of AstA cells, and suggest that AstA gut endocrine cells, which had received little attention in previous functional studies, regulate locomotor activity and food transit. Thus, we can show that AstA is involved in several interrelated processes to promote metabolic and behavioral adaptability to internal and environmental requirements.

Key words: insect metabolism, brain-gut peptide, enteroendocrine cell, feeding, locomotor activity, midgut peristalsis

Introduction

Animals regulate food intake as well as the storage and remobilization of nutrients to maintain a balanced energetic and nutritional state. It is known from mammals that this balance is controlled by a network of signaling molecules—mainly neuropeptides and peptide hormones—between the CNS and peripheral tissues, and that signals from the gastrointestinal tract, adipose tissue and endocrine glands regulate feeding behavior, which eventually is controlled by the brain [1–3]. Nutrients are made available to the organism by the digestive tract, which therefore represents an important source of information for the control of metabolism. Many of the mammalian gut peptides (e.g. cholecystokinin, pancreatic polypeptide, peptide YY, glucagon-like peptide-1 and oxyntomodulin) reduce appetite, while others such as orexin [4] and ghrelin serve as potent appetite-stimulating signals [1–3]. Disruption of the signaling network between the CNS and the periphery leads to an imbalanced energy metabolism and can result in diseases like e.g. diabetes or obesity [1–3].

A role in the regulation of food intake and metabolism is also established for a number of insect regulatory peptides, most of which are neuropeptides [5, 6]. In insects, peptide signals are produced by peptidergic neurons and also by numerous enteroendocrine cells (EECs) that lie scattered throughout the epithelium of the midgut. Comprehensive immunohistological or peptidomic studies about peptides produced in insect EECs exist for the dipterans *Aedes aegypti* [7, 8], *Drosophila melanogaster* [9–11] and *Delia radicum* [12]. These studies showed that all peptides produced in insect EECs represent "brain-gut" peptides which are also synthesized by the nervous system.

Allatostatin A (AstA) peptides are brain-gut peptides found in brain interneurons, in efferent neuronal processes innervating the gut, and in EECs in a number of insect species [13]. AstA has been shown to exert pleiotropic effects and to affect metabolism-related processes. In several species it inhibits the motility of certain parts of the gut, e.g. in cockroaches [14–18], moth larvae [19–22], locusts [23] and in the blowfly [24]. AstA has also been found to influence the release and activity of digestive enzymes in the midgut of several cockroach species *in vitro* [17, 18, 25], and to reduce food intake [18]. When administered to isolated glandular lobes of locust corpora cardiaca, AstA increased the cAMP level and stimulated the release of AKH, which regulates the mobilization of energy stores [26].

Both in larval and adult *Drosophila*, AstA is widely distributed and was found in interneurons within the CNS, in neurons innervating the hindgut (in adults also the most posterior midgut) and in EECs of the posterior midgut [9, 10, 27]. Two AstA receptors, DAR-1 (=AlstR) and DAR-2, have been identified [28–32].

Ubiquitous expression of *AstA*- or *DAR-1-RNAi* in fruit fly larvae resulted in shortened foraging path lengths in the presence, but not in the absence of food, as well as a reduction of *foraging* mRNA levels. These are characteristics known from the "sitter" phenotype [33]. In adult flies, activation of AstA cells reduced feeding and inhibited the starvation-induced increase of glucose responsiveness as shown by Hergarden et al. [34]. They suggested that AstA neurons in the subesophageal ganglion are underlying the observed effects on glucose responsiveness, and that a different population of AstA neurons controls feeding. For their experiments, Hergarden et al. used an *AstA-Gal4* driver line that targeted a large number of AstA cells, including brain neurons (protocerebrum, medulla and subesophageal ganglion neurons), gut-innervating thoracico-abdominal ganglion neurons and EECs in the posterior midgut.

Further evidence for a role of AstA in the control of metabolism was shown by Hentze et al. [35]. Their results suggest that AstA positively affects signaling of AKH- and insulin-producing cells, which are important regulators of energy metabolism and starvation resistance [36].

While some functions for AstA cells in *Drosophila* have been demonstrated up to now, it remains unclear which AstA cell subset is responsible for the respective effects. For example, it is not known whether AstA neurons in the CNS, AstA EECs in the midgut or both are underlying the reduction of food intake observed by Hergarden et al. [34]. Moreover, the broad distribution of *AstA*-expressing cells and the data from other insects (see above) suggests additional functions of *Drosophila* AstA.

Here, we set out to dissect the roles of the AstA cell population with regard to metabolism and feeding. For this we used a restricted *AstA-Gal4* transgene that allowed us to manipulate different subsets of AstA cells. We show that two pairs of AstA neurons in the posterior lateral protocerebrum and/or the AstA EECs in the gut are sufficient to regulate food intake, but also—contrary to what previously was suggested—strongly affect locomotor activity. Furthermore, we demonstrate a new AstA function in the reduction of midgut motility. This effect is mediated by DAR-2. Taken together, our data suggest an important role of the so far neglected AstA EECs for feeding-related behavior.

Materials and methods

Flies

The following fly strains were used for crossings and experiments: *UAS-TrpA1* (Bloomington Stock Center stock no. 26263), *10XUAS-IVS-myr::GFP* (Bloomington Stock Center; [37]), *tsh-Gal80* (kindly provided by J. Simpson, Janelia Farm; [38, 39]), *UAS-AstA(1)-Gal4* (kindly provided by the lab of D. Anderson, Caltech; [34]), *UAS-Dcr-2* (VDRC stock no. 60007), *UAS-DAR-1-RNAi* (101395 KK, VDRC), *UAS-DAR-2-RNAi* (108648 KK, VDRC), *Mef2-Gal4* (kindly provided by the lab of R. Renkawitz-Pohl, University of Marburg; [40]), *Canton-S* as wild-type strain and w^{1118} for control crossings (both from Bloomington Stock Center).

Fly crossings were kept on standard *Drosophila* medium (see supplement for recipe) with a 12:12 h light-dark cycle at 25°C, except for the crossings used in TrpA1 experiments, which were kept at 20 or 22°C.

Creation of *AstA promoter-Gal4* transgenic flies

The putative *D. melanogaster* allatostatin A promoter was amplified from genomic DNA by PCR using the following primers:
5'-GCCGGATCCAGAGGTTCCGCGGACTAAAT-3' and
5'-GCGCAATTGAGTAGAAGCTGCGCCAGAAG-3'.
The resulting PCR product was digested with MunI and BamHI, gel purified and cloned into the *P{pAkh-Gal4}* vector [41], previously digested with EcoRI and BamHI in order to remove the *Akh* promoter. The *P{pAstA-Gal4}* plasmid was injected into *Drosophila* embryos by BestGene Inc. (Chino Hills, CA, USA) and 5 independent transformant lines were obtained.

Immunostaining

Tissue of feeding 3rd instar larvae or adult flies (approx. 1 week after eclosion) was dissected in HL3.1 solution [42] and fixed in 4% PFA/PBS (pH 7.2) at room temperature. Fixation time was 45 min for guts and larval CNS, and 90 min for adult CNS. After several washes with PBT (=PBS with 0.3% Triton X), followed by an overnight blocking step with PBT containing 10% normal goat serum at room

temperature, the tissue was incubated in primary antibody solution on a shaker for about 1 d at 4°C, then several h at room temperature. Primary anti-GFP (1:100) antibody and anti-AstA (1:3500) antiserum were diluted in PBT containing 3% normal goat serum. 1 d of washing steps with PBT followed, after which the samples were incubated with secondary antibodies diluted 1:300 in PBT containing 3% normal goat serum. Samples were washed several times with PBT, then twice with PBS and were finally mounted onto microscope slides using 80% glycerol/20% PBS. Images were acquired with a Leica TCS SPE (Leica, Wetzlar, Germany) through sequential scanning with different diode lasers. Fiji [43] was applied for maximum intensity projection and contrast enhancement. Figures were generated with Adobe Photoshop CS2. The description of neuronal arborizations in the adult brain was facilitated by the adult brain stack of Virtual Fly Brain [44].

Antibodies

Primary antibodies used were a monoclonal anti-GFP IgG (A11120, Invitrogen GmbH, Karslruhe, Germany) and a polyclonal antiserum directed against Dippu-AstA-7 (old name Dip-allatostatin I, [45], Jena Bioscience GmbH, Jena, Germany), which apparently recognizes the C-terminal YXFGL-amide of other AstA peptides [45], including that of Drome-AstA-1–3 [46]. It potentially also reacts with the C-terminal residues of the Drome-AstA-4 (FNFGL-amide). Alexa Fluor 647- or DyLight 488-conjugated IgG (H+L) secondary antibodies were purchased from Dianova GmbH, Hamburg, Germany.

Quantitative real time-PCR

For egg laying, adult wild-type flies (*Canton-S*) were incubated on apple juice plates at 25°C with a 12:12 h light-dark cycle. After 24 h, 40 eggs were transferred into a new vial and flies raised on standard *Drosophila* medium at 25°C. 1 week after eclosion, total RNA was extracted from brains, thoracico-abdominal ganglia and guts of 10 flies using Quick-RNA™ MicroPrep (Zymo Research Europe GmbH, Freiburg, Deutschland) according to the manufacturer's protocol, and cDNA was synthesized using QuantiTect® Reverse Transcription Kit (Qiagen, Hilden, Germany) according to the manufacturer's protocol.

The primers for qPCR were:

for *DAR-1*:
forward 5'-CAAACCTTCCGCAGAGTC-3',
reverse 5'-GAGGATGACATGAATGGGC-3';

for *DAR-2*:
forward 5'-GGATGATGAGGACGGAGAAC-3',
reverse 5'-GTAATCCACCACCACGTCG-3';

for *αTub84B* (as reference):
forward 5'-TCTGCGATTCGATGGTGCCCTTAAC-3',
reverse 5'-GGATCGCACTTGACCATCTGGTTGGC-3'.

Thermal cycling conditions for the Rotor-Gene Q real-time PCR cycler (Qiagen, Hilden, Germany) were as follows: initial denaturation at 95°C for 2 min, followed by 40 cycles of 95°C for 5 s and 63°C for 20 s. The reaction was performed using SensiFast™ SYBR No-ROX Kit (Bioline GmbH, Luckenwalde, Germany) and 50 nM of each primer. The procedure from egg collection to reverse transcription was conducted 5 times, and each of the 5 cDNA samples was analyzed for *DAR-1*, *DAR-2* and *α-tubulin* expression 3 times by qPCR.

Relative expression levels are presented as ratios (ΔCt method). ΔCt was calculated as difference of the Ct value for the target gene to the reference gene, i.e. ΔCt=Ct(*α-tubulin*)-Ct(*DAR-1* or *DAR-2*).

Capillary Feeder (CAFE) assay

The CAFE protocol was based on the method described in [47]. 7–9 d old male flies were anesthetized on ice and transferred into 24-well plates (1 fly per well) containing several small holes in each well to allow for air exchange. A piece of moist filter paper was added to each well to provide the flies with water separately from the food. Capillaries (5 µl glass capillary pipettes, Megro GmbH & Co. KG, Wesel, Germany) were filled with liquid food (see below), and 1 capillary per well was inserted through a hole in the lid of the well plate so that the bottom was easily accessible to the fly. Food capillaries in wells without flies were used to control for evaporation, which was negligible. The plates were put into an airtight, humid container, which prevented the filter paper from drying, and placed into an incubator with a 12:12 h light-dark cycle at 20/22°C or 29°C. Liquid food was prepared daily of the following ingredients: 5.4% sucrose, 3.6% yeast extract (Yeast Extract BioChemica, AppliChem, Darmstadt, Germany) and 0.03% BPB (Bromophenol blue sodium salt Electrophoresis grade, AppliChem, Darmstadt, Germany) (all m/v) in ultrapure water. Capillaries were exchanged each day at the same time. Food consumption was not measured for the first day to give the flies some time to acclimatize to the change of environment and food. Values measured for day 2 and 3 (descent of the meniscus) were summed up for each fly.

Defecation assay

The protocol for the defecation assay was based on the procedure described in [48]. For preparation of BPB food 5.4% sucrose, 3.6% brewer's yeast powder, 0.15% nipagin (Methyl-4-hydroxybenzoate, Merck KGaA, Darmstadt, Germany), 0.5% BPB (Bromophenol blue sodium salt Electrophoresis grade, AppliChem, Darmstadt, Germany) and 1% agar (all m/v) were dissolved in ultrapure water, pH was adjusted to ~ 5.5, then the mixture was boiled briefly. The food was stirred constantly until it had cooled down to ~ 60°C, and was immediately poured into petri dishes for rapid solidification. Around 12 d old male flies were fed with BPB food for ½ d. Then flies were transferred to petri dishes (Ø ~ 55 mm) containing a defined amount of BPB food. 5 dishes per genotype with 5 flies each were set up and left, for 2 d at 22°C or 1 d at 29°C, with lids facing downwards in an incubator set to a 12:12 h light-dark cycle. Afterwards, digital images of the petri dish lids were obtained by high resolution backlight scanning, and deposits were detected and analyzed with the QAFF software ("Quantitative analysis of fly faeces", written by Matt Wayland, University of Cambridge, UK) in an automated manner. The software registered information about size, shape, lightness and color for each deposit. The median values for the single deposits were used to calculate the mean value of each analyzed quality per dish, yielding an N of 5 per genotype and temperature.

Activity measurement

Drosophila Activity Monitors (TriKinetics Inc., Waltham, MA, USA) were used to measure locomotor activity. 7 d old adult males were transferred to separate glass tubes containing an agar-sucrose food medium (prepared from 2% agar and 4% sucrose in ultrapure water by brief boiling), after which the tubes were closed with foam plugs. The tubes were inserted into holes in the monitor and centered. As a fly walked back and forth within its tube, it interrupted an infrared beam that crossed the tube at its midpoint. Light beam interruptions were counted for individual flies at 1-min intervals as a measure of fly activity. Flies were monitored under a 12:12 h light-dark cycle with 10 lux light intensity for 8 d at 22°C and subsequently for 10 d at 29°C, and average minute-by-minute activities were calculated for both conditions.

Measurement of midgut movement

6 d old feeding 3rd instar larvae were carefully washed out of the food and transferred into a small volume of HL3.1 solution [42] for 3–4 h. During this time the larvae expelled a part of their gut contents, which prevented rupture of tissue during dissection and filming. Larval guts were dissected in HL3.1 and fixed in a loosely stretched condition at the bottom of a small HL3.1 filled chamber using needles and a small droplet of 3% low-melt agarose in the anterior midgut region (close to the proventriculus) and at the hindgut. Following 2 gentle washes with fresh HL3.1, the guts were left undisturbed in 1 mL of HL3.1 for about 25 min. Then, backlight images were captured with a Leica M165FC fluorescent stereo microscope (Leica Microsystems, Heerbrugg, Switzerland) equipped with a Leica DFC450 C camera using the open-source software Micro-Manager (v. 1.4.13; [49]) with multi-dimensional acquisition. Acquisition was run for 9 min with a frame rate of 0.5 Hz. 3 min after start, 0.5 mL HL3.1 was added at the far side of the chamber with a pipette and immediately and gently intermixed, after which 0.5 mL HL3.1 was removed from the chamber to restore the initial volume. In the same way, synthetic AstA peptide, dissolved in 0.5 mL HL3.1 ringer according to the desired final concentration, was added 6 min after start.

The recorded image sequence was converted to a grayscale AVI file. Then, brightness and contrast were enhanced to achieve high contrast between gut tissue and surrounding fluid prior to analysis with the program AviLine 0.99 ([50], freely available at [51]). For this, usually 1 line per gut was drawn in a middle portion of the posterior midgut and measurements were carried out with the option “begin at white end”. For final analysis, the pixel changes from picture to picture were summed up for period 1:00 (min:s)–2:58 (=A, start conditions), period 4:00–5:58 (=B, after wash with HL3.1) and 7:00–8:58 (=C, after AstA application).

Changes of movement were quantified as follows: First, for each gut 4 ratios were calculated: $R_1=A/(A+B)$, $R_2=B/(A+B)$, $R_3=B/(B+C)$ and $R_4=C/(B+C)$. Then, we calculated the means of these ratios for each trial (3 guts), which was finally used to calculate the change of gut movement ($\Delta M/M_0$) after wash with HL3.1 as $M_{wash}=(R_{2mean}-R_{1mean})/R_{1mean}$, and the change after application of AstA as $M_{AstA}=(R_{4mean}-R_{3mean})/R_{3mean}$.

Synthetic peptides

Drome-AstA-1 (VERYAFGL-amide) and Drome-AstA-4 (TTRPQPFNFGL-amide) were custom-synthesized at a purity of > 90 % and obtained from Iris Biotech GmbH (Marktredwitz, Germany).

Statistics

Plotting and statistical analysis were performed using the R environment [52]. ANOVA with post-hoc Tukey's HSD tests were applied if criteria for normal distribution (Shapiro-Wilk normality test, $p > 0.05$) and homogeneity of variances (Levene's test, $p > 0.05$) were met, otherwise Kruskal-Wallis and post-hoc Mann-Whitney U tests (with Holm correction) were applied. Exceptions are stated in the figure legends. In boxplot graphs, circles represent outliers, plots show the median, 25th and 75th percentile (upper and lower box boundary), 10th and 90th percentile (whiskers).

Results

Our aim was to investigate the effects and dissect the functional subgroups of allatostatin A-producing cells in *Drosophila* with regard to metabolism and feeding. As a tool to specifically manipulate a subset of AstA cells in functional experiments, we created *AstA-Gal4* constructs by combining specific parts of the putative *AstA* 5' regulatory region with the *Gal4* sequence. By P-element transformation we obtained transgenic *AstA(34)-Gal4* flies.

Expression pattern of the new *AstA(34)-Gal4* line

In order to test for the specificity of the *AstA(34)-Gal4* expression, we analyzed *AstA(34)>GFP* (*AstA(34)-Gal4/UAS-GFP*) flies for colocalization of GFP and AstA peptides by immunostaining.

The results of the AstA staining were consistent with the pattern described in earlier studies ([9, 10, 27, 46, 53], Figs. 1, 2). Table 1 provides an overview of the localisation of *AstA(34)-Gal4*-driven GFP expression in relation to results from the AstA staining and previous studies. We adopted the nomenclature of [27], although the designation of the DLAa (dorsolateral abdominal a) cells seems not fully accurate because part of their somata lie centrally or slightly ventrally within the abdominal VG (larval ventral ganglion) or TAG (adult thoracico-abdominal ganglion).

In addition to the neurons already described in [27] (see Table 1), which in general showed clear and strong staining, we noticed several somata with weaker AstA immunoreactivity (IR) in the CNS of larvae and adults. As these cells were not included in the *AstA(34)-Gal4* expression pattern and projections were difficult to follow, we did not analyze them further.

Adult

In each brain hemisphere of *AstA(34)>GFP* flies, GFP was detected in two AstA-immunoreactive (-IR) cells belonging to the three PLP (posterior lateral protocerebrum) cells [27] with somata in the PLP and arborizations in the superior protocerebrum (Fig. 1A, B). Furthermore, GFP could be found in two to four cells per hemisphere with somata in the lateral cell body region (LCBR) close to the lateral horn. These LCBR neurons were not AstA-IR and run ventro-posteriorly to arborize mainly within the PLP and the posterior slope (Fig. 1A, B). In addition, a varying number of AstA-IR neurons in the medulla showed a mostly weak GFP expression (Fig. 1A, B). However, in some preparations, single medulla neurons exhibited a stronger GFP signal (Fig. 1B3).

Three pairs of AstA-IR DLAa cells within the posterior abdominal TAG were found to send neurites via the median abdominal nerve to innervate the gut ([27], Fig. 1A, C). Besides the DLAa cell somata, which were clearly co-labeled, all GFP-labeled structures in this TAG region apparently are varicosities and arborizations of projections from these six DLAa neurons (Fig. 1C). The DLAa neurons generally exhibited strong GFP expression, while the brain neurons showed noticeable variability of GFP labeling intensity between preparations (examples are shown in Fig. 1B). In many preparations, one or a few additional non-AstA-IR interneurons within the TAG showed a weak GFP signal, but their location seemed to differ between individual flies.

Outside of the CNS, two pairs of peripheral AstA-IR neurons with somata located on the segmental nerves leading to the wings and the halteres [27] expressed GFP (Fig. 1A). Furthermore, GFP was detectable in the processes of the DLAa cells that target the hindgut (including the rectum) and posterior midgut, and in the majority of AstA-IR EECs in the posterior part of the midgut (Fig. 1E–G). The staining results are summarized in Table 1.

To analyze the function of AstA neurons that are not included in the *AstA(34)-Gal4* pattern, we also used the *AstA(1)-Gal4* driver strain [34] in our experiments. The expression pattern of *AstA(1)-Gal4* includes the following AstA-IR neurons per brain hemisphere: three PLP cells, ~ 30 medulla neurons and three neurons with cell bodies in the SOG (subesophageal ganglion). In comparison, *AstA(1)-Gal4* drives expression in a larger number of AstA brain neurons than *AstA(34)-Gal4*, while expression in the TAG is similar (Table 1, [34, 54]). In contrast, *AstA(34)-Gal4* seems to include a larger proportion of AstA EECs.

Larva

GPF expression could not be detected in the brain hemispheres of *AstA(34)>GFP* larvae. In the central part of the VG, a pair of AstA-IR VMA (ventromedial abdominal) cells [27] ramifying within the VG were co-labeled for GFP (Fig. 2A). The posterior abdominal neuromeres contain three pairs of AstA-IR DLAa cells [27] that showed strong GFP labeling (Fig. 2A, B). Projections of these cells leave the tip of the VG through the posteriormost segmental nerve to innervate the hindgut ([27], Fig. 2B, E, F). Outside the CNS, GFP expression was detectable in AstA-producing EECs of the posterior midgut (Fig. 2D). Like adults, larvae contain two pairs of AstA-IR peripheral neurons with cell bodies apparently lying on thoracic nerves 2 and 3 [27]. Due to our focus on adult behavior, we did not analyze these cells further.

GFP expression in few AstA-negative interneurons was also frequently observed in *AstA(34)>GFP* larvae. This unspecific expression was generally weak or very weak and the location varied among preparations.

Expression pattern of *tsh-Gal80; AstA(34)-Gal4*

We showed above that *AstA(34)-Gal4* drives expression in a subset of AstA cells. In order to dissect functional subgroups of *AstA(34)* cells in more detail, we generated a *tsh-Gal80; AstA(34)-Gal4* driver strain to restrict the *AstA(34)-Gal4* expression pattern to the brain and EECs. *Tsh-Gal80* suppresses *Gal4* expression in the thoracic and abdominal part of the CNS [39, 55, 56]. We then analyzed the expression pattern via immunostaining against AstA and GFP in *tsh-Gal80; AstA(34)>GFP* (*tsh-Gal80/+; AstA(34)-Gal4/UAS-GFP*) flies.

The GFP pattern in the brain of *tsh-Gal80; AstA(34)>GFP* flies corresponded to that in *AstA(34)>GFP* flies as described above. In contrast, the GFP signal of the DLAa cells in the TAG (and their gut-innervating processes) and of the four peripheral cells was absent (Fig. 1D). GFP expression in AstA-IR midgut EECs was unaffected by the *tsh-Gal80* construct (Fig. 1H).

Similar to adults, GFP staining of AstA cells in the larval VG (and hence in the gut-innervating neurons) was suppressed by the *tsh-Gal80* construct (Fig. 2C), while AstA EECs were still labeled in *tsh-Gal80; AstA(34)>GFP* larvae.

In summary, we successfully generated *AstA-Gal4* flies which express Gal4 in a defined subset of AstA cells and in a small number of unspecifically and mostly weakly expressing cells. By combination with *tsh-Gal80* we further refined the expression of Gal4 to AstA cell subsets in the brain and the gut.

Table 1: Expression patterns of *AstA(34)-Gal4* and *tsh-Gal80; AstA(34)-Gal4*. Data from earlier studies are given in the last two columns.

Stage	Organ	Cells with *AstA(34)-Gal4*-driven GFP expression	GFP expression with *tsh-Gal80; AstA(34)-Gal4* driver	AstA immunoreactivity[1]	Expression of GPF or LacZ with *AstA(1)-Gal4* driver[2]
adult	central brain	2 per hemisphere in the posterior lateral protocerebrum	+	+ (belong to PLP cells [27])	+ [34]
		2–4 per hemisphere in the lateral cell body region (LCBR cells)	+	-	- [34]
	optic lobes	small number of cells in the medulla	+	+	+ [34]
	TAG	3 pairs of abdominal cells at the posterior end of the TAG (innervate the gut)	-	+ (DLAa cells in abdominal neuromeres [27])	+ [34]
	peripheral NS	2 pairs of cells on segmental nerves exiting the thoracic part of the TAG	-	+ (peripheral cells on the wing and haltere nerves [27])	+ [34]
	gut	EECs in the posterior midgut	+	+	+ [34]
3rd instar larva	VG	2 cells ventro-medially in the anterior abdominal region of the VG	-	+ (VMA cells in abdominal neuromeres 1–2 [27, 46])	+ [54]
		3 pairs of abdominal cells at the posterior end of the VG (innervate the hindgut)	-	+ (DLAa cells in abdominal neuromeres 8–9 [27, 46])	+ [54]
	peripheral NS	? (not analyzed)	?	+ (1 pair of peripheral cells each in the meso- and metathoracic segment [27])	? (not analyzed)
	gut	EECs in the posterior midgut	+	+	+ [54]

[1] Details relate to AstA IR detected in this study, as well as results from [27] and [46], which are consistent with our findings.
[2] data from Hergarden et al. [34, 54]
DLAa dorsolateral abdominal a, EECs enteroendocrine cells, LCBR lateral cell body region, NS nervous system, PLP posterior lateral protocerebrum, TAG thoracico-abdominal ganglion, VG ventral ganglion, VMA ventromedial abdominal

Activation of a subset of AstA cells in the brain and the gut epithelium reduces food intake

To analyze a possible role of AstA as a signal to control food intake, we employed the CAFE assay [47] to measure food intake while AstA cells were thermogenetically activated to secrete AstA peptides. We measured the volume of liquid food consumed by male flies, which had been kept on food at 20 or 22°C following eclosion, over a period of two days at 29°C to activate AstA cells by ectopic expression of the *Drosophila* TrpA1 channel. TrpA1 is a heat sensor that is widely used to conditionally activate neurons by temperatures above ~ 25°C [e.g. 57, 58].

First, we measured food intake of *AstA(34)>TrpA1* (*UAS-TrpA1/+; AstA(34)-Gal4/+*) flies. At 29°C, but not at 20°C, consumption by *AstA(34)>TrpA1* flies was significantly lower than that of controls (Fig. 3). A similar reduction of food intake at 29°C was detected for *AstA(1)>TrpA1* flies (Fig. 4). This is in accordance with the results from a different feeding assay performed by Hergarden et al. [34], who observed that constitutive activation of AstA cells with *AstA(1)-Gal4* driven NaChBac reduced starvation-induced feeding behavior [34]. In contrast to TrpA1, expression of NaChBac, a bacterial voltage-gated sodium channel, results in a constant increase of neuronal excitability throughout development [59].

In *tsh-Gal80; AstA(34)>TrpA1* (*UAS-TrpA1/tsh-Gal80; AstA(34)-Gal4/+*) flies with TrpA1 expression limited to *AstA(34)* central brain neurons (PLP cells, LCBR cells), medulla neurons and EECs, cellular activation by a shift to 29°C was sufficient to reproduce the feeding phenotype found in *AstA(34)>TrpA1* flies (Fig. 5). This shows that the AstA neurons in the TAG and SOG, as well as the two pairs of peripheral AstA neurons, are dispensable for the feeding effect, and suggests that signaling via AstA-producing PLP cells and/or EECs, i.e. the cells that are included in the expression patterns of *AstA(34)-Gal4*, *tsh-Gal80; AstA(34)-Gal4* and *AstA(1)-Gal4*, controls food intake. A role for the AstA neurons in the optic lobe cannot be excluded but seems unlikely, since *AstA(34)-Gal4* driven expression in these neurons is inconsistent and weak, and their processes do not leave the medulla.

AstA cell activation considerably reduces locomotor activity

As shown above, activation of a specific subset of AstA cells resulted in reduced food intake. As locomotor activity affects energy expenditure and thus appetite, we asked whether AstA might indirectly reduce feeding by decreasing the activity of the flies. To analyze locomotor activity, flies were kept in small glass tubes and their movements were monitored using Drosophila Activity Monitors.

Compared to control flies, the average locomotor activity of *AstA(1)>TrpA1* flies was significantly reduced at 29°C, but not at 22°C (Fig. 6), contradicting the findings of Hergarden et al. [34]. This implies that activation of AstA cells leads to a strong inhibition of locomotion. To find out which AstA cells are underlying this effect, we simultaneously measured *AstA(34)>TrpA1* flies (Fig. 6) and repeated the experiment with *tsh-Gal80; AstA(34)>TrpA1* flies (Suppl. Fig. S1). Activity in *AstA(34)>TrpA1* flies was reduced to a similar level as in *AstA(1)>TrpA1* flies (Fig. 6), and the *tsh-Gal80* construct did not influence the reduction of locomotion (Suppl. Fig. S1). This indicates that the PLP neurons or the AstA EECs, but not the DLAa neurons or the four peripheral AstA neurons are mediating an inhibitory influence on locomotion. The circadian clock, a strong modulator of lomocotor activity, was not affected by activation of AstA cells, as activity of *AstA(1)>TrpA1* and *AstA(34)>TrpA1* flies at 29°C under constant darkness was—albeit reduced—rhythmic and period length did not differ from controls (Suppl. Fig. S2).

AstA regulates defecation behavior

An important function of the insect hindgut is the reabsorption of water and ions from the material transferred by the midgut and the Malpighian tubules. The *Drosophila* hindgut and the posteriormost midgut are innervated by the AstA-producing DLAa neurons (Fig. 1E, F, H). Regions with innervations include the pyloric valve and the rectal valve, which control transit of gut contents and urine from the midgut to the ileum and from the ileum to the rectum. The central innervation of these valves suggests a neuronal regulation of their function [48]. Furthermore, AstA EECs are found in the midgut region adjacent to the midgut-hindgut transition and might influence pyloric valve function.

Processes of the DLAa neurons innervating the rectum in part extend through the muscle layer (Fig. 7), thus their peptide signals might target the rectal epithelium and regulate its reabsorptive action. To detect possible effects of AstA on the activity of the hindgut and its valves, we fed male flies with food containing BPB. After that, analysis of fly deposits (number, size, color, dye density etc.) provided a readout for the investigation of defecation and excretion [48].

The defecation assay was repeated several times, but results were quite variable, both at 22 and 29°C, and statistical analysis did not reveal robust significant differences. In general, deposits of *AstA(34)>TrpA1* flies at 29°C were larger than those of controls, and the number of excreta was smaller (Fig. 8). The same tendency to larger and less numerous deposits is also seen in *tsh-Gal80; AstA(34)>TrpA1* flies at 29°C, although here the effect is less prominent (Fig. 8). No such tendencies were seen at 22°C (not shown). Our results suggest that AstA cells in the brain and in the gut affect defecation behavior. The observed effect is at least in part attributable to the diminished feeding and locomotion seen in *AstA(34)>TrpA1* and *tsh-Gal80; AstA(34)>TrpA1* flies. In comparison of *AstA(34)>TrpA1* and *tsh-Gal80; AstA(34)>TrpA1* flies, the different magnitude of the tendency to excrete less and larger deposits at 29°C suggests that the DLAa neurons and/or the four peripheral AstA neurons are involved in the regulation of defecation without measurably influencing food intake or locomotor activity, which are similar in both genotypes (Fig. 5, Suppl. Fig. S1). In summary, we could show that AstA cells in the brain and/or the AstA EECs, as well as the DLAa neurons and/or the peripheral AstA neurons directly or indirectly influence defecation behavior.

Clear tendencies for changes in the shape, lightness or color of the deposits could not be found. These features are indicators for the water content and pH of excreta, thereby providing information about (anti)diuretic and acid-base-homeostatic activity by the gut [48]. Thus, regarding the regulation of water and ion balance, we could not assign any distinct function to the hindgut-innervating DLAa neurons.

DAR-2 is required for AstA-induced inhibition of midgut motility

In a variety of insects, including *Drosophila*, AstA peptides have been detected in neurons innervating the gut and in EECs of the midgut epithelium [13, 27]. Furthermore, AstA has been shown to reduce motility of different parts of the gut in several insects [e. g. 15–19, 21–24]. However, an effect of AstA peptides on the activity of the gut muscle in *Drosophila* has not been demonstrated so far.

In preliminary tests on dissected midguts of w^{1118} larvae we observed a reduction of spontaneous movements after application of 10^{-6} M AstA-4, which was visible by eye without further analysis. We therefore tested the effect of AstA on gut motility by measuring the movement of larval midguts dissected from feeding 3rd instars before and after application of different concentrations of AstA-4. In HL3.1 saline, the midguts showed spontaneous contractions that were inhibited in a dose-dependent manner by AstA-4 dissolved in HL3.1 saline (Fig. 9). Application of HL3.1 saline alone did not affect or slightly increased gut motility (data not shown). Our data suggests that 10^{-6} M AstA-4

causes maximal inhibition and that higher concentrations would not reduce the measured value to -1, because the relaxation of midgut tension, which can be observed in addition to a cessation of contractions, generates itself a slow movement during the period analyzed. To find out which AstA receptor mediates the myoinhibitory effect of AstA-4, we first tested by qPCR which receptor is expressed in the gut including associated muscles.

Table 2: FlyAtlas gene expression data for *DAR-1* and *DAR-2* in selected body regions of larval and adult *Drosophila* [60].

Stage	Tissue	DAR-1 (CG2872)		DAR-2 (CG10001)	
		mRNA Signal	Affy Call	mRNA Signal	Affy Call
adult (7 d old)	brain	143 ± 1	up	9 ± 1	down
	eye	147 ± 7	up	40 ± 3	up
	TAG	87 ± 1	up	20 ± 1	up
	crop	2 ± 1	none	116 ± 3	up
	midgut	1 ± 0	none	157 ± 8	up
	tubule	1 ± 0	down	54 ± 5	up
	hindgut	1 ± 0	none	262 ± 7	up
	heart	1 ± 0	none	44 ± 4	up
feeding 3rd instar larva	CNS	45 ± 13	up	28 ± 3	up
	midgut	0 ± 0	none	103 ± 8	up
	tubule	1 ± 0	none	47 ± 2	up
	hindgut	1 ± 0	none	196 ± 12	up
	carcass	3 ± 1	none	128 ± 13	up
whole fly (reference)		2 ± 1	–	13 ± 0	–

TAG thoracico-abdominal ganglion

According to the FlyAtlas [60], only *DAR-2*, but not *DAR-1* is expressed at a detectable level in the gut of adult and larval *Drosophila* (Table 2). Since GPCRs are often expressed at low levels, we re-measured mRNA levels of both receptors in adult flies by qPCR. Our results show that both receptors are expressed in the gut, with *DAR-1* mRNA occurring at a lower level than *DAR-2*, partly confirming the data from FlyAtlas (Table 3). The gut contains different types of cells that might potentially express *DAR-1* or *DAR-2*, e.g. enterocytes, EECs or the surrounding muscle cells. According to the function of the cell type, AstA might provoke different effects in the gut.

Table 3: Relative expression levels of *DAR-1* and *DAR-2* in the brain, the thoracico-abdominal ganglion and the midgut of adult flies were detected by qPCR. $2^{\Delta Ct}$ values represent the relative expression ratios of *DAR-1* or *DAR-2* in comparison to the reference gene (*α-tubulin*).

Tissue	DAR-1		DAR-2	
	mean ΔCt / SEM	$2^{\Delta Ct}$	mean ΔCt / SEM	$2^{\Delta Ct}$
brain	-4.1 / ± 0.19	0.0596	-6.9 / ± 0.25	0.0085
TAG	-5.6 / ± 0.15	0.0211	-8.1 / ± 0.21	0.0035
midgut	-11.5 / ± 0.25	0.0004	-4.5 / ± 0.18	0.0430

TAG thoracico-abdominal ganglion

To find out which receptor is mediating the myoinhibitory effect of AstA, we downregulated both DAR-1 and DAR-2 by expressing either *DAR-1*- or *DAR-2-RNAi* using the *Mef2-Gal4* driver, which—in the gut—directs expression specifically to the musculature. While AstA-4 had a similar myoinhibitory effect on guts from *Mef2>Dcr-2; DAR-1-RNAi* larvae than in controls, downregulation of *DAR-2* expression rendered the peptide ineffective at *Mef2>Dcr-2; DAR-2-RNAi* guts (Fig. 9).

The C-terminus of Drome-AstA-4 is FXFGL-amide, while Drome-AstA-1–3 terminate with YXFGL-amide. To make sure that the observed effects are not restricted to AstA-4 only, we repeated the measurements with 10^{-7} M AstA-1. Similar to AstA-4 we found a reduction of motility for guts from *Mef2>Dcr-2; DAR-1-RNAi* and control larvae, but not for *Mef2>Dcr-2; DAR-2-RNAi* larvae (not shown). These results imply that all AstA peptides exert an inhibitory effect on gut motility. This effect is mediated by DAR-2, which is expressed in the muscle cells surrounding the midgut, and not DAR-1.

Discussion

With this study we show that AstA cells of the fruit fly regulate several behaviors related to metabolism and that the pleiotropic action of AstA peptides is more complex than previously shown. In addition, we could assign different regulatory functions to specific subsets of AstA cells.

Activation of AstA-producing PLP neurons and EECs resulted in reduced food intake and a striking decrease of locomotor activity of fruit flies. Besides, activation of the PLP neurons and AstA EECs altered defecation behavior towards fewer but larger deposits, though our results suggest an additional involvement of the gut-innervating DLAa neurons in the TAG and/or the peripheral AstA neurons. Moreover, AstA peptides were found to act as inhibitors of midgut motility and therefore regulate food transit, which has not been demonstrated for *Drosophila* so far.

Subset-dependent functions of AstA cells: brain PLP cells regulate feeding, gut EECs control activity

Using the *AstA(1)-Gal4* driver, Hergarden et al. found that flies consumed less food if AstA cells were activated via UAS-NaChBac [34]. They ruled out that this feeding phenotype was an indirect consequence—caused by an effect on locomotor activity, gustatory abilities, energy reserves, starvation resistance or food content in the gut—by showing that these characteristics were not significantly altered by activation of AstA cells.

In contrast to the results of Hergarden et al., we found a strong and almost immediate effect on locomotion when AstA cells were thermogenetically activated via TrpA1. The observed difference might be a result of the different nature of the activators. NaChBac constantly activates the cells, while activation with TrpA1 is inducible. Hence, one possible explanation might be a downregulation of AstA receptors caused by constant exposure to the ligand if NaChBac is used for activation. This explanation implies that the adaptive downregulation is differential, so it affects cells involved in locomotion but not feeding.

A more reasonable explanation lies in the differences between the physiological properties of EECs and neurons. EECs are supposed to be activated by an influx of Ca^{2+} but not Na^{+}, thus *AstA-Gal4*-driven TrpA1 activates both AstA EECs and neurons at temperatures above 25°C and induces AstA release, while *AstA-Gal4*-driven NaChBac activates only AstA neurons, as EECs as endocrine cells are most likely non-excitable. This would suggest that the reduction of locomotion is caused by activation of the AstA EECs, but not by activation of AstA neurons. AstA from the EECs might reach

the somatic musculature or (motor)neurons controlling locomotion via the hemolymph and inhibit movements of the fly, thus effectively acting as a hormone, while neuronal release does not measurably contribute to this effect. Locomotor activity influences energy expenditure and therefore reduced locomotion should result in reduced feeding. Still, the results from Hergarden et al. demonstrated that the inhibitory effect of AstA on feeding is not (or only in part) a consequence of a reduced activity of the flies, and suggest that AstA neurons influence the motivation to feed [34]. A caveat of our study is that we cannot genetically distinguish between *AstA*-expressing neurons and EECs, as so far no EEC-specific drivers are known. First experiments designed to use *elav-Gal80* to separate AstA neurons from EECs showed that *elav* is strongly expressed not only in neurons, but also in EECs. This is fully in line with the finding that Elav antibodies marked EECs (data not shown).

Since the effect of thermogenetic cell activation on feeding and locomotor activity was similar regardless of which *AstA-Gal4* construct was used to drive TrpA1 expression, we reasoned that the LCBR neurons, which are included in the expression patterns of *AstA(34)-Gal4* and *tsh-Gal80; AstA(34)-Gal4* but not of *AstA(1)-Gal4*, did not influence the characteristics investigated in this study. However, we cannot fully exclude a possible effect of LCBR neuron activation on our results.

The myoinhibitory function of allatostatin A is conserved in *Drosophila*

The regulation of gut motility is important for the transport of food through the gut as well as for effective digestion [e.g. 23]. *Drosophila* foregut and hindgut peristalsis are conducted by associated circular muscles, while the midgut is surrounded by a bi-layered meshwork of muscle fibers: an inner layer of circular muscles and an outer layer of longitudinal muscles [61].

We found that AstA peptides dose-dependently inhibit the activity of the *Drosophila* larval midgut musculature, and that this inhibition is dependent on the DAR-2 receptor. For practical reasons, we measured motility effects on the bigger and more robust larval guts. Since the longitudinal and circular muscles of the *Drosophila* midgut persist during metamorphosis [62, 63], it appears likely that AstA and DAR-2 also mediate inhibition of gut peristalsis in the adult. This assumption is further supported by FlyAtlas expression data [60], which shows abundant expression of *DAR-2* in the gut of both adults and larvae (Table 2). Moreover, AstA-producing EECs can be found in the same region, i.e. the posteriormost midgut, in both stages [9, 10, 27]. Since the larval midgut is not innervated by processes of AstA neurons, the effect of AstA on gut peristalsis indicates a paracrine or hormonal role of the AstA EECs in the regulation of food transit through the gut.

In a heterologous cell assay, the four *Drosophila* AstA peptides activated DAR-2 with an EC_{50} of $1–8\times10^{-8}$ M [31]. In our experiments a somewhat higher concentration (10^{-7} M) of AstA-4 or AstA-1 was necessary to evoke a significant reduction in midgut muscle activity. The bath-applied peptide may not as effectively reach the muscle receptors as the native peptides in the living fruit fly. Muscles in gut regions containing AstA EECs or lying adjacent to neuronal AstA release sites are likely exposed to high doses of the peptides that—due to the convoluted arrangement of the gut *in vivo*—might effectively inhibit large portions of the gut muscle. A tight temporal restriction of the effect might be achieved by rapid degradation of the peptides in the hemolymph or at the gut epithelium after release [64–66].

AstA is a possible satiety factor

Recent studies indicated that AstA is involved in the regulation of metabolism [33–35]. Along this line, Hentze et al. showed that AstA regulates insulin and AKH signaling, and that AstA signaling itself responds to the uptake of food in a nutrient type-depending manner [35].

Our findings further strengthen the assumption that AstA is a component of the signaling network that promotes satiety and affects neural circuits and neurohemal centers in the brain, and identify the PLP neurons and the EECs as principal components. Extending this, our findings also show—perhaps not surprisingly for a brain-gut peptide—that AstA exerts pleiotropic actions, which are functionally connected, and appears to provide a link to functionally related processes (digestion, locomotion) in non-nervous tissues. After intake of nutritious food, AstA from the PLP neurons might cause inhibition of further feeding, and—as the need for food search behavior is relieved—a rise of hemolymph AstA levels, caused by activity of AstA EECs, might reduce locomotion of the fly. As another consequence of feeding, food transit through the gut, including defecation, need to be regulated by interplay of myoinhibitory factors such as AstA from EECs and gut-innervating DLAa neurons on the one hand, and myoactivators on the other hand, thus assuring effective digestion and adequate removal of metabolic and excretory waste products. However, we are aware that under wild-type conditions different AstA cell subsets are not necessarily active in the same circumstances.

AstA EECs in *Drosophila* are “open type” EECs [9], i.e. they possess apical extensions that reach the gut lumen. Hence, these cells might sense nutrients in the gut and thereupon exert their effects via paracrine and endocrine signaling [67, 68]. Besides the effects on gut motility and locomotor activity described above, further feeding-related functions of AstA signaling by EECs, which we did not analyze in this study, are possible. These might involve stimulation of digestive enzyme activity in the midgut, as it has been described for AstA cells in other insects [17, 18, 25].

Acknowledgements

The authors wish to thank Matt Wayland (University of Cambridge) for programming of and help with the QAFF software, Susanne Klühspies, Gertrud Gramlich and Sylwia Febocolon for excellent technical assistance, Pamela Menegazzi and Dirk Rieger for help with locomotor activity analysis, Mareike Pauls-Selcho for helpful discussion, Charlotte Helfrich-Förster and the members of her lab for general support and discussion. We also greatly acknowledge funding by the Deutsche Forschungsgemeinschaft (DFG WE 2652/4-2, to CW) and the DAAD (“Kurzstipendium für Doktoranden” to WR).

Figures

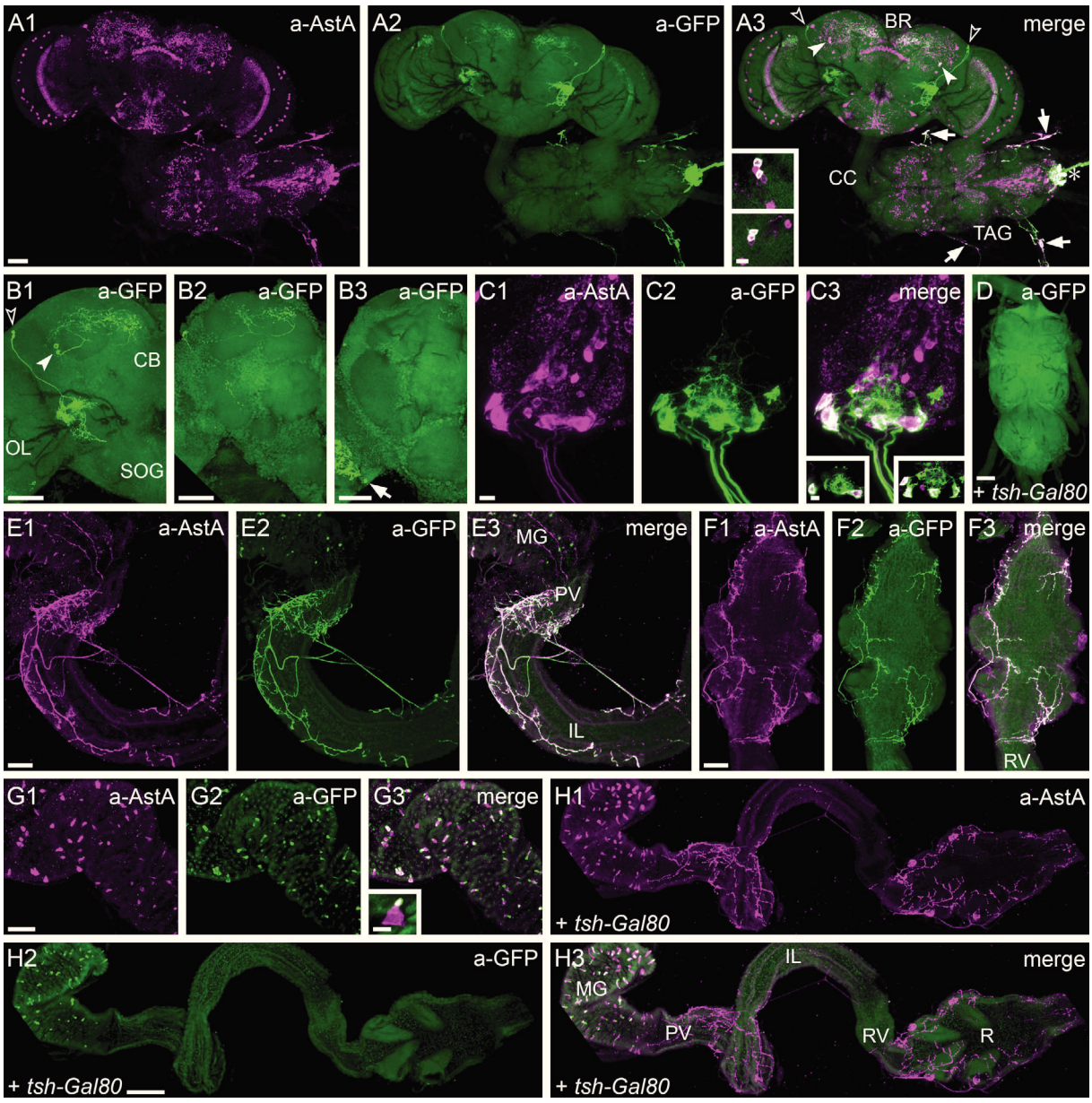
A1
a-AstA
A2
a-GFP
A3
BR
merge
CC
TAG
B1
a-GFP
CB
OL
SOG
B2
a-GFP
B3
a-GFP
C1
a-AstA
C2
a-GFP
C3
merge
D
a-GFP
+ tsh-Gal80
E1
a-AstA
E2
a-GFP
E3
MG
merge
PV
IL
F1
a-AstA
F2
a-GFP
F3
merge
RV
G1
a-AstA
G2
a-GFP
G3
merge
H1
a-AstA
+ tsh-Gal80
H2
a-GFP
+ tsh-Gal80
H3
IL
merge
MG
PV
RV
R
+ tsh-Gal80

◀ **Figure 1:**

AstA and GFP labeling of nervous systems and guts of adult *AstA(34)>GFP* (A–C, E–G) and *tsh-Gal80; AstA(34)>GFP* (D, H) flies.

A: GFP expression is detectable in two paired groups of brain neurons. In each hemisphere, one group with two somata in the posterior lateral protocerebrum (PLP cells, solid arrowheads in A3) and a second group with two to four somata in the lateral cell body region (LCBR cells, open arrowheads in A3) are labeled (see also B). The LCBR neurons are anti-AstA-negative. Some of the AstA-IR medulla neurons also express GFP. In the abdominal TAG, the six AstA-IR DLAa cells show strong anti-GFP staining and project through the median abdominal nerve towards the gut (asterisk in A3). Four peripheral cells located on nerves that exit the TAG dorso-laterally also exhibit co-labeling (arrows in A3). Inset in A3: Single optical sections showing double-labeled PLP cells of both hemispheres.

B: The GFP signal in brains of different individuals illustrates the variability of expression intensity. The PLP cells (solid arrowhead in B1) innervate the superior protocerebrum, while the ramifications of the LCBR neurons (open arrowhead in B1) lie mainly within the posterior lateral protocerebrum and the posterior slope. Arrow in B3 marks strongly stained neuron in the medulla.

C: Detail of the abdominal TAG. Three pairs of AstA-IR DLAa neurons co-express GFP and run through the median abdominal nerve to innervate the hindgut and posterior midgut (see E). The membrane-targeted GFP distinctly marks the projections of these neurons. Two single optical sections (insets in C3) reveal six co-labeled cell bodies.

D: *AstA(34)-Gal4* expression in the TAG is absent with *tsh-Gal80*.

E: AstA and GFP labeling are present in neuronal processes at the hindgut, which extend onto the posterior midgut. (Malpighian tubules have been removed during dissection.)

F: The rectal part of the hindgut is likewise innervated by double-labeled neurons.

G: GFP is expressed in most of the AstA-producing EECs that are scattered within the epithelium of the posterior midgut. The maximum intensity projection of a single EEC in the inset of G3 illustrates that the main GFP signal is restricted to the narrow apical portion of the cells.

H: GFP expression is absent from gut neurons in individuals carrying *tsh-Gal80*, but remains in the AstA EECs. (Malpighian tubules have been removed during dissection.)

Scale bars: in A, B and D–G 50 µm; in C and insets 10 µm; in H 100 µm.

BR brain, CB central brain, CC cervical connective, IL ileum, MG midgut, OL optic lobe, PV pyloric valve, R rectum, RV rectal valve, SOG subesophageal ganglion, TAG thoracico-abdominal ganglion.

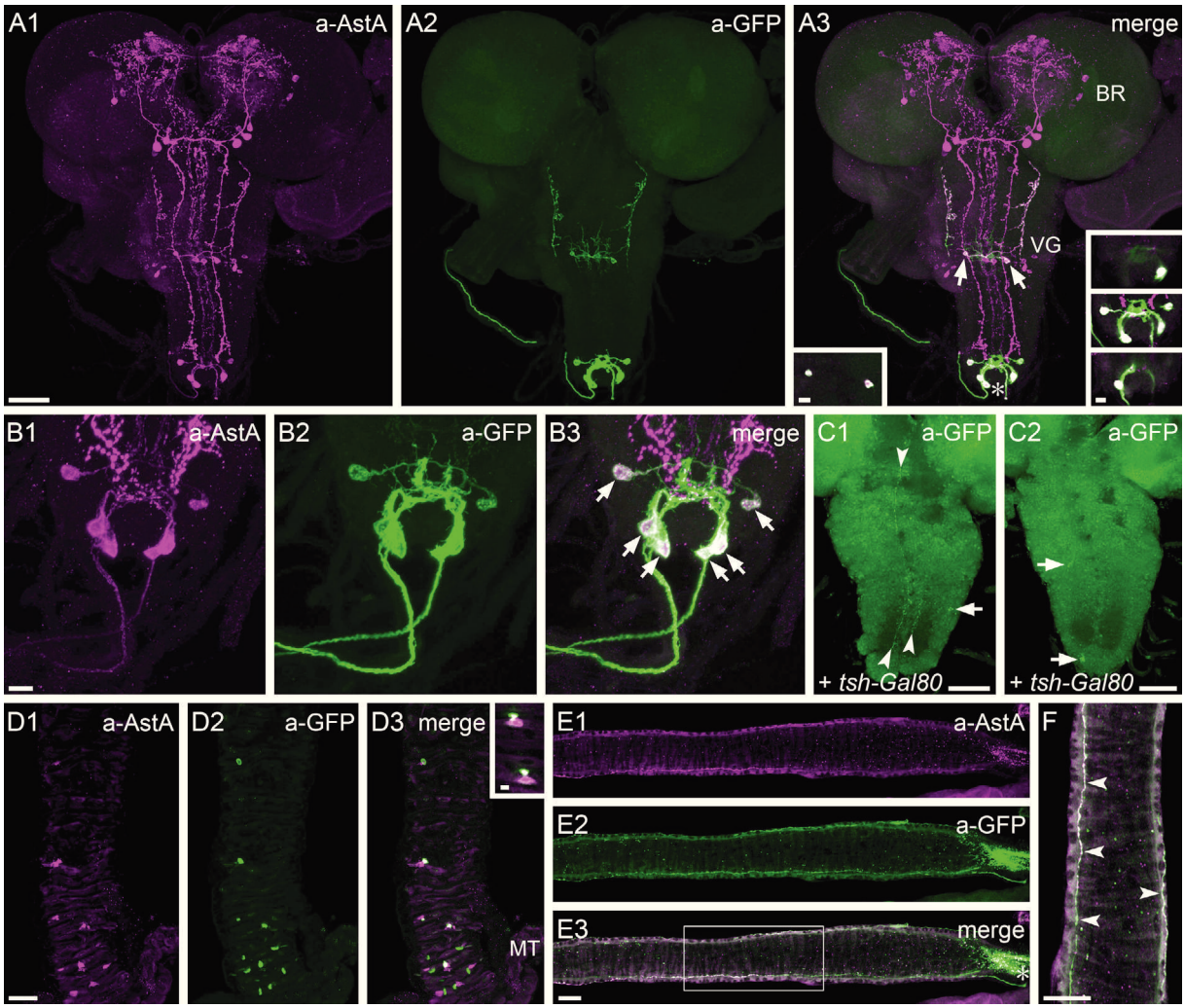
A1
a-AstA
A2
a-GFP
A3
merge
BR
VG
B1
a-AstA
B2
a-GFP
B3
merge
C1
a-GFP
+ tsh-Gal80
C2
a-GFP
+ tsh-Gal80
D1
a-AstA
D2
a-GFP
D3
merge
MT
E1
a-AstA
E2
a-GFP
E3
merge
F

◀ **Figure 2:**

AstA IR and GFP expression in *AstA(34)>GFP* (A, B, D–F) and *tsh-Gal80; AstA(34)>GFP* (C) feeding 3rd instar larval CNS and guts. C and F show maximum intensity projections of optical sections representing only a part of the z-axis of the object to improve visibility of stained neurons.

A: *AstA(34)-Gal4* is expressed in a subset of AstA neurons in the VG: one pair with cell bodies in the anterior abdominal VG (VMA cells, arrows in A3) and three pairs in the posterior tip (DLAa cells, asterisk in A3). Left inset in A3: Single optical section through VMA cell bodies. Right inset in A3: Three single optical sections demonstrate six double-labeled DLAa cells in the posterior VG.

B: Detail of the posterior VG. Co-labeled DLAa cells (arrows in B3) send projections through the last abdominal nerves (segmental nerves a8/9) to the hindgut.

C: *AstA(34)-Gal4*-driven GFP expression in two different VG preparations of larvae with *tsh-Gal80*. GFP expression is abolished in the VMA and DLAa cells. Only a weak labeling of variable anti-AstA-negative (C1) or anti-AstA-positive (C2) cells was frequently observed. Arrows point to somata, arrowheads mark processes.

D: AstA-producing EECs in the posterior midgut are co-labeled for GFP. Inset in D3: Detail with two EECs. While anti-AstA staining is stronger in the basal part of the EECs, most of the GFP localizes to the apical part.

E: Double-labeled neuronal processes of the DLAa cells innervate the hindgut and run up to its posterior end (asterisk in E3). Box: Higher magnification of this portion is shown in F.

F: Detail of the hindgut. Two neurites labeled for AstA and GFP (arrowheads) run along the outside of the hindgut.

Scale bars: in A and C–F 50 µm; in B and insets 10 µm.

BR brain, MT Malpighian tubule, VG ventral ganglion.

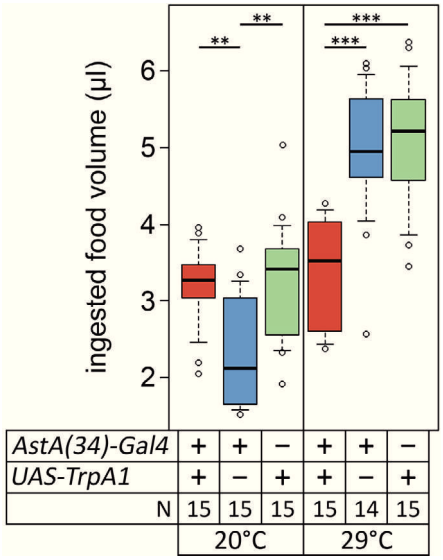

Figure 3:

Thermogenetic activation of the AstA(34) cells resulted in reduced food intake. The total food volume consumed within two days was measured via the CAFE assay. At 20°C, *AstA(34)>TrpA1* flies did not consume less food than the controls. Activation of the TrpA1 channel by 29°C resulted in significantly reduced food intake in *AstA(34)>TrpA1* flies compared to the controls. * $p \leq 0.05$, ** $p \leq 0.01$, *** $p \leq 0.001$. Genotypes were: *UAS-TrpA1/+; AstA(34)-Gal4/+, +/+; AstA(34)-Gal4/+, UAS-TrpA1/+; +/+.*

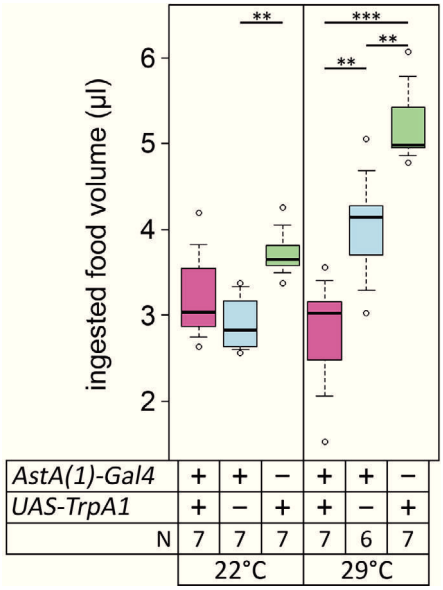

Figure 4:

Food intake of flies was reduced if AstA(1) cells were thermogenetically activated. *AstA(1)>TrpA1* flies consumed significantly less food than controls when AstA cells were activated at 29°C, but not at 22°C. * $p \leq 0.05$, ** $p \leq 0.01$, *** $p \leq 0.001$. Genotypes were: *UAS-TrpA1/+; AstA(1)-Gal4/+, +/+; AstA(1)-Gal4/+, UAS-TrpA1/+; +/+.*

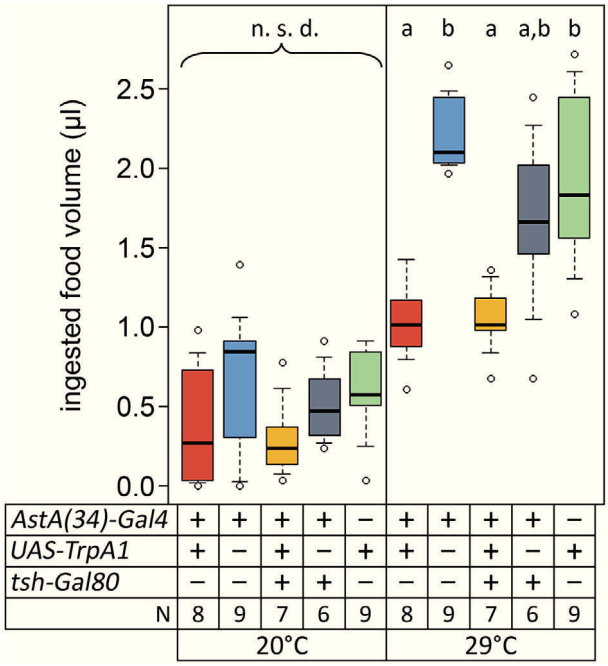

Figure 5:

Restricted thermogenetic activation of AstA(34) cells in the brain and midgut was sufficient to inhibit feeding. No significant differences (n. s. d.) of food consumption were measured at 20°C. After a shift to 29°C, food intake of *tsh-Gal80; AstA(34)>TrpA1* flies was significantly lower than that of control flies, and not different from *AstA(34)>TrpA1* flies. The *tsh-Gal80; AstA(34)-Gal4* control showed an intermediate phenotype.

The setup for the CAFE assay here slightly differed from the previous tests (Figs. 3, 4): flies were left at 20°C for two days and were then switched to 29°C for two days. Food intake was measured for day 2 ("20°C") and day 4 ("29°C"). All genotypes were tested simultaneously, and two independent tests were performed that gave similar results. Mortality during the assay was higher in the two groups with *tsh-Gal80*, hence N numbers are lower. Genotypes were assigned to different statistical groups "a" or "b" if $p \leq 0.05$. ** $p \leq 0.01$, *** $p \leq 0.001$. Genotypes were: *UAS-TrpA1/+; AstA(34)-Gal4/+, +/+; AstA(34)-Gal4/+, UAS-TrpA1/tsh-Gal80; AstA(34)-Gal4/+, +/tsh-Gal80; AstA(34)-Gal4/+, UAS-TrpA1/+; +/+.*

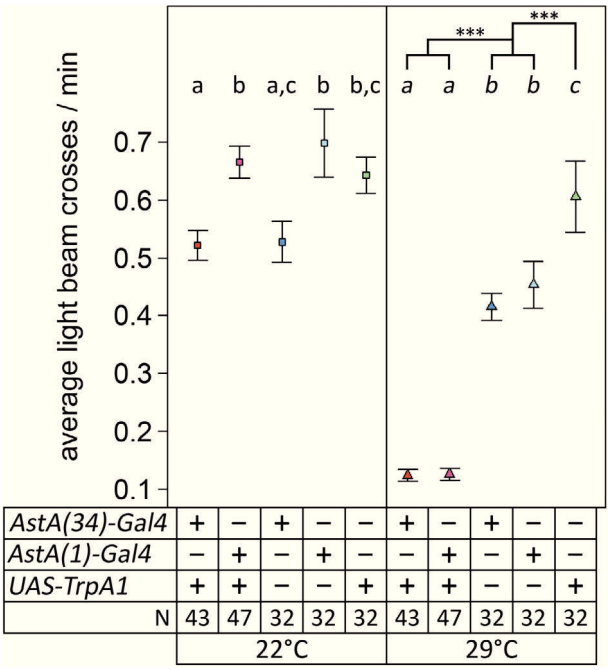

Figure 6:

Thermogenetic activation of AstA cells resulted in a strongly inhibited locomotion. At 29°C, activity levels of both experimental genotypes, *AstA(1)>TrpA1* and *AstA(34)>TrpA1*, were similar and significantly lower than those of control genotypes. At 22°C, activity of *AstA(1)>TrpA1* flies was similar to controls, while the *AstA(34)>TrpA1* flies were on a level with the *AstA(34)-Gal4* control flies, but moved less than *UAS-TrpA1* control flies. Genotypes were assigned to different statistical groups "a", "b" or "c" (22°C) or groups "*a*", "*b*" or "*c*" (29°C) if $p \leq 0.05$. ** $p \leq 0.01$, *** $p \leq 0.001$. Graph shows means and SEM. Genotypes were: *UAS-TrpA1/+; AstA(34)-Gal4/+, UAS-TrpA1/+; AstA(1)-Gal4/+, +/+; AstA(34)-Gal4/+, +/+; AstA(1)-Gal4/+, UAS-TrpA1/+; +/+.*

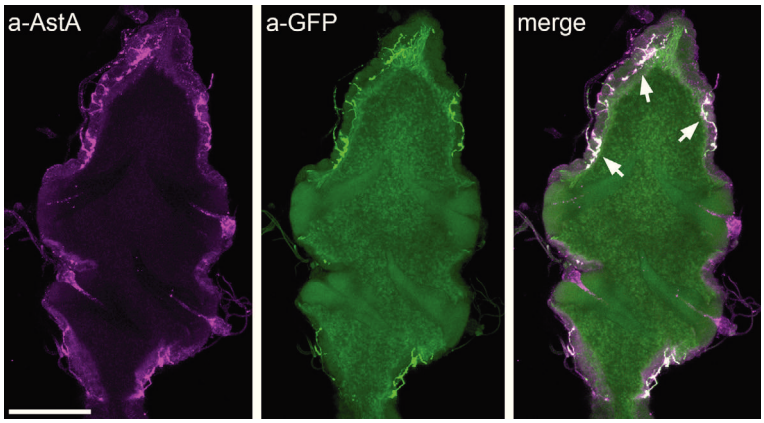

Figure 7:

Rectum of *AstA(34)>GFP* flies stained for AstA and GFP. A part of the DLAa neuron arborizations, which are co-labeled for AstA and GFP, permeate the rectal muscle layer and run in proximity to the epithelial cells (arrows). Maximum intensity projection of optical sections representing ~ 24 µm in z-axis. Scale bar: 100 µm.

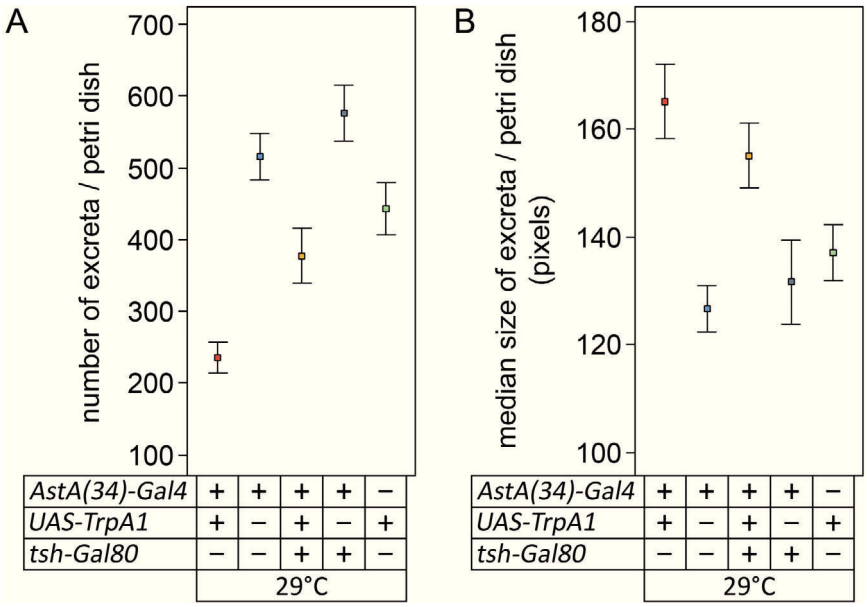

Figure 8:

Thermogenetic activation of AstA cells affects defecation behavior. Exemplary results from one defecation assay demonstrate that *AstA(34)>TrpA1* flies by trend defecate less frequently than control flies over a period of 24 hours at 29°C (A), but deposits tend to be larger (B). A similar but weaker tendency to fewer (A) and larger (B) excreta could be detected upon activation of the *tsh-Gal80; AstA(34)-Gal4* cell subset. Graphs show means and SEM; N=5. Genotypes were: *UAS-TrpA1/+; AstA(34)-Gal4/+, +/+; AstA(34)-Gal4/+, UAS-TrpA1/tsh-Gal80; AstA(34)-Gal4/+, +/tsh-Gal80; AstA(34)-Gal4/+, UAS-TrpA1/+; +/+.*

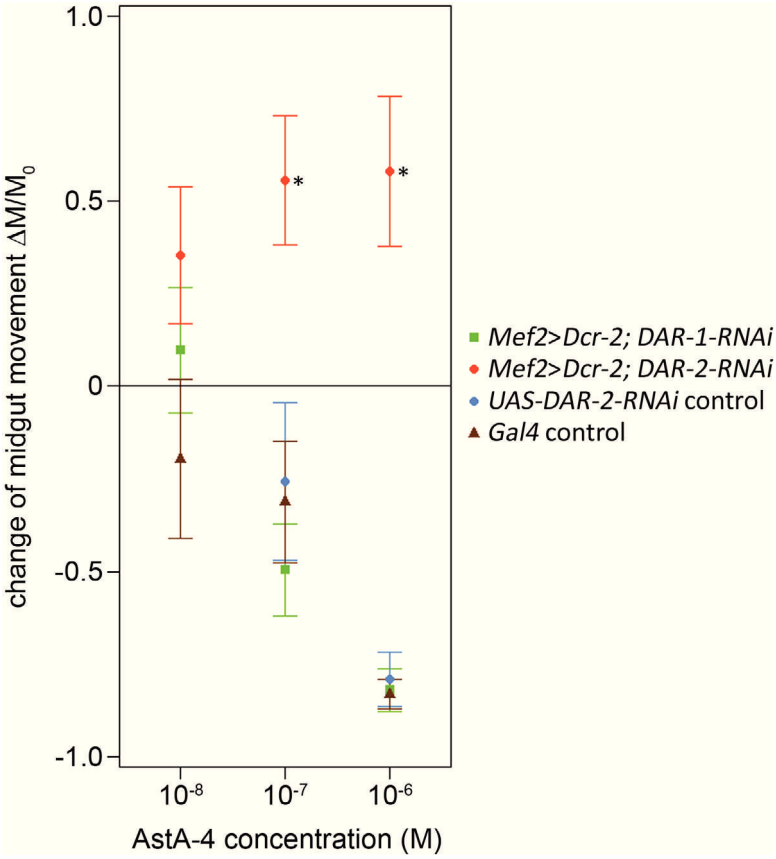

Figure 9:

Inhibition of larval midgut motility by AstA-4 is dose- and DAR-2-dependent. Values were calculated as relative changes in gut movements ($\Delta M/M_0$). The *UAS-DAR-1-RNAi* control was not measured because no differences were visible for *Mef2>Dcr-2; DAR-1-RNAi* guts in comparison to the *Gal4* control. Graph shows means and SEM; N=4–6. * $p \leq 0.05$, ** $p \leq 0.01$, *** $p \leq 0.001$ (significant difference to controls, Mann-Whitney U test). Genotypes were the following: *UAS-Dcr-2/+; UAS-DAR-1-RNAi/+; Mef2-Gal4/+* (*Mef2>Dcr-2; DAR-1-RNAi*), *UAS-Dcr-2/+; UAS-DAR-2-RNAi/+; Mef2-Gal4/+* (*Mef2>Dcr-2; DAR-2-RNAi*), *UAS-Dcr-2/+; UAS-DAR-2-RNAi/+; +/+* (*UAS-DAR-2-RNAi* control), *UAS-Dcr-2/+; +/+; Mef2-Gal4/+* (*Gal4* control).

Supplement

Recipe for standard *Drosophila* medium:

5.9 kg corn semolina was mixed with 34 L water, boiled for 3 min, and then constantly and slowly stirred for 4 h while cooling down. The next day, 6 L water, 1.8 kg malt extract, 1.8 kg sugar beet molasses, 0.4 kg soy flour, 0.74 kg yeast powder and 0.25 kg agar-agar were added, and the mixture was boiled for 3 min under constant stirring. When the medium had cooled down to ~ 80°C, 0.1 kg methyl-4-hydroxybenzoate (nipagin) was intermixed.

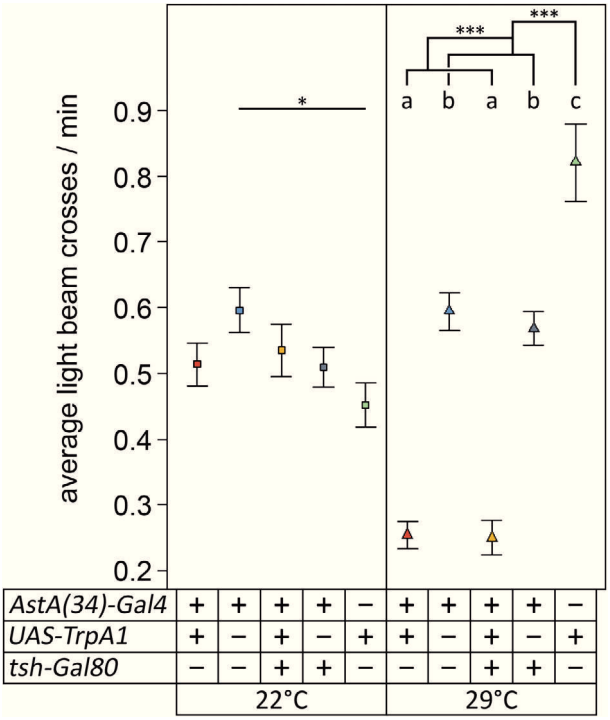

Supplemental Figure S1:

Thermogenetic activation of the brain and the midgut subset of AstA(34) cells was sufficient to reduce locomotion of flies. Average locomotor activity of *AstA(34)>TrpA1* and *tsh-Gal80; AstA(34)>TrpA1* flies was not different from control flies at 22°C. After a temperature increase to 29°C, locomotion of *AstA(34)>TrpA1* and *tsh-Gal80; AstA(34)>TrpA1* flies was still similar in both genotypes, but significantly lower than that of controls.

Average minute-by-minute activity of male flies was analyzed using Drosophila Activity Monitors. During monitoring, flies were kept in an incubator with a 12:12 hour light-dark cycle provided via a fluorescent tube. Temperature was initially set to 22°C. After several days for acclimatization, activity was measured for 72 hours. Then, temperature was switched to 29°C and activity was again measured for 72 hours.

Graph shows means and SEM; N=32. Genotypes were assigned to different statistical groups “a”, “b” or “c” (29°C) if $p \leq 0.05$. * $p \leq 0.05$, ** $p \leq 0.01$, *** $p \leq 0.001$. Genotypes were: *UAS-TrpA1/+; AstA(34)-Gal4/+, +/+; AstA(34)-Gal4/+, UAS-TrpA1/tsh-Gal80; AstA(34)-Gal4/+, +/tsh-Gal80; AstA(34)-Gal4/+, UAS-TrpA1/+; +/+.*

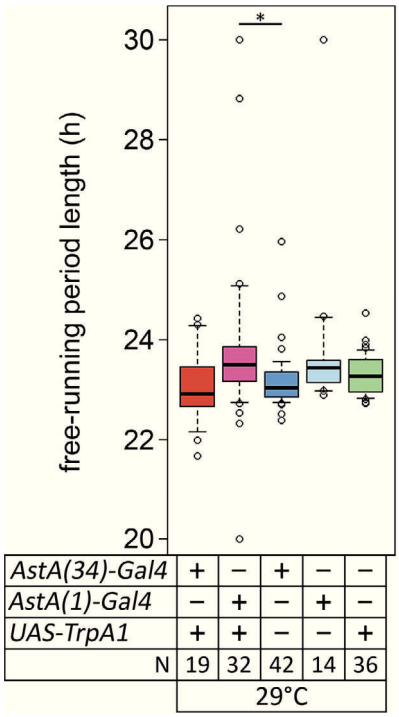

Supplemental Figure S2:

Free-running period length is not influenced by thermogenetic activation of AstA cells. The circadian locomotor activity rhythm of *AstA(34)>TrpA1* and *AstA(1)>TrpA1* flies in constant darkness at 29°C did not significantly differ from control flies.

Average minute-by-minute activity of male flies was analyzed using Drosophila Activity Monitors. Flies were synchronized for 3 days with a 12:12 h light-dark cycle at 29°C. Then, to calculate the free-running period, locomotor activity was recorded in constant darkness for 8 days and analyzed by chi-square periodogram analysis [69] using the ActogramJ software package (http://actogramj.neurofly.de/, [70]). * $p \leq 0.05$, ** $p \leq 0.01$, *** $p \leq 0.001$.

Genotypes were: *UAS-TrpA1/+; AstA(34)-Gal4/+, UAS-TrpA1/+; AstA(1)-Gal4/+, +/+; AstA(34)-Gal4/+, +/+; AstA(1)-Gal4/+, UAS-TrpA1/+; +/+*.

References

1. Stanley S, Wynne K, McGowan B, Bloom S (2005) Hormonal regulation of food intake. Physiol Rev 85:1131–1158. doi: 10.1152/physrev.00015.2004

2. Broberger C (2005) Brain regulation of food intake and appetite: molecules and networks. J Intern Med 258:301–327. doi: 10.1111/j.1365-2796.2005.01553.x

3. Chaudhri OB, Salem V, Murphy KG, Bloom SR (2008) Gastrointestinal Satiety Signals. Annu Rev Physiol 70:239–255. doi: 10.1146/annurev.physiol.70.113006.100506

4. Kirchgessner AL (2002) Orexins in the brain-gut axis. Endocr Rev 23:1–15.

5. Audsley N, Weaver RJ (2009) Neuropeptides associated with the regulation of feeding in insects. Gen Comp Endocrinol 162:93–104. doi: 10.1016/j.ygcen.2008.08.003

6. Spit J, Badisco L, Verlinden H, et al. (2012) Peptidergic control of food intake and digestion in insects. Can J Zool-Rev Can Zool 90:489–506. doi: 10.1139/Z2012-014

7. Veenstra JA, Lau GW, Agricola HJ, Petzel DH (1995) Immunohistological localization of regulatory peptides in the midgut of the female mosquito Aedes aegypti. Histochem Cell Biol 104:337–347.

8. Predel R, Neupert S, Garczynski SF, et al. (2010) Neuropeptidomics of the mosquito Aedes aegypti. J Proteome Res 9:2006–2015. doi: 10.1021/pr901187p

9. Veenstra JA, Agricola H-J, Sellami A (2008) Regulatory peptides in fruit fly midgut. Cell Tissue Res 334:499–516. doi: 10.1007/s00441-008-0708-3

10. Veenstra JA (2009) Peptidergic paracrine and endocrine cells in the midgut of the fruit fly maggot. Cell Tissue Res 336:309–323. doi: 10.1007/s00441-009-0769-y

11. Reiher W, Shirras C, Kahnt J, et al. (2011) Peptidomics and peptide hormone processing in the Drosophila midgut. J Proteome Res 10:1881–1892. doi: 10.1021/pr101116g

12. Zoephel J, Reiher W, Rexer K-H, et al. (2012) Peptidomics of the Agriculturally Damaging Larval Stage of the Cabbage Root Fly Delia radicum (Diptera: Anthomyiidae). PLoS ONE 7:e41543. doi: 10.1371/journal.pone.0041543

13. Tobe SS, Bendena WG (2006) Chapter 31 - Allatostatins in the Insects. In: Kastin AJ (ed) Handb. Biol. Act. Pept., 1st ed. Academic Press, Burlington, pp 201–206

14. Lange AB, Chan KK, Stay B (1993) Effect of allatostatin and proctolin on antennal pulsatile organ and hindgut muscle in the cockroach, Diploptera punctata. Arch Insect Biochem Physiol 24:79–92. doi: 10.1002/arch.940240203

15. Lange AB, Bendena WG, Tobe SS (1995) The effect of the thirteen Dip-allatostatins on myogenic and induced contractions of the cockroach (Diploptera punctata) hindgut. J Insect Physiol 41:581–588. doi: 10.1016/0022-1910(95)00008-I

16. Duve H, Wren P, Thorpe A (1995) Innervation of the foregut of the cockroach Leucophaea maderae and inhibition of spontaneous contractile activity by callatostatin neuropeptides. Physiol Entomol 20:33–44. doi: 10.1111/j.1365-3032.1995.tb00798.x

17. Fusé M, Zhang JR, Partridge E, et al. (1999) Effects of an allatostatin and a myosuppressin on midgut carbohydrate enzyme activity in the cockroach Diploptera punctata. Peptides 20:1285–1293.

18. Aguilar R, Maestro JL, Vilaplana L, et al. (2003) Allatostatin gene expression in brain and midgut, and activity of synthetic allatostatins on feeding-related processes in the cockroach Blattella germanica. Regul Pept 115:171–177. doi: 10.1016/S0167-0115(03)00165-4

19. Duve H, Johnsen AH, Maestro JL, et al. (1997) Identification, tissue localisation and physiological effect in vitro of a neuroendocrine peptide identical to a dipteran Leu-callatostatin in the codling moth Cydia pomonella (Tortricidae: Lepidoptera). Cell Tissue Res 289:73–83.

20. Duve H, East PD, Thorpe A (1999) Regulation of lepidopteran foregut movement by allatostatins and allatotropin from the frontal ganglion. J Comp Neurol 413:405–416.

21. Duve H, Audsley N, Weaver RJ, Thorpe A (2000) Triple co-localisation of two types of allatostatin and an allatotropin in the frontal ganglion of the lepidopteran Lacanobia oleracea (Noctuidae): innervation and action on the foregut. Cell Tissue Res 300:153–163.

22. Matthews HJ, Audsley N, Weaver RJ (2007) Interactions between allatostatins and allatotropin on spontaneous contractions of the foregut of larval Lacanobia oleracea. J Insect Physiol 53:75–83. doi: 10.1016/j.jinsphys.2006.10.007

23. Robertson L, Rodriguez EP, Lange AB (2012) The neural and peptidergic control of gut contraction in Locusta migratoria: the effect of an FGLa/AST. J Exp Biol 215:3394–3402. doi: 10.1242/jeb.073189

24. Duve H, Thorpe A (1994) Distribution and functional significance of Leu-callatostatins in the blowfly Calliphora vomitoria. Cell Tissue Res 276:367–379. doi: 10.1007/BF00306122

25. Sakai T, Satake H, Takeda M (2006) Nutrient-induced alpha-amylase and protease activity is regulated by crustacean cardioactive peptide (CCAP) in the cockroach midgut. Peptides 27:2157–2164. doi: 10.1016/j.peptides.2006.04.009

26. Clark L, Lange AB, Zhang JR, Tobe SS (2008) The roles of Dippu-allatostatin in the modulation of hormone release in Locusta migratoria. J Insect Physiol 54:949–958. doi: 10.1016/j.jinsphys.2008.03.007

27. Yoon JG, Stay B (1995) Immunocytochemical localization of Diploptera punctata allatostatin-like peptide in Drosophila melanogaster. J Comp Neurol 363:475–488. doi: 10.1002/cne.903630310

28. Birgül N, Weise C, Kreienkamp HJ, Richter D (1999) Reverse physiology in Drosophila: identification of a novel allatostatin-like neuropeptide and its cognate receptor structurally related to the mammalian somatostatin/galanin/opioid receptor family. EMBO J 18:5892–5900. doi: 10.1093/emboj/18.21.5892

29. Lenz C, Søndergaard L, Grimmelikhuijzen CJ (2000) Molecular cloning and genomic organization of a novel receptor from Drosophila melanogaster structurally related to mammalian galanin receptors. Biochem Biophys Res Commun 269:91–96. doi: 10.1006/bbrc.2000.2251

30. Lenz C, Williamson M, Grimmelikhuijzen CJ (2000) Molecular cloning and genomic organization of a second probable allatostatin receptor from Drosophila melanogaster. Biochem Biophys Res Commun 273:571–577. doi: 10.1006/bbrc.2000.2964

31. Lenz C, Williamson M, Hansen GN, Grimmelikhuijzen CJ (2001) Identification of four Drosophila allatostatins as the cognate ligands for the Drosophila orphan receptor DAR-2. Biochem Biophys Res Commun 286:1117–1122. doi: 10.1006/bbrc.2001.5475

32. Larsen MJ, Burton KJ, Zantello MR, et al. (2001) Type A allatostatins from Drosophila melanogaster and Diplotera puncata activate two Drosophila allatostatin receptors, DAR-1 and DAR-2, expressed in CHO cells. Biochem Biophys Res Commun 286:895–901. doi: 10.1006/bbrc.2001.5476

33. Wang C, Chin-Sang I, Bendena WG (2012) The FGLamide-allatostatins influence foraging behavior in Drosophila melanogaster. PloS One 7:e36059. doi: 10.1371/journal.pone.0036059

34. Hergarden AC, Tayler TD, Anderson DJ (2012) Allatostatin-A neurons inhibit feeding behavior in adult Drosophila. Proc Natl Acad Sci U S A 109:3967–3972. doi: 10.1073/pnas.1200778109

35. Hentze JL, Carlsson MA, Andersen O, et al. (SUBMITTED) The neuropeptide allatostatin A coordinates feeding decisions and metabolism in Drosophila.

36. Nässel DR, Winther ÅME (2010) Drosophila neuropeptides in regulation of physiology and behavior. Prog Neurobiol 92:42–104. doi: 10.1016/j.pneurobio.2010.04.010

37. Pfeiffer BD, Ngo T-TB, Hibbard KL, et al. (2010) Refinement of Tools for Targeted Gene Expression in Drosophila. Genetics 186:735–755. doi: 10.1534/genetics.110.119917

38. Shiga Y, Tanaka-Matakatsu M, Hayashi S (1996) A nuclear GFP/β-galactosidase fusion protein as a marker for morphogenesis in living Drosophila. Dev Growth Differ 38:99–106. doi: 10.1046/j.1440-169X.1996.00012.x

39. Clyne JD, Miesenböck G (2008) Sex-Specific Control and Tuning of the Pattern Generator for Courtship Song in Drosophila. Cell 133:354–363. doi: 10.1016/j.cell.2008.01.050

40. Ranganayakulu G, Elliott DA, Harvey RP, Olson EN (1998) Divergent roles for NK-2 class homeobox genes in cardiogenesis in flies and mice. Development 125:3037–3048.

41. Isabel G, Martin JR, Chidami S, et al. (2005) AKH-producing neuroendocrine cell ablation decreases trehalose and induces behavioral changes in Drosophila. Am J Physiol - Regul Integr Comp Physiol 288:R531–R538.

42. Feng Y, Ueda A, Wu C-F (2004) A modified minimal hemolymph-like solution, HL3.1, for physiological recordings at the neuromuscular junctions of normal and mutant Drosophila larvae. J Neurogenet 18:377–402. doi: 10.1080/01677060490894522

43. Schindelin J, Arganda-Carreras I, Frise E, et al. (2012) Fiji: an open-source platform for biological-image analysis. Nat Methods 9:676–682. doi: 10.1038/nmeth.2019

44. Milyaev N, Osumi-Sutherland D, Reeve S, et al. (2012) The Virtual Fly Brain browser and query interface. Bioinformatics 28:411–415. doi: 10.1093/bioinformatics/btr677

45. Vitzthum H, Homberg U, Agricola H (1996) Distribution of Dip-allatostatin I-like immunoreactivity in the brain of the locust Schistocerca gregaria with detailed analysis of immunostaining in the central complex. J Comp Neurol 369:419–437. doi: 10.1002/(SICI)1096-9861(19960603)369:3<419::AID-CNE7>3.0.CO;2-8

46. Santos JG, Vömel M, Struck R, et al. (2007) Neuroarchitecture of Peptidergic Systems in the Larval Ventral Ganglion of Drosophila melanogaster. PLoS ONE 2:e695. doi: 10.1371/journal.pone.0000695

47. Ja WW, Carvalho GB, Mak EM, et al. (2007) Prandiology of Drosophila and the CAFE assay. Proc Natl Acad Sci U S A 104:8253–8256. doi: 10.1073/pnas.0702726104

48. Cognigni P, Bailey AP, Miguel-Aliaga I (2011) Enteric Neurons and Systemic Signals Couple Nutritional and Reproductive Status with Intestinal Homeostasis. Cell Metab 13:92–104. doi: 10.1016/j.cmet.2010.12.010

49. Edelstein A, Amodaj N, Hoover K, et al. (2010) Computer control of microscopes using μManager. Curr Protoc Mol Biol 92:14.20.1–14.20.17. doi: 10.1002/0471142727.mb1420s92

50. Middleton CA, Nongthomba U, Parry K, et al. (2006) Neuromuscular organization and aminergic modulation of contractions in the Drosophila ovary. BMC Biol 4:17. doi: 10.1186/1741-7007-4-17

51. Elliott C (2005) AviLine. http://biolpc22.york.ac.uk/avianal/avi_line/. University of York

52. R Core Team (2013) R: A Language and Environment for Statistical Computing. R Foundation for Statistical Computing, Vienna, Austria

53. Carlsson MA, Diesner M, Schachtner J, Nässel DR (2010) Multiple neuropeptides in the Drosophila antennal lobe suggest complex modulatory circuits. J Comp Neurol 518:3359–3380. doi: 10.1002/cne.22405

54. Hergarden AC (2011) The role of peptidergic neurons in the regulation of satiety in Drosophila. Dissertation (Ph.D.), California Institute of Technology

55. Yu JY, Kanai MI, Demir E, et al. (2010) Cellular organization of the neural circuit that drives Drosophila courtship behavior. Curr Biol CB 20:1602–1614. doi: 10.1016/j.cub.2010.08.025

56. Tsubouchi A, Caldwell JC, Tracey WD (2012) Dendritic filopodia, Ripped Pocket, NOMPC, and NMDARs contribute to the sense of touch in Drosophila larvae. Curr Biol CB 22:2124–2134. doi: 10.1016/j.cub.2012.09.019

57. Hamada FN, Rosenzweig M, Kang K, et al. (2008) An internal thermal sensor controlling temperature preference in Drosophila. Nature 454:217–220. doi: 10.1038/nature07001

58. Pulver SR, Pashkovski SL, Hornstein NJ, et al. (2009) Temporal dynamics of neuronal activation by Channelrhodopsin-2 and TRPA1 determine behavioral output in Drosophila larvae. J Neurophysiol 101:3075–3088. doi: 10.1152/jn.00071.2009

59. Nitabach MN, Wu Y, Sheeba V, et al. (2006) Electrical hyperexcitation of lateral ventral pacemaker neurons desynchronizes downstream circadian oscillators in the fly circadian circuit and induces multiple behavioral periods. J Neurosci Off J Soc Neurosci 26:479–489. doi: 10.1523/JNEUROSCI.3915-05.2006

60. Chintapalli VR, Wang J, Dow JAT (2007) Using FlyAtlas to identify better Drosophila melanogaster models of human disease. Nat Genet 39:715–720. doi: 10.1038/ng2049

61. Lee H-H, Zaffran S, Frasch M (2006) Development of the Larval Visceral Musculature. In: Sink H (ed) Muscle Dev. Drosoph. Springer New York, New York, pp 62–78

62. Klapper R (2000) The longitudinal visceral musculature of Drosophila melanogaster persists through metamorphosis. Mech Dev 95:47–54.

63. Klapper R, Stute C, Schomaker O, et al. (2002) The formation of syncytia within the visceral musculature of the Drosophila midgut is dependent on duf, sns and mbc. Mech Dev 110:85–96.

64. Bendena WG, Garside CS, Yu CG, Tobe SS (1997) Allatostatins: Diversity in Structure and Function of an Insect Neuropeptide Family. Ann N Y Acad Sci 814:53–66. doi: 10.1111/j.1749-6632.1997.tb46144.x

65. Garside CS, Hayes TK, Tobe SS (1997) Degradation of Dip-Allatostatins by Hemolymph From the Cockroach, Diploptera punctata. Peptides 18:17–25. doi: 10.1016/S0196-9781(96)00244-6

66. Nachman RJ, Garside CS, Tobe SS (1999) Hemolymph and tissue-bound peptidase-resistant analogs of the insect allatostatins. Peptides 20:23–29. doi: 10.1016/S0196-9781(98)00149-1

67. Žitňan D, Šauman I, Sehnal F (1993) Peptidergic innervation and endocrine cells of insect midgut. Arch Insect Biochem Physiol 22:113–132. doi: 10.1002/arch.940220110

68. Robertson L, Lange AB (2010) Neural substrate and allatostatin-like innervation of the gut of Locusta migratoria. J Insect Physiol 56:893–901. doi: 10.1016/j.jinsphys.2010.05.003

69. Sokolove PG, Bushell WN (1978) The chi square periodogram: its utility for analysis of circadian rhythms. J Theor Biol 72:131–160.

70. Schmid B, Helfrich-Förster C, Yoshii T (2011) A new ImageJ plug-in "ActogramJ" for chronobiological analyses. J Biol Rhythms 26:464–467. doi: 10.1177/0748730411414264

6 Final discussion

6.1 Conclusions

The peptidomic investigation of *Drosophila* (5.1) demonstrated that—both during the larval and the adult stage—not only the CNS, but also the midgut produces diverse peptide signals. All midgut peptides represent "brain-gut" peptides that are likewise generated by the CNS.

We are aware that we detected the peptide products of most, but not all, regulatory peptide precursor genes expressed in the *Drosophila* gut. The detectability of a peptide is influenced by several factors, like the concentration, size, structure and ionization efficiency of the peptide, as well as sample composition and factors that are due to the equipment used for analysis, e.g. the type of mass spectrometer. As mentioned in publication 5.1, NPF could not be detected, although other studies demonstrated its presence in enteroendocrine cells (EECs) [e.g. 1–3]. We also did not discover orcokinin B, although in a recent investigation orcokinin B-immunoreactive EECs were found in adult and larval midguts [3]. Moreover, this study confirmed the presence of CCHa1 and CCHa2—two peptides structurally characterized in 5.1—in the midgut and showed that both peptides are produced by EECs of larval and adult fruit flies [3].

The finding that the peptides produced by the gut are also produced by neurons of the CNS is just one of the characteristics that EECs and neurons have in common. Both cell types share further molecular features, e.g. expression of *elav* (see discussion of 5.3). In addition, the developmental mechanism for the specification of both cell types shows noticeable similarities, suggesting a common phylogenetic origin [see e.g. 4 and references therein].

Similar to our first study, the peptidomic analysis of *Delia radicum* larvae (5.2) revealed numerous regulatory peptides, several of them appearing both in the gut and in the CNS of this dipteran pest species. It is nevertheless clear that we did not identify all peptide signals present in *Delia* larvae, and that a number of further peptides will be predicted and verified once the genome sequence of this species is available. Apart from that, the peptidomic studies shown in this thesis (i.e. 5.1 and 5.2) are completed, and results are discussed comprehensively within the respective publications.

Knowledge of the structures and distribution of peptide signals provides a basis for functional research. In general—and analogous to neuropeptides and their multiple tasks—we expect the diversity of insect gut peptides to be reflected in a variety of functions. The peptidergic systems of *Delia* and *Drosophila* showed extensive similarity, suggesting that *Drosophila* could be used as a genetically accessible model to study peptide actions in *Delia* (and most likely in other fly species as well). Considering the relevance of peptide signals for the regulation of e.g. metabolism, research on *Drosophila* peptides might reveal new strategies for the control of pest species.

In our functional study (5.3), we could show that allatostatin A (AstA)—a peptide family detected in the CNS and the gut of both *Drosophila* (5.1) and *Delia* (5.2)—regulates several metabolism-related processes and behaviors in adult fruit flies. As different subsets of AstA-producing cells apparently fulfill different functions, the pleiotropy of AstA peptides seems to correlate with their wide distribution over different regions of the nervous system and the gut.

6.2 AstA analogs are candidates for new pest control agents

Due to their variety and importance for growth and other processes crucial for insect fitness (Fig. 6.1), different peptide families have been investigated with regard to their potential application for targeted and environmentally compatible pest control [5–7].

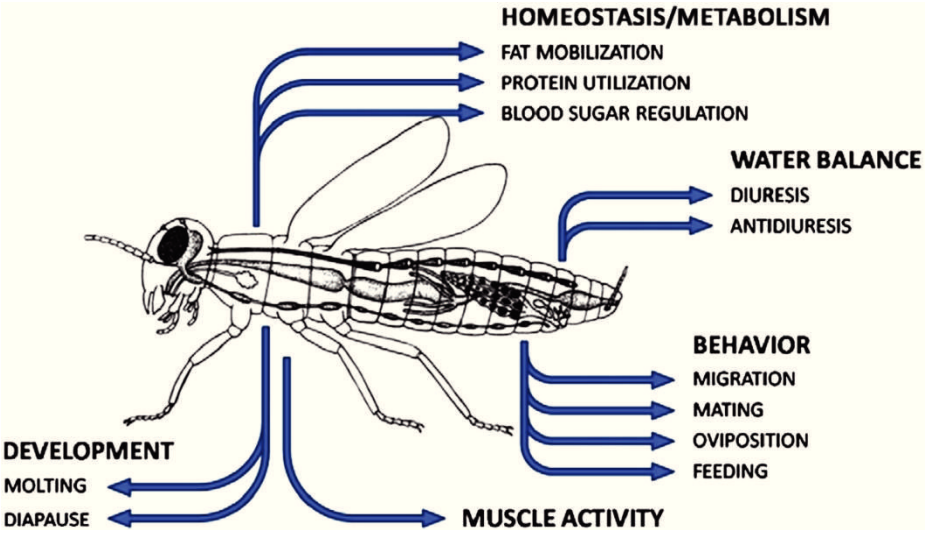

Figure 6.1: Overview of major processes regulated by insect regulatory peptides, which—besides their receptors—represent promising starting points for the development of new insect pest control agents. Modified after [6].

AstA peptides are among the peptide groups for which a multitude of analogs have been synthesized and tested as to whether they can combine the bioactivity of the original, native peptides with improved properties like high stability. In order to overcome the problem of rapid inactivation of AstA peptides by peptidases [8, 9], different chemical approaches were undertaken to create peptidase-resistant analogs by introduction of peptide bond surrogates [10] or by replacement of amino acid residues by unnatural moieties [11–13]. In more recent studies, Kai et al. [14–16] focused on the AstA active core region, i.e. the C-terminal (Y/F)XFGL-amide pentapeptide, to reduce analog size and production cost. They could show that several of the different pentapeptide analogs possessed a potency comparable to that of native Dippu-AstA peptides [15]. The same group pursued this approach even further in order to attain simple and potent substitutions for AstA peptides: Xie et al. synthesized YXFGL-amide analogs which conserved the benzene rings of Y and F, as well as the terminal L-amide, while other portions of the original pentapeptide were altered to simplify synthesis of the compound [17]. Although less effective than the native Dippu-AstA peptides, two of these analogs still showed considerable potency (IC_{50} of ~ 10^{-7} M for the inhibition of JH release by *D. punctata* corpora allata *in vitro* [17]). In addition, the lower potency is potentially compensated by the longer lasting effect of the degradation-resistant analogs [12].

The main focus of the above-mentioned publications was the applicability of AstA mimetics to manipulate JH production and thereby growth, development and reproduction of pest species. The potency of the analogs presented in these studies was predominantly tested for the inhibition of JH synthesis by cockroach corpora allata [10–17], for which a well-established *in vitro* assay exists. Due to the pleiotropic effects of AstA in insects (see 4.4), the potential use of AstA analogs goes beyond

the exploitation of their allatostatic properties and therefore is not limited to those species in which AstA inhibits the corpora allata.

AstA does not regulate JH production in *Drosophila* [18], but the results presented in this thesis (chapter 5.3), as well as other recent studies on *Drosophila*, showed that AstA influences metabolism, food intake, gut peristalsis and locomotor activity [19–21]. As the distribution of AstA cells in *Delia* resembles that of *Drosophila* (see 5.2, 5.3), AstA-mimicking substances are likely to show similar effects in both species and thus might offer a potential strategy to reduce agricultural damage by cabbage maggots (and other fly species).

A problem that remains to be solved is the development of a method to effectively administer the AstA mimetics to the insect, so that an adequate concentration in the hemolymph can be achieved. The analogs developed so far, although being bioactive and stable, most likely do not sufficiently penetrate the gut wall or cuticle of the animal [13, 16]. A possible way to overcome these difficulties might be the use of a carrier protein that enables passage of the gut epithelium and effective transport into the hemolymph. This approach was successfully employed by Fitches et al. [22], who created a fusion product of Manse-allatostatin (AstC) and a plant lectin. This fusion protein, which might be expressed in transgenic crop plants in the future, was detected in the hemolymph of tomato moth larvae following oral ingestion [22]. Furthermore, uptake of the fusion protein by the larvae resulted in inhibition of feeding and growth, thus resembling the effect of direct injection of AstC peptide into the hemolymph of the larvae [22, 23].

6.3 Perspectives

The functional study of AstA (chapter 5.3) brought up several interesting questions and directions for future experiments. For a deeper understanding of AstA function, the following issues deserve further attention:

• Analysis of the influence of nutritional conditions on AstA production, secretion and reception

Whole-fly *AstA* and *DAR-2* mRNA levels were shown to be lower in starved flies than in fed flies, and to rise considerably if starved flies were refed with carbohydrate-rich food [21], suggesting a nutrient-dependent regulation of AstA signaling.

It will be interesting to measure the effect of constant feeding versus starvation versus refeeding after starvation—separately for the brain, the TAG and the gut—both for the level of the *AstA* transcript (RT-qPCR) and for the peptide stores. Relative comparison of peptide quantities is possible via metabolic labeling with ^{15}N followed by mass spectrometric analysis [24]. The combination of information for both the transcript and the peptide levels allows us to speculate on the regulation of peptide production and secretion. We expect to find a higher level of *AstA* mRNA and a lower level of AstA peptides in fed flies compared to starved flies, which would suggest that both *AstA* expression and AstA secretion are increased upon feeding. The mRNA levels for the two AstA receptors will be analyzed in parallel to reveal possible regulation of AstA signaling at the receptor level.

With this method, it will be possible to find out in which way AstA cells react to changing nutritional conditions, and whether the responses differ depending on the location of the AstA subset.

• Confirmation of the role of AstA signaling for feeding and activity

Manipulation of AstA neurons does not only affect secretion of AstA peptides, but also of other neuromodulators/neurotransmitters that potentially are co-localized in the cells. To unequivocally confirm the relevance of AstA signaling for the effects on feeding and activity (demonstrated in 5.3),

experiments using RNAi to inhibit expression of *AstA* and the two receptors genes will be needed, or the experiments have to be repeated within an *AstA* null mutant background [25].

For example, we plan one experiment in which we will use a combination of TrpA1 to activate the AstA cells and RNAi to downregulate *AstA* expression, and then try to rescue the phenotypes (reduced food intake and locomotor activity) we found upon activation of AstA cells.

• Elucidation of the pathway for AstA function

It is not known which signals activate certain AstA cells *in vivo*. To address this question, imaging methods, for example calcium imaging, could be applied. Moreover, in order to understand the downstream effects of AstA, further target cells expressing *DAR-1* or *DAR-2* need to be identified.

In a recent publication, blood fructose was identified to be a key indicator of the nutritional value of ingested food [26]. It is sensed by protocerebral neurons expressing the fructose receptor Gr43a. Following ingestion of sugars, a strong relative increase of blood fructose can be observed. As a consequence, the Gr43a neurons are activated and affect feeding behavior in a manner depending on the nutritional state of the fly: in starved flies food intake is increased, while in satiated flies feeding is decreased [26]. The signal for the nutritional state, i.e. the decisive factor for the outcome of the fructose-induced activation of protocerebral Gr43a neurons, is not known. AstA might be involved in this pathway, e.g. as a signal that indicates a satiated nutritional state. Thus, it would be interesting to test for possible contacts of Gr43a neurons with AstA neurons in the protocerebrum.

• Investigation of a possible interaction between AstA and PKG

The activity of the cGMP-dependent protein kinase G (PKG) encoded by *foraging* depends on the *for* allele, with for^R generating a higher PKG activity than for^S [27]. In the presence of food, for^R ("rover") larvae show more locomotion and consume less than for^S ("sitter") larvae, while no significant differences were detected when food was scarce or absent [28, 29], or when larvae had been food-deprived for at least two hours [30]. Rover/sitter differences in the locomotive response to food were likewise seen in adults [28, 31]. Among further characteristics [e.g. 32, 33], rovers and sitters also differ in the expression levels of genes involved in energy metabolism [31] and the strategies for storing energy as lipids or carbohydrates [30, 31]. The data of Kent et al. suggested that the effects of for^R and for^S in adults are in part caused by interaction of *for* with the insulin signaling pathway [31]. In addition, *akh* mRNA levels were found to be lower in larval rovers than sitters [30].

For larvae, a possible connection between AstA signaling and PKG activity has been found, as *DAR-1* and *AstA* RNAi resulted in reduced *for* mRNA levels and shortened foraging path lengths if food was present [19]. With regard to the influence of AstA on AKH and insulin signaling [21] and the interrelation of AstA and feeding ([20, 21], section 5.3), the question whether a link between AstA and PKG exists in adults might offer an opportunity to reveal further details of a complex signaling network for the control of energy balance.

6.4 References

1. Veenstra JA, Agricola H-J, Sellami A (2008) Regulatory peptides in fruit fly midgut. Cell Tissue Res 334:499–516. doi: 10.1007/s00441-008-0708-3

2. Veenstra JA (2009) Peptidergic paracrine and endocrine cells in the midgut of the fruit fly maggot. Cell Tissue Res 336:309–323. doi: 10.1007/s00441-009-0769-y

3. Veenstra JA, Ida T (SUBMITTED) More Drosophila enteroendocrine peptides: Orcokinin B and the CCHamides 1 and 2.

4. Takashima S, Adams KL, Ortiz PA, et al. (2011) Development of the Drosophila entero-endocrine lineage and its specification by the Notch signaling pathway. Dev Biol 353:161–172. doi: 10.1016/j.ydbio.2011.01.039

5. Gäde G, Goldsworthy G (2003) Insect peptide hormones: a selective review of their physiology and potential application for pest control. Pest Manag Sci 59:1063–1075.

6. Scherkenbeck J, Zdobinsky T (2009) Insect neuropeptides: structures, chemical modifications and potential for insect control. Bioorg Med Chem 17:4071–4084. doi: 10.1016/j.bmc.2008.12.061

7. Caers J, Verlinden H, Zels S, et al. (2012) More than two decades of research on insect neuropeptide GPCRs: an overview. Front Endocrinol 3:151. doi: 10.3389/fendo.2012.00151

8. Garside CS, Hayes TK, Tobe SS (1997) Degradation of Dip-Allatostatins by Hemolymph From the Cockroach, Diploptera punctata. Peptides 18:17–25. doi: 10.1016/S0196-9781(96)00244-6

9. Garside CS, Hayes TK, Tobe SS (1997) Inactivation of Dip-allatostatin 5 by membrane preparations from the cockroach Diploptera punctata. Gen Comp Endocrinol 108:258–270. doi: 10.1006/gcen.1997.6968

10. Piulachs MD, Vilaplana L, Bartolomé JM, et al. (1997) Ketomethylene and methyleneamino pseudopeptide analogues of insect allatostatins inhibit juvenile hormone and vitellogenin production in the cockroach Blattella germanica. Insect Biochem Mol Biol 27:851–858.

11. Nachman RJ, Moyna G, Williams HJ, et al. (1998) Synthesis, biological activity, and conformational studies of insect allatostatin neuropeptide analogues incorporating turn-promoting moieties. Bioorg Med Chem 6:1379–1388.

12. Nachman RJ, Garside CS, Tobe SS (1999) Hemolymph and tissue-bound peptidase-resistant analogs of the insect allatostatins. Peptides 20:23–29. doi: 10.1016/S0196-9781(98)00149-1

13. Garside CS, Nachman RJ, Tobe SS (2000) Injection of Dip-allatostatin or Dip-allatostatin pseudopeptides into mated female Diploptera punctata inhibits endogenous rates of JH biosynthesis and basal oocyte growth. Insect Biochem Mol Biol 30:703–710.

14. Kai Z, Huang J, Tobe SS, Yang X (2009) A potential insect growth regulator: Synthesis and bioactivity of an allatostatin mimic. Peptides 30:1249–1253. doi: 10.1016/j.peptides.2009.03.010

15. Kai Z, Huang J, Xie Y, et al. (2010) Synthesis, Biological Activity, and Hologram Quantitative Structure−Activity Relationships of Novel Allatostatin Analogues. J Agric Food Chem 58:2652–2658. doi: 10.1021/jf902156k

16. Kai Z, Xie Y, Huang J, et al. (2011) Peptidomimetics in the Discovery of New Insect Growth Regulators: Studies on the Structure−Activity Relationships of the Core Pentapeptide Region of Allatostatins. J Agric Food Chem 59:2478–2485. doi: 10.1021/jf200085d

17. Xie Y, Kai ZP, Tobe SS, et al. (2011) Design, synthesis and biological activity of peptidomimetic analogs of insect allatostatins. Peptides 32:581–586. doi: 10.1016/j.peptides.2010.10.016

18. Wang C, Zhang J, Tobe SS, Bendena WG (2012) Defining the contribution of select neuropeptides and their receptors in regulating sesquiterpenoid biosynthesis by Drosophila melanogaster ring gland/corpus allatum through RNAi analysis. Gen Comp Endocrinol 176:347–353. doi: 10.1016/j.ygcen.2011.12.039

19. Wang C, Chin-Sang I, Bendena WG (2012) The FGLamide-allatostatins influence foraging behavior in Drosophila melanogaster. PloS One 7:e36059. doi: 10.1371/journal.pone.0036059

20. Hergarden AC, Tayler TD, Anderson DJ (2012) Allatostatin-A neurons inhibit feeding behavior in adult Drosophila. Proc Natl Acad Sci U S A 109:3967–3972. doi: 10.1073/pnas.1200778109

21. Hentze JL, Carlsson MA, Andersen O, et al. (SUBMITTED) The neuropeptide allatostatin A coordinates feeding decisions and metabolism in Drosophila.

22. Fitches E, Audsley N, Gatehouse JA, Edwards JP (2002) Fusion proteins containing neuropeptides as novel insect contol agents: snowdrop lectin delivers fused allatostatin to insect haemolymph following oral ingestion. Insect Biochem Mol Biol 32:1653–1661.

23. Audsley N, Weaver RJ, Edwards JP (2001) In vivo effects of Manduca sexta allatostatin and allatotropin on larvae of the tomato moth, Lacanobia oleracea. Physiol Entomol 26:181–188. doi: 10.1046/j.0307-6962.2001.00233.x

24. Gouw JW, Tops BBJ, Krijgsveld J (2011) Metabolic Labeling of Model Organisms Using Heavy Nitrogen (15N). In: Gevaert K, Vandekerckhove J (eds) Gel-Free Proteomics. Humana Press, pp 29–42

25. Kondo S, Ueda R (2013) Highly Improved Gene Targeting by Germline-Specific Cas9 Expression in Drosophila. Genetics [Epub ahead of print]. doi: 10.1534/genetics.113.156737

26. Miyamoto T, Slone J, Song X, Amrein H (2012) A Fructose Receptor Functions as a Nutrient Sensor in the Drosophila Brain. Cell 151:1113–1125. doi: 10.1016/j.cell.2012.10.024

27. Osborne KA, Robichon A, Burgess E, et al. (1997) Natural Behavior Polymorphism Due to a cGMP-Dependent Protein Kinase of Drosophila. Science 277:834–836. doi: 10.1126/science.277.5327.834

28. Pereira HS, Sokolowski MB (1993) Mutations in the larval foraging gene affect adult locomotory behavior after feeding in Drosophila melanogaster. Proc Natl Acad Sci U S A 90:5044–5046.

29. Kaun KR, Riedl CAL, Chakaborty-Chatterjee M, et al. (2007) Natural variation in food acquisition mediated via a Drosophila cGMP-dependent protein kinase. J Exp Biol 210:3547–3558. doi: 10.1242/jeb.006924

30. Kaun KR, Chakaborty-Chatterjee M, Sokolowski MB (2008) Natural variation in plasticity of glucose homeostasis and food intake. J Exp Biol 211:3160–3166. doi: 10.1242/jeb.010124

31. Kent CF, Daskalchuk T, Cook L, et al. (2009) The Drosophila foraging Gene Mediates Adult Plasticity and Gene–Environment Interactions in Behaviour, Metabolites, and Gene Expression in Response to Food Deprivation. PLoS Genet 5:e1000609. doi: 10.1371/journal.pgen.1000609

32. Kaun KR, Hendel T, Gerber B, Sokolowski MB (2007) Natural variation in Drosophila larval reward learning and memory due to a cGMP-dependent protein kinase. Learn Mem 14:342–349. doi: 10.1101/lm.505807

33. Scheiner R, Sokolowski MB, Erber J (2004) Activity of cGMP-dependent protein kinase (PKG) affects sucrose responsiveness and habituation in Drosophila melanogaster. Learn Mem 11:303–311. doi: 10.1101/lm.71604

Danksagung

An erster Stelle möchte ich Christian Wegener für die Möglichkeit danken, meine Doktorarbeit in seiner Arbeitsgruppe durchführen zu können. Ich bin dankbar für seine sehr gute, engagierte Betreuung, für die Organisation von Retreats und anderen Unternehmungen für die AG, und für das schnelle Korrekturlesen.

Uwe Homberg danke ich für die Übernahme des Zweitgutachtens und die Unterstützung der AG Wegener, als diese noch in Marburg weilte.

Ich danke den Marburger „Neuros“, d.h. den betreffenden aktuellen bzw. ehemaligen Mitgliedern der AGs Homberg, Schachtner und Wegener, für die gute Arbeitsatmosphäre und – im Besonderen auch Martina und den Leuten aus jenem Büro, in dem ich „immer herzlich willkommen“ war/bin – für gemeinsame Unternehmungen sowie interessante bis verrückte Gespräche. Bei den Mitgliedern der AG Entwicklungsbiologie in Marburg möchte ich mich dafür bedanken, dass ich in ihren Räumen arbeiten und meine Fliegen unterbringen konnte, außerdem für die Hilfsbereitschaft und viele frische Fliegenflaschen. Anja gebührt zusätzlich noch Dank für die Weitergabe ihres Erfahrungsschatzes zur Arbeit mit den Drosos und für unser In-situ-Projekt. Jörg vom MPI danke ich für seine stete Bereitschaft zu helfen, seine Freude daran Dinge zu erklären und seine Begeisterung für das MALDI.

Den Würzburger Neurobiologen/Genetikern danke ich für ihre Unterstützung im letzten Jahr meiner praktischen Arbeit, das häufige Kuchenessen, viele unterhaltsame Zusammentreffen im Seminarraum sowie das gute Arbeitsklima im D-„Keller“. Danke an Irina für ihren unermüdlichen Einsatz für die AG mit D-Zug-Tempo. Susanne, Franzi und Pamela danke ich für die Sorge um mein Wohlergehen, schöne Gespräche und gelegentliche Übernachtungsmöglichkeiten. Dennis und Agi bin ich dankbar für die Hilfe beim Umzug, und Agi außerdem dafür, dass sie mir so schnell ihre Wohnung überlassen hat, als ich eine brauchte.

Den Mitgliedern von Irene Miguel-Aliagas „Poo Lab“ danke ich für die freundliche Aufnahme in die AG trotz etwas beengter Verhältnisse im Labor, und für die schöne und produktive Zeit in Cambridge. Außerdem danke ich ihnen und den anderen „Basement“-Leuten des Zoologischen Instituts für das angenehme Arbeitsklima.

Vielen Dank an alle TAs, die gekocht, gespült, umgeklopft, präpariert, gefilmt, gefärbt, ... haben, sowie an alle Werkstatt-Mitarbeiter, die repariert, gebastelt und sich um allerlei weitere Probleme und Problemchen gekümmert haben.

Ich danke den Freunden, die ich in Marburg kennengelernt habe (Anja, Katja, Addi, Nicole, Bianca, Daniel...), für offene Ohren, Unterhaltung, Ablenkung, Verständnis, gemeinsames Biertrinken und schweißtreibende Bewegung zu lauter Musik. Danke natürlich auch an meine „alten“ Freunde für ihre moralische Unterstützung, Post, Telefonate und Besuche.

Meinen Eltern möchte ich dafür danken, dass sie immer für mich da sind und mich unterstützen, wenn ich sie brauche.

René danke ich für seine Geduld, den Halt, den er mir gibt, seine Hilfe bei meinen Umzügen, die vielen Fahrten zum Bahnhof bzw. nach Hause, und für sein Verständnis für die zukünftigen Platzverhältnisse auf unserem Klingelschild.

Erklärung

Ich versichere, dass ich die vorliegende Dissertation mit dem Titel

„Characterization of the gut peptidome and the function of brain-gut peptides with regard to food intake and metabolism in *Drosophila melanogaster* and the agricultural pest *Delia radicum*“

selbst und ohne unerlaubte Hilfe verfasst, keine anderen als die in der Dissertation angegebenen Quellen oder Hilfsmittel benutzt und alle vollständig oder sinngemäß übernommenen Zitate als solche gekennzeichnet habe.

Die Dissertation wurde in der vorliegenden oder einer ähnlichen Form noch bei keiner anderen in- oder ausländischen Hochschule anlässlich eines Promotionsgesuchs oder zu anderen Prüfungszwecken eingereicht und stellt meinen ersten Promotionsversuch dar.

Marburg, ……

Wencke Reiher

Die nachfolgenden Seiten (Lebenslauf) enthalten persönliche Daten. Sie sind deshalb nicht Bestandteil der Online-Veröffentlichung.